University of Naples Federico II
Polytechnic and Basic Sciences School

Department of Chemical Sciences

Ph.D. in Chemical Sciences

Study of Secondary Metabolites Produced by Fungi from Diverse Environmental Contexts using Combined Analytical Techniques

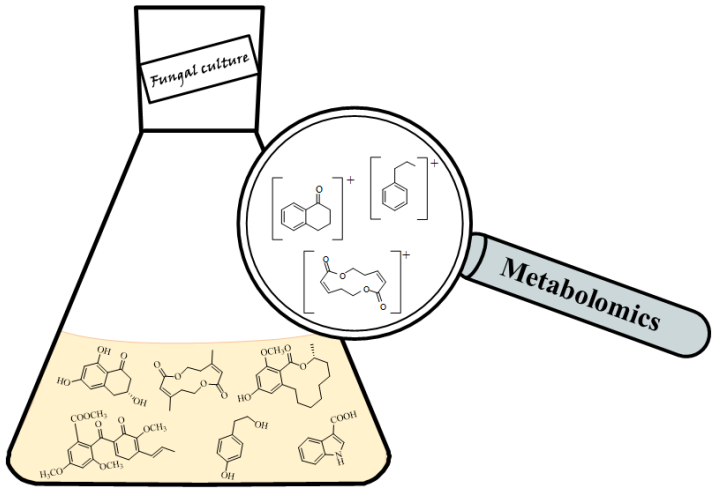

Maria Michela Salvatore

Advisor:
Prof. Anna Andolfi

Examiner:
Prof. Antonio Molinaro

XXXII Cycle 2017 – 2020
Coordinator: prof. Angela Lombardi

University of Naples “Federico II”

Polytechnic and Basic Sciences School

Ph.D. School of Chemical Sciences

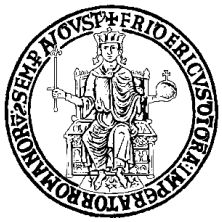

Study of Secondary Metabolites Produced by Fungi from Diverse Environmental Contexts using Combined Analytical Techniques

Maria Michela Salvatore

Supervisor:

Prof. Anna Andolfi

Examiner:

Prof. Antonio Molinaro

XXXII Cycle 2017-2020

Coordinator: Prof. Angela Lombardi

ABSTRACT

In the last decades the scientific community has focused on the study of secondary metabolites produced by fungi. In this respect, fungi from diverse habitat and/or associated to organisms are prime targets of a vigorous investigational activity, based on the employment of the most advanced analytical and structure elucidation techniques. In addition to the classic procedure of isolating and identifying bioactive fungal substances, the metabolomic approaches represent emerging tools for metabolite identification in complex samples.

In this thesis, robust and comprehensive analytical strategies, essentially based on NMR and mass spectrometry, were employed for the structural and stereostructural elucidations of new and known compounds produced in vitro by fungi.

The importance of study the fungal metabolomic profiles is related to the important biological roles of secondary metabolites as virulence factors, chemical defense agents and chemical signals for the communication with other organisms. In fact, many fungi are responsible of severe damages in plants and causing infections in immunocompromised patients. To this end, in this work fungi from the family of Botryospheraceae (i.e. *Lasiodiplodia theobromae*, *Macrophomina phaseolina*, *Neofusicoccum vitifusiforme*) were studied for their capacity to switch with unfavourable environmental conditions from asymptomatic endophytes to virulent pathogens. Their ability to produce lipophilic secondary metabolites (e.g. lasiodiplodins, melleins, botryodiplodins) and the effect of abiotic factors, such as temperature, on the metabolite profile were investigated to better understand the dynamic between host and pathogen.

Furthermore, the increasing awareness of the importance to exploit natural resources for the finding of new bioactive products that may be useful in the search for drugs stimulated us to study fungi as potential biosynthetic factories for a

plethora of biological active and structurally diverse natural products. Our analytical strategies allowed the identification of biological important and taxonomically informative types of compounds (e.g. thiosilvatins, diketopiperazines, funicones) from marine-derived strains collected in the Naples bay (*Trichoderma citrinoviride*, *Aspergillus niger*, *Penicillium brevicompactum*) and from *Talaromyces pinophilus* isolated from the rhizosphere of tobacco plant.

TABLE OF CONTENTS

THESIS OUTLINE

The present work is focused on the role of fungi as producers of secondary metabolites and on the useful information which can be derived from an increasing knowledge of them.

Chapter 1 corresponds to a general introduction addressing the main topics of the work and, in the end of this first section, there are the aims of the work. In chapter 2, the state of art about the instrumental approaches for the detection of secondary metabolites by fungi is described. In chapters 3, 4, and 5 all the results obtained are discussed. In particular, chapter 3 addresses the involvement of secondary metabolites produced by phytopathogenic fungi (i.e. botryosphaeriaceae fungi) in fungal infections. A more specific work regarding the metabolome profiles of *Lasiodiplodia theobromae* strains is reported, in order to understand the importance of the variables "host" and "abiotic factors". As showed in chapter 4, fungal secondary metabolites are also valuable for their biotechnological applications and metabolites produced by marine-derived fungi are of special interest for their original structures and bioactivity. Chapter 5 includes the investigation of secondary metabolites produced by *Talaromyces pinophilus* and the characterization of a new compound with unusual structure. In chapter 6, general procedure information, about the data discussed in chapters 3, 4 and 5, was reported. Finally, the proposed goals and final remarks are discussed.

It should be noted that the realization of this project has been possible thanks to the synergy of different skills and expertise which have defined the chemical and biological aspects of this topic. This work is in collaboration with:

- Prof. Artur Alves, Dr. Ana Cristina Esteves - Department of Biology, University of Aveiro, Portugal;

- Dr. Rosario Nicoletti - Council for Agricultural Research and Economics, Research Centre for Olive, Citrus and Tree Fruit, Caserta, Italy;
- Prof. Francesco Vinale: Institute for Sustainable Plant Protection, National Research Council, Portici (NA), Italy;
- Prof. Santella Burruano, Dr. Selene Giambra, Department of Agricultural, Food and Forest Sciences (SAAF), University of Palermo, Italy;
- Prof. Francesca Borrelli, Department of Pharmacy, School of Medicine and Surgery, University of Naples Federico II, Italy.

Moreover, thanks to the support of Short Terms Scientific Mission COST Action FA1303 (1 month) and Erasmus+ (6 months), I had the opportunity to work on the biological part of my thesis project with the team of Prof. Artur Alves.

Some chapters presented in this thesis have been published on scientific journals. In the followed list, the papers included in this thesis are reported:

- Félix, C., **Salvatore, M.M.**, DellaGreca, M., Ferreira, V., Duarte, A. S., Salvatore, F., Naviglio, D., Gallo, M., Gallo, M., Alves, A., Esteves, A. C., Andolfi, A. (2019). Secondary metabolites produced by grapevine strains of *Lasiodiplodia theobromae* grown at two different temperatures. Mycologia *111*, 466-476. Doi: 10.1080/00275514.2019.1600342
- Félix, C., **Salvatore, M.M.**, DellaGreca, M., Meneses, R., Duarte, A. S., Salvatore, F., Naviglio, D., Gallo, M., Jorrín-Novo, J.V., Alves, A., Andolfi, A., Esteves, A. C. (2018). Production of toxic metabolites by two trains of *Lasiodiplodia theobromae*, isolated from a coconut tree and a human patient. Mycologia *110*, 642-653. Doi: 10.1080/00275514.2018.1478597
- Marra, R., Nicoletti, R., Pagano, E., DellaGreca, M., **Salvatore, M.M.**, Borrelli, F., Lombardi, N., Vinale, F., Woo, S.L., Andolfi, A. (2019). Inhibitory effect of trichodermanone C, a sorbicillinoid produced by

Trichoderma citrinoviride associated to the green alga *Cladophora* sp., on nitrite production in LPS-stimulated macrophages. Natural product research *33*, 3389-3397. Doi: 10.1080/14786419.2018.1479702.

- **Salvatore, M.M.**, Nicoletti, R., Salvatore, F., Naviglio, D., Andolfi, A. (2018). GC–MS approaches for the screening of metabolites produced by marine-derived *Aspergillus*. Marine Chemistry *206*, 19-33. Doi: 10.1016/j.marchem.2018.08.003.
- **Salvatore, M.M.**, DellaGreca, M., Nicoletti, R., Salvatore, F., Vinale, F., Naviglio, D., Andolfi, A. (2018). Talarodiolide, a new 12-membered macrodiolide, and GC/MS Investigation of culture filtrate and mycelial extracts of *Talaromyces pinophilus*. Molecules 23, 950. Doi: 10.3390/molecules23040950.
- **Salvatore, M.M.**, Giambra, S., Naviglio, D., DellaGreca, M., Salvatore, F., Burruano, S., Andolfi, A. (2018). Fatty Acids Produced by *Neofusicoccum vitifusiforme* and *N. parvum*, Fungi Associated with Grapevine Botryosphaeria Dieback. Agriculture *8*, 189. Doi: 10.3390/agriculture8120189.
- Vinale, F., **Salvatore, M.M.**, Nicoletti, R., Staropoli, A., Manganiello, G., Venneri, T., Borrelli, F., DellaGreca, M., Salvatore, F., Andolfi, A. (2020). Identification of Main Metabolites of a Marine-derived Strain of *Penicillium brevicompactum* using LC and GC MS Techniques. Metabolites, *10*, 55. Doi: 10.3390/metabo10020055.
- **Salvatore, M.M.**, Félix, C., Lima, F., Ferreira, V., Naviglio, D., Salvatore, F., Duarte, A.S., Alves, A., Andolfi, A., Esteves a.C. (2020). Secondary Metabolites Produced by *M. phaseolina* Isolated from *E. globulus*. Agriculture, *10*, 72. Doi: 10.3390/agriculture10030072.

CHAPTER 1

General Introduction

Fungi are among the most important organisms in the world, including a large number of taxa, morphologies, ecologies, and life history strategies. In fact, they are one of the largest and most diverse kingdoms of eukaryotes, with special importance because[1]:

1. they are the primary decomposers with ecological roles in the carbon cycle and in nutrient recycling;
2. they are able to establish essential associations with many groups of organisms (i.e. mutualism);
3. many of them are human, plant, or animal pathogens;
4. they show great potential for pharmaceutical, agricultural and industrial applications.

With about 120,000 species described so far, studies on fungal biodiversity propose that the actual number of fungal species may be around 2.2 to 3.8 million[2].

Fungi are widely distributed in all habitats and ecosystems as reported by a recent literature which shows that multiple fungal taxa have cosmopolitan distribution based on 365 global soil samples collected from diverse natural ecosystems[3]. Moreover, fungi can be found in special ecological niches:

1. endophytes (i.e. plant-fungus symbiosis);
2. in marine contexts (i.e. fungi associated with marine algae, seagrass, and mangroves; fungi cohabiting with marine invertebrates, such as corals and sponges; and fungi in marine detritus and in marine extreme environments)[4];
3. anaerobic fungi (e.g. fungi inhabit the gastrointestinal tract of mammalian herbivores);
4. in cold oligotrophic soils from Antarctica[5];
5. in hypersaline environments[6];

6. in areas with naturally higher radiation levels or radioactively contaminated (e.g. space stations, Antarctic mountains, and the Chernobyl exclusion zone)[7-9].

The huge capacity of fungi to occupy areas with a wide variety of environmental conditions of the world is linked to their unique and unusual biochemical pathways. A plethora of low-molecular-weight metabolites are produced by fungi and classified as secondary metabolites.

By definition, secondary metabolites are opposed to primary ones, in fact they are not generally included in the standard metabolic charts. They are organic compounds that are not directly involved in the normal growth, development, or reproduction of organisms. Although secondary metabolites are not strictly needed for the survival of their producers (producer organisms can grow without synthesizing these metabolites), these compounds are often bioactive and each of them is produced only by small number of species[10].

Fungal secondary metabolites are produced by common biosynthesis pathways, such as acetate, shikimate, mevalonate and methylthritol phosphate pathways and alkaloids derived. For this reason, fungi produce metabolites with enormous structural diversity belonging to different classes of natural compounds, such as anthraquinones, statins, melleins, aflatoxins, cumarins, funicones, diketopiperazines, thiosilvatins, fatty acids and derivatives[11].

This structural variability also explains their broad spectrum of activities and functions. A vast number of fungal secondary metabolites is produced as physiological response to multiple biotic and abiotic stimuli. Of great interest is the role of secondary metabolites during fungal interaction with other organisms. In fact, they fulfil very different functions, such as mediating communication, nutrient acquisition, and interactions[12,13]. The recent availability of defined mutants in the biosynthesis of secondary metabolites enables to confirm the hypothesis that these compounds play a major role when the fungus acting as

symbiotic partner of plants, promoting plant growth and development. In turn, the plant delivers carbohydrates to the fungus contributing to a stable association between interaction partners[13].

There is a wide variety of symbiotic plant-fungal interactions which include endophytic fungi. Endophytes show symptomless growth inside living tissues of roots, stems or leaves. The prove that the production of secondary metabolites is one of the ecological benefits in the symbiotic associations between fungi and hosts derives from several genetic studies. In general, the biosynthesis genes for secondary metabolites are in clusters in the fungal genome, and most of them contain one or several central biosynthesis genes encoding extremely large multidomain, multimodular enzymes belonging to the polyketide synthases (PKSs) or non-ribosomal peptide synthetases (NRPSs). Some gene clusters, including aflatoxins[14] and penicillin[15], were identified by generating mutations in these genes and analyzing the profile of the resultant mutants. In fact, the gene deletions may result in abrogation of the biosynthetic pathway[16-18].

For instance, peramine, a modified non-ribosomal peptide (pyrrolopyrazine) from *Epichloë* group of fungal endophytes, is a potent insect feeding deterrent. The genetic evidence, obtained from the identification and mutation of the peptide synthetase in the peramine biosynthetic pathway, confirms the hypothesis that this fungal product protects the host plant from insects. In fact, as endophyte-free organisms, plants associated with mutants are preferentially consumed by the insects, while plants with wild-type fungi are less attractive to predators[19,20]. However, the endophytes may break the fine balance of mutual benefit to become pathogens, prompted by environmental or nutritional conditions[21,22].

For pathogenic interactions, fungi employ an array of strategies to distress, weaken or kill the host in order to gain access to nutrients. One of these strategies is the production of secondary metabolites which play crucial roles as virulence factors and can be observed for fungi infecting animals and plants. These toxins

are compounds produced by the pathogens and their effect on hosts is characterized by the appearance of specific symptoms. The role of a toxin as a disease determinant is proved by the occurrence of this compound in an infected plant and the ability of the toxin alone to elicit at least part of the symptoms of the disease[23]. They belong to different classes of natural compounds, such as polyketides, peptides, terpenoids, organic acids, fatty acids and derivatives. Some of these products are non-host specific because are active toward a broad range of species contributing to the virulence or disease symptom development in the organism which they occur. Other toxins are host-specific and affect only certain species[24]. Understanding the exact functions and mechanisms of action might give an opportunity to successfully combat fungal infections.

Not only does the role of secondary metabolites in the dynamics host-fungus make them interesting to study, but also their biomedical applications. Different fungal strains are being used in biotechnological processes for production of economically important compounds, such as organic acids (e.g. citric, lactic, and succinic acids), antibiotics (e.g. penicillin), and antitumorals (e.g. taxol), among them the ascomycete fungi *Aspergillus*, *Trichoderma*, and *Penicillium* are valuable producers. Furthermore, some metabolites are both toxic and pharmaceutically useful, such as the griseofulvin[25].

After the discovery and development of penicillin[26], the scientific community has focused its attention on fungal metabolites and by 1950[27], prompted by pharmaceutical companies, extensive screening programmes revealed a treasure of microbial products with pharmaceutical applications.

The economic interest on natural products and the improvements of the analytical instrumentations for their detection led to the discovery of one of the most important compounds in terms of biomedical application and commercial value (i.e. millions of dollars per year), the anticancer drug taxol (generic name paclitaxel), reported for the first time as product of the Pacific yew (*Taxus*

brevifolia) in very low concentrations[28]. In 1993[29], the production of taxol was reported from *Taxomyces andreanae*, an endophytic fungus of the Pacific yew. The phenomenon known as horizontal gene transfer (HGT) has disclosed a more reasonable biological explanation of this finding, according to which fungi and plants thriving in the same ecological niche may somehow establish a successful interaction at the genetic level resulting in modification of their metabolome[18,30-32]. This important finding represented the start point for new search in terms addressed to possible applicative opportunities for mere economic production to be exploited in view of increase the drug development.

The search for compounds with new pharmacological properties (i.e. safe, potent, and with broader spectrum) is crucial, especially those applying to new targets and based on different mechanisms. Compounds of great interest to the pharmacological sector are those that combat pathogens, tumours and physiological diseases. Furthermore, these compounds are regarded for new biochemical detection methods and diagnostics, or new metabolic pathways for the selective production of substances with novel pharmacological properties. In this respect, fungi are a promising source of novel antibiotics and drugs with a variety of valued properties, such as anti-inflammatory inhibitors, anti-tuberculosis and anticancer drugs, agonists or antagonists at adrenergic, dopaminergic, and serotonergic receptors, and hypercholesterolemia treatment agents[12,33,34].

Genetic analyses showed the capability of fungi to produce secondary metabolites has been underestimated, because many of the fungal secondary metabolite biosynthesis gene clusters are silent under standard cultivation conditions; the production is strain-specific and environment-dependent[17,35,36] .

1.1. Aims

In the present thesis, secondary metabolites produced by fungi collected from different environmental contexts were studied in order to improve the knowledge on the role of secondary metabolites in the fungal infections, as well as on fungi as source of valuable bioactive compounds in the pharmaceutical, agricultural and industrial fields.

The main goal of the first part of this thesis was the isolation, chemical characterization and bioactivity investigations of secondary metabolites produced *in vitro* by *Botryosphaeriaceae* species (i.e. *Lasiodiplodia theobromae*, *Macrophomina phaseolina* and *Neofusicoccum vitifusiforme*), involved in plant diseases and responsible of significant losses in several crops of economic importance. Of special interest for their huge host/environment adaptability was the evaluation of the effect of abiotic factors (i.e. temperature, nutrient availability and GABA presence) on the metabolomic profiles of *Lasiodiplodia theobromae* strains.

The aim of the second part of this work was the screening and bioactivity investigations of secondary metabolites by marine-derived fungi (*Trichoderma citrinoviride*, *Aspergillus niger* and *Penicillium brevicompactum*) as rich and promising sources of bioactive compounds with original structures and with potential biomedical applications. The metabolome of *Talaromyces pinophilus* isolated from the rhizosphere of tobacco plant was also studied.

To achieve these goals, a comprehensive and robust strategy based on several instrumental techniques was employed, with slight modifications for each case study, considering that this class of natural products has an enormous variety of compounds with different physico-chemical proprieties.

The fungal strains object of this thesis are summarized in the following scheme.

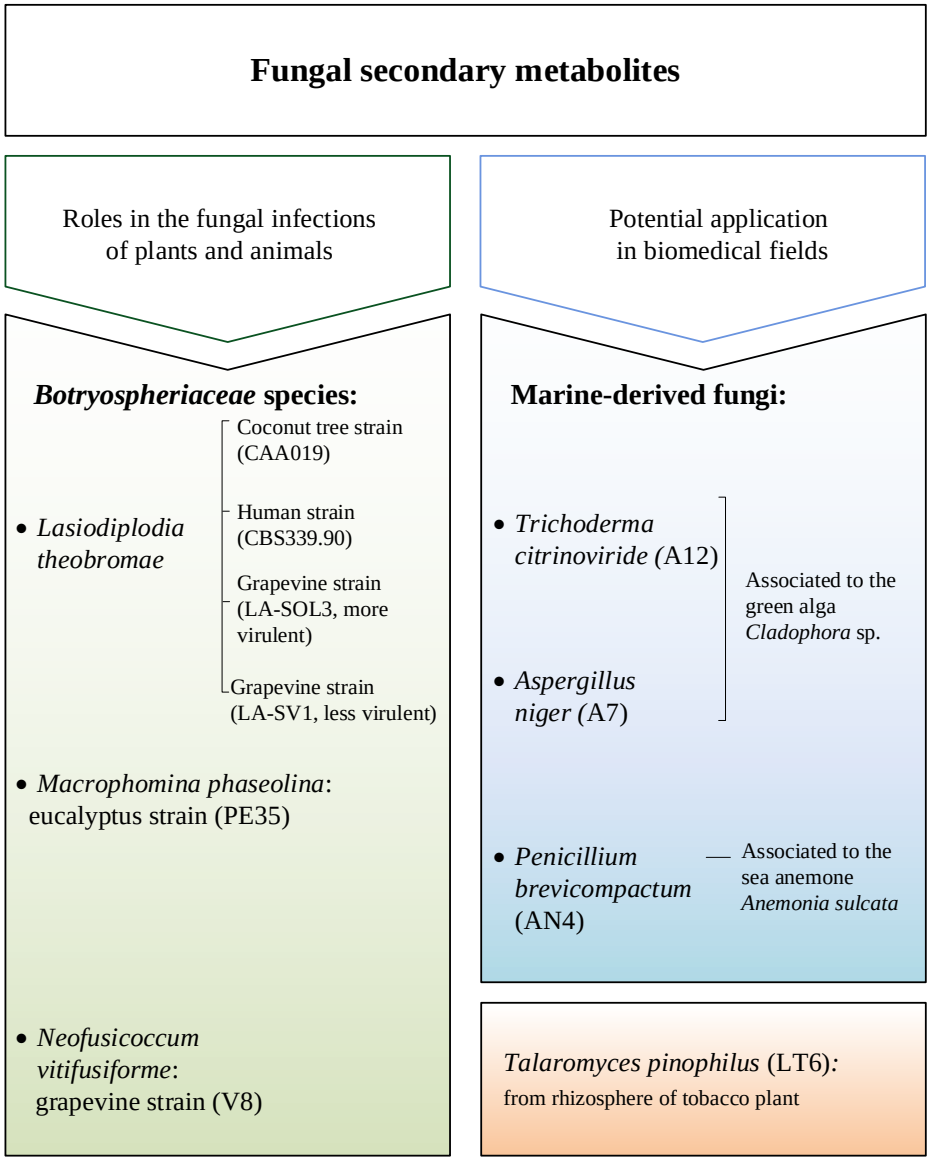
Fungal secondary metabolites
Roles in the fungal infections of plants and animals
Potential application in biomedical fields
Botryospheriaceae species:
Lasiodiplodia theobromae
Coconut tree strain (CAA019)
Human strain (CBS339.90)
Grapevine strain (LA-SOL3, more virulent)
Grapevine strain (LA-SV1, less virulent)
Macrophomina phaseolina: eucalyptus strain (PE35)
Neofusicoccum vitifusiforme: grapevine strain (V8)
Marine-derived fungi:
Trichoderma citrinoviride (A12)
Aspergillus niger (A7)
Associated to the green alga Cladophora sp.
Penicillium brevicompactum (AN4)
Associated to the sea anemone Anemonia sulcata
Talaromyces pinophilus (LT6): from rhizosphere of tobacco plant

1.2. References

1. Baker, S.E., Thykaer, J., Adney, W.S., Brettin, T.S., Brockman, F.J., D'haeseleer, P., Martinez, A.D., Miller, R.M., Rokhsar, D.S., Schadt, C.W., Torok, T., Tuskan, G., Bennett, J., Berka, R.M., Briggs, S.P., Heitman, J., Taylor, J., Turgeon, B.G., Werner-Washburne, M., Himmel, M.E. (2008) Fungal genome sequencing and bioenergy. Fungal Biol. Rev. *22*, 1–5
2. Hawksworth, D.L., Lücking, R. (2017). Fungal diversity revisited: 2.2 to 3.8 million species. In The fungal kingdom, Wiley, Hoboken, NJ, USA, pp 79-95, ISBN: 978-1-55581-957-6.
3. Tedersoo, L., Bahram, M., Polme, S., Koljalg, U., Yorou, N.S., Wijesundera, R., Villarreal Ruiz, L., Vasco-Palacios, A,M., Thu, P.Q., Suija, A., Smith, M.E., Sharp, C., Saluveer, E., Saitta, A., Rosas, M., Riit, T., Ratkowsky, D., Pritsch, K., Poldmaa, K., Piepenbring, M., Phosri, C., Peterson, M., Parts, K., Partel, K., Otsing, E., Nouhra, E., Njouonkou, A.L., Nilsson, R.H., Morgado, L.N., Mayor, J., May, T.W., Majuakim, L., Lodge. D.J., Lee, SS., Larsson, K.H., Kohout, P., Hosaka, K., Hiiesalu, I., Henkel, T.W., Harend, H., Guo, L.D., Greslebin, A., Grelet, G., Geml, J., Gates, G., Dunstan, W., Dunk, C., Drenkhan, R., Dearnaley, J., De Kesel, A., Dang, T., Chen, X., Buegger, F., Brearley, F.Q., Bonito, G., Anslan, S., Abell, S., Abarenkov, K. (2014) Fungal biogeography. Global diversity and geography of soil fungi. Science *346*,1256688.
4. Nicoletti, R., Vinale, F. (2018). Bioactive compounds from marine-derived *Aspergillus, Penicillium, Talaromyces* and *Trichoderma* species. Mar. Drugs *16*, 408.
5. Godinho, V.M., Goncalves, V.N., Santiago, I.F., Figueredo, H.M., Vitoreli, G.A., Schaefer, C.E., Barbosa, E.C., Oliveira, J.G., Alves, T.M., Zani, C.L., Junior, P.A., Murta, S.M., Romanha, A.J., Kroon, E.G., Cantrell, C.L., Wedge, D.E., Duke, S.O., Ali, A., Rosa, C.A., Rosa, L.H. (2015). Diversity and bioprospection of fungal community present in oligotrophic soil of continental Antarctica. Extremophiles *19*, 585–596.
6. Cantrell, S.A., Casillas-Martinez, L., Molina, M. (2006). Characterization of fungi from hypersaline environments of solar salterns using morphological and molecular techniques. Mycol Res. *110*, 962–970.

7. Dadachova, E., Casadevall, A. (2008). Ionizing radiation: how fungi cope, adapt, and exploit with the help of melanin. Curr. Opin. Microbiol. *11*, 525–531.
8. Dighton, J., Tugay, T., Zhdanova, N. (2008) Fungi and ionizing radiation from radionuclides. FEMS Microbiol. Lett. *281*, 109–120.
9. Tugay, T.I., Zheltonozhskaya, M.V., Sadovnikov, L.V., Tugay, A.V., Farfan, E.B. (2011) Effects of ionizing radiation on the antioxidant system of microscopic fungi with radioadaptive properties found in the Chernobyl exclusion zone. Health Phys. *101*, 375–382.
10. Karlovsky, P. (2008). Secondary metabolites in soil ecology. In Secondary metabolites in soil ecology. Springer, Berlin, Germany, pp. 1-19, ISBN: 978-3-54074-542-6.
11. Cole, R.J., Schweikert, M.A. Handbook of secondary fungal metabolites. Academic Press, San Diego, California, USA. ISBN: o-12-179460-1.
12. Meyer, V., Andersen, M.R., Brakhage, A.A., Braus, G.H., Caddick, M.X., Cairns, T.C., de Vries, R.P., Haarmann, T., Hansen, K., Hertz-Fowler, C., et al. (2016). Current challenges of research on filamentous fungi in relation to human welfare and a sustainable bio-economy: A white paper. Fungal Biol. Biotechnol. *3*, 6.
13. Chambergo, F.S.; Valencia, E.Y. (2016). Fungal biodiversity to biotechnology. Appl. Microbiol. Biotechnol., *100*, 2567-2577.
14. Bennett, J.W., Chang, P.-K., Bhatnagar, D. (1997). One gene to whole pathway: the role of norsolorinic acid in aflatoxin research. Adv. Appl. Microbiol. *45*, 1–15.
15. Luengo, J.M., Penalva, M.A. (1994) Penicillin Biosynthesis. In *Aspergillus*: 50 Years On. Elsevier, Amsterdam, Netherlands, pp 603–638, ISBN: 978-0-44481-762-4
16. Khaldi, N., Seifuddin, F.T., Turner, G., Haft, D., Nierman, W.C., Wolfe, K.H., Fedorova, N.D. (2010). SMURF: Genomic mapping of fungal secondary metabolite clusters. Fungal Genet. Biol. *47*, 736–741
17. Brakhage, A.A. (2013). Regulation of fungal secondary metabolism. Nat. Rev. Microbiol. *11*, 21–32.
18. Salvatore, M.M., Nicoletti, R., DellaGreca, M., Andolfi, A. (2019). Occurrence and Properties of Thiosilvatins. *Mar. Drugs*, 17, 664.

19. Fox, E.M., Howlett, B.J. (2008). Secondary metabolism: regulation and role in fungal biology. Curr. Opin. Microbiol. *11*, 481-487.
20. Tanaka, A., Tapper, B. A., Popay, A., Parker, E. J., Scott, B. (2005). A symbiosis expressed non-ribosomal peptide synthetase from a mutualistic fungal endophyte of perennial ryegrass confers protection to the symbiotum from insect herbivory. Mol. Microbiol., *57*, 1036-1050.
21. Schulz, B., Boyle, C. (2005). The endophytic continuum. Mycol. Res. *109*, 661-686.
22. Nicoletti, R., Fiorentino, A. (2015). Plant bioactive metabolites and drugs produced by endophytic fungi of *Spermatophyta*. Agriculture, *5*, 918-970.
23. Hamid, K., Strange, R. N. (2000). Phytotoxicity of solanapyrones A and B produced by the chickpea pathogen *Ascochyta rabiei* (Pass.) Labr. and the apparent metabolism of solanapyrone A by chickpea tissues. Physiol. Mol. Plant. Pathol., 56, 235-244.
24. Walton, J. D. (1996). Host-selective toxins: agents of compatibility. Plant Cell, *8*, 1723.
25. Dewick, P.M. (2011) Medicinal natural products. A biosynthetic approach. Wiley, Hoboken, NJ, USA. ISBN: 978-0-470-74168-9.
26. Bennett, J., Chung, K. (2001). Alexander Fleming and the discovery of penicillin. Adv. Appl. Microbiol. *49*, 163–184
27. Raistrick, H. (1950). A region of biosynthesis. Proc. R. Soc. Lond. B Biol. Sci. *136*, 481–508.
28. Suffness, M. . (1995). Taxol: science and applications. CRC press, Boca Raton, Fl, USA, Volume 22, ISBN: 0-849383-82-X.
29. Stierle, A., Strobel, G., Stierle, D. (1993). Taxol and taxane production by *Taxomyces andreanae*, an endophytic fungus of Pacific yew. Science *260*, 214-216.
30. Fitzpatrick, D.A. (2012). Horizontal gene transfer in fungi. FEMS Microbiol. Lett. *329*, 1-8.
31. Manganiello, G.; Marra, R.; Staropoli, A.; Lombardi, N.; Vinale, F.; Nicoletti, R. (2019). The shifting mycotoxin profiles of endophytic *Fusarium* strains: A case study. Agriculture *9*, 143.

32. Richards, T.A., Soanes, D.M., Foster, P.G., Leonard, G., Thornton, C. R., Talbot, N.J. (2009). Phylogenomic analysis demonstrates a pattern of rare and ancient horizontal gene transfer between plants and fungi. Plant. Cell. *21*, 1897-1911.
33. Nicoletti, R., Salvatore, M.M., Andolfi, A. (2018). Secondary metabolites of mangrove-associated strains of *Talaromyces*. Mar. Drugs *16*, 12.
34. Ana, M.L., Pinto, D.C. (2019). Biological Potential and Medical Use of Secondary Metabolites. Medicines, MDPI, Basel, Switzerland, ISBN 978-3-03921-187-6.
35. Van den Berg, M.A., Albang, R., Albermann, K., Badger, J.H., Daran, J.M., Driessen, A.J., Garcia-Estrada, C., Fedorova, N.D., Harris, D.M., Heijne, W.H., Joardar, V., Kiel, J.A., Kovalchuk, A., Martin, J.F., Nierman, W.C., Nijland, J.G., Pronk, J.T., Roubos, J.A., van der Klei, I.J., van Peij, N.N., Veenhuis, M., von Dohren, H., Wagner, C., Wortman, J., Bovenberg, R.A. (2008) Genome sequencing and analysis of the filamentous fungus *Penicillium chrysogenum*. Nat. Biotechnol. *26*, 1161–1168.
36. Nutzmann, H.W., Reyes-Dominguez, Y., Scherlach, K., Schroeckh, V., Horn, F., Gacek, A., Schumann, J., Hertweck, C., Strauss, J., Brakhage, A.A. (2011) Bacteria-induced natural product formation in the fungus *Aspergillus nidulans* requires Saga/Ada-mediated histone acetylation. Proc. Natl. Acad. Sci. USA *108*, 14282–14287.

CHAPTER 2

Instrumental Approaches for the Screening of Secondary Metabolites Produced by Fungi

2.1. Introduction

Fungi are prime targets of a vigorous investigational activity, based on the employment of the most advanced analytical and structure elucidation techniques, as well as sophisticated software tools and databases for their interpretation and filing. In addition to the classic procedure of isolating and identifying bioactive fungal substances, the metabolomics approach represents an emerging tool for metabolite identification in complex samples. As a robust and comprehensive analytical method, metabolomics measures changes of metabolites representing the functional phenotypes which are the net result of genomic, transcriptomic, and proteomic modifications. This approach can also be used to optimize a biosynthetic pathway to selectively produce biologically active secondary metabolites. The combination of different instrumental techniques (e.g. GC-MS, LC-MS, NMR, IR, X-ray crystallography, etc…) can be considered for the detection of metabolites produced by fungi, each of them presenting different advantages and limitations.

2.2. Sample Preparation for Metabolomic Analysis

Investigations on the biochemical properties of a fungal strain require appropriate treatments finalized to its cultivation *in vitro* in either a solid or a liquid medium (Figure 2.1). When a fungus is grown on solid phase, many classes of volatile organic compounds are released, and GC-MS has long been the main method for their identification. In fact, static and/or dynamic headspace is used to investigate volatile compounds with low molecular weight[1]. To perform analysis of a larger range of metabolites, an extraction step with an organic solvent is necessary to yield a crude extract including both extrolites and mycelial metabolites. In several instances metabolomic profiling of fungi grown in liquid medium is preferred because it enables separation of the mycelial part from the broth by means of filtration or centrifugation, and the independent analysis of the

two components of the culture. Analysis of the mycelial extract can be preceded by further manipulations, such as washing, freeze-drying, sonication, centrifugation, extraction, etc. In the case of culture filtrates, a preliminary extraction with an organic solvent is generally carried out to reduce the mixture complexity and select extrolites according to their polarity[2].

The chemical composition of the cultivation medium influences fungal growth and metabolite production. In fact, media with a rich composition, such as potato-dextrose broth (PDB), allow fast and more conspicuous fungal development. Possible derivation of the extracted products from metabolites originally contained in the medium should be considered when the fungus is grown in a rich substrate. In this respect, it would be meaningful to include a sterile sample of the selected medium for comparison. On a different investigational instance, provided that it can effectively support fungal growth, preference can be granted to a minimal medium, such as Czapek-Dox broth (CDB) only containing sucrose as carbon source, in view of exclusively extracting products deriving from fungal metabolism[3].

Another sensitive methodological aspect is definitely the choice of a suitable solvent for extraction, considering that a higher efficiency at this stage provides a greater range of compounds. In principle, the sequential use of solvents of diverse polarity for the extraction of non-polar compounds enables to perform more complete analyses; however, more frequently the extraction procedure is only based on a single solvent with a broad polarity range, such as ethyl acetate. pH of the aqueous phase to be extracted is of great importance because compounds of interest can be acid or basic species[2]. The resulting crude extract might be highly complex, therefore further separation steps are generally adopted to obtain one or more substances, and many chromatographic methods may be employed[4].

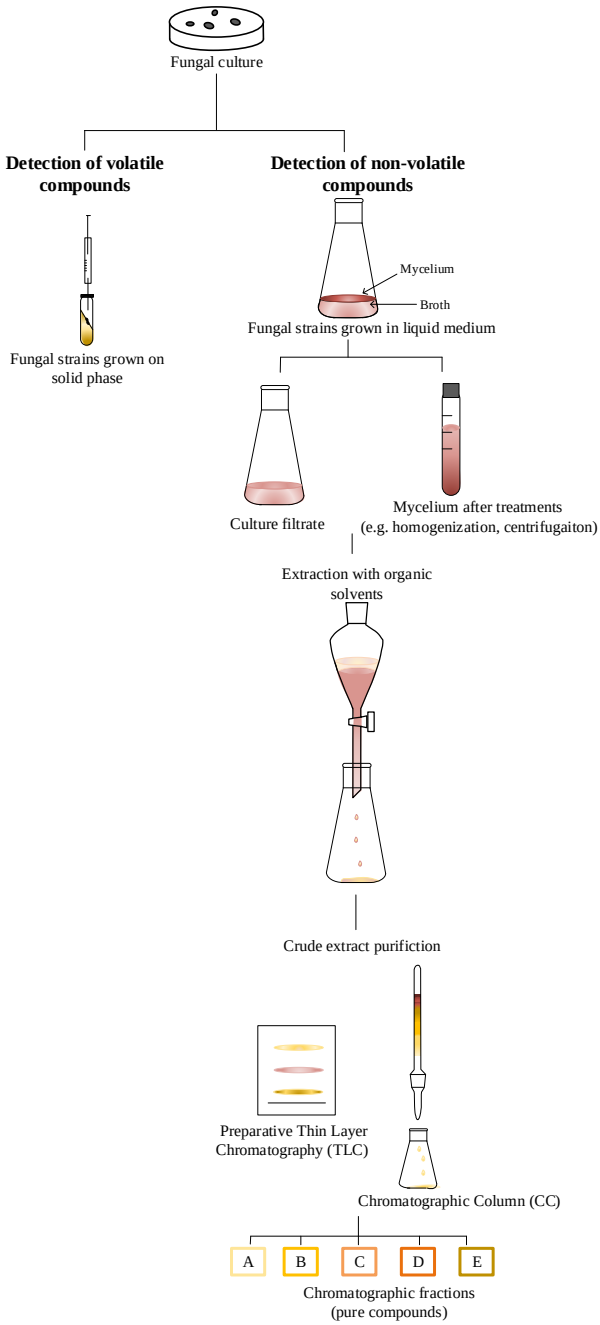

Figure 2.1. Sample preparation for identification of secondary metabolites via instrumental techniques.

2.3. An Overview of Instrumental Strategies for the Detection of Fungal Secondary Metabolites

An accurate identification of secondary metabolites can be obtained through the application of several instrumental techniques, considering their advantages and limitations (Table 2.1). In fact, fungal metabolites have very diverse physico-chemical proprieties and occur at different abundance levels. Consequently, comprehensive metabolomics investigation is a challenge for researchers involved in this field. This complex task requires a special strategy to have a complete screening of detectable compounds in a sample (e.g. culture filtrate, organic extract).

Table 2.1. Comparison between GC-MS, LC-MS and NMR.

	GC-MS	**LC-MS**	**NMR**
Possibility of identifying compounds in a complex matrix	✔	✔	
Availability of commercial libraries for rapid compounds identification	✔		
Identification of new compounds	✔		✔
Suitable for polar/poorly volatile and thermolabile compounds	*derivatization step required	✔	✔
Suitable for high molecular weight compounds (more than 1000 u)		✔	✔
Suitable for compounds with very similar structures (e.g., fatty acids)	✔	✔	
High sensitivity	✔	✔	
Easy to operate and maintain	✔		
Instrument and software cost	Low-Medium	Medium-High	High

As a matter of fact, NMR is considered the most reliable technique for the *de novo* structural elucidation of new compounds occurring in fungal organic extracts but requires preliminary purification processes to dispel interferences among the different components.

Gas chromatography coupled to mass spectrometry (GC-MS) is a mature technology and represents a very convenient tool to avoid the usual more complex procedures necessary to separate metabolites in sufficient pure amounts. The main GC-MS disadvantage is that polar or poorly volatile compounds require a derivatization step, which complicates the sample preparation. Furthermore, GC is not suitable for thermolabile compounds because of the elevated temperature of the injector and separation column. Analogously, compounds with molecular weight above 1000 u which cannot be volatilized without decomposition cannot be analysed by GC-MS.

Liquid chromatography (LC) is better suited for polar and thermolabile compounds. However, coupling MS to LC is much more difficult than coupling to GC. The development of Atmospheric Pressure Ionisation (API) sources made it possible to couple LC and MS. Accurate mass measurements (which require a high resolution mass analyzer, e.g. a Time of Fly (TOF) mass analyzer) and multiple stages of mass analysis (e.g. LC-MS/MS) are used to compensate for the lack of structural information of LC-MS mass spectra acquired with an API ion source but at the cost of a more complex and expensive instrumentation. Even so, LC-MS and LC-MS/MS data are more instrument-dependent and, consequently, the possibility of identification of analytes via comparison with published MS data in libraries is much reduced. Custom MS libraries can be created by users, but at the cost of additional work.

The strength of our approaches to the study of fungal metabolites is the use of several instrumentations, but in particular the use of GC-MS had certainly the advantage to make possible the identification with an excellent sensitivity and

reproducibility for compounds occurring in complex matrices. In this respect, the followed section is dedicated to GC-MS analysis.

2.4. GC-MS Analysis

The workhorse for GC-MS is a Gas Chromatograph, equipped with a capillary column, hyphenated to a Mass Spectrometer based on a quadrupole Mass Analyzer and an Electron Ionization (EI) ion source operated with a 70 eV electron beam. EI is a hard ionization technique and EI mass spectra show the mass of molecules eluted from the GC and of pieces from it (Figure 2.2).

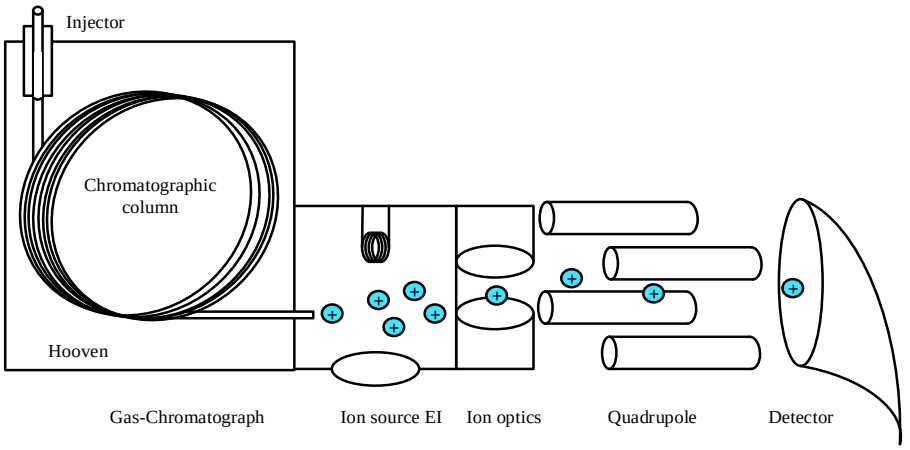

Figure 2.2. Schematic representation of a GC-EI-MS.

More advanced GC-MS instruments can alternate the EI ion source with a soft CI (Chemical Ionization) ion source which can provide complementary information to the EI mass spectrum.

EI mass spectra acquired under standardized conditions (70 eV electrons energy and 200 – 250 °C ion source temperature) are very reproducible. So much so that identification of compounds via GC-MS can be conveniently done by comparing the acquired mass spectrum with reference mass spectra of pure compounds collected in dedicated MS libraries, such as the National Institute of

Standards and Technology (NIST) library[5], and databases. Further support to the GC-MS identification is also provided by chromatographic retention indices (RI) calculated from the Reconstructed Total Ion Gas Chromatogram (TIC).

The identification of compounds via GC-MS is conveniently done by combining the retention indices (RI) and the reference mass spectra gathered in dedicated databases such as the National Institute of Standards and Technology (NIST) libraries[5] (Figure 2.3).

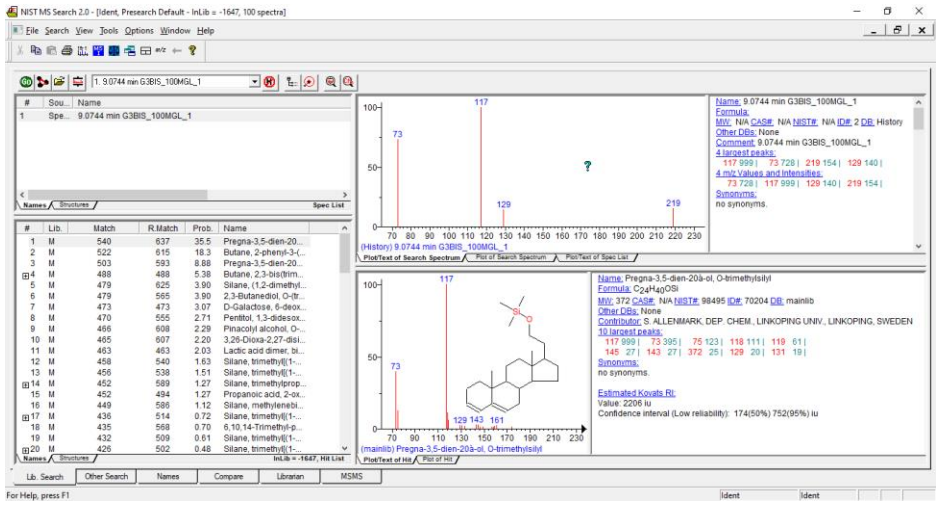

Figure 2.3. Lib. Search window of the mass spectral database NIST14.

Modern GC-MS methods use capillary columns with low bleed characteristics, which are typically 30 m long with a 0.25 mm internal diameter. By increasing the column length, the analysis time increases and this is a drawback for a high throughput laboratory. Longer columns provide greater chromatographic resolution but doubling column length will not double resolution. In any case, any reduction of time in separation of complex samples should not prejudice the possibility to resolve the different peaks in the reconstructed gas chromatogram.

In a GC-MS system the job of the chromatographic column is to present in sequence to the Mass Spectrometer pure compounds separated from the injected mixture. The ability to separate sample components depends, among others, on the nature of the column stationary phase. For instance, two compounds that co-elute on a stationary phase may be separated on a different phase. For this reason, a variety of capillary column phases are commercially available providing specific analyte-stationary phase interactions. A non-polar column is recommended for the separation of non-polar compounds. On the other hand, polar columns are used for the analysis of polar compounds. Generally a non-polar/slight polar column (such as DB-1, DB-5MS, HP-5MS) is used for a broad-spectrum analysis of components present in the samples[6,7]. In fact, identification of products in complex mixtures could become problematic when components of the injected mixture are not fully separated or even co-elute from the column which is detected as overlapping peaks in the resulting gas chromatogram and impure mass spectra. When components of a mixture are not fully separated, identification is still possible through the process of deconvolution of GC-MS data which is implemented by several computer programs, such as the NIST program AMDIS (Automated Mass spectral Deconvolution and Identification System)[8,9] (Figure 2.4).

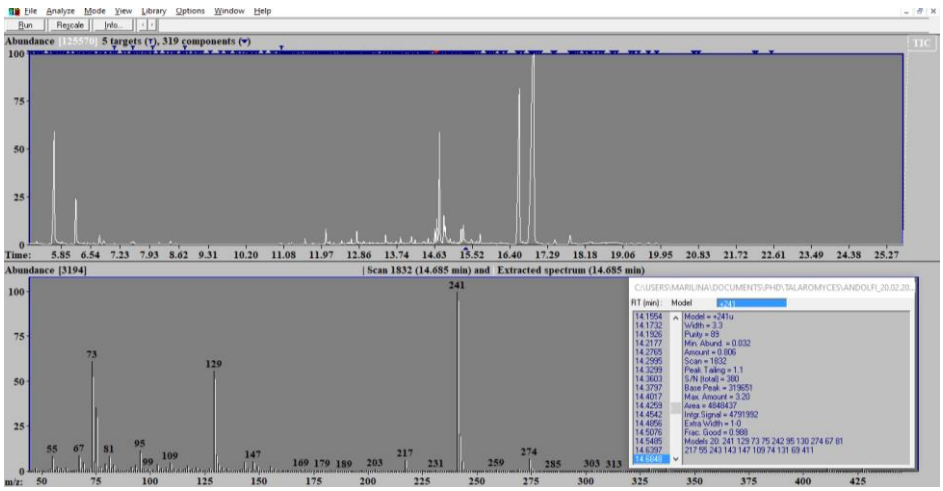

Figure 2.4. Window of NIST program AMDIS for deconvolution process of GC-MS data.

Certainly, the best column for fungal metabolite screening should have high sensitivity, high efficiency and should operate under high temperature limits to provide the utmost confidence in results.

The above identification procedure is appropriate for compounds which are unknown to the operator, but which are already known to the scientific community and whose EI mass spectra have already been acquired and compiled in a MS database. Obviously, compounds which are truly unknown (that is, new compounds which have not been previously reported) cannot be identified in the way described above.

The strength of GC-MS with an EI ion source is that even truly unknown substances can, in abstract, still be identified through the *ab initio* interpretation of the EI mass spectrum. In fact, in the course of several decades, a key discipline has evolved which allows the determination of a structure from an EI mass spectrum. Even for very complex structures, the interpretation of the EI mass spectrum by a trained mass spectrometrist would at least unravel the main structural features of the compound.

MS Interpreter is one of a number of softwares which, from the postulated structure of a compound, derives a theoretical mass spectrum (*in silico* mass spectrum) which can be compared with the experimental mass spectrum in order to check its consistency with the postulated structure. The process starts by importing in MS Interpreter both the postulated structure and the experimental spectrum. As soon as the two files are imported, MS interpreter calculates the *in silico* MS spectrum and compares it with mass peaks in the experimental spectrum. As a result of this operation, mass peaks in the experimental spectrum are divided into two groups.

The first group contains mass peaks which can be justified on the basis of the imported structure. These peaks assume a full black colour in the mass spectrum window of the program interface. By selecting with the mouse click one of the black MS peaks, the program readily highlights, in the structure window of the interface, the fragmentation pathway through which the selected fragment has been created from the imported structure. On the contrary, mass peaks in the experimental MS spectrum which are considered incompatible with the imported structure are coloured in white and are insensitive to the mouse click. Finally, the imported structure is considered consistent with the mass spectrum when the number of white coloured MS peaks is a small fraction of the total number of mass peaks in the MS spectrum (Figure 2.5).

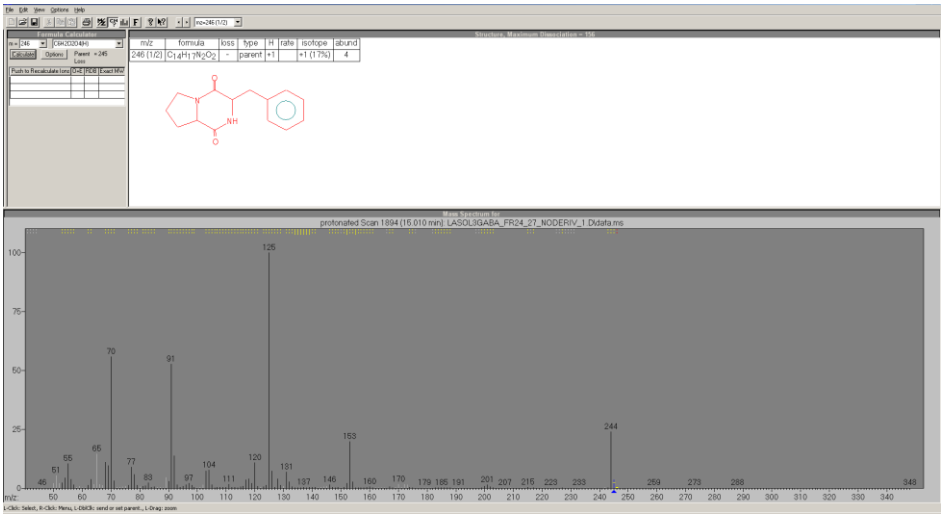

Figure 2.5. Window of MS interpreter.

Many secondary metabolites in the fungal extract are non-volatile compounds with polar functionalized groups and, in general, not suitable for GC-MS analysis because very prone to decomposition during high temperature flash vaporization in the GC injector. In order to reduce the risk of decomposition, before GC-MS measurements, metabolites with polar functionalized groups should be converted in other substances which are more easily detected (derivatization). Although it is not completely excluded that GC-MS measurements for some polar compounds be possible without chemical derivatization of samples, this procedure is highly recommended to reduce the polarity of the functional groups, facilitate the separation by gas chromatography, and increase sensitivity[10-12].

Derivatization of compounds for GC-MS is the substitution on the polar function using a reagent that reacts with active hydrogen. Among the derivatization procedures[6,10-12], the most commonly used are methylation and trimethylsilylation. Ethereal diazomethane is widely employed in the methylation reaction of carboxylic acids (e.g., fatty acids) or phenols to obtain methyl esters of the original compounds[13]. Trimethylsilylation is usually done as single step

derivatization with reagents such as *N*,*O*-bis(trimethylsilyl)trifluoroacetamide (BSTFA), a donor which substitutes hydrogen atoms in -OH, -NH, -SH groups with trimethylsilyl groups (TMS). Frequently, during derivatization with BSTFA a single compound originates more than one derivative. By way of example, a compound with two functionalized groups in its structure may give rise to its mono- and bis-trimethylsilyl derivatives[14,15].

2.5. References

1. Larsen, T.O., Frisvad, J.C. (1995). Comparison of different methods for collection of volatile chemical markers from fungi. J. Microbiol. Methods *24*, 135–144.
2. Harvey, D. (2000). Modern analytical chemistry. Vol. 381 McGraw-Hill, New York, NY, USA, ISBN 0-07-237547-7.
3. Nicoletti, R., Ferranti, P., Caira, S., Misso, G., Castellano, M., Di Lorenzo, G., Caraglia, M. (2014). Myrtucommulone production by a strain of *Neofusicoccum australe* endophytic in myrtle (*Myrtus communis*). World J. Microbiol. Biotechnol. *30*, 1047–1052.
4. Grob, R.L., Barry, E.F. (2004). Modern practice of gas chromatography. John Wiley & Sons, New York, NY, USA, ISBN: 978-0-471-65115-4.
5. Schauer, N., Steinhauser, D., Strelkov, S., Schomburg, D., Allison, G., Moritz, T., Lundgren, K., Roessner-Tunali, U., Forbes, M.G., Willmitzer, L., Fernie, A.R., Kopka, J. (2005). GC–MS libraries for the rapid identification of metabolites in complex biological samples. FEBS Lett. *579*, 1332–1337.
6. Sparkman, O.D., Penton, Z., Kitson, F.G. (2011). Gas chromatography and mass spectrometry: a practical guide, 2nd ed. Academic Press, Oxford, UK ISBN: 978-0-12-373628-4.
7. Lebedev, A. (2012). Comprehensive environmental mass spectrometry. ILM Publications, Hertfordshire, UK ISBN: 978-1-906799-12-0.
8. Stein, S.E. (1999). An integrated method for spectrum extraction and compound identification from gas chromatography/mass spectrometry data. J. Am. Soc. Mass Spectrom. *10*, 770–781.
9. AMDIS NET http://www.amdis.net/ (accessed on 14 12 2019).
10. Knapp, D.R. (1979). Handbook of analytical derivatization reactions. John Wiley & Sons, New York NY, USA, ISBN: 0-471-03469-X.

11. Halket, J.M., Waterman, D., Przyborowska, A.M., Patel, R.K., Fraser, P.D., Bramley, P.M. (2004). Chemical derivatization and mass spectral libraries in metabolic profiling by GC/MS and LC/MS/MS. J. Exp. Bot. *56*, 219–243.
12. Frei, R.W. (2013). Chemical derivatization in analytical chemistry. Springer Science & bussines media, New York, NY, USA, ISBN: 978-1-4615-9194-8.
13. Levitt, M.J. (1973). Rapid methylation of microamounts of nonvolatile acids. Anal. Chem. *45*, 618–620.
14. Schummer, C., Delhomme, O., Appenzeller, B.M., Wennig, R., Millet, M. (2009). Comparison of MTBSTFA and BSTFA in derivatization reactions of polar compounds prior to GC/MS analysis. Talanta *77*, 1473–1482.
15. Guida, M., Salvatore, M.M., Salvatore, F. (2015). A strategy for GC/MS quantification of polar compounds via their silylated surrogates: silylation and quantification of biological amino acids. J. Anal. Bioanal. Tech. *6*, 1–16.

CHAPTER 3

Study of Secondary Metabolites, Produced by Botryosphaeriaceae, Potentially Involved in Host-Pathogen Interactions

3.1. Introduction

The Botryosphaeriaceae is an ascomycete family with a worldwide distribution in all climatic areas playing important roles in the ecology of woody plants. It counts with 187 species grouped in 23 genera[1], the best-known of which are *Lasiodiplodia*, *Neofusicoccum*, *Diplodia*, *Macrophomina* and *Dothiorella*[2], occurring as saprophytes, parasites and endophytes on a wide range of annual and perennial plants[3]. The Botryosphaericeae include a range of morphologically diverse fungi which can live as endophytes in plant organs, in a latent phase, but with unfavourable environmental conditions they can switch to virulent pathogens. In fact, they are frequently associated with plant diseases causing diverse symptoms, such as leaf spots, fruit rots, dieback and cankers and eventually death. With meaningful economic impact in some crops (e.g. grapevine, mango, eucalypt).

To date, several species are known for producing bioactive toxic metabolites, which are probably involved in the plant diseases. There are no effective fungicides against these commonly occurring diseases and the best control practice consists in providing the appropriate cultural management avoiding plant stress and injury, and employing appropriate sanitation measures. However, enriching the existing literature with new data on secondary metabolites produced by isolates from different hosts might be useful in understanding[3]:

1. the ecology and host-pathogen relationships;
2. the mechanisms of action;
3. the resistant mechanisms and possible application for the screening of diseases;
4. possible applications of secondary metabolites as natural antimicrobial, insecticidal and herbicidal.

This knowledge in turn can be applied where recommendations for disease management strategies are required.

In this study, secondary metabolites produced by strains of *Lasiodiplodia theobromae*, *Neofusicoccum vitifusiforme* and *Macrophomina phaseolina* were investigated using the experimental approach explained in detail in Chapter 2.

3.2. Effects of Abiotic Factors on Secondary Metabolites Produced by Strains of *Lasiodiplodia theobromae*

The objectives of this study were a) to investigate secondary metabolites production by four strains of *L. theobromae*; b) to evaluate the effect of abiotic factors (i.e. temperature and GABA concentration) on metabolomic profiles of isolates of *L. theobromae*; c) to test the phytotoxicity and cytotoxicity of culture filtrates and compounds isolated from cultures.

3.2.1. Phytotoxicity and Cytotoxicity of Culture Filtrates

The culture filtrates produced by strains isolated from coconut tree (i.e. CAA019), human (i.e. CBS339.90) and grapevines (i.e. LA-SOL3 and LA-SV1) grown in Czapek medium at two temperatures (i.e. 25 and 37°C) were evaluated for toxicity on tomato stems and on mammalian cells. Furthermore, culture filtrates produced by LA-SOL3 and LA-SV1 strains grown in Potato Dextrose Agar (PDB) in presence and absence of 10 mM γ-amminobutyric acid (GABA) were also tested for phytotoxicity. Phytotoxicity of the culture filtrates from the strains of *L. theobromae* was evaluated by an assay on tomato stems of rootless plants. All the strains induced phytotoxicity symptoms, such as wilting and dry leaves (Figure 3.1).

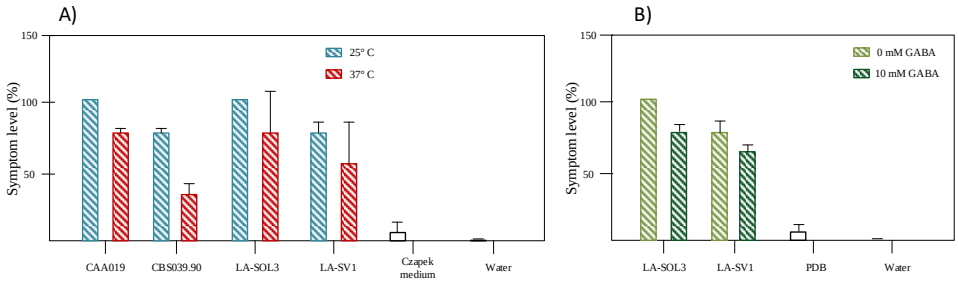

Figure 3.1. Phytotoxicity assay on tomato stems using A) strains CAA019, CBS339.90, LA-SOL3 and LA-SV1 of *L. theobromae* grown in Czapek medium at 25 and 37°C and B) strains LA-SOL3 and LA-SV1 of *L. theobromae* grown in PDB at 25°C in presence and absence of GABA. Symptoms were recorded and converted to a percentage to evaluate the phytotoxic activity using a 0-4 scale (0 = no symptoms; 1 = slight withering; 2 = intermediate withering; 3 = severe withering; 4 = full withering). Data are shown as the average of three independent replicates for each condition.

Severity of symptoms steadily decreased with culture filtrate dilution. The culture filtrates more toxic to stems were those from fungi grown at 25°C and the strains that induced more severe symptoms were the ones isolated from plants.

This supports the presence of one or more toxic metabolites in the culture filtrates of fungi grown at 25°C that are not produced (or produced in lower amounts) at 37°C. Concerning strains isolated from grapevine, LA-SOL3 turns out to be more phytotoxic compared to LA-SV1 in all the growth conditions tested. Interestingly, when the strains were grown in presence of GABA there is a decrease of phytotoxic activity of the culture filtrates. It suggests the presence of different metabolites in culture filtrates from strains under examinations.

In addition to phytotoxicity, we evaluated the cytotoxicity of the culture filtrates. Vero (African green monkey kidney epithelial cells) and 3T3 (mouse fibroblasts) cells were selected to assess the effect of pure metabolites. Vero and 3T3 cells may display different sensitivity to test materials/compounds and for that reason are broadly used to assess general toxicity, mainly for detection of the

biological activity of test natural or synthetic substances. Epithelial cells and fibroblasts are the two cell types mainly involved in tissue repair after injury/infection. Monkey kidney cells (Vero) were shown to be more robust, and fibroblasts (3T3) more sensitive, to strain CBS339.90, which was responsible for causing higher mammalian cell mortality, especially when grown at 37 °C. The culture filtrate of the strain of *L. theobromae* (grown either at 25 or 37°C) induced only slight decrease in viability of Vero cells (Figure 3.2A). However, the culture filtrate of strain CBS339.90 grown at 37°C caused significant cytotoxicity ($P < 0.0001$), leading to the loss of about 80% of cell viability. When the strain was grown at 25°C, no cytotoxicity was detected. The same trend was observed for 3T3 cell line: strain of *L. theobromae* isolated from plants showed low toxic effect, whereas strain CBS339.90 grown at 37°C induced a significant severe mortality (10% viability, $P < 0.0001$) of 3T3 cells (Figure 3.2B). Cytotoxicity of culture filtrates of LA-SOL3 and LA-SV1 strain, grown in presence and in absence of GABA, was not tested on mammalian cell cultures. In fact, GABA, as a neurotransmitter in animals, affects the vitality of the cells not allowing the evaluation of the culture filtrates toxicity.

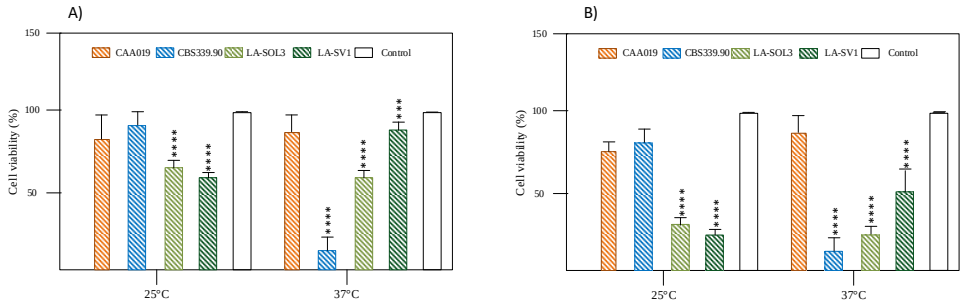

Figure 3.2. Cytotoxicity in Vero (A) and 3T3 (B) cells of the culture filtrates of strains CAA019, CBS339.90, LA-SOL3 and LA-SV1 in Czapek medium at 25 and 37°C. Data are presented as average ± standard error. Two-way ANOVA, followed by a Bonferroni multiple comparison test, was used to determine the statistical significance of cytotoxicity of each strain within the same temperature versus the control. **P < 0.01; ****P < 0.0001

3.2.2. Isolation and Identification of Secondary Metabolites in Different Cultures

In order to identify bioactive lipophilic compounds (Figure 3.3) that may be involved in the biological activities of the culture filtrates, their crude extracts were subjected to purification processes by combined column and thin-layer chromatography. When possible, metabolites were identified by comparison of experimental data with those reported in literature for botryosphaerilactone A[4], lasiolactols A and B[5], (3*S*,4*R*,5*R*)-hydroxymethyl-3,5-dimethyldihydro 2-furanone[4,6], (-)-botryodiplodin[7], (3*S*,4*S*)- and (3*R*,4*S*)-4-acetyl-3-methyl-2-dihydrofuranone[8], 3-indolecarboxylic acid (identification by certified standard), (-)-jasmonic acid[9,10], (*R*)-mellein[11,12], *cis*-(3*R*,4*R*)- 4-hydroxymellein[10,12], and tyrosol[13] (Figure 3.3).

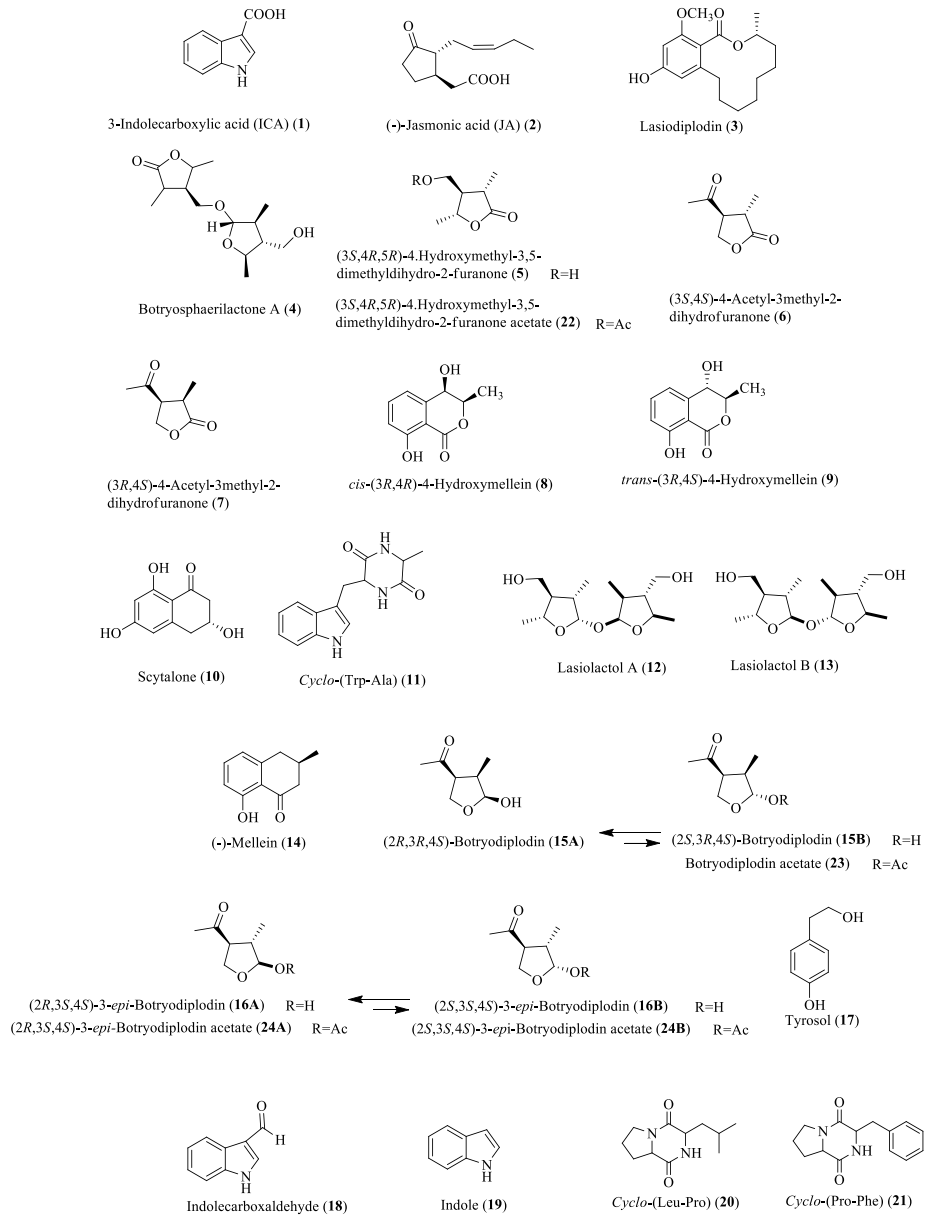

Figure 3.3. Pure metabolites and derivatives (**1-24**) from strains CAA019, CBS339.90, LA-SOL3 and LA-SV1 grown in Czapek medium at 25 and 37°C, and metabolites from LA-SOL3 and LA-SV1 grown in PDB at 25°C in presence and absence of GABA.

3.2.3. Structure Determination of (2R/2S,3S,4S)-3-epi-botryodiplodin

(2*R*/2*S*,3*S*,4*S*)-3-*epi*-botryodiplodin (**16**, Figure 3.3.) has a molecular formula $C_7H_{12}O_3$, indicating degree of unsaturation of 2, according to the sodiated cluster peak at *m/z* 167.0660 $[M+Na]^+$ in the High Resolution (HR)-ESI-MS spectrum. The ^{1}H NMR spectrum showed the presence of doublets at δ 5.38 (J = 4.5 Hz) and a broad singlet at δ 5.08 in 1:2 ratio. These signals were assigned to hemiacetalic functional groups based on their correlations in the heteronuclear single-quantum coherence (HSQC) experiment to the carbons at δ 100.1 and 104.7, respectively. The NMR spectroscopic data of (2*R*/2*S*,3*S*,4*S*)-3-*epi*-botryodiplodin resembled those of (3*R*,4*S*)-botryodiplodin[7] except the H-2, H-4, and H_3-6 signals. These data could indicate that (2*R*/2*S*,3*S*,4*S*)-3-*epi*-botryodiplodin is a diastereomer of (2*R*/2*S*,3*R*,4*S*)-botryodiplodin. Furthermore, the ^{1}H NMR spectrum showed double doublets at δ 4.19 (H_2-5), a doublet of double doublets at δ 2.93 (H-4), and a multiplet at δ 2.47 (H-3), which were assigned to the main diastereoisomer **16**A, also on the basis of correlation spectroscopy (COSY). The couplings in the HSQC spectrum allowed assigning the chemical shifts to the corresponding carbons at δ 68.5 (C-5), δ 57.8 (C-4), and δ 43.8 (C-3). Finally, the methyl groups at δ 2.31 and 1.15 were correlated to the carbons at δ 29.9 and 17.9. The heteronuclear multiple bond correlation (HMBC) experiment furnished useful data to solve the structure. The main correlations observed were between H-2 and C-5, H-3 and C-7, and H-8 and C-4. These data were in accordance with the structure of **16**A. Its relative stereochemistry was defined by a nuclear Overhauser effect spectroscopy (NOESY) experiment. This spectrum showed nuclear Overhauser effects (NOEs) of H-2 with protons H_3-6, indicating a trans relation between methyl and hydroxy groups. For isomer **16**B, the same NMR spectra allowed assigning chemical shifts to all carbons and protons. In particular, in addition to the H-2 signals, the main differences between **16**A and **16**B in ^{1}H NMR spectrum were due to methylene protons at C-5 resonating as triplets at δ 4.30 and 3.51. On the other hand, the analysis of NOESY

spectrum evidenced for **16**B NOE between H-2 (δ 5.38) and H-3 (δ 2.39), indicating a cis relation between methyl and hydroxy groups. NMR and optical rotation data of 5 agreed with (2*R*/2*S*,3*S*,4*S*)-3-*epi*-botryodiplodin (**16**) as reported for the synthetic compound[14].

The structure and stereostructure of **16** were confirmed by preparing its 2-acetyl derivatives. In contrast to (2*R*/2*S*,3*S*,4*S*)-botryodiplodin (**15**, Figure 3.3.) compound (2*R*/2*S*,3*S*,4*S*)-3-*epi*-botryodiplodin yielded 2-*O*-acetyl derivative epimers at C-2. (2*S*,3*S*,4*S*)- and (2*R*,3*S*,4*S*)-3-*epi*-botryodiplodin acetate (**24**A/B, Figure 3.3.) were isolated and their structures and stereostructures determined by ^{1}H and ^{13}C NMR and COSY. In particular, ^{1}H and ^{13}C NMR data of (2*R*,3*S*,4*S*)-3-*epi*-botryodiplodin acetate (**24**A) were in agreement with those previously reported for the same compound[15], but the data of the compound **16** are here reported for the first time. The main difference between proton spectra of compounds 15 and 16 is at the H-2 proton signal resonating as a broad singlet at δ 5.91 for 15 and as doublets (J = 4.5 Hz) at δ 6.27 for 16. The ESI-MS(+) spectrum of (2*S*,3*S*,4*S*)-3-*epi*-botryodiplodin acetate (**24**B) showed the sodiated cluster $[M+Na]^+$ at *m/z* 209, whereas the ESI-MS(+) spectrum of (2*R*,3*S*,4*S*)-3-*epi*-botryodiplodin acetate (**24**A) showed the potassium $[M+K]^+$ and sodiated $[M+Na]^+$ clusters at *m/z* 225 and 209, respectively. Also, (-)-botryodiplodin structure was confirmed by preparation of its acetate derivate and by comparison of **23** data with those previously reported[16].

3.2.4. Structure Determination of (3S,4R,5R)-4-hydroxymethyl-3,5-dimethyldihydro-2-furanone

4-Hydroxymethyl-3,5-dimethyldihydro-2-furanone (**5**, Figure 3.3.) was acetylated, and its spectroscopic data were compared with those of its parent compound[4]. In particular, ^{1}H NMR spectrum of 13 showed, as the only differences from that of the parent compound, the presence of a singlet at δ 2.11, attributed to the acetyl group, and the characteristic downfield shift of hydroxymethylene

protons H_2-8, which resonated as double doublets at δ 4.26 (*J* = 4.4 and 11.5 Hz) and 4.18 (*J* = 5.9 and 11.5 Hz). The ESI-MS spectrum of 13 recorded in the positive mode gave $[M+Na]^+$, $[M+H]^+$, and $[M-CH_3COO]^+$ at *m/z* 209, 187, and 127, respectively.

3.2.5. GC-MS Analysis

Within the frame of the overall strategy, a very important outcome of the separation procedures arises from the fact that all crude extract and separated fractions were analyzed by GC-MS. Therefore, the EI mass spectrum at 70 eV of all isolated metabolites was acquired and compiled in a custom target mass spectral library to be employed to check that they are actually present as such in crude extracts and are not artefacts created by chemical events taking place during the many steps of separation procedures.

However, most secondary metabolites in Figure 3.3 are functionalized compounds which, in general, are very prone to decomposition during high temperature flash vaporization in the GC injector. In order to reduce to a minimum the risk of decomposition, metabolites were converted, before GC-MS measurements, to their trimethylsilyl derivatives using *N*,*O*-bis(trimethylsilyl)trifluoroacetamide (BSTFA), which is a trimethylsilyl (TMS) donor which substitutes hydrogen atoms in -OH, -NH, -SH groups with trimethylsilyl groups (TMS). For most of the separated fractions, the total ion chromatogram (TIC) presented a single well-developed peak, which implies that, as expected from an efficient separation procedure, the chromatographed sample mainly consisted of a single metabolite. However, in many cases, several peaks were observed, which not necessarily implies that several metabolites are present in the analyzed fraction. GC-MS measurements served several purposes within our strategy. First, when the mass spectrum of the metabolite could be retrieved from a MS database, the acquired mass spectrum provided a definitive proof of its identity (e.g. as in the case of jasmonic acid). Furthermore, GC-MS was also useful for the

quantification of ICA as methyl derivative in the extract of LA-SOL3 and LA-SV1 strains grown in presence and absence of 10 mM of GABA. For quantification of ICA, the derivatization with diazomethane was preferred because the methylation of this compound gives only one derivative.

When no mass spectrum satisfactorily matching the acquired mass spectrum could be retrieved from a database, the unknown metabolite had to be otherwise identified (this was accomplished mainly via ESI-TOF LC-MS and $^{1}H/^{13}C$ NMR mono and bi-dimensional) but interpretation of the acquired mass spectrum served as a guide in the identification process by setting restrictions on possible structures.

In all cases, the acquired mass spectrum was incorporated in the custom MS library to be used for interpreting GC-MS measurements to be performed directly on samples of the crude extracts.

The full set of mass spectra of trimethylsilyl derivatives of metabolites produced by *L. theobromae* strains under examination, which constitute the custom MS target library, are exposed in Chapter 6, Experimental Section, where retention data of the identified metabolites are also reported in the form of Kovats retention indexes (RI).

As an example, Figures 3.4A and B show the total ion chromatograms (TICs) of the crude extracts of LA-SOL3 grown in Czapek medium at 25 and 37°C, respectively.

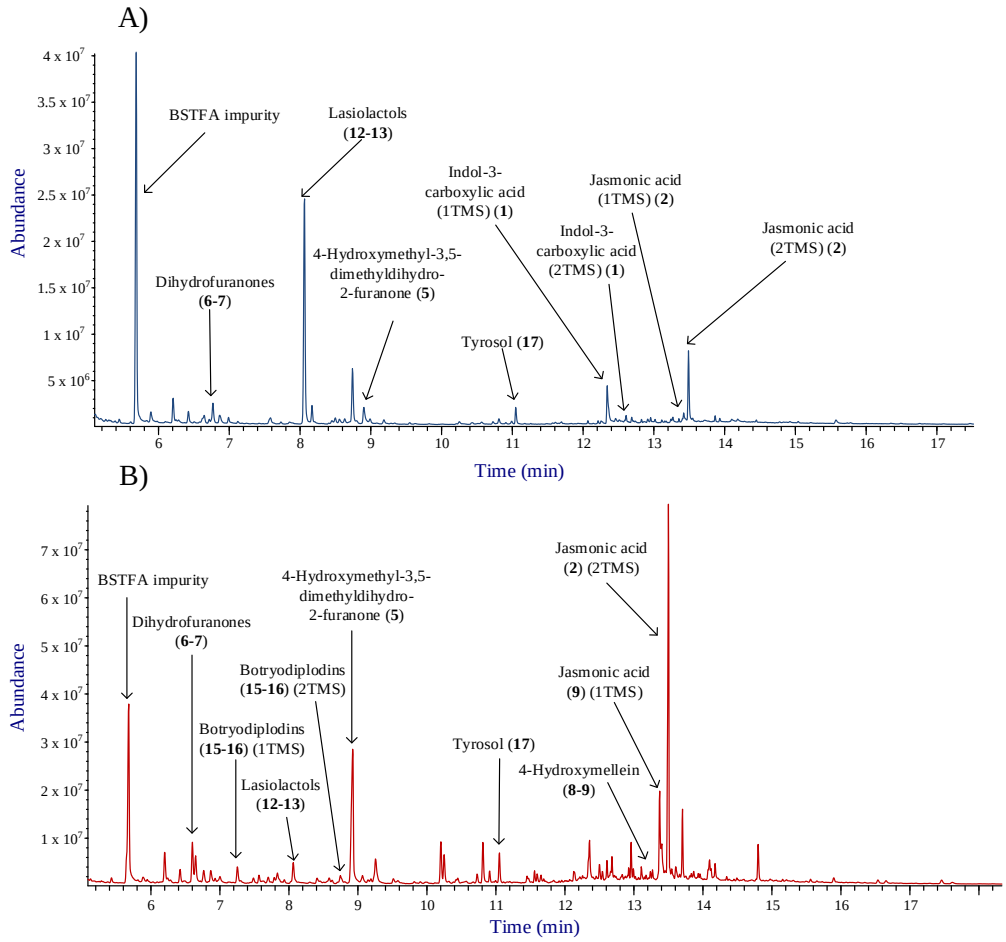

Figure 3.4. Annotated total ion chromatograms (TICs) acquired by processing samples from two cultures of the strain LA-SOL3 grown in Czapek medium at 25°C (A) and 37°C (B)

3.2.6. Distribution of Secondary Metabolites

Metabolites identified as product of *L. theobromae* CAA019, CBS339.90, LA-SOL3 and LA-SV1 in Czapek medium at 25 and 37°C are presented in Table 3.1. Metabolites identified as product of *L. theobromae* LA-SOL3 and LA-SV1 in Potato Dextrose Agar (PDB) at 25°C in presence and absence of GABA are presented in Table 3.2.

Table 3.1. Distribution of secondary metabolites produced by strains of *Lasiodoplodia theobromae*, according to strain and temperature.

Name		CAA019		CBS339.90		LA-SOL3		LA-SV1	
		25 °C	37°C	25°C	37°C	25°C	37°C	25°C	37°C
3-Indolecarboxylic acid (ICA)	**1**	+	+	+	+	+	+	+	+
(-) Jasmonic acid (JA)	**2**	+		+		+		+	
Lasiodiplodin	**3**	+	+						
Botryosphaerilactone A	**4**		+		+				
(3*S*,4*R*,5*R*)-4-Hydroxymethyl-3,5-dimethyldihydro-2-furanone	**5**		+		+	+	+	+	+
(3*S*,4*S*)-4-Acetyl-3-methyl-2-dihydrofuranone	**6**		+		+		+		
(3*R*,4*S*)-4-Acetyl-3-methyl-2-dihydrofuranone	**7**		+		+	+	+	+	+
cis-(3*R*,4*R*)-4-Hydroxymellein	**8**			+	+		+	+	
trans-(3*R*,4*S*)-4-Hydroxymellein	**9**			+	+				
Scytalone	**10**			+					
Cyclo-(Trp-Ala)	**11**		+		+				
Lasiolactols A and B	**12-13**					+	+	+	+
(-)-Mellein	**14**							+	+
Botryodiplodin	**15**						+		+
3-*epi*-Botryodiplodin	**16**						+		+
Tyrosol	**17**					+	+	+	+

Table 3.2. Distribution of secondary metabolites produced by strains of *Lasiodoplodia theobromae* isolated from grapevine, according to strain and presence of GABA.

Name		**LA-SOL3**		**LA-SV1**	
		/	**GABA**	**/**	**GABA**
3-Indolecarboxylic acid (ICA)	**1**	71mg/$g_{extract}$	59mg/$g_{extract}$	68mg/$g_{extract}$	62mg/$g_{extract}$
(-) Jasmonic acid	**2**	+	+		+
(*R*)-Mellein	**14**	+	+	+	+
(3*R*,4*S*)-Botryodiplodin	**15**	+	+		+
Tyrosol	**17**		+	+	
3-Indolecarboxaldehyde	**18**	+	+		
cis-(3*R*,4*R*)-4-Hydroxymellein	**8**		+		+
Indole	**19**		+	+	+
Cyclo-(Leu-Pro)	**20**	+	+	+	+
Cyclo-(Pro-Phe)	**21**	+	+	+	+

The metabolic profiles of each strain of *L. theobromae* were distinct, and strains behaved differently when growth temperature was increased. In fact, only one metabolite (ICA) was produced by all the strains under examination at both growth temperatures. Lasiodiplodin was produced only by strain CAA019, *trans*-(3*R*,4*S*)-4-hydroxymellein and scytalone were produced only by strain CBS339.90, (*R*)-mellein was produced only by strain LA-SV1. Furthermore, some metabolites are characteristic of *L. theobromae* strains isolated from grapevine. The findings obtained comparing fungal metabolome obtained when *L. theobromae* was grown

in presence and absence of GABA, show the decrease of ICA production when both strains were exposed to the phytohormone. This is justified because ICA is a phytotoxic compound which is involved in the fungal infections. Hence, GABA is produced by the plants as defence agent and reduces the pathogen activity.

3.2.7. Phytotoxicity and Cytotoxicity of Pure Metabolites

Scytalone, jasmonic acid and *cis*-(3*R*,4*R*)- and *trans*-(3*R*,4*S*)-hydroxymellein are known to contribute to fungal pathogenicity to plants. Phytotoxicity of the pure metabolites was evaluated by a leaf puncture assay on tomato leaves, and the results are presented in Table 3.3.

Table 3.3. Phytotoxicity of pure compounds and derivatives in leaf puncture assay on tomato leaves. Results are reported as lesion size in mm after 10 d.

Code	Compound	Lesion size (mm)
24	Botryodiplodin acetate	8.7 ± 1.5
16	3-*epi*-Botryodiplodin	7.3 ± 1.5
7	(3*R*,4*S*)-4-Acetyl-3-methyl-2-dihydrofuranone	5 ± 1.0
2	(-) Jasmonic acid	4.7 ± 1.5
3	Lasiodiplodin	3.3 ± 1.0
1	3-Indolecarboxylic acid	2.3 ± 1.0
5	(3*S*,4*R*,5*R*)-4-Hydroxymethyl-3,5-dimethyldihydro-2-furanone	0
4	Botryosphaerialactone A	0
12-13	Lasiolactols A and B	0
22	(3*S*,4*R*,5*R*)-4-Hydroxymethyl-3,5-dimethyldihydro-2-furanone acetate	0
15	Botryodiplodin	0
6	(3*S*,4*S*)-4-Acetyl-3-methyl-2-dihydrofuranone	0
	Control (4% methanol)	0

Data show that lasiodiplodin, jasmonic acid, (2*R*/2*S*,3*S*,4*S*)-3-*epi*-botryodiplodin and (3*R*,4*S*)-4-acetyl-3-methyl-dihy-dro-furan-2-one are phytotoxic to tomato leaves. Pure metabolites (Figure 3.5.) were also cytotoxic for both cell lines.

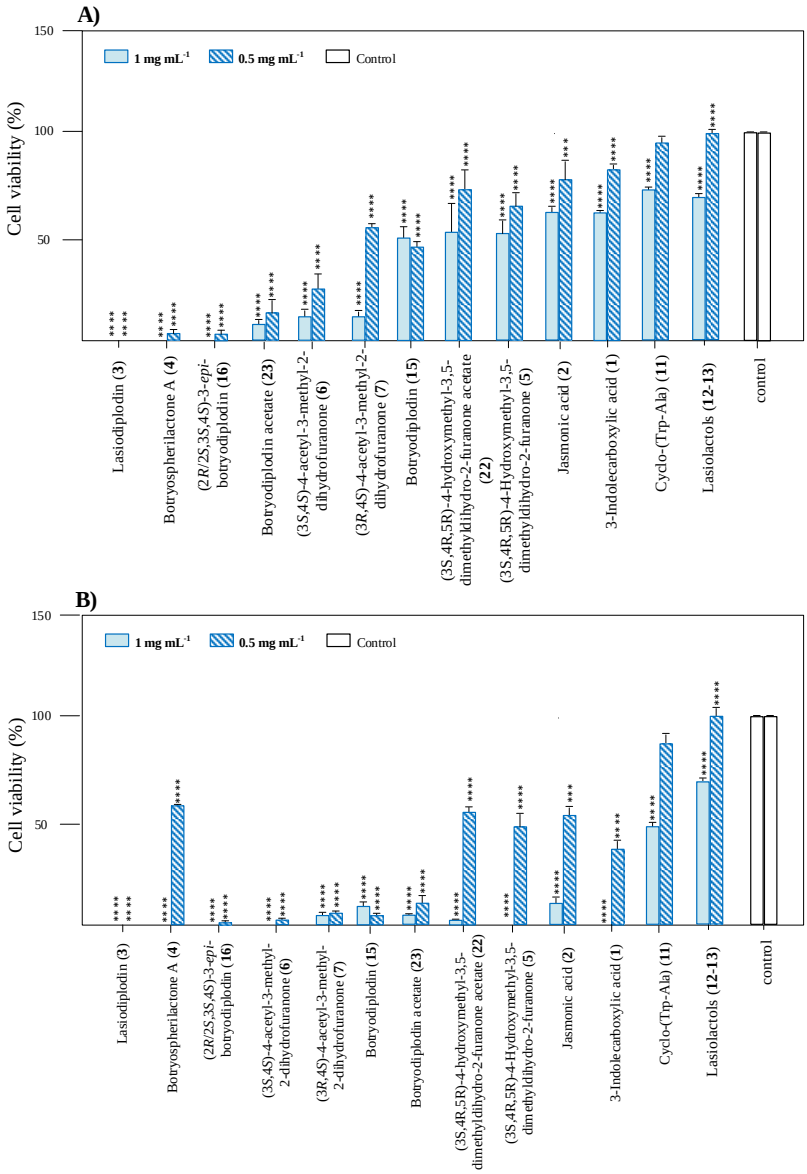

Figure 3.5. Evaluation of cytotoxicity in Vero (A) and 3T3 (B) cells of pure metabolites and derivatives from strains CAA019, CBS339.90, LA-SOL3, LASV1. Open and striped bars correspond to metabolite concentrations of 1 and 0.5 mg mL^{-1}, respectively. Data are presented as average ± standard error. Two-way ANOVA, followed by a Bonferroni multiple comparison test, was used to determine the statistical significance of cytotoxicity between pure metabolites and control (A, B). *P < 0.05; **P < 0.01; ***P < 0.001; ****P < 0.0001.

The cytotoxicity assays on mammalian cell lines, Vero and 3T3 cells (Figure 3.5.), show that 3-*epi*-botryodiplodin and botryodiplodin acetate, lasiodiplodin, botryosphaerialactone A are the most cytotoxic compounds to Vero cells. Concerning the 3T3 cell line, all pure compounds induced more than 80% cell mortality, with the exception of lasiolactols A and B, which induced low toxicity to cells (cell mortality below 50%). Until now, none of these metabolites was known to induce damages to nontumoral mammalian cells.

3.2.8. Discussion

Lasiodiplodia theobromae (pat.) Griffon & Maubl. is a phytopathogenic fungus from the family botryospheraceae typically found in tropical and subtropical regions. It has been associated with many hosts, causing diverse diseases and being responsible for serious damages on crops. It has also been reported as a human opportunistic pathogen causing keratomycosis and phaeohyphomycosis[17]. The host adaptability of *L. theobromae* is a result of the capacity to produce different metabolites at different environmental conditions, particularly those involved in host-pathogen interactions. In this regard, until now there were no studies on the production of secondary metabolites by *Lasiodiplodia* strains causing human infections. It is known that *L. theobromae* biosynthesizes a variety of lipophilic and hydrophilic metabolites with different biological activities. Moreover, the production of metabolites may be affected by abiotic factors, such as temperature.

In fact, Paolinelli Alfonso et al. (2016)[18] showed that heat stress facilitates *L. theobromae* colonization, since this fungus can degrade phenylpropanoid precursors and salicylic acid, compounds known to control host defense. Controlling fermentation conditions by altering process parameters (e.g. media composition, pH, temperature, agitation) and studying their effects on metabolite profile might give an opportunity to effectively combat infections by *L. theobromae*. The characterization of the secondary metabolite production of plant-isolated *L. theobromae* strains is scarce, and none describe the effect of abiotic factors.

Boosted by the preliminary investigation on the toxicity of culture filtrates, studies were conducted on the production of secondary bioactive lipophilic metabolites that could be involved in the toxic activity of culture filtrates. Sixteen metabolites were isolated from four strains (i.e. CAA019, CBS339.90, LA-SOL3, LA-SV1) of *L. theobromae* grown in Czapek medium at 25 and 37°C (Table 3.1.). Ten metabolites were produced by *L. theobromae* strains, isolated from grapevine (i.e. LA-SOL3 and LA-SV1), grown in Potato Dextrose Broth (PDB) at 25°C in presence and absence of γ-amminobutyric acid (GABA) (Table 3.2.). In addition to several known secondary metabolites, such as jasmonic acid and ICA, this is the first time that the phytotoxin scytalone was identified in a *Lasiodiplodia* species. Furthermore, 3-*epi*-botryodiplodin was identified for the first time as natural product. Biological activities of metabolites produced by *L. theobromae* strains are discussed below for some representative compounds.

Scytalone (**10**, Figure 3.3.) is produced by several fungi and is thought to be a precursor in the synthesis of dihydronaphtalene (DHN)-melanin, which is involved in the melanin pathway[19]. Due to the potential toxicity of the oxidative products of melanin precursors, certain melanotic fungi seem to secrete those products to induce injuries in their hosts. Indeed, several phytotoxins derived from DHN-melanin have

been described[20]. Furthermore, absolute configuration of **10** has also been determined[21].

In 1993, Husain and co-workers described (-)-jasmonic acid (**2**, Figure 3.3.) as a phytotoxin, capable of inducing dieback symptoms caused by *Botryodiplodia theobromae* (= *L. theobromae*) in infected rose plants[22]. Recent studies also demonstrated that the production of JA by pathogenic fungi, such as *L. theobromae*, leads to the inhibition of the defense pathway of the plant host, facilitating the infection process[23,24]. Our results agree with these observations: **2** was extremely phytotoxic for tomato plants. Moreover, about the temperature role in the JA production, a maximum was reported at about 33°C, and this is in line with our data[25]. We also showed that **2** is cytotoxic for mammalian 3T3 cells, which may have implications in the ability of *L. theobromae* to infect animal hosts.

The metabolites *cis*-(3*R*,4*R*)- and *trans*-(3*R*,4*S*)-4-hydroxymellein (**8** and **9**, Figure 3.3.), 3,4-dihydroisocoumarins from the family of pentaketides, are toxins known to be typically found in Botryosphaeriaceae culture filtrates contributing, in synergy with other extracellular metabolites, to several diseases in grapevines[26] and other plants (e.g. tomato plants)[26,27]. In fact, Andolfi et al. (2011)[19] proposed mellein as a diagnostic marker of diseased plants.

(3*R*,4*S*)-Botryodiplodin (**15**, Figure 3.3.), 3-*epi*-botryodiplodin (**16**, Figure 3.3.), (3*S*,4*S*)-4-acetyl-3-methyl-2-dihydrofuranone (**5**, Figure 3.3.) and (3*R*,4*S*)-4-acetyl-3-methyl-2-dihydrofuranone (**6**, Figure 3.3.) are structurally related and, for the first time, were isolated from the same natural source. (3*R*,4*S*)-Botryodiplodin is a natural mycotoxin with a variety of biological activities[28]. It is a 2:3 mixture of (2*R*) and (2*S*) diastereomers, and its absolute configuration at C-3 and C-4 was established as (3*R*,4*S*)[29]. Acetylation of compound **15** yielded a unique derivative: the (2*R*,3*R*,4*S*)-2-*O*-acetylbotryodiplodin[16]. Recently, botryodiplodin was isolated as a secondary metabolite produced by *Lasiodiplodia mediterranea* associated with grapevine declining in Sardinia, Italy[4]. Until now, none of the botryodiplodin

stereoisomers had been isolated from natural sources. In particular, it was speculated that 4-*epi*-botryodiplodin could only be produced after treatment of botryodiplodin with ethyl acetate and $NaHCO_3$[30]. On the other hand, the botryodiplodin isomer produced by strains LASOL3 and LA-SV1 is the C-3 epimer. In the present study, the acetylation of compound **16**, which yielded two 2-*O*-acetyl derivative epimers at C-2, is also reported. As previously documented[4], 3*R*,4*S* (3*R*,4*S*)-botryodiplodin turns out not to be a phytotoxic compound, but its epimerization on C-3 and its acetylation yielded phytotoxic derivatives. Interestingly, (3*R*,4*S*)-botryodiplodin and its acetate derivative have the same cytotoxicity to 3T3 cells. Conversely, (3*R*,4*S*)-botryodiplodin is more toxic than botryodiplodin acetate to Vero cells. However, for Vero cells, 3-*epi*-botrydiplodin was the most cytotoxic metabolite, inducing 100% cell mortality. The production of botryodiplodins at 37°C could be considered an important feature of fungal adaptation during host infection at higher temperatures. Pure dihydrofuranolactones were also tested for toxicity. The C-3 stereochemistry has a larger influence on phytotoxicity than on cytotoxicity; in particular, the (3*R*,4*S*) isomer showed major toxicity in the leaf puncture test. Lasiolactols, two dimeric γ-lactols, were isolated for the first time from *L. mediterranea* associated with grapevine decline in Sicily[5]. Regarding the toxicity of these compounds, no effect was visible in tomato leaves, but lasiolactols induced 20–50% cell mortality (Vero and 3T3 cells, respectively).

4-Hydroxymethyl-3,5-dimethyldihydro-2-furanone acetate (**22**, Figure 3.3.) is not toxic for tomato leaves but is cytotoxic for mammalian cells. As its parent compound, **22** is more cytotoxic to 3T3 cells than to Vero cells[4,5].

Tyrosol (**17**, Figure 3.3.) is a well-known compound produced by plants and microorganisms, and it is frequently isolated from Botryosphaeriaceae fungi[31]. In this study, **17** was produced by both strains grown at both temperatures. It is also known to contribute to biofilm formation by *Candida albicans*, which could be relevant for the infection process of *L. theobromae*[32].

We produced evidence that abiotic factors influence phytotoxicity and cytotoxicity of *L. theobromae* strains, apparently due to the different production of secondary metabolites which synergic effect contribute to their activities. The metabolite profile of both strains was revealed to be significantly affected by abiotic factors, leading to relevant implication for plant pathogenicity.

3.3. Secondary Metabolites Produced by a Strain of *Macrophomina phaseolina* Isolated from *Eucalyptus globulus*

The aim of this study was to investigate for the first time the *in vitro* secondary metabolite production of the strain PE35 of *M. phaseolina* isolated from *Eucalyptus globulus*.

3.3.1. Phytotoxicity and Cytotoxicity of Culture filtrates and Crude Extracts

Phytotoxicity of culture filtrate (Figure 3.6.). and crude extract (Figure 3.7.) of *M. phaseolina* PE35 was assessed on tomato plant cuttings and on tomato leaves, respectively, as reported in Chapter 6, Experimental Section.

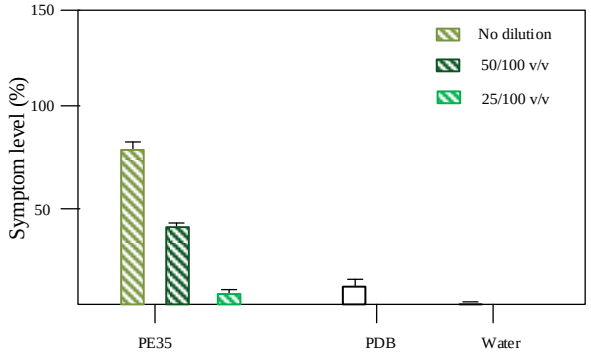

Figure 3.6. Phytotoxicity assay on tomato stems of culture filtrates (no diluted, 50/100 and 25/100 *v/v*) of *M. phaseolina* PE35 grown in PDB at 25°C. Symptoms were recorded and converted to a percentage to evaluate the phytotoxic activity using a 0-4 scale (0 = no symptoms; 1 = slight withering; 2 = intermediate withering; 3 = severe withering; 4 = full withering). Data are shown as the average of three independent replicates for each condition.

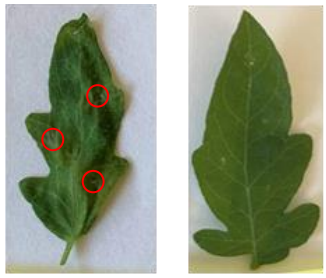

Figure 3.7. Phytotoxicity of crude extract of filtrate of *M. phaseolina* PE35. Lesion size at concentration of 1mg mL^{-1} is 0.48cm.

Both culture filtrate and crude extract of *M. phaseolina* PE35 were able to induce symptoms on tomato plants and the severity of symptoms steadily decreased with dilution.

When the culture filtrate was used, it was possible to observe a significant cytotoxicity on 3T3 cell lines at the highest concentration tested. The crude extract showed the higher cytotoxicity at 0.1 mg mL^{-1} (Figure 3.8.).

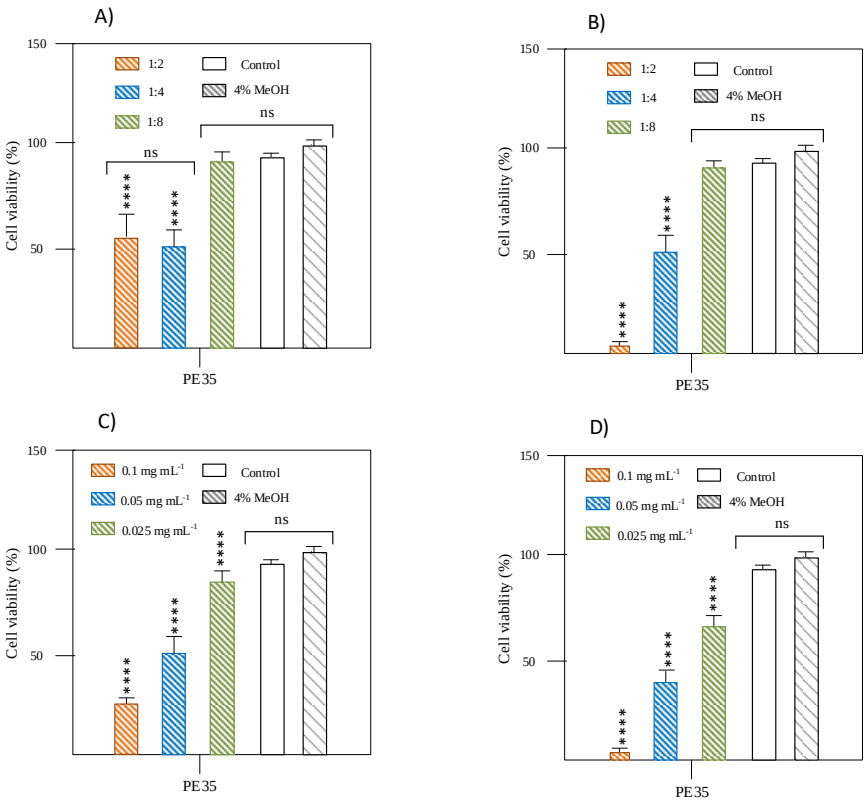

Figure 3.8. Cytotoxicity results of culture filtrate (A, B) and crude extract (C, D) in Vero Cells (A, C) and 3T3 cells (B, D). Statistical analysis performed using ANOVA followed by a Tukey multiple comparison test. Equal letters and asterisk correspond to data with statistical difference ($p < 0.05$), and (ns) match non-significant differences ($p > 0.01$).

3.3.2. Metabolites Isolation and Identification

The culture filtrate of *M. phaseolina* PE35 was extracted with ethyl acetate (EtOAc) as described in Chapter 6, Experimental Section. GC-MS measurements were conducted on extracts after trimethylsilylation. All metabolites were identified comparing their EI mass spectra at 70 eV with the ones present in the NIST 14 mass spectral library[33] and the custom GC-MS library built in the study of *Lasiodiplodia theobromae* strains reported in the previous paragraph. The definitive proof of the

identity of metabolites reported in Figure 3.9 and the stereostructure elucidation of some compounds [i.e. (3*R*,4*S*)-botryodiplodin, cis-(3*R*,4*R*)-4-hydroxymellein and (-)-mellein] were obtained after fractionation by column chromatography of the crude extracts and the comparison of the ^{1}H NMR spectra and optical rotation of pure compounds with those reported in the previous paragraph.

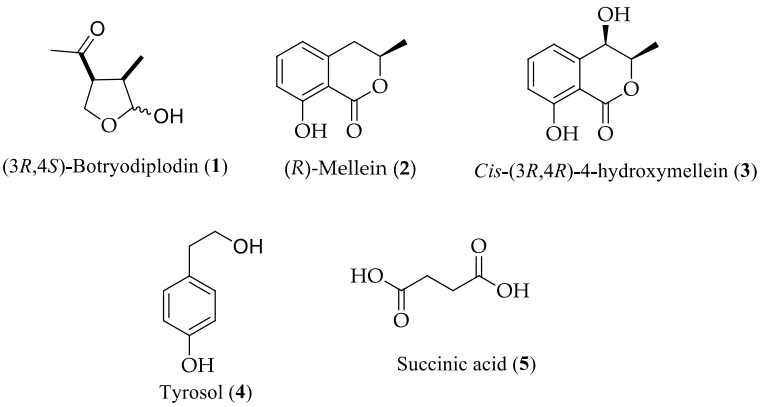

Figure 3.9. Secondary metabolites (**1**-**5**) produced by *Macrophomina phaseolina* PE35.

Total ion chromatograms (TIC) of crude extracts, treated with *N*,*O*-bis(trimethylsilyl)trifluoroacetamide (BSTFA), of *M. phaseolina* PE35 was showed in Figure 3.10.

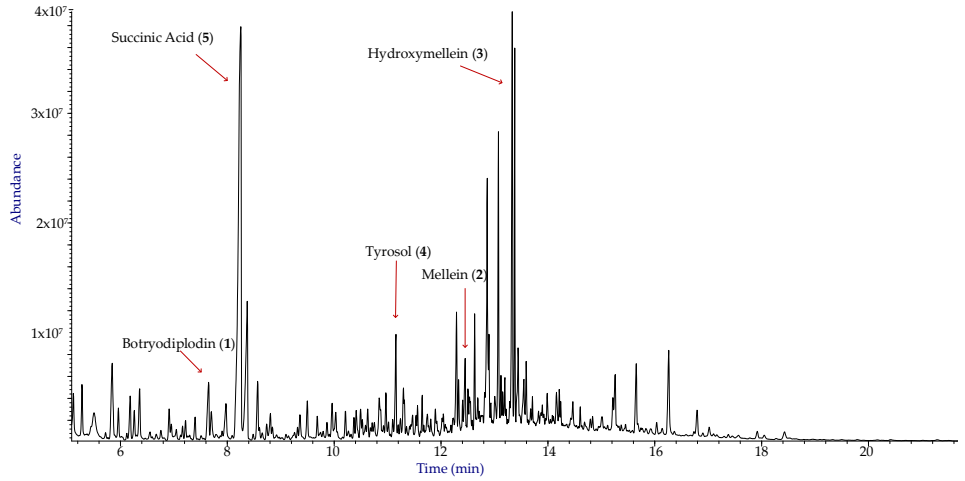

Figure 3.10. Annotated total ion chromatograms (TICs) acquired by processing samples from crude extracts. a. *M. phaseolina* PE35.

3.3.3. Discussion

Macrophomina phaseolina (Tassi) Goid. is responsible of serious damages of eucalypt plantations[34] and other economically important crops, such as soybean, sunflower, sesame, melon and strawberry[35-39]. In fact, it attacks a wide range of hosts belonging to more than 500 cultivated and wild plant species[40]. Furthermore, *M. phaseolina* is a smart pathogen also capable to infect animals and human and an example of emerging fungal infections[41]. The diseases caused by this fungus are well-documented, but few reports are present in literature on secondary metabolites produced by *M. phaseolina*, although they might play a role in the charcoal rot and other plant diseases. In fact, *M. phaseolina* is reported so far only as producer of few metabolites, such as asperlin, isoasperlin, phomalactone, phaseolinic acid, phomenone and phaseolinone[42,43].

In this study, for the first time, findings from the investigation of secondary metabolites by a *M. phaseolina* strain isolated from *Eucalyptus globulus* were reported. The culture filtrate and the crude extract were evaluated for toxicity on tomato and mammalian cells, showing toxicity (Figure 3.8.).

Five metabolites, belonging to diverse classes of natural compounds were identified in the crude extract of *M. phaseolina*.

Among the identified metabolites, **1**-**4** are typical metabolites produced by fungi from the family botryosphaeriaceae[4,26,31], but only botryodiplodin (**1**, Figure 3.9.) was already known as product of *M. phaseolina*. In 2007, Ramezani et al. identified **1** in the culture of *M. phaseolina*, isolated from soybean, but phaseolinone, the most common metabolite produced by this fungal species[42], was not observed. Subsequently, **1** was detected in many cultures of *M. phaseolina* isolated from several plants (e.g. melon, strawberry, soybean), and also as *vivotoxin* in studies on plant tissues naturally infected with charcoal rot disease[44]. Interestingly, also the strain under examination produces **1**, but not phaseolinone. Although it has been proposed that **1** may be involved in fungal infection of plants, its role remains to be clarified. Certainly, the (3*R*,4*S*)-botryodiplodin stereostructure significantly influences the biological activities. In fact, (3*R*,4*S*)-botryodiplodin is not reported as a phytotoxic compound[4], but its epimer turns out to be phytotoxic and also the cytotoxicity on mammalian cells was higher for 3-*epi*-botryodiplodin than (3*R*,4*S*)-botryodiplodin (see previous paragraph, Figure 3.5.).

The toxic metabolite **1** present in culture crude extracts of *M. phaseolina* is responsible of high toxicity against mammalian cells (i.e. Vero and 3T3 cell lines), consistent with the opportunistic nature of this fungal species towards the human host. In fact, it was tested for cytotoxicity on Vero and 3T3 cell lines in the previous paragraph, Figure 3.5. In general, 3T3 cells seems to be more sensitive then Vero cells when exposed to culture filtrate and crude extract of *M. phaseolina* PE35.

3.4. Fatty acids produced by a strain of *Neofusicoccum vitifusiforme* isolated from grapevine

In the present study, the composition of fatty acids produced in liquid medium by a grapevine strain of *N. vitifusiforme* (B8)[45] was evaluated and the pathogenicity *in planta* was assayed and discussed.

3.4.1. Pathogenic Activity

N. vitifusiforme B8 strain showed pathogenic activity on the inoculated grapevines. Six months after inoculation, vascular discolorations were found upward and downward starting from the point of inoculation and were observed in all inoculated plants (Figure 3.11.). Mean discoloration length produced by B8 strain was 12.0 ± 3.0 cm (mean ± S.E). The inoculated fungi were always re-isolated from the inoculated canes, but never from the control.

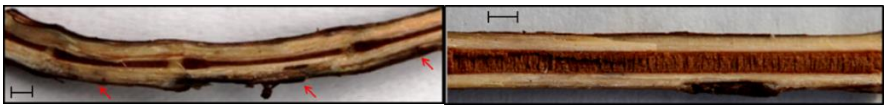

Figure 3.11. Brown necrosis (indicated by the red arrow) caused by *N. vitifusiforme* extending along a large part of the trunk of 2-year-old grapevine plants of cv. Inzolia in longitudinal section (left) and absence of xylematic symptom in the control (right). Scale bars = 1 cm.

3.4.2. Identification and Quantification of Fatty Acids

The preliminary spectroscopic investigation conducted for the crude extract of *N. vitifusiforme* showed typical signals of saturated and unsaturated fatty acids[46].

Samples were analyzed via GC-MS after esterification with diazomethane in ether (see subparagraphs 6.4.2 and 6.4.3.). In Figure 3.12. is reported the total ion chromatogram obtained from *N. vitifusiforme*. Particularly important is the composition of the crude extract of *N. vitifusiforme* which presents azelaic acid.

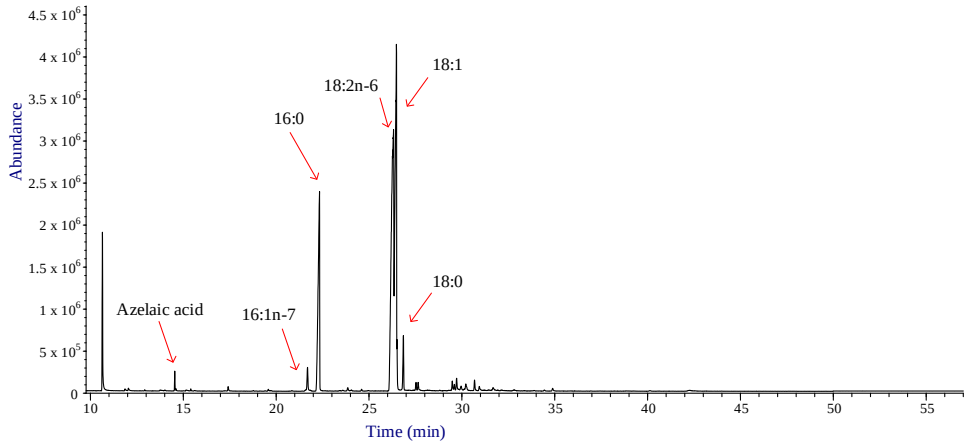

Figure 3.12. TIC of methylated compounds from *N. vitifusiforme* B8 acquired with the following method: the injector temperature was 250°C and, during the run, a temperature ramp raised the column temperature from 50°C to 240°C: 50°C for 2 min; 10°C min^{-1} until reaching 180°C, 180 °C for 5 min, and 5°C min^{-1} until reaching 240°C; 240°C for 25 min.

Fatty acids, and, eventually, related compounds, in the extract of the strain B8 of *N. vitifusiforme* have been quantified and results are summarized in Table 3.4. as percentage.

Table 3.4. Quantitative results of compounds in the extract of the strain B8 of *N. vitifusiforme*

Code	Name	KI[1]	Abundance (%)
-	Azelaic acid	1548	0.5
16:1n-7	Palmitoleic acid	1903	1.5
16:0	Palmitic acid	1926	10.4
18:2n-6	Linoleic acid	2092	48.2
18:1	Elaidic acid	2109	38.0
18:0	Stearic acid	2125	1.4

[1]KI are referred to methyl esters of compounds reported.

3.4.3. Discussion

Several fungal pathogens from the family Botryosphaeriaceae are involved in the Grapevine Trunk Diseases (GTDs). In fact, these fungi have become an impending threat to the productivity and longevity in most wine-growing areas

cause the so-called Botryosphaeria dieback. Annual losses for Botryosphaeria dieback can vary depending on wine-growing area. For instance, in the Bordeaux area (France), annual losses are estimated to be 4-20%[47] and in some regions in China are over 30-50%[48]. Several pathogens involved in GTDs produce secondary metabolites *in vitro* and *in vivo* whose mode of action is sometimes reported[4,5,19,27,31,49,50]. Many secondary metabolites were isolated from diverse species of *Neofusicoccum* associated to grapevine dieback. Among these metabolites, several natural compounds belong to cyclohexenones, melleins, naphtalenones, and phenols[19,31,49,51,52], and some of them are reported as vivotoxins[27]. Despite several studies on species of *Neofusicoccum* associated to grapevine dieback, the production in liquid medium of fatty acids had not been reported. In fact, fatty acids and modified fatty acids are important compounds during colonization of plants by pathogenic fungi and may be involved in their virulence[53]. In this work, five different fatty acids and one dicarboxylic acid were detected in the crude extract of the culture filtrate of *N. vitifusiforme*. From Table 3.4., it can be seen that linoleic acid (48.2%) and elaidic acid (38%), are the most abundant components in the crude extract of strain B8 of *N. vitifusiforme*, while palmitic acid (10.4%), palmitoleic acid (10.5%) and stearic acid (1.4%) are present in much less amounts. Octadecanoid acids have influence in the fungal virulence because many of them are precursors of jasmonic acid[54], a plant hormone capable of inducing phytotoxic effects[4,5,22-24]. Furthermore, Farmer and Ryan (1992)[55] tested the capacity of octadecanoid precursors of jasmonic acid, such as linolenic acid and linoleic acid (which can be converted to linolenic acid by the plant) to be inducers of proteinase inhibitors in tomato, tobacco, and alfalfa leaves. The results suggest that the octadecanoid intermediates may participate in the signalling pathway in response to the pathogen attack and in the plant colonization.

Even if in low concentration, *N. vitifusiforme* produce also azelaic acid, a dicarboxylic acid well-known for its bacteriostatic and bactericidal proprieties against diverse microorganisms[56].

The investigations carried out during the last ten years induce to hypothesize that, as well as cultivar kind and environmental conditions, also the type of secondary metabolite, produced by different botryosphaeriaceous fungi can be correlated with the foliar chlorosis expression in declining grapevine.

3.5. References

1. Dissanayake, A.J., Phillips, A.J., Li, X.H., Hyde, K.D. (2016). Botryosphaeriaceae: Current status of genera and species. *Mycosphere*, *7*, 1001-1073.
2. Crous, P.W., Slippers, B., Wingfield, M.J., Rheeder, J., Marasas, W.F., Philips, A.J., Alves, A., Burgess, T., Barber, T., Groenewald, J. Z. (2006). Phylogenetic lineages in the Botryosphaeriaceae. Stud. Mycol. *55*, 235-253.
3. Slippers, B., Wingfield, M.J. (2007). Botryosphaeriaceae as endophytes and latent pathogens of woody plants: diversity, ecology and impact. Fungal Biol. Rev. *21*, 90–106.
4. Andolfi, A., Maddau, L., Cimmino, A., Linaldeddu, B.T., Basso, S., Deidda, A., Serra, S., Evidente, A. (2014). Lasiojasmonates A–C, three jasmonic acid esters produced by *Lasiodiplodia* sp., a grapevine pathogen. Phytochemistry *103*:145–153.
5. Andolfi, A., Basso, S., Giambra, S., Conigliano, G., Lo Piccolo, S., Alves, A., Burruano, S. (2016). Lasiolactols A and B produced by the grapevine fungal pathogen *Lasiodiplodia mediterranea*. Chem. Biodivers. *13*, 395–402.
6. Ravi, B.N., Armstrong, R.W., Faulkner, D.J. (1979). Some aromatic compounds from the marine sponge *Plakortis halichondrioides*. J. Org. Chem. *44*, 3109–3113.
7. Ramezani, M., Shier, W.T., Abbas, H.K., Tonos. J.L., Baird. R.E., Sciumbato, G.L. (2007). Soybean charcoal rot disease fungus *Macrophomina phaseolina* in Mississippi produces the phytotoxin (−)-botryodiplodin but no detectable phaseolinone. J. Nat. Prod. *70*, 128–129.
8. Forzato, C., Furlan, G., Nitti, P., Pitacco, G., Marchesan, D., Coriani, S., Valentin, E. (2005). A combined experimental and computational strategy in the

assignment of absolute configurations of 4-methyl-5-oxo-tetrahydrofuran-3-carboxylic acids and their esters. Tetrahedron: Asymmetry *16*, 3011–3023.

9. Aldridge, D.C., Galt, S., Giles, D., Turner, W.B. (1971). Metabolites of *Lasiodiplodia theobromae*. J. Chem. Soc. C, 1623–1627.
10. Carvajal, M., Espinoza, L., Caggia, S., Cardile, V., Garbarino, J.A., Peña-Cortés, H., Russo, A. (2011). New stereoisomeric derivatives of jasmonic acid generated by biotransformation with the fungus *Gibberella fujikuroi* affect the viability of human cancer cells. Electron. J. Biotechnol. *14*, 7.
11. Dimitriadis, C., Gill, M., Harte, M.F. (1997). The first stereospecific approach to both enantiomers of mellein. Tetrahedron: Asymmetry *8*, 2153–2158.
12. Cabras, A., Mannoni, M.A., Serra, S., Andolfi, A., Fiore, M., Evidente, A. (2006). Occurrence, isolation and biological activity of phytotoxic metabolites produced in vitro by *Sphaeropsis sapinea*, pathogenic fungus of *Pinus radiata*. Eur. J. Plant Pathol. *115*, 187–193.
13. Capasso, R., Cristinzio, G., Evidente, A., Scognamiglio, F. (1992). Isolation, spectroscopy and selective phytotoxic effects of polyphenols from vegetable waste waters. Phytochemistry *31*, 4125–4128.
14. Rehnberg, N., Magnusson, G. (1990). Total synthesis of (−)- and (+)-botryodiplodin and (+)- and (−)-epibotryodiplodin. Acta Chem. Scand. *44*, 377–383.
15. De Buyck, L., Forzato, C., Ghelfi, F., Mucci, A., Nitti, P., Pagnoni, U. M., Parsons, A.F., Pitacco, G., Roncaglia, F. (2006). A new and effective route to (±)-botryodiplodin and (±)-*epi*-botryodiplodin acetates using a halogen atom transfer Ueno–Stork cyclization. Tetrahedron Lett., *47*, 7759-7762.
16. Moreau, S., Lablache-Combier, A., Biguet, J., Foulon, C., Delfosse, M. (1982). Botryodiplodin, a mycotoxin synthesized by a strain of P. roqueforti. J. Org. Chem. 47, 2358–2359.

17. Summerbell, R.C., Krajden, S., Levine, R., Fuksa, M. (2004). Subcutaneous phaeohyphomycosis caused by *Lasiodiplodia theobromae* and successfully treated surgically. Med. Mycol. *2*, 543–547.
18. Paolinelli-Alfonso, M., Villalobos-Escobedo, J.M., Rolshausen, P., Herrera-Estrella, A., Galindo-Sánchez, C., López-Hernández, J., Hernandez-Martinez, R. (2016). Global transcriptional analysis suggests *Lasiodiplodia theobromae* pathogenicity factors involved in modulation of grapevine defensive response. BMC Genomics *17*, 615.
19. Andolfi, A., Mugnai, L., Luque, J., Surico, G., Cimmino, A., Evidente, A. (2011). Phytotoxins produced by fungi associated with grapevine trunk diseases. Toxins *3*,1569–1605.
20. Jacobson, E.S. (2000). Pathogenic roles for fungal melanins. Clin. Microbiol. Rev. *13*, 708–717.
21. Evidente, A., Andolfi, A., Cimmino, A. (2011). Relationships between the stereochemistry and biological activity of fungal phytotoxins. Chirality *23*, 674–693.
22. Husain, A., Ahmad, A., Agrawal, P.K. (1993). (−)-jasmonic acid, a phytotoxic substance from *Botryodiplodia theobromae*: characterization by nmr spectroscopic methods. J. Nat. Prod. *56*, 2008–2011.
23. Tsukada, K., Takahashi, K., Nabeta, K. (2010). Biosynthesis of jasmonic acid in a plant pathogenic fungus, *Lasiodiplodia theobromae*. Phytochemistry *71*, 2019–2023.
24. Chanclud, E., Morel, J.B. (2016). Plant hormones: a fungal point of view. Mol. Plant. Pathol. *17*, 1289–1297.
25. Dhandhukia, P.C., Thakkar, V.R. (2007). Standardization of growth and fermentation criteria of *Lasiodiplodia theobromae* for production of jasmonic acid. Afr. J. Biotechnol. *6*, 707–712.

26. Ramirez-Suero, M., Benard-Gellon, M., Chong, J., Laloue, H., Stempien, E., Abou-Mansour, E., Fontaine, F., Larignon, P., Mazet-Kieffer, F., Farine, S., Bertsch, C. (2014). Extracellular compounds produced by fungi associated with *Botryosphaeria* dieback induce differential defence gene expression patterns and necrosis in *Vitis vinifera* cv. Chardonnay cells. Protoplasma *251,* 1417–1426.
27. Abou-Mansour, E., Débieux, J.L., Ramírez-Suero, M., Bénard-Gellon, M., Magnin-Robert, M., Spagnolo, A., Chong, J., Farine, S., Bertsch, C., L'Haridon, F., Serrano, M., Fontaine, F., Rego, C., Larignon, P. (2015). Phytotoxic metabolites from *Neofusicoccum parvum*, a pathogen of Botryosphaeria dieback of grapevine. Phytochemistry *115*, 207–215.
28. Nouguier, R., Gastaldi, S., Stien, D., Bertrand, M., Villar, F., Andrey, O., Renaud, P. (2003). Synthesis of (±)- and (−)-botryodiplodin using stereoselective radical cyclizations of acyclic esters and acetals. Tetrahedron: Asymmetry *14*, 3005–3018.
29. Sakai, K., Amemiya, S., Inoue, K., Kojima, K. (1979). The conversion of methylenomycin A to natural botryodiplodin and their absolute configurations. Tetrahedron Lett. *20*, 2365–2368.
30. Fujimoto, Y., Kamiya, M., Tsunoda, H., Ohtsubo, K., Tatsuno, T. (1980). Recherche toxicologique des substances métaboliques de *Penicillium carneo-lutescens*. Chem. Pharm. Bull. *28*, 1062-1066.
31. Andolfi, A.; Maddau, L.; Cimmino, A.; Linaldeddu, B.T.; Franceschini, A.; Serra, S.; Basso, S.; Merck, D.; Evidente, A. (2012) Cyclobotryoxide, a phytotoxic metabolite produced by the plurivorous pathogen *Neofusicoccum australe*. J. Nat. Prod. *75*, 1785–1791.
32. Albuquerque, P., Casadevall, A. (2012). Quorum sensing in fungi−a review. Med. Mycol. *50*, 337−345.
33. NIST Standard Reference Data. http://www.nist.gov/srd/nist1a.cfm (accessed on 14 12 2019).

34. Soni, K.K., Dadwal, V. S. (1985). Charcoal root and stem rot of Eucalyptus. Eur. J. Forest Pathol., *15*, 397-401.
35. Su, G., Suh, S.O., Schneider, R.W., Russin, J.S. (2001). Host specialization in the charcoal rot fungus, *Macrophomina phaseolina*. Phytopathology *91*, 120–126.
36. De, B.K., Chattopadhya, S.B., Arjunan, G. (1992). Effect of potash on stem rot diseases of jute caused by *Macrophomina phaseolina*. J. Mycopathol. Res. *30*, 51-5.
37. Khan, S.N. (2007). *Macrophomina phaseolina* as causal agent for charcoal rot of sunflower. Mycopathology *5*, 111-8.
38. Jacob, C.J., Krarup, C., Diaz, G.A., Latorre, B.A. (2013). A severe outbreak of charcoal rot in cantaloupe melon caused by *Macrophomina phaseolina* in Chile. Plant Dis. *97*, 141-142.
39. Sánchez, S., Henríquez, J.L., Urcola, L.A., Scott, A., Gambardella, M. (2016). Susceptibility of strawberry cultivars to root and crown rot caused by *Macrophomina phaseolina*. J. Berry Res. *6*, 345-354.
40. Kaur, S., Dhillon, G.S., Brar, S.K., Vallad, G.E., Chand, R., Chauhan, V.B. (2012). Emerging phytopathogen *Macrophomina phaseolina*: biology, economic importance and current diagnostic trends. Crit. Rev. Microbiol., *38*, 136-151.
41. Arora, P., Dilbaghi, N., Chaudhury, A. (2012). Opportunistic invasive fungal pathogen *Macrophomina phaseolina* prognosis from immunocompromised humans to potential mitogenic RBL with an exceptional and novel antitumor and cytotoxic effect. *Eur. J. Clin. Microbiol. 31*, 101-107.
42. Dhar, T.K., Siddiqui, K.A., Ali, E. (1982). Structure of phaseolinone, a novel phytotoxin from *Macrophomina phaseolina*. Tetrahedron Lett. *23*, 5459-5462.
43. Mahato, S.B., Siddiqui, K.A., Bhattacharya, G., Ghosal, T., Miyahara, K., Sholichin, M., Kawasaki, T. (1987). Structure and stereochemistry of

phaseolinic acid: A new acid from *Macrophomina phaseolina*. J. Nat. Prod. *50*, 245-247.

44. Abbas, H.K.; Bellaloui, N.; Accinelli, C.; Smith, J.R.; Shier, W.T. (2009). Toxin Production in Soybean (*Glycine max* L.) Plants with Charcoal Rot Disease and by *Macrophomina phaseolina*, the fungus that causes the disease. Toxins *11*, 645.
45. Mondello, V., Lo Piccolo, S., Conigliaro, G., Alfonzo, A., Torta, L., Burruano, S. (2013). First report of *Neofusiccoccum vitifusiforme* and presence of other Botryosphaeriaceae species associated with Botryosphaeria dieback of,grapevine in Sicily (Italy). Phytopathol. Mediterr. *52*, 388–396.
46. Nieva-Echevarría, B., EncarnaciónGoicoechea, M., Manzanos, J., Guillén, M.D. (2014). A method based on ^{1}H NMR spectral data useful to evaluate the hydrolysis level in complex lipid mixtures. Food Res. Int. *66*, 379–387.
47. Larignon, P., Fulchic, R., Cere, L., Dubos, B. (2001). Observation on black dead arm in French vineyards. Phytopathol. Mediterr. *40*, S336–S342.
48. Yan, J.Y., Xie, Y., Zhang, W., Wang, Y., Liu, J.K., Hyde, K.D., Seem, R.C., Zang, G.Z., Wang, Z.Y., Yao, S.W., et al. (2013). Species of Botryosphaeriaceae involved in grapevine dieback in China. Fungal Divers. *61*, 221–236.
49. Larignon, P., Dubos, B. (1997). Fungi associated with esca disease in grapevine. Eur. J. Plant Pathol. *103*, 147–157.
50. Burruano, S.; Giambra, S.; Mondello, V.; DellaGreca, M.; Basso, S.; Tuzi, A.; Andolfi, A. (2016). Naphthalenone polyketides produced by *Neofusicoccum parvum*, a fungus associated with grapevine Botryosphaeria dieback. Phytopathol. Mediterr. *55*, 197–206.
51. Mondello, V., Songy, A., Battiston, E., Pinto, C., Coppin, C., Trotel-Aziz, P., Clément, C., Mugnai, L., Fontaine, F. (2018) Grapevine Trunk Diseases: A review of fifteen years of trials for their control with chemicals and biocontrol agents. Plant Dis. *102*, 1189–1217.

52. Evidente, A., Punzo, B., Andolfi, A., Cimmino, A., Melck, D., Luque, J. (2010). Lipophilic phytotoxins produced by *Neofusicoccum parvum*, a grapevine canker agent. Phytopathol. Mediterr. *49*, 74–79.
53. Uranga, C.C., Beld, J., Mrse, A., Córdova-Guerrero, I., Burkart, M.D., Hernández-Martínez, R. (2016). Fatty acid esters produced by *Lasiodiplodia theobromae* function as growth regulators in tobacco seedlings. *Biochem. Biophys. Res. Commun.* 472, 339–345.
54. Schaller, A., Stintzi, A. (2009). Enzymes in jasmonate biosynthesis–structure, function, regulation. Phytochemistry *70*, 1532–1538.
55. Farmer, E.E., Ryan, C.A. (1992). Octadecanoid precursors of jasmonic acid activate the synthesis of wound-inducible proteinase inhibitors. Plant Cell *4*, 129–134.
56. Fitton, A., Goa, K.L. (1991). Azelaic acid. Drugs, *41*, 780-798.

CHAPTER 4

Marine-derived Fungi as Producers of Taxonomically and Biotechnologically Relevant Secondary Metabolites

4.1. Introduction

Marine-derived fungi are an ecological rather than a taxonomic group and they occur in all marine habitats. Fungi are major decomposers of woody and herbaceous substrates in marine ecosystems. Their importance lies in their ability to aggressively degrade lignocellulose.

Marine-derived fungi are also important pathogens of plants and animals and for symbiotic relationships with other organisms. The diversity, biological activity and secondary metabolite production of these fungi were investigated in order to assess their potential to produce novel biologically active secondary metabolites.

In fact, the spread of studies on biodiversity in different environmental contexts is particularly fruitful for natural product discovery, with the finding of novel secondary metabolites and structural models, which are sometimes specific to certain organisms. Bioactive metabolites produced by marine microorganisms have received considerable attention as new therapeutic agents. In fact, recently, marine-derived fungi have been isolated from various habitats, including sponges, sea water and algae, and found to be excellent producers of new compounds[1-4]. Pharmaceutical industry revealed great interest in the exploitation of metabolites from marine microbes as novel drugs and the combination of multiple analytical approaches in the 'omics' field will certainly improve drug discovery from such natural sources[5].

In order to search for microbial compounds with novel biotechnological applications, fungi associated to marine organisms in Naples bay were investigated for the production of secondary metabolites. In particular, strains of *Trichoderma citrinoviride* and *Aspergillus niger* were collected from the shoreside of Miliscola (Naples, Italy) in association to the green alga *Cladophora* sp., and a strain of *Penicillium brevicompactum* was collected in association to the sea anemone *Anemonia sulcata* near to the island of Procida (Naples, Italy).

4.2. *Trichoderma citrinoviride* Associated to *Cladophora* sp.

In this study, the major secondary metabolites of a *Trichoderma citrinoviride* strain, named A12, isolated from the green alga *Cladophora* sp. were examined. The effect on nitrite levels of the main product (i.e. trichodermanone C) of this fungus in lipopolysaccharide-stimulated J774A.1 macrophages was tested.

4.2.1. Purification and Identification of Secondary Metabolites

The crude EtOAc extract from the culture filtrates of A12 was fractionated by combined column and thin layer chromatography, leading to the purification of six known compounds. Structures were confirmed by comparison of the obtained data (OR, NMR, and ESI MS) with those reported in the literature for: trichodermanone C (**1**)[6], spirosorbicillinol A (**2**)[7], (*R*)-vertinolide (**3**)[8], sorbicillin (**4**)[9], tyrosol (**5**)[10], and 2-phenylethanol (**6**) (Figure 4.1). Furthermore, NMR data of trichodermanone C and spirosorbicillinol A recorded in $CDCl_3$ (instead of CD_3OD) are reported in Chapter 6, Experimental Section (paragraph 6.5.).

Each chromatographic fraction was analysed by LC-ESI-HRMS, allowing the putatively identification of other compounds (see paragraph 6.5.). In particular, trichodimerol (**7**) was detected as $[M + H]^+$, $[M + Na]^+$, $[M + K]^+$ and $[M - OH]^+$ precursors at *m/z* 497.2166, 519.1981, 535.1713 and 479.2056, respectively. Rezishanone A (**8**, Figure 4.1.) was confidently identified from the ions at *m/z* 363.1436 (pseudomolecular ion $[M + H]^+$) and 345.1327 ($[M\text{-}OH]^+$), 2,3′-dihydrosorbicillin (**9**, Figure 4.1.) from ions at *m/z* 235.1339 $[M + H]^+$ and 217.1223 $[M\text{-}OH]^+$, and bisvertinol (**10**, Figure 4.1.) from ion at *m/z* 499.2332 $[M + H]^+$. However, their characterization by spectroscopic analysis was not carried out, because of the low amount.

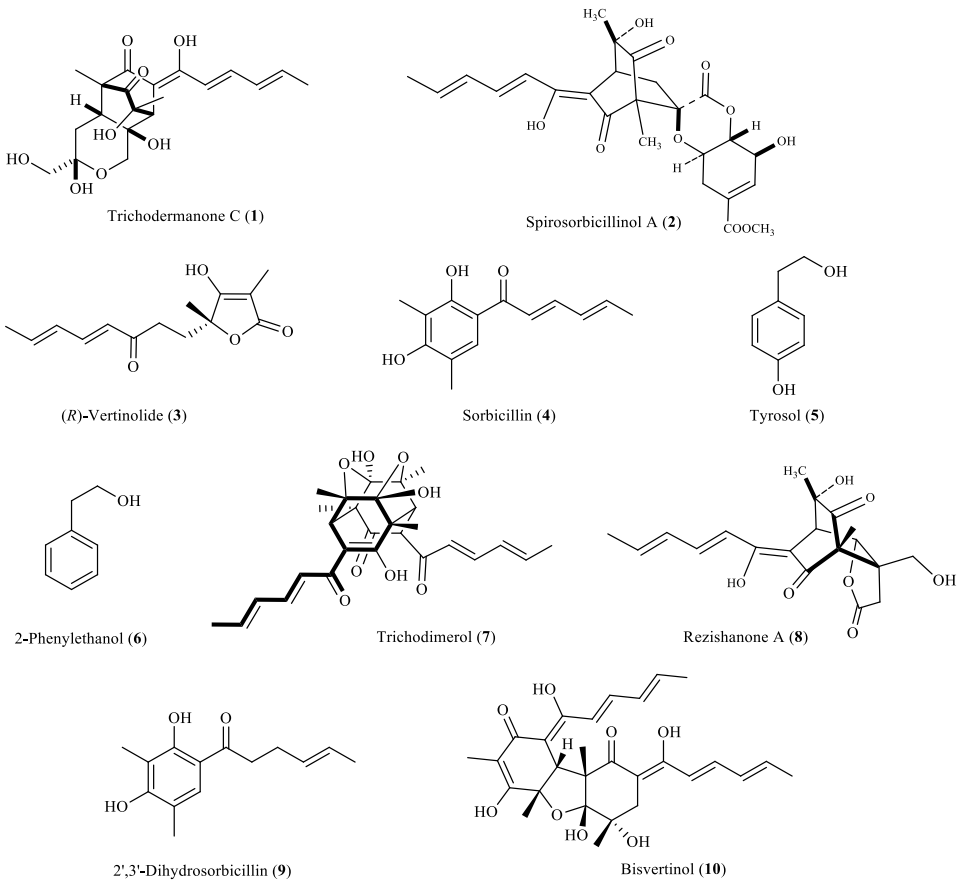

Figure 4.1. Structures of the major secondary metabolites produced by *T. citrinoviride* strain A12 in liquid culture

4.2.2. Anti-inflammatory and Cytotoxicity Assays

The capacity of **1** to reduce the production of nitrites in the macrophages cell line J774A.1 stimulated by lipopolysaccharide (LPS) was evaluated. In the reported experiments, exposure of macrophages to LPS (1 μg/mL for 24 h) significantly promoted the production of the pro-inflammatory molecules nitrites (stable final products of NO metabolism) (Figure 4.2). A pre-treatment with **1**, in the range concentration of 3–60 μM, reduced in a concentration-dependent

manner the nitrites production induced by LPS incubation, being the effect significant starting from the 10 μM concentration.

Trichodermanone C at the highest concentration (60 μM) did not modify *per se* basal nitrite levels (e.g. cells not treated with LPS) (Figure 4.2). The effect of **1** on nitrite production was not due to a cytotoxic response since the exposure of **1** to J774A.1 cells did not affect mitochondrial respiration after 24 h treatment [cell viability (%) ± SEM: vehicle: 100 ± 2.36, (**1**) 3 μM: 106.2 ± 2.19; (**1**) 10 μM: 104.0 ± 2.38; (**1**) 30 μM: 102.90 ± 2.11; (**1**) 60 μM: 105.0 ± 2.07]. DMSO, used as a positive control, significantly reduced cell viability (vehicle: 100 ± 2.36, DMSO 20%: 4.45 ± 0.235 $p < 0.001$).

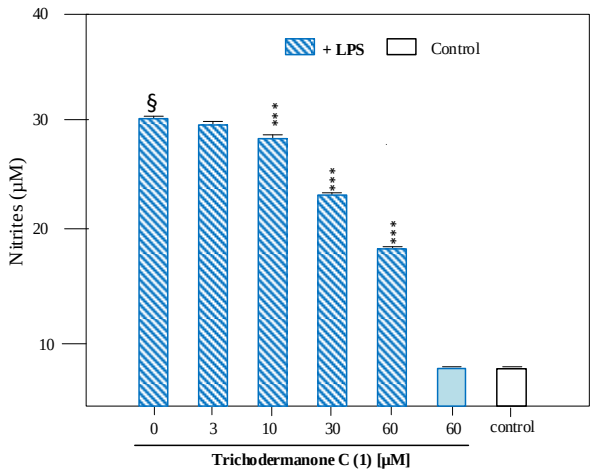

Figure 4.2. Inhibitory effect of trichodermanone C (**1**) on nitrite levels in the cell medium of J774A.1 macrophages incubated with lipopolysaccharide (LPS, 1 μg/mL) for 24 h. (**1**), used at the not cytotoxic concentrations (3-60 μM), was added to the cells 30 min before LPS stimulus. Results are mean ± SEM of three experiments (in triplicates). §$p < 0.001$ vs control; ***$p < 0.001$ vs LPS alone.

4.2.3. Discussion

The genus *Trichoderma* (teleomorph *Hypocrea*, class Sordariomycetes, order Hypocreales) includes fungal species adapted to both terrestrial and marine environments. Rhizosphere colonizing strains of *Trichoderma* spp. may act as plant opportunistic symbionts and are widely used as biocontrol agents against different fungal phytopathogens[11-13]. Species of *Trichoderma* isolated from marine habitats showed great attitude in producing bioactive secondary metabolites, displaying diverse chemical structures and biological activities[14-16].

The strain A12 of *Trichoderma citrinoviride*, isolated from the green alga *Cladophora* sp. collected in Miliscola (Naples, Italy), was identified and characterized. Chromatographic techniques and spectroscopic methods were used to isolate and characterize the major secondary metabolites produced by this strain in liquid medium. Numerous compounds identified in this study (Figure 4.1) belong to the family of sorbicillinoids, a group of hexaketide metabolites isolated from both marine and terrestrial fungi[17]. Sorbicillinoid-related compounds include over 90 monomeric, dimeric, trimeric and hybrid products which have been reported from several fungi, including marine-derived strains, namely *Paecilomyces*, *Penicillium*, *Verticillium* and *Trichoderma*[18]. In particular, *T. citrinoviride* or the closely related species *T. longibrachiatum* isolated from marine substrates were found to produce epoxysorbicillinol, bisvertinol, bisvertinolone, dihydrotrichodimerol, bislongiquinolide, trichodimerol and sorbiquinol[9,19,20]. This class of metabolites exhibited a broad range of biological activities including pronounced radical scavenging, antitumor properties and cytotoxicity[17,18,21,22].

Among the isolated compounds, trichodermanone C (**1**, Figure 4.1.) resulted to be the main metabolite produced by A12 strain. This compound has been previously isolated, along with its analogues trichodermanones A, B and D, by Neumann et al. (2007)[6] from a sponge-derived strain of *Trichoderma* sp.

Previous pre-clinical studies demonstrated that trichodermanone C (**1**) possesses a moderate radical scavenging activity[6] and in this study we produced evidence that 1 has an interesting anti-inflammatory activity in LPS-stimulated J774A.1 cells. It is well known that macrophages can be activated by LPS and play a key role in inflammation through the production of several pro-inflammatory mediators, including nitric oxide (NO). In fact, NO plays an important role in the regulation of several pathophysiological processes[23]. Moreover, an overproduction of NO has been proved to be responsible of cell damage caused by inflammation[23]. Therefore today, inflammation-associated to nitric oxide production is largely used as a potential therapeutic target from complementary and alternative medicines to prevent and treat inflammation[24]. To the best of our knowledge, this is the first work that shows an inhibitory effect of trichodermanone C on nitrite production evoked by LPS in macrophages.

Some representative compounds identified in liquid culture of *Trichoderma citrinoviride* A12 are discussed below.

Spirosorbicillinol A (**2**, Figure 4.1.) was identified, together with its analogues spirosorbicillinols B-C, from culture extracts of *Trichoderma* sp. isolated from soil, and displayed a weak DPPH-radical scavenging activity[7]. These compounds are also produced by a strain of *T. citrinoviride* isolated from an indoor air sample collected in Montreal (Canada) along with vertinolide, bisvertinol and trichotetronine[25].

Vertinolide (**3**, Figure 4.1.) was isolated from *Trichoderma* sp.[26,27], as well as from other fungi[28]. Vertinolide and its derivatives, 5-hydroxyvertinolide and 5-epihydroxyvertinolide, can be defined as a subfamily of the sorbicillinoids because of their particular configuration and structure[17].

Sorbicillin (**4**, Figure 4.1.) is the precursor of the class of sorbicillinoids, a group of monomeric and sorbicillin-related natural products, and represents an example of hexaketide where the cyclization took place on the carboxylate

terminus. This compound has been previously isolated from marine-derived *Trichoderma* sp. with other sorbicillinoids and bisorbicillinoids, such as 2′,3′-dihydrosorbicillin, bisvertinolone, trichodimerol, bisvertinoquinol[29].

4.3. *Aspergillus niger* Associated to *Cladophora* sp.

4.3.1. Identification of Secondary Metabolites

The crude EtOAc extract of strain A7 of *Aspergillus niger*, isolated from the green alga *Cladophora* sp. collected in Miliscola (Naples, Italy), was analysed both directly and after trimethylsilylation with BSTFA by GC-MS (Figure 4.3), as described in Chapter 6 (see subparagraphs 6.1.4. and 6.6.1.). Metabolites were identified by comparing their mass spectra with those present in database by employing the NIST Mass Spectral Search Program v.2.0 g which, among others, could explore the NIST 14 Mass Spectral library (2014) and the Golm Metabolome Database[30].

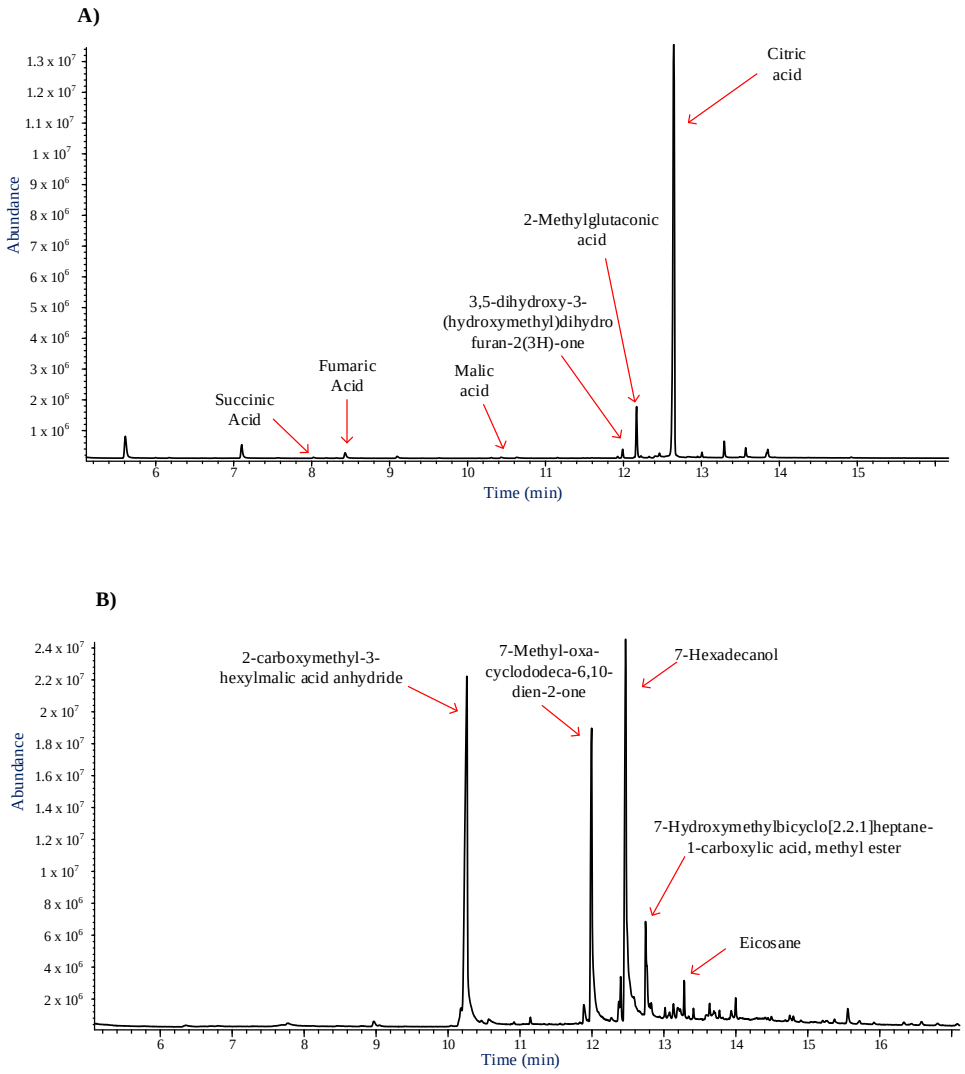

Figure 4.3. Annotated total ion chromatograms (TICs) acquired from crude extract of strain A7 of *A. niger* after derivatization with BSTFA (A) and without any treatment (B).

GC–MS analysis of crude extract after derivatization with BSTFA revealed the presence of dicarboxylic acids (i.e., succinic acid, fumaric acid, malic acid), 3,5-dihydroxy-3-(hydroxymethyl)dihydrofuran-2(3H)-one, 2-methylglutaconic acid and citric acid. GC–MS analysis of the crude extract disclosed the presence

of 2-carboxymethyl-3-hexylmaleic acid anhydride, 7-methyloxa-cyclododeca-6,10-dien-2-one, 7-hexadecanol, 7-hydroxymethylbicyclo[2.2.1]heptane-1-carboxylic acid methyl ester and eicosane (Table 4.1.).

Table 4.1. Secondary metabolites produced *by Aspergillus niger* A7. * RI are referred to silylated compounds

Name	Structure	KI	Sample preparation
2-Carboxymethyl-3-hexylmaleic acid anhydride	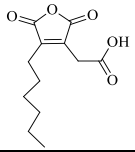	1134	/
7-Methyloxa-cyclododeca-6,10-dien-2-one	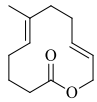	1734	/
7-Hexadecanol	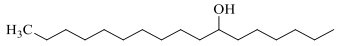	1962	/
7-Hydroxymethylbicyclo[2.2.1]heptane-1-carboxylic acid methyl ester	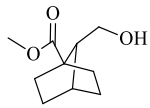	1881	/
Eicosane	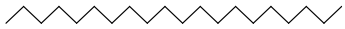	2077	/
Succinic acid	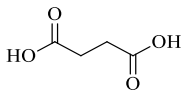	1318*	Sylilation
Fumaric acid	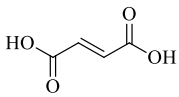	1351*	Sylilation
Malic acid	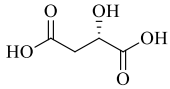	1498*	Sylilation
3,5-Dihydroxy-3-(hydroxymethyl)dihydrofuran-2(3H)-one	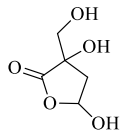	1733*	Sylilation

2-Methylglutaconic acid	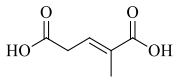	1837*	Sylilation
Citric acid	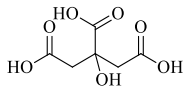	1941*	Sylilation

4.3.2. Discussion

Well-known for its ubiquity and cosmopolitan distribution, *Aspergillus* (Eurotiales, Aspergillaceae) includes 344 species grouped in 4 subgenera and 19 sections according to the Raper & Fennel's classification scheme proposed 50 years ago[31]. It also represents the most common genus of Ascomycetes at sea[32]. Since the recent affirmation of the single name principle in fungal nomenclature[33], this genus has incorporated species previously classified according to their teleomorphic stages in *Emericella*, *Eurotium*, *Neosartorya* and *Chaetosartorya*. However, this new taxonomic arrangement is not consolidated yet, and it is quite possible that further modifications be introduced in future[34].

Aspergillus species, a good number of which have been used for some extent of biotechnological application, can be recovered from all sorts of peculiar or even extreme habitats, from deep-sea sediments[35] to coastal salterns[36], passing through a wide range of symbiotic relationships with any kind of marine organisms[37-39], due to an extraordinary capacity to adapt their metabolism to very diverse environmental conditions.

In this study, secondary metabolites in the culture crude extract of strain A7 of *Aspergillus niger* isolated from *Cladophora* sp. were identified via GC-MS, both directly and after trimethylsililation with BSTFA.

A few dicarboxylic acids were detected in the extract after derivatization; among these compounds, succinic acid has an industrial potential deriving from possible application in chemical industry producing food and pharmaceutical products[40,41]. A well-developed peak of silylated citric acid appears in the

chromatogram obtained injecting the sample derivatized with BSTFA. This tricarboxylic acid has been reported as a product of some strains of *A. niger* cultured in medium with initial pH of 2.5–3.5 since a century ago[42,43], and its production is known to be stimulated by the availability of sucrose[44]. Anyway, citric acid is used in the household and in the preparation of many industrial products (e.g., food, pharmaceuticals, cleaning agents), and *A. niger* is the main producer exploited in biotechnology[43]. On the other hand, 2-carboxymethyl-3-hexylmaleic acid anhydride was detected in the non-derivatized extract. It was isolated for the first time in 1972 as a metabolite produced by a strain of *A. niger*, showing a weak *in vitro* activity against gram positive bacteria[45].

4.4. *Penicillium brevicompactum* Associated to *Anemonia sulcata*

4.4.1. Identification of Secondary Metabolites

The crude EtOAc extract from the culture filtrate was subjected to GC-MS analysis after derivatization with BSTFA and without any treatment. The acquired gas chromatograms (Total Ion Current Chromatograms, TICs) showed that the EtOAc extract was very rich in metabolites.

However, a number of metabolites in the extract, associated with well-developed chromatographic peaks in the TICs, could not be readily identified by the standard procedure of comparison of the 70 eV EI mass spectrum with spectra in the commercial NIST14 or in custom MS libraries available in our laboratory and on the WEB[46].

In particular, we located, in the TIC, nine chromatographic peaks which appeared to be of good purity and associated them with as many metabolites which become the target products in this investigation. At this stage, the nine target metabolites were tagged by their Kovats non-isothermal retention index and associated EI mass spectrum.

In the following, for brevity, we shall refer to each of the nine target metabolites with an ascending integer from **1** to **9**.

After this, the crude EtOAc extract of the the culture broth was fractionated by combined column and thin layer chromatography and each fraction was presented to the GC-MS system. This revealed that, although most of the separated fractions contained mixtures of compounds, two fractions contained each a single substance in a good degree of purity. These two fractions were submitted to NMR structural analysis which led to the identification of *cis*-bis-(methylthio)silvatin ($C_{20}H_{28}N_2O_3S_2$) and mycophenolic acid ($C_{17}H_{20}O_6$) which correspond to structures in Figure 4.4:

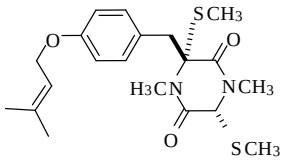

Cis-bis-(methylthio)silvatin

($C_{20}H_{28}N_2O_3S_2$)

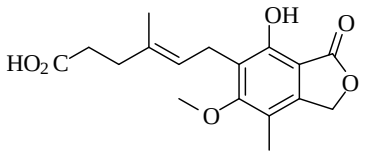

Mycophenolic acid

($C_{17}H_{20}O_6$)

Figure 4.4. Structures of *cis*-bis(methylthio)silvatin (**1**) and mycophenolic acid (**8**) determined via NMR analysis of purified fractions of *Penicillium brevicompactum* AN-4 culture broth extract

In order to identify the remaining seven metabolites, chromatographic fractions, which contained one or more of the target metabolites, were subjected to LC-ESI-HRMS analysis.

To each of the non-identified target metabolites, an accurate value of the the monoisotopic mass, within an uncertainty of ± 0.0002-0.0005 u, was assigned from the high-resolution LC-ESI-HRMS mass spectra acquired. From the accurate mass, the atomic composition of each target metabolite was readily

derived by using standard MS tools. The accurate mass and formulas associated to each target metabolite are reported in Table 4.2.

Table 4.2. Data concerning nine targeted metabolites of strain AN4 collected via GC-EI-MS and LC-ESI-HRMS. Uncertainty on the reported values of the accurate mass is tipically ± 0.0002-0.0005 u.

Code	Compound	RI (GC-MS)	Formula	Accurate Mass (u)	RDB
1	*Cis*-bis(methylthio)silvatin	RI = 3229	$C_{20}H_{28}N_2O_3S_2$	408.1538	8
2	Metabolite 2	RI = 2892	$C_{19}H_{26}N_2O_3S_2$	394.1388	8
3	Metabolite 3	RI = 2083	$C_{19}H_{24}N_2O_3S$	360.1510	9
4	Metabolite 4	RI = 3203	$C_{19}H_{24}N_2O_4S$	376.1462	9
5	Metabolite 5	RI = 3047	$C_{20}H_{30}N_2O_5S_2$	442.1593	7
6	Metabolite 6	RI = 2014 (TMS derivative)	$C_{15}H_{20}N_2O_3S_2$	340.0919	7
7	Metabolite 7	RI = 1876 (TMS derivative)	$C_{13}H_{16}N_2O_3S_2$	312.0600	7
8	Mycophenolic acid	RI = 2871	$C_{17}H_{20}O_6$	320.1268	8
9	Metabolite 9	RI = 3227 (TMS derivative)	$C_{21}H_{23}N_3O_3$	365.1725	12

In the last column of Table 4.2, it is also reported the RDB (Ring + Double Bonds) number which is calculated from the empirical formulas by a standard algorithm[47]. Data in Table 4.2, and the corresponding EI mass spectra, were employed to assign a structure to each of the unidentified target metabolites, as described in some detail in the Discussion subparagraph below. Hence, LC-ESI-HRMS and GC-MS allowed the putative identification of other compounds (Figure 4.5), a number of which were found to belong to the thiosilvatin series[48].

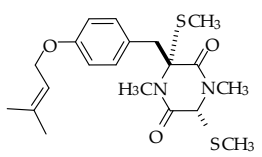

Cis-bis(methylthio)silvatin (**1**)

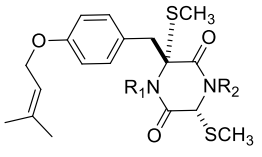

Saroclazine A (**2A**) $R_1 = CH_3$, $R_2 = H$
Saroclazine B (**2B**) $R_1 = H$, $R_2 = CH_3$

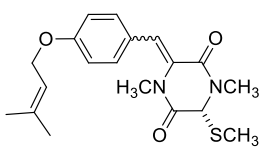

Fusaperazine E/F (**3**)

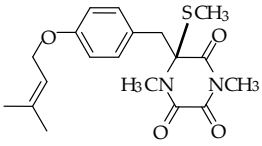

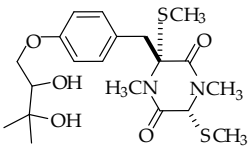

Bilain B (**5**)

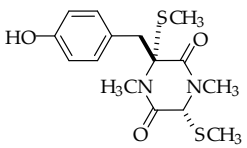

Deprenyl-bis(methylthio)silvatin (**6**)

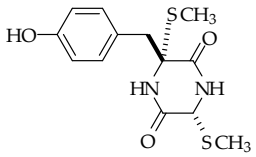

Fusaperazine A (**7**)

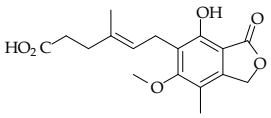

Mycophenolic acid (**8**)

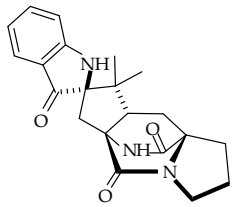

Brevianamide A (**9**)

Figure 4.5. Structures of secondary target metabolites identified in culture organic extract of *P. brevicompactum* AN-4.

Please note that, unlike *cis*-bis(methylthio)silvatin (**1**, Figure 4.5.) whose configuration was assigned by NMR, determination of stereochemistry was not possible for compounds identified via MS. Hence, their configuration in Figure 4.5. was arbitrarily assigned.

4.4.2. Cytotoxicity of cis-bis(methylthio)silvatin

Cytotoxic activity of *cis*-bis(methylthio)silvatin was evaluated at different concentrations (0.3-100 μM) on two colorectal cancer cell lines (HCT116 and Caco-2) and a healthy colonic epithelial cell line (HCEC). By using the MTT assay we found that **1** significantly reduced cells viability in HCT116 and Caco-2

cells in a dose-dependent manner, starting from 1 µM for HCT116 and 3 µM for Caco-2 cells (Figure 4.6.A and B), with EC_{50} of 29.29 µM and 35.31 µM, respectively. Similarly, the compound exerted a cytotoxic activity on HCEC, with a significant effect starting from 1 µM, and EC_{50} of 0.57 µM (Figure 4.6.C).

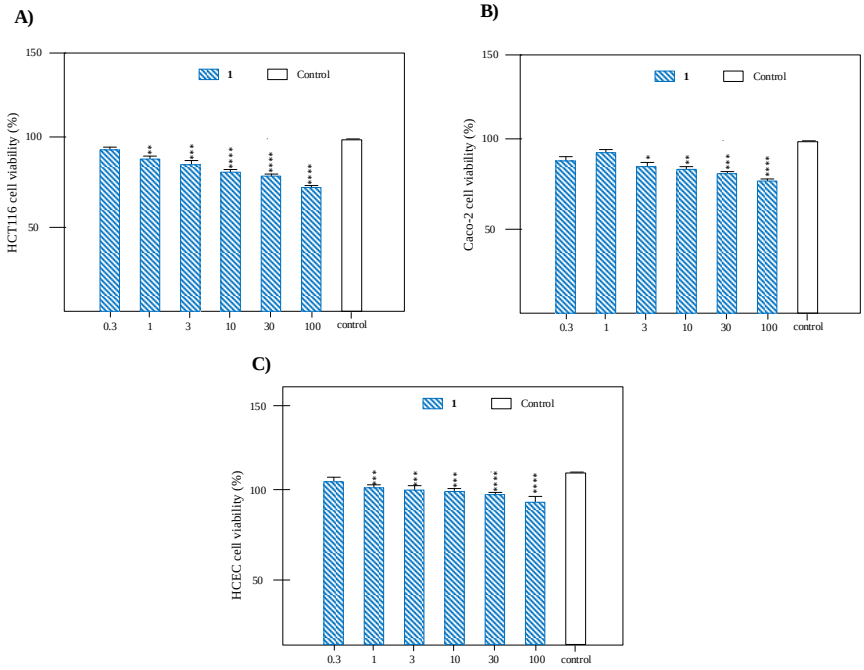

Figure 4.6. Effect of *cis*-bis(methylthio)silvatin (0.3-100 µM) on cell viability, evaluated by the MTT assay, in the colorectal cancer cell lines HCT116 (A) and Caco-2 (B), and in the healty colonic epithelial cell line HCEC (C). Cells were incubated with increasing concentration of compound (24h exposure). Each bar represents the mean ± SEM of three independent experiments. *P < 0.05, **P < 0.01, ***P < 0.001 and ****P < 0.0001 versus control (ctrl, untreated cells).

4.4.3. Discussion

Within the many Ascomycetes reported from the sea environment, the genus *Penicillium* is particularly widespread in association to any kind of marine organisms, and represents one of the most prolific taxa with reference to

production of bioactive compounds[2,49]. Besides the continuous finding of novel secondary metabolites[2,50,51], the metabolomic characterization of *Penicillium* isolates from marine substrates is relevant in terms of comparison with conspecific terrestrial strains.

To perform an accurate identification of secondary metabolites produced by strain AN4, parallel application of several instrumental techniques was employed (i.e NMR, LC-ESI-HRMS, GC-MS).

An important question to be discussed concerns the way structures presented in Figure 4.5 have been derived from data in Table 4.2 and the associated EI mass spectra collected via GC-MS analysis of chromatographic fractions from the EtOAc extract of strain AN4.

By considering the formulas and RDB numbers of metabolites **1-7** in Table 4.2, as presented in Figure 4.7., hardly one can avoid the perception that these formulas refer to a group of structurally related molecules, probably being part of a common metabolic pathway.

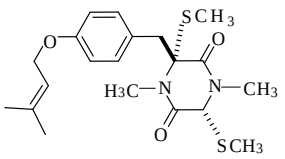

cis-bis(methylthio)silvatin (**1**)

(**1**→$C_{20}H_{28}N_2O_3S_2$)$^{RDB = 8}$

(**2**→$C_{19}H_{26}N_2O_3S_2$)$^{RDB = 8}$

(**3**→$C_{19}H_{24}N_2O_3S$)$^{RDB = 9}$

(**4**→$C_{19}H_{24}N_2O_4S$)$^{RDB = 9}$

(**5**→$C_{20}H_{30}N_2O_5S_2$)$^{RDB = 7}$

(**6**→$C_{15}H_{20}N_2O_3S_2$)$^{RDB = 7}$

(**7**→$C_{13}H_{16}N_2O_3S_2$)$^{RDB = 7}$

Figure 4.7. Comparison of *cis*-bis(methylthio)silvatin (**1**) with metabolites **2-7** for structure assignment

As can be seen from Figure 4.7, the RDB = 8 number of *cis*-bis(methylthio)silvatin (**1**), whose structure was unambigously assigned by NMR analysis of the purified compound, is accounted for: 1) by the benzene ring which

consumes 4 RDB units; 2) by the heterocyclic 6-membered ring, which consumes 1 RDB unit; 3) by two C=O functional groups which consume two RDB units; 4) by the double bond in the alkyl side chain attached to the benzene ring which accounts for one RDB unit.

The RDB of the targeted metabolites **2-7** ranges between 7 and 9, so that all of them can accommodate the benzene ring and several additional rings and/or double bonds. Furthermore, all the molecules in Figure 4.7 expose two nitrogen atoms which are necessary to the formation of the six members heterocyclic ring of **1**.

Based on these considerations, it is a reasonable starting point to assume that structures of **2-7** share the same basic structural pattern of **1**.

This fundamental consideration can be used in various ways to tentatively assign a structure to our targeted metabolites.

One most obvious way is to make a similarity structure search in a database of known chemical molecules (e.g. PubChem) starting with the known structure of *cis*-bis(methylthio)silvatin (**1**).

A second, very intriguing approach is to exercise, guided by the pertinent EI mass spectra, our chemical understanding and knowledge on breaking and closing bonds, to translate into structural variations the differences between formulas of the unidentified metabolites and compound **1.** This function can also be supported by an *ad hoc* program which is capable of predicting mass spectra from a hypothesized structure on the basis of well-established fragmentation rules. To this purpose we have used the NIST program MS Interpreter[52], which is a well-known MS *fragmenter* and which can be freely downloaded from the internet.

As an example of the procedure we have employed throughout to assign a structure to metabolites from 2 to 7 (and which is sketched for each single metabolite below) we discuss, in the following, as briefly as possible, how a structure can be associated to the target metabolite 2 on the basis of data in Table

1, its EI mass spectrum and the EI mass spectrum of the fully characterized *cis*-bis(methylthio)silvatin(**1**).

First, if we compare formula of **2** ($C_{19}H_{26}N_2O_3S_2$) with formula of **1** ($C_{20}H_{28}N_2O_3S_2$), we see immediately that these two molecules, which have the same RDB number, simply differ by a CH_2 group. When we look at the structure of **1** in Figure 4.8, we see that there are several ways in which metabolite **2** can be generated by substitution of a -CH_3 group with hydrogen.

For better clarifying, two possible conversion processes, which produce supposed structures for metabolite **2** are described in Figure 4.8.

Please note that although structures 2A and 2B, hypothesized in Figure 4.8, refer to two different isomeric compounds, in the following we will treat them as a single hypthetical structure for metabolite **2** (since it can be anticipated that it will be impossible to distinguish between them on the basis of MS data).

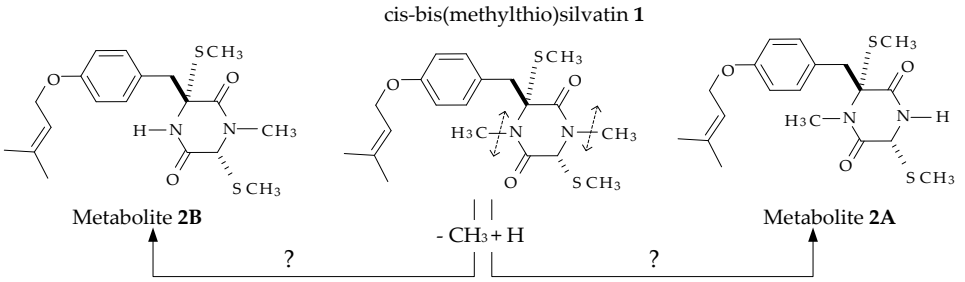

Figure 4.8. Hypothetical pathways for the conversion of the formula of *cis*-bis(methylthio)silvatin (**1**) to the formula of metabolite **2** in Table 1

Second, we can provide substantial support for hypothetical structure in Figure 4.5, by confronting the EI mass spectra of *cis*-bis(methylthio)silvatin (**1**) with the mass spectrum of metabolite **2**, which is done in Figure 4.9.

As can be seen, the EI mass spectra of both compounds do not exhibit the molecular ion mass peak. However, this is irrelevant in the present case because

we already know the empirical formula of the two compounds (which has been derived from HR MS data, see Table 4.2.).

Even a superficial inspection of Figure 4.9 will show a strict correlation of the mass spectra which, obviously, derives from structural relationships.

For instance, well developed mass peaks are present at *m/z* 107, 158, 186, 233, 245, 293, etc., in both spectra.

The main difference between the two spectra appears to be a peak at *m/z* 361 which is only present in the spectrum of *cis*-bis(methylthio)silvatin (**1**).

In primis, we consider that the base peak, both in spectrum (A) and (B), appears at *m/z* = 107. This peak is readily assigned to the ion $C_7H_7O^+$ whose composition is derived from the analysis of its well-developed isotopic pattern.

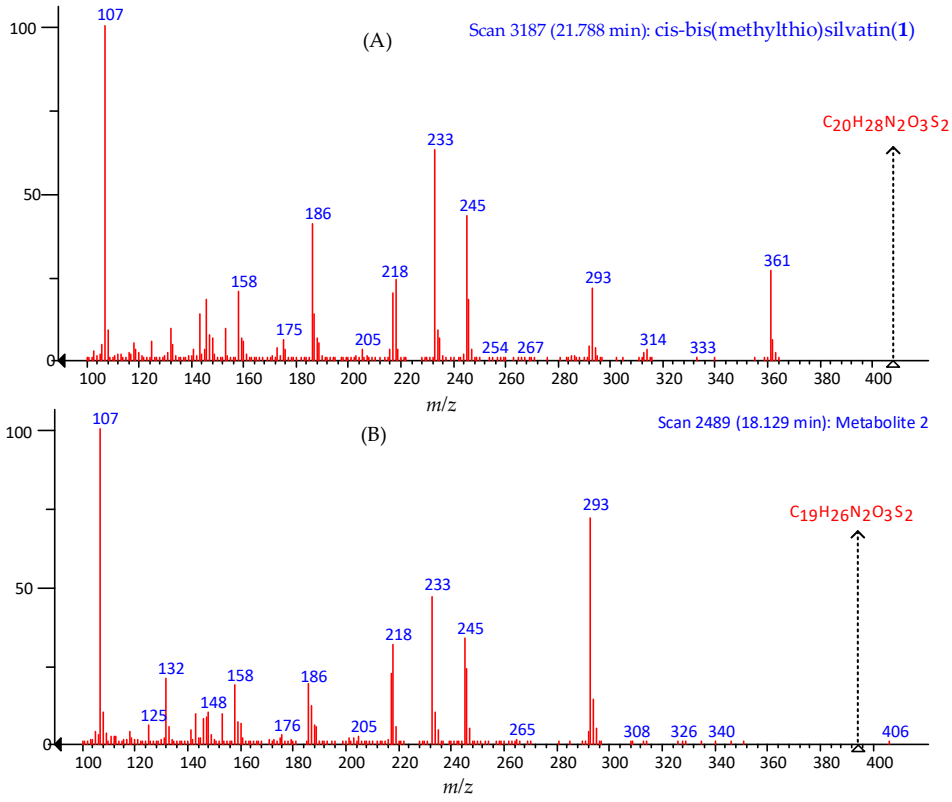

Figure 4.9. Comparison of 70 eV EI MS of the NMR characterized *cis*-bis(methylthio)silvatin (**1**, Figure 4.5.), A, with the spectrum of the unidentified target Metabolite **2**, B.

In addition, the substructure coloured in red in Figure 4.10. is assigned to this fragment on the basis the known structure of *cis*-bis(methylthio)silvatin (**1**).

This assignment is also supported by MS Interpreter, which readily connects the red coloured substructure to the *m/z* 107 peak in the mass spectrum of *cis*-bis(methylthio)silvatin (**1**).

From the above, there can be no doubt that *cis*-bis(methylthio)silvatin (**1**) and metabolite **2** share the substructure drawn in red in Figure 4.10.

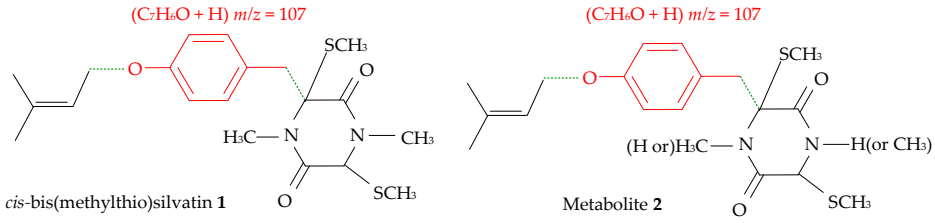

Figure 4.10. Substructure coloured in red has been assigned to ion $C_7H_7O^+$ at *m/z* = 107 in Figure 4.9 while substructures in black represent the neutral losses for its formation from the parent ion.

The second most abundant mass peak in the spectrum of *cis*-bis(methylthio)silvatin (**1**) has *m/z* 233. Formula $C_8H_{13}N_2O_2S_2^+$, is assigned to this peak from its isotopic pattern.

In Figure 4.11. it is shown that a fragment of composition $C_8H_{13}N_2O_2S_2^+$ can be readily created from the structure of *cis*-bis(methylthio)silvatin (**1**) by the simple scission of the benzylic σ bond (benzylic cleavage).

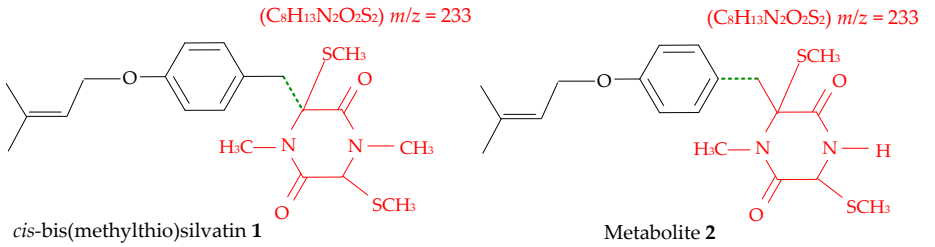

Figure 4.11. Substructure coloured in red has been assigned to ion $C_8H_{13}N_2O_2S_2^+$ at m/z = 233 in Figure 4.9 while substructure in black represents the neutral loss for its formation from the parent ion.

However, the analogous benzylic scission in the hypothetical structure of metabolite **2** would create the fragment $C_7H_{11}N_2O_2S_2^+$ which would appear as a peak at *m/z* 219, which is not.

In Figure 4.11. it is shown how this apparent contradiction can be resolved by simply replacing the scission at the benzylic position (which takes place for *cis*-bis(methylthio)silvatin (**1**)) with the scission of the phenylic σ bond (which presumably predominates for metabolite **2**.

The mass peak at *m/z* 293 is also shared by *cis*-bis(methylthio)silvatin (**1**) and metabolite **2**.

In the case of *cis*-bis(methylthio)silvatin (**1**), based on the known composition of its parent ion and its isotopic pattern, to this ion can be attributed the formula $C_{14}H_{17}N_2O_3S^+$ which implies a loss of $C_6H_{11}S$ from the molecular ion. This loss is interpreted structurally as shown in Figure 4.12.

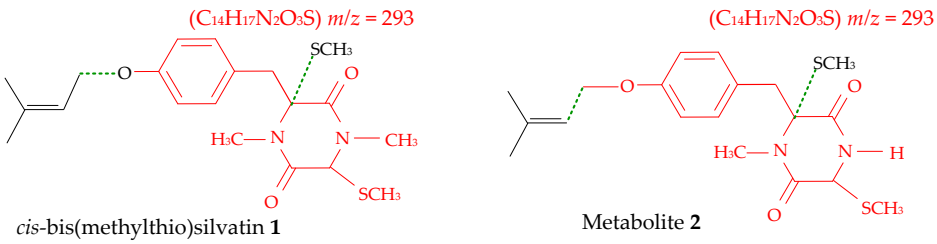

Figure 4.12. Substructure coloured in red has been assigned to ion $C_{14}H_{17}N_2O_3S^+$ at m/z = 293 in Figure 4.9 while substructures in black represent the neutral losses for its formation from the parent ion.

A loss of $C_6H_{11}S$ from the molecular ion of metabolite **2**, would create the ion $C_{13}H_{15}N_2O_3S^+$ at *m/z* = (394 - 115) = 279, which is not.

In Figure 4.12. it is shown that the shared ion $C_{14}H_{17}N_2O_3S^+$ (*m/z* = 293) can be created from the hypothesized structure of metabolite **2** by a loss of C_5H_9S, instead, which is produced by moving the scission of the σ bond from the allylic position [in the case of *cis*-bis(methylthio)silvatin (**1**)] to the C-C σ bond starting at the double bond of the alkyl side chain.

The two bonds scission which from *cis*-bis(methylthio)silvatin (**1**) produces the ion at *m/z* 293 takes place in two steps. In the first step only one of the two CH_3S- groups is eliminated and this produces the well-developed peak at *m/z* 361 (i.e., $C_{19}H_{25}N_2O_3S^+$) in spectrum (A). The formed ion then evolves to the shared ion $C_{14}H_{17}N_2O_3S^+$ (*m/z* = 293) by dissociation of the alkyl chain bonded to the phenolic oxygen atom.

On the contrary, there is no signal at *m/z* = 394 - 47 = 347 due to the dissociation of the CH_3S- group (which would produce the ion $C_{18}H_{23}N_2O_3S^+$) in the mass spectrum of metabolite **2**, but the intensity of peak at *m/z* 293 is about three times the intensity of the corresponding peak in the spectrum of *cis*-bis(methylthio)silvatin (**1**). This simply implies that the intermediate ion $C_{18}H_{23}N_2O_3S^+$ (*m/z* = 347) produced from metabolite **2** evolves, after its formation in the ion source, with a larger speed than ion $C_{19}H_{25}N_2O_3S^+$ (*m/z* = 361) to the shared ion $C_{14}H_{17}N_2O_3S^+$ (*m/z* = 293). So much so that the abundance lost at *m/z* = 347 in spectrum (B) is fully recovered as an increase of abundance at *m/z* 293. This explains the fundamental qualitative difference between the spectra in Figure 4.9.

For brevity, we omit further correlations which can be stated between the mass spectra in Figure 4.9 and which support the hypothesized structure of metabolite **2** exposed in Figure 4.8.

We also mention that when the spectrum of *cis*-bis(methylthio)silvatin (**1**) exposed in Figure 4.9 is submitted, along with the known structure, to the algorithm of MS Interpreter, as expected, about 85% of the total ionic abundance (i.e. 7078) in the spectrum is explained. The analogous operation performed with the mass spectrum of metabolite **2** and its hypothetical structure results in 83.8% of the total ionic abundance (i.e. 6322) being explained.

As anticipated above, the response of MS Interpreter was the same regardless of which of structures **2**A and **2**B in Figure 4.8. is submitted, implying that it is impossible to distinguish between these two isomers.

Finally, as a matter of fact, structures **2**A and **2**B in Figure 4.8. correspond to isomers A/B of saroclazine which are known fungal metabolites[53]. Then, it appears very reasonable to identify metabolite **2** with saroclazine A/B.

In this way, as sketched below, we have arrived at structures of compounds in Table 4.2. which could not be recovered in sufficient quantity and/or in a suitable degree of purity for NMR analysis. This strategy allows the specific detection of fungal compounds as well as the unambiguous determination of their structures. Metabolite structures reported in Figure 4.5. were assigned following the same way used for metabolite **2**.

Below is explained briefly the identification for each metabolite.

Formula of metabolite **3** ($C_{19}H_{26}N_2O_3S_2$) can be obtained from formula 1 of *cis*-bis(methylthio)silvatin by elimination of one molecule of methanethiole (CH_3SH) with the simultaneous formation of a double bond. On the basis of this observation structure of **1** is easily converted in the structure of metabolite **3** in Figure 4.5. which is strongly supported by the interpretation of the EI mass spectrum via MS Interpreter.

Apart from that, a search of PubChem database for the structure assigned to metabolite **3**, results in a structure identified by the PubChem CID101520130 (i.e. fusaperazine E).

On the other side, the case of metabolite **4** could not unambiguously be resolved in this way. In fact, from one side, metabolite **4** appears to be formed in the same way as metabolite **3** by elimination of a methanethiole molecule from the formula of **1**. As in the case of metabolite **3**, this justifies the fact that this metabolite molecule has one C, four H and one S atom less than **1** and a RDB

number one unit higher. However, this does not justify the fact that metabolite **4** exposes in its formula one more oxygen atom than **1**.

To solve this problem, we performed a structure similarity search in PubChem by starting with the SMILES (*Simplified Molecular Input Line Entry Specification*) string of **1**. This search resulted in a list of 61 compounds which, according to the PubChem search algorithm, had structures related to the structure of **1**.

By parsing this list, we found a single structure whose formula ($C_{19}H_{24}N_2O_4S$) coincides with formula assigned to metabolite **4**.

This structure is identified by the PubChem CID 122229044 and the IUPAC name: (6*S*)-1,4-dimethyl-6-[[4-(3-methylbut-2-enoxy)phenyl]methyl]-6-methylsulfanylpiperazine-2,3,5-trione.

The structure of this compound was readily downloaded from the PubChem site (as an .SDF structure file) and imported in MS Interpreter with the experimental mass spectrum associated to metabolite **4**.

This showed a very high degree of consistency between the downloaded structure and the mass spectrum and on this basis, structure exposed in Figure 4.5. was assigned to metabolite **4**.

Now we consider metabolites **5**, **6** and **7** in the last three rows of Figure 4.7. (formulas: $C_{20}H_{30}N_2O_5S_2$, $C_{15}H_{20}N_2O_3S_2$, $C_{13}H_{16}N_2O_3S_2$).

All of these metabolites share the same RDB which is one unit less than the RDB number of *cis*-bis(methylthio)silvatin (**1**). It is most reasonable to start with the idea that this decrease of the RDB takes place at the expenses of the double bond in the alchil side chain attached to the benzene ring in the structure of **1**. This idea is readily confirmed, by parsing the above-mentioned PubChem list of structures similar to **1** for the formula, $C_{20}H_{30}N_2O_5S_2$, associated to metabolite **5**. A single structure is associated to this formula which is identified by the PubChem CID 24179621 (common name: bilain B). The structure of bilain B (Figure 4.5.)

is formally derived from that of **1** by converting the double C=C bond of the alkyl side chain in a diol functional group. This beautifully justifies the decrease in RDB, the increase in O and H atoms in passing from the formula of **1** to $C_{20}H_{30}N_2O_5S_2$.

As in the previous case, we obtained a positive response when the structure of the bis TMS derivative of bilain B was compared, via MS Interpreter, to the EI Mass spectrum associated to metabolite **5**.

Unfortunately, in the above-mentioned PubChem list there was no structure associated to the formula of metabolite **6**, but there was a structure associated to the formula of metabolite **7**. This structure is identified by the PubChem CID 10267534 (i.e. fusaperazine A) and its structure is presented in Figure 4.5. The structure of the fusaperazine A can be derived from structure of **1** by the simultaneous substitution of the $-C_5H_9$ side chain and of the two $-CH_3$ methyl groups, bonded to the N atoms of the heterocyclic ring, with H atoms. This beautifully accounts for the decrease in the number of C and H atoms and RDB in passing from the formula ($C_{20}H_{28}N_2O_3S_2$) of **1** to the formula ($C_{13}H_{16}N_2O_3S_2$) associated to metabolite **7**.

As in previous cases, the structure of the TMS derivative of fusaperazine A was found to explain satisfactorily the mass spectrum associated with metabolite **7** using MS Interpreter and our own knowledge of fragmentation rules. In the light of the way in which the structure of fusaperazine A is connected to the structure of **1**, the structure of metabolite **6**, can easily be inferred.

In fact, the formula ($C_{15}H_{20}N_2O_3S$) of metabolite **6** can easily be derived from that of **1** through a path in which (as in the case of fusaperazine A) the alkyl side chain, $-C_5H_9$, is disconnected from the benzene ring and substituted with one H atom. The difference between this path and the path that leads from **1** to Fusaperazine A consists simply in the fact that the $-CH_3$ groups attached to the nitrogen atoms are left unchanged.

From this inference a structure is created which corresponds to the SMILES string: CN1C(C(=O)N(C(C1=O)(CC2=CC=C(C=C2)O)SC)C)SC.

When this SMILES string is searched in PubChem database, the searching algorithm readily finds a structure identified by the PubChem CID 13989134 and the IUPAC name (3*R*,6*R*)-3-[(4-hydroxyphenyl)methyl]-1,4-dimethyl-3,6-bis(methylsulfanyl)piperazine-2,5-dione.

After checking for its consistency with the mass spectrum associated to metabolite **6**, the above structure was definitely attributed to metabolite **6** (Figure 4.5).

Please note that structures of metabolites **4**, **5**, **6** and **7** reported in Figure 4.7 refers to the stereoisomer indexed in PubChem database but, since mass spectrometry cannot distinguish between stereoisomers, it is, strictly, not significant.

As can be easily predicted from its formula, ($C_{21}H_{23}N_3O_3$) and from the very large value of RDB (RDB = 13) the above approach cannot be extended to metabolite **9** in Table 4.2.

Furthermore, a blind formula search in PubChem database is immaterial because it finds thousands of results corresponding to formula $C_{21}H_{23}N_3O_3$. Nonetheless, a mycotoxin of formula $C_{21}H_{23}N_3O_3$ (named Brevianamide A, CAS#: 23402-09-7) is a well-known product from *Penicillium brevicompactum* and some other *Penicillium* species.

Brevianamide A is an aromatic heteropolycyclic compounds which, as can be predicted from its structure, can be silylated at least at one of the three nitrogen atoms. This is in agreement with the fact that the mass spectrum associated with metabolite **9** is the spectrum of its TMS derivative. When the structure of the TMS derivative of Brevianamide A is imported in MS Interpreter, a conspicuous number of peaks in the experimental mass spectrum are judged compatible, although several mass peaks are not predicted and are coloured in white. This is

to be expected in view of the structural complexity of brevianamide A which makes the prediction of fragmentation paths a difficult task. On this basis metabolite **9** is identified with brevianamide A (or its conformer brevianamide B, CAS#: 38136-92-4) whose structure can be seen in Figure 4.5.

Several thousand secondary metabolites have been isolated from fungi. Depending on their chemical structure, fungi-derived metabolites can display beneficial or harmful effects on human health. Several fungal metabolites have been reported to possess a broad range of biological activities (including antitumoral, antiviral, antimicrobial, anti-inflammatory and antioxidant effects) and therefore, they have been used as lead compounds in medicine for the development of effective therapies. However, a lot of fungal metabolites with negative effects on human health (for example mycotoxins) have also been identified. In this study, two main secondary metabolites were purified from the culture filtrate, which are typical products of the species *P. brevicompactum*. Particularly, mycophenolic acid is considered to characterize the metabolomic profile of this species so that, together with brevianamide A which was also detected through LC-MS and GC, it is regarded as a chemotaxonomic marker[54,55]. Conversely, asperphenamate, that is another product which is typical of all the species in the section *Brevicompacta*[56], was not detected in our study. The second purified product is *cis*-bis(methylthio)silvatin, a member of a homogeneous family of compounds within the large class of the epipolythiodioxopiperazines (ETPs)[57], has already been reported to display antibacterial activity against *Staphylococcus aureus* and, more importantly, cytotoxic effect against P388 lymphocytic leukemia and NS-1 cells[58]. Here, for the first time, we have investigated the effect of *cis*-bis(methylthio)silvatin on both two colorectal cancer cell lines, which have a different genetic profile: HCT116 expresses mutant β-catenin and K-RAS while Caco-2 has APC, β-catenin and p53 gene mutations[59] and, for comparison, an healthy human colon cell line. Our results have shown

that the compound exerts cytotoxic effect on the two human colon adenocarcinoma cell lines (i.e. Caco-2 and HCT116) with similar efficacy and potency (EC_{50} 29.3 µM and 35.3 µM for HCT 116 and Caco-2 respectively; % of inhibition at 100 µM 33.3 % and 25,3 % for HCT 116 and Caco-2, respectively). However, *cis*-bis(methylthio)silvatin is also able to reduce cell viability in the healthy epithelial cell line HCEC with more potency (EC_{50}: 0.57 µM) but less efficacy (% of inhibition at 100 µM: 22.1 %) compared to cancer cell lines. Because of a lack of selectivity on cancer cells as opposed to healthy cells, we cannot propose the use of this compound for the development of drugs with antitumoral effect on colorectal cancer. It was previously reported from just a single strain of *P. brevicompactum*[60], indicative of either its infrequent occurrence or inherent difficulties in its extraction and/or identification. Interestingly, our metabolomic analysis disclosed the ability by strain AN4 to produce several compounds belonging to the thiosilvatin series[48], in evident connexion with their biosynthetic relationships. So far thiosilvatins have been reported from just 23 strains belonging to 17 species from both marine and terrestrial sources[48]. Half of these strains belong to *Penicillium* species, indicating that the genetic basis for thiosilvatin biosynthesis may be rooted in this genus. At the same time the rest of the known producing strains are taxonomically unrelated, leaning for a much wider diffusion of these secondary metabolites. Considering that biosynthesis of ETPs is known to be encoded by a gene cluster[61], it seems likely that the occurrence of these compounds is independent from the phylogenetic relationships among the producing fungi, and may be more logically explained taking into account the transmission of the pertinent gene cluster by means of horizontal gene transfer (HGT). Such hypothesis is more and more considered realistic by experts in the field, based on the ecological opportunity resulting from hyphal contacts involving strains colonizing the same host[62]. It is to be expected

that additional findings concerning thiosilvatins may help to shed light on the mechanisms subtending the intriguing phenomenon of HGT.

4.5. References

1. Blunt, J.W., Copp, B.R., Hu, W.P., Munro, M.H., Northcote, P.T., Prinsep, M.R. (2009). Marine natural products. Nat. Prod. Rep. *26*, 170–244.
2. Nicoletti, R, Trincone, A. (2016). Bioactive compounds produced by strains of *Penicillium* and *Talaromyces* of marine origin. Mar Drugs. *14*, 37.
3. Ha, T.M., Ko, W., Lee, S.J., Kim, Y.-C., Son, J.-Y., Sohn, J.H., Yim, J.H., Oh, H. (2017). Anti-inflammatory effects of curvularintype metabolites from a marine-derived fungal strain *Penicillium* sp. SF-5859 in lipopolysaccharideinduced RAW264.7 Macrophages. Mar. Drugs. *15*, 282.
4. Moharram, A.M., Zohri, A.A., Omar, H.M., Abd El-Ghani, O.A. (2017). In vitro assessment of antimicrobial and anti-inflammatory potential of endophytic fungal metabolites extracts. Eur. J. Biol. Res. *7*, 234–244.
5. Dias, D.A., Urban, S., Roessner, U. (2012). A historical overview of natural products in drug discovery. Metabolites *2*, 303–336.
6. Neumann, K., Abdel-Lateff, A., Wright, A.D., Kehraus, S., Krick, A., König, G.M. (2007). Novel sorbicillin derivatives with an unprecedented carbon skeleton from the sponge-derived fungus *Trichoderma* species. Eur. J. Org. Chem. *14*, 2268–2275. Correction. Eur. J. Org. Chem. *2007*, 4125–4125.
7. Washida, K., Abe, N., Sugiyama, Y., Hirota, A. (2009). Novel secondary metabolites, spirosorbicillinols A, B, and C, from a fungus. Biosci. Biotechnol. Biochem. *73*, 1355–1361.
8. Matsuo, K., Sakaguchi, Y. (1997). Enantioselective synthesis of (-)-vertinolide. Chem Pharm Bull. *45*, 1620–1625.
9. Andrade, R., Ayer, W.A., Mebe, P.P. (1992). The metabolites of *Trichoderma longibrachiatum*. Part 1. Isolation of the metabolites and the structure of trichodimerol. Can. J. Chem. *70*, 2526–2535.

10. Evidente, A., Punzo, B., Andolfi, A., Cimmino, A., Melck, D., Luque, J. (2010). Lipophilic phytotoxins produced by *Neofusicoccum parvum*, a grapevine canker agent. Phytopathol. Mediterr. *49*, 74–79.
11. Harman, G.E., Howell, C.R., Viterbo, A., Chet, I., Lorito, M. (2004). Trichoderma species-opportunistic, avirulent plant symbionts. Nature Rev Microbiol. *2*, 43–56.
12. Vinale, F., Sivasithamparam, K., Ghisalberti, E.L., Marra, R., Woo, S.L., Lorito, M. (2008). *Trichoderma*–plant–pathogen interactions. Soil Biol. Biochem. *40*, 1–10.
13. Lorito, M., Woo, S.L., Harman, G.E., Monte, E. (2010). Translational research on Trichoderma: from 'Omics to the feld. Annu Rev Phytopathol. *48*, 395–417.
14. Ruiz, N., Roullier, C., Petit, K., Sallenave-Namont, C., Grovel, O., Pouchus, Y.F. (2013). Marine-derived *Trichoderma*: a source of new bioactive metabolites. In Trichoderma: biology and applications; Mukherjee PK, Horwitz BA, Singh US, Mukherjee M, Schmoll M, Eds.; CABI: Wallingford, UK. p. 247–279.
15. Vinale, F., Sivasithamparam, K., Ghisalberti, E.L., Woo, S.L., Nigro, M., Marra, R., Lombardi, N., Pascale, A., Ruocco, M., Lanzuise, S., et al. (2014). *Trichoderma* secondary metabolites active on plants and fungal pathogens. Open Mycol. J. *8*, 127–139.
16. Wu, B., Oesker, V., Wiese, J., Schmaljohann, R., Imhoff, J.F. (2014). Two new antibiotic pyridones produced by a marine fungus, *Trichoderma* sp. strain MF106. Mar Drugs *12*, 1208–1219.
17. Harned, A.M., Volp, K.A. (2011). The sorbicillinoid family of natural products: isolation, biosynthesis, and synthetic studies. Nat. Prod. Rep. *28*, 1790–1810.

18. Meng, J., Wang, X., Xu, D., Fu, X., Zhang, X., Lai, D., Zhou, L., Zhang, G. (2016). Sorbicillinoids from fungi and their bioactivities. Molecules *21*, 715.
19. Cram, D.J. (1948). Mold metabolites. II. The structure of sorbicillin, a pigment produced by the mold *Penicillium notatum*. J. Am. Chem. Soc. *70*, 4240–4243.
20. Evidente, A., Andolfi, A., Cimmino, A., Ganassi, S., Altomare, C., Favilla, M., De Cristofaro, A., Vitagliano, S., Sabatini, A.M. (2009). Bisorbicillinoids produced by the fungus *Trichoderma citrinoviride* affect feeding preference of the aphid Schizaphis graminum. J. Chem. Ecol. *35*, 533.
21. Abe, N., Murata, T., Yamamoto, K., Hirota, A. (1999). Bisorbibetanone, a novel oxidized sorbicillin dimer, with 1,1-diphenyl-2-picrylhydrazyl radical scavenging activity from a fungus. Tetrahedron Lett. *40*, 5203–5206.
22. Bringmann, G., Lang, G., Gulder, T.A.M., Tsuruta, H., Mühlbacher, J., Maksimenka, K., Steffens, S., Schaumann, K., Stöhr, R., Wiese, J., et al. (2005). The first sorbicillinoid alkaloids, the antileukemic sorbicillactones A and B, from a sponge-derived *Penicillium chrysogenum* strain. Tetrahedron. *61*, 7252–7265.
23. Sharma, J.N., Al-Omran, A., Parvathy, S.S. (2007). Role of nitric oxide in inflammatory diseases. Inflammopharmacology *15*, 252–259.
24. Hofseth, L.J. (2008). Nitric oxide as a target of complementary and alternative medicines to prevent and treat inflammation and cancer. Cancer Lett. *268*, 10–30.
25. Miller, J.D., McMullin, D.R. (2014). Fungal secondary metabolites as harmful indoor air contaminants: 10 years on. Appl Microbiol Biotechnol. *98*, 9953–9966.
26. Newman, D.J., Cragg, G.M. (2007). Natural products as sources of new drugs over the last 25 years. J. Nat. Prod. *70*, 461–477.

27. Abdel-Lateff, A., Fisch, K., Wright, A.D. (2009). Trichopyrone and other constituents from the marine spongederived fungus *Trichoderma* sp. Z Naturforsch *64c*, 186–192.
28. Trifonov, L.S., Dreiding, A.S., Hoesch, L., Rast, D.M. (1981). Isolation of four hexaketides from *Verticillium intertextum*. Helv Chim. Acta. *64*, 1843.
29. Du, L., Zhu, T., Li, L., Cai, S., Zhao, B., Gu, Q. (2009). Cytotoxic sorbicillinoids and bisorbicillinoids from a marinederived fungus *Trichoderma* sp. Chem. Pharm. Bul. *57*, 220–223.
30. Kopka, J., Schauer, N., Krueger, S., Birkemeyer, C., Usadel, B., Bergmüller, E., Dormann, P., Weckwerth, Y.G., Fernie, A.R., Steinhauser, D., Willmitzer, L. (2004). GMD@ CSB. DB: the Golm metabolome database. Bioinformatics *21*, 1635–1638.
31. Samson, R.A., Visagie, C.M., Houbraken, J., Hong, S.B., Hubka, V., Klaassen, C.H.W., Perrone, G., Seifert, K.A., Susca, A., Tanney, J.B., Varga, J., Kocsubé, S., Szigeti, G., Yaguchi, T., Frisvad, J.C., (2014). Taxonomy, identification and nomenclature of the genus *Aspergillus*. Stud. Mycol. *78*, 141–173.
32. Jones, E.B.G., Suetrong, S., Sakayaroj, J., Bahkali, A.H., Abdel-Wahab, M.A., Boekhout, T., Pang, K.L. (2015). Classification of marine Ascomycota, Basidiomycota, Blastocladiomycota and Chytridiomycota. Fungal Diver. *73*, 1–72.
33. Hawksworth, D.L., Crous, P.W., Redhead, S.A., Reynolds, D.R., Samson, R.A., Seifert, K.A., Taylor, J.W., Wingfield, M.J., Abasi, Ö., Aime, C., Asan, A., Bai, F.Y., de Beer,Z.W., Gegerow, D., Berikten, D., Boekhout, T., Buchanan, P.K., Burgess, T., Buzina, W., Cai, L., Cannon, P.F., Crane, J.L., Damm, U., Daniel, H.M., van Diepeningen, A.D., Druzhinina, I., Dyer, P.S., Eberhardt, U., Fell, J.W., Frisvad, J.C., Geiser, D.M., Geml, J., Glienke, C., Gräfenhan, T., Greonewald, J.Z., Groenewald, M., de Gruyter, J., Guého-

Kellerman, E., Guo, L.D., Hibbett, D.S., Hong, S.B., de Hoog, G.S., Houbraken, J., Huhndorf, S.M., Hyde, K.D., Ismail, A., Johnston, P.R., Kadaifciler, D.G., Kirk, P.M., Kõljalg, U., Kurtzman, C.P., Lagneau, P.E., Lévesque, C.A., Liu, X., Lombard, L., Meyer, W., Miller, A., Minter, D.W., Najafzadeh, M.J., Norvell, L., Ozeweskaya, S.M., Öziç, R., Pennycock, S.R., Peterson, S.W., Pettersson, O.V., Quaedvlieg, W., Robert, V.A., Riubal, C., Schnürer, J., Schroers, H.J., Shivas, R., Slippers, B., Spierenburg, H., Takashima, M., Takin, E., Thines, M., Thrane, U., Uztan, A.H., van Raak, M., Varga, J., Vasco, A., Verkley, G., Videira, S.I.R., de Vries, R.P., Weir, B.S., Yilmaz, N., Yurkov, A., Zhang, N. (2011). The Amsterdam declaration on fungal nomenclature. IMA Fungus *2*, 105–112.

34. Frisvad, J.C., Larsen, T.O. (2015). Chemodiversity in the genus Aspergillus. Appl. Microbiol. Biotechnol. *99*, 7859–7877.
35. Wang, Y.T., Xue, Y.R., Liu, C.H. (2015). A brief review of bioactive metabolites derived from deep-sea fungi. Mar. Drugs *13*, 4594–4616.
36. Xiao, L., Liu, H., Wu, N., Liu, M., Wei, J., Zhang, Y., Lin, X. (2013). Characterization of the high cytochalasin E and rosellichalasin producing-*Aspergillus* sp. nov. F1 isolated from marine solar saltern in China. World J. Microbiol. Biotechnol. *29*, 11–17.
37. Debbab, A., Aly, A.H., Proksch, P. (2013). Mangrove derived fungal endophytes–a chemical and biological perception. Fungal Diver. *61*, 1–27.
38. Yarden, O. (2014). Fungal association with sessile marine invertebrates. Front. Microbiol. *5*.
39. Zhang, Y., Wang, S., Li, X.M., Cui, C.M., Feng, C., Wang, B.G. (2007). New sphingolipids with a previously unreported 9-methyl-C20-sphingosine moiety from a marine algous endophytic fungus *Aspergillus niger* EN-13. Lipids *42*, 759–764.

40. Arora, D.K., Mukerji, K.G., Marth, E.H. (1991). Foods and feeds. In: Fungal metabolites in food processing. Handbook of applied mycology. Volume 3. Marcel Dekker, inc., New York, NY, USA, pp. 415–443 ISBN: 0-8247-8491-X.
41. Zeikus, J.G., Jain, M.K., Elankovan, P. (1999). Biotechnology of succinic acid production and markets for derived industrial products. Appl. Microbiol. Biotechnol. *51*, 545–552.
42. Currie, J.N. (1917). The citric acid fermentation of *A. niger*. J. Biol. Chem. *31*, 15–37.
43. Papagianni, M. (2007). Advances in citric acid fermentation by *Aspergillus niger*: biochemical aspects, membrane transport and modeling. Biotechnol. Adv. *25*, 244–263.
44. Hossain, M., Brooks, J.D., Maddox, I.S. (1984). The effect of the sugar source on citric acid production by *Aspergillus niger*. Appl. Microbiol. Biotechnol. *19*, 393–397.
45. Weidenmüller, H.L., Cavagna, F., Fehlhaber, H.W., Praeve, P. (1972). 2-Carboxymethyl-3-N-hexyl-maleic acid anhydride, a novel metabolite from an *Aspergillus*. Tetrahedron Let. *13*, 3519–3522.
46. NIST Standard Reference Data. Available online: http://www.nist.gov/srd/nist1a.cfm (accessed on 14 12 2019).
47. Sparkman, O.D., Penton, Z.E., Kitson, F.G. (2011). Gas Chromatography and Mass Spectrometry: A Practical Guide, 2nd ed. Elsevier Inc., Burlington, Massachusetts.
48. Salvatore, M.M., Nicoletti, R., DellaGreca, M., Andolfi, A. (2019). Occurrence and proprieties of thiosilvatins. Mar. Drugs *17*, 664.
49. Koul, M., Singh, S. (2017). *Penicillium* spp.: Prolific producer for harnessing cytotoxic secondary metabolites. Anti- Cancer Drugs *28*, 11–30.

50. Liu, S., Su, M., Song, S.J., Jung, J.H. (2017). Marine-derived *Penicillium* species as producers of cytotoxic metabolites. Mar. Drugs *15*, 329.
51. Nicoletti, R., Vinale, F. (2018). Bioactive compounds from marine-derived *Aspergillus*, *Penicillium*, *Talaromyces* and *Trichoderma* species. Mar. Drugs *16*, 408.
52. NIST program MS Interptreter. Available online: https://chemdata.nist.gov/mass-spc/interpreter/ (accessed on 14 12 2019).
53. Li, F., Guo, W., Wu, L., Zhu, T., Gu, Q., Li, D., Che, Q. (2018). Saroclazines A–C, thio-diketopiperazines from mangrove-derived fungi *Sarocladium kiliense* HDN11-84. Arch. Pharm. Res., *41*, 30-34.
54. Andersen, B. (1991). Consistent production of phenolic compounds by *Penicillium brevicompactum* for chemotaxonomic characterization. Antonie van Leeuwenhoek *60*, 115–123.
55. Frisvad, J.C., Smedsgaard, J., Larsen, T.O., Samson, R.A. (2004). Mycotoxins, drugs and other extrolites produced by species in *Penicillium* subgenus *Penicillium*. Stud. Mycol. *49*, 201–241.
56. Frisvad, J.C., Houbraken, J., Popma, S., Samson, R.A. (2013). Two new *Penicillium* species *Penicillium buchwaldii* and *Penicillium spathulatum*, producing the anticancer compound asperphenamate. FEMS Microbiol. Lett. *339*, 77–92.
57. Welch, T.R., Williams, R.M. (2014). Epidithiodioxopiperazines. occurrence, synthesis and biogenesis. Nat. Prod. Rep. *31*, 1376-1404.
58. Capon, R.J., Stewart, M., Ratnayake, R., Lacey, E., Gill, J.H. (2007). Citromycetins and bilains A–C: new aromatic polyketides and diketopiperazines from Australian marine-derived and terrestrial *Penicillium* spp. J. Nat. Prod. *70*, 1746-1752.

59. Ahmed, D., Eide, P.W., Eilertsen, I.A., Danielsen, S.A., Eknaes, M., Hektoen, M., Hektoen, M., Lothe, R.A. 2013. Epigenetic and genetic features of 24 colon cancer cell lines. Oncogenesis *2*, 71.
60. Ayer, W.A., Altena, I.V., Browne, L.M. (1990). Three piperazinediones and a drimane diterpenoid from *Penicillium brevi-compactum*. Phytochemistry *29*, 1661–1665.
61. Fox, E.M., Howlett, B.J. (2008). Biosynthetic gene clusters for epipolythiodioxopiperazines in filamentous fungi. Mycol. Res. *112*, 162–169.
62. Fitzpatrick, D.A. (2012). Horizontal gene transfer in fungi. FEMS Microbiol. Lett. *329*, 1–8.

CHAPTER 5

Secondary Metabolites Produced by a Strain of *Talaromyces pinophilus* from the Rhizosphere of Tobacco Plant

5.1. Introduction

Talaromyces is a genus described for the first time by Benjamin in 1955[1] as a sexual state of *Penicillium* characterised by soft walled ascomata covered with interwoven hyphae. The establishment of the recent concept of "one fungus, one name" in mycology[2] has stimulated reconsideration of the nomenclature of fungi. In fact, as a result of taxonomic revisions, *Penicillium* and *Talaromyces* are now ascribed to different families, belonging to distant phylogenetic lineages[3]. With a widespread occurrence in very diverse environmental contexts, from the soil to the sea[4-6], the species *Talaromyces pinophilus* (= *Penicillium pinophilum*) (Eurotiales: Trichocomaceae) has received increasing attention in mycological research for its ability to act as a fungal antagonist and plant-growth promoter[4,7,8], and for possible biotechnological applications based on the production of enzymes[9,10] and bioactive metabolites[11,12]. Data concerning the production of secondary metabolites can be quite informative for these fungi, particularly when they are indicative of the ability to synthesize some structural models that are only, or predominantly, found in *Talaromyces*[5]. In the present work, culture filtrate and mycelial extract of *T. pinophilus* strain LT6 isolated from the rhizosphere of tobacco plant in Lecce (Apulia, Italy) were investigated for the production of secondary metabolites. A new product with an unusual structure for a natural compound, namely talarodiolide, was purified from the culture filtrate.

5.2. Isolation and Identification of Metabolites

The crude $CHCl_3$ extract from the culture filtrates of *T. pinophilus* strain LT6 was purified by combined column (CC) and thin layer chromatography (TLC), leading to isolation of one new (**1**, Figure 5.1) and four known compounds (**2-5**, Figure 5.1). Structures of known compounds were confirmed by comparison of data obtained from OR, ^{1}H and ^{13}C NMR, and ESI-TOF MS with those reported

in the literature for 3-*O*-methylfunicone (OMF)[13], *cyclo*-(*S*-Pro-*R*-Leu), *cyclo*-(*S*-Pro-*S*-Ile)[14], and *cyclo*-(*S*-Pro-*S*-Phe)[15] (**2-5**).

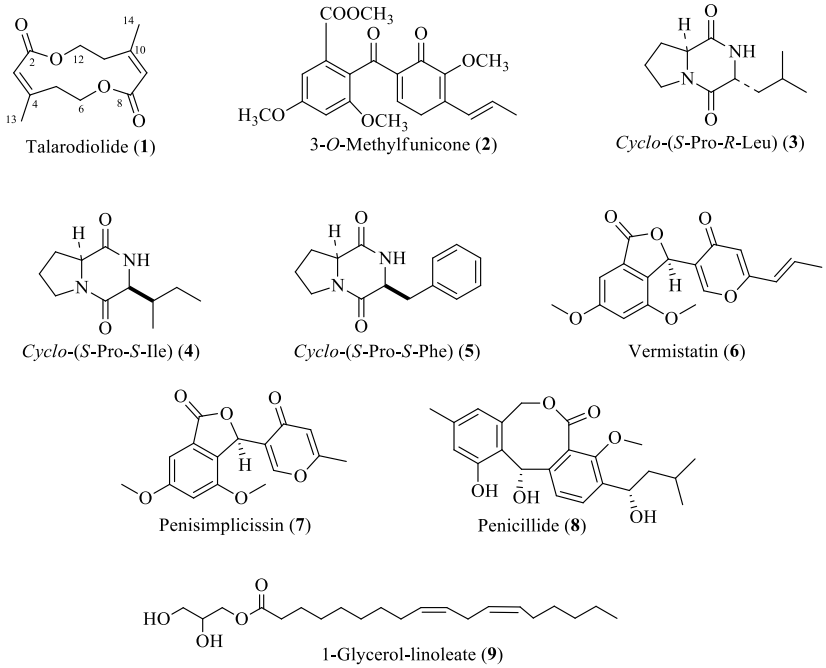

Figure 5.1. Structures of secondary metabolites produced by *Talaromyces pinophilus* LT6.

Compound **1**, isolated as amorphous solid, has a molecular weight of 224 *m*/*z* accounting for a molecular formula of $C_{12}H_{16}O_4$ and five degrees of unsaturation deduced from ESI-TOF MS. The ^{1}H NMR spectrum (see Chapter 6, Experimental Section) revealed one broad singlet methyl, one broad triplet and one triplet in aliphatic region, and a broad singlet of olefinic signals, in the ^{13}C NMR spectrum (See Chapter 6, Experimental Section) only six carbon signals were present indicating a highly symmetric molecule. The ^{1}H and ^{13}C resonances of **1** were assigned by combination of COSY and HSQC experiments. The COSY experiment showed homocorrelations among the olefinic proton at δ 5.84 with the

methyl at δ 2.03 and methylene at δ 2.40, this latter was also correlated with methylene at δ 4.40. The HSQC (see Chapter 6, Experimental Section) spectrum showed correlations of methyl at δ 2.03 with carbon at δ 22.4, two methylenes at δ 2.40 and 4.40 with carbons at δ 29.2 and 65.8, respectively, and one methine at δ 5.84 with carbon 116.8. The carbons at δ 164.6 and 157.7 were assigned to a carboxyl group and substituted sp^2 carbon, respectively. According to the structure in the HMBC (Table 5.1) spectrum the H_2-6 protons were correlated to the C-2 at 164.4, C-4 at 157.7 and C-5 at 29.2; furthermore the H_3-13 protons were correlated to C-3, C-4 and C-5 carbons. The analysis of NOESY (See Chapter 6, Experimental Section) spectrum evidenced NOE of the methyl at δ 2.03 and olefinic H-3 proton indicating a Z configuration at double bond.

Table 5.1. NMR data and HMBC correlations for talarodiolide (**1**) recorded in $CDCl_3$

1			
Position	**δ_C**	**δ_H (*J* in Hz)**	**HMBC**
2, 8	164.6 C	-	
3, 9	116.8 CH	5.84, brs	
4,10	157.7 C	-	
5, 11	29.2 CH_2	2.40, brt, 6.3	
6, 12	65.8 CH_2	4.40, t, 6.3	C-2,C-4, C-5
13, 14	22.4 CH_3	2.03, brs	C3, C-4, C-5

These results, and the molecular formula of $C_{12}H_{16}O_4$ suggest that **1** is a symmetrical macrodiolides, 4,10-dimethyl-1,7-dioxa-cyclododeca-3,9-diene-2,8-dione. This structure was confirmed by data from ESI-TOF MS recorded in positive mode. The spectrum showed the sodiated dimeric, dimeric, sodiated and pseudomolecular ions $[2M+Na]^+$, $[2M+H]^+$, $[M+Na]^+$, $[M+H]^+$ at *m/z* 471, 449, 247, and 225, respectively.

In this study, an EI mass spectrum at 70eV of all isolated metabolites was acquired and compiled in a custom MS target library to be employed to detect metabolites separated in the crude extracts. The acquired mass spectrum was incorporated in the custom MS library to be used for interpreting GC-MS measurements to be performed directly on samples of mycelium and culture filtrates extracts obtained.

5.3. Discussion

The present work describes the isolation and structural characterization of the first 12-membered macrodiolide, named talarodiolide, from the culture filtrate of this strain. The structure of 4,10-dimethyl-1,7-dioxa-cyclododeca-3,9-diene-2,8-dione (i.e. talarodiolide) was assigned essentially on the basis of NMR and MS data. Symmetric macrodiolides have been reported from many natural sources, and displayed some interesting effects, such as antibacterial, antifungal and cytotoxic activities[15]. However, in the light of the current knowledge no 12-membered macrodiolide has been isolated from natural sources so far.

In addition, the production of secondary metabolites by *T. pinophilus* LT6 was investigated after extraction of mycelium. Separation and purification procedures (i.e. CC and TLC) afforded the isolation of 3-*O*-methylfunicone (OMF) (**2**), and other known compounds identified as vermistatin (**6**)[16] penisimplicissin (**7**)[17], penicillide (**8**)[18], and 1-glycerol-linoleate (**9**) (Figure 5.1). OMF is part of a homogeneous family comprising about 20 structurally related secondary metabolites which have been mainly characterized from cultures of *Talaromyces* strains[19]. It has disclosed notable antitumor properties based on several biomolecular mechanisms of action resulting from a series of preclinical assays[20-24]. In the case of **9**, preliminary NMR investigation showed typical signals of monoglycerides of polyunsatured fatty acids[25]. GC-MS measurements confirmed NMR data and unequivocally revealed the presence of this

monoglyceride by comparison its mass spectrum with the reference mass spectra gathered in NIST 14 Mass Spectral library (2014)[26].

Figure 5.2A and B show the total ion chromatograms (TICs) of the extracts of culture filtrate and mycelium, respectively.

Apart from the isolated metabolites, Figure 5.2A shows the presence of some fatty acids and their methyl esters in the mycelial extract. In fact, due to the high sensitivity of this technique, GC/MS was able to detect them, combining the retention indices and the reference mass spectra gathered in NIST 14 Mass Spectral library (2014)[26].

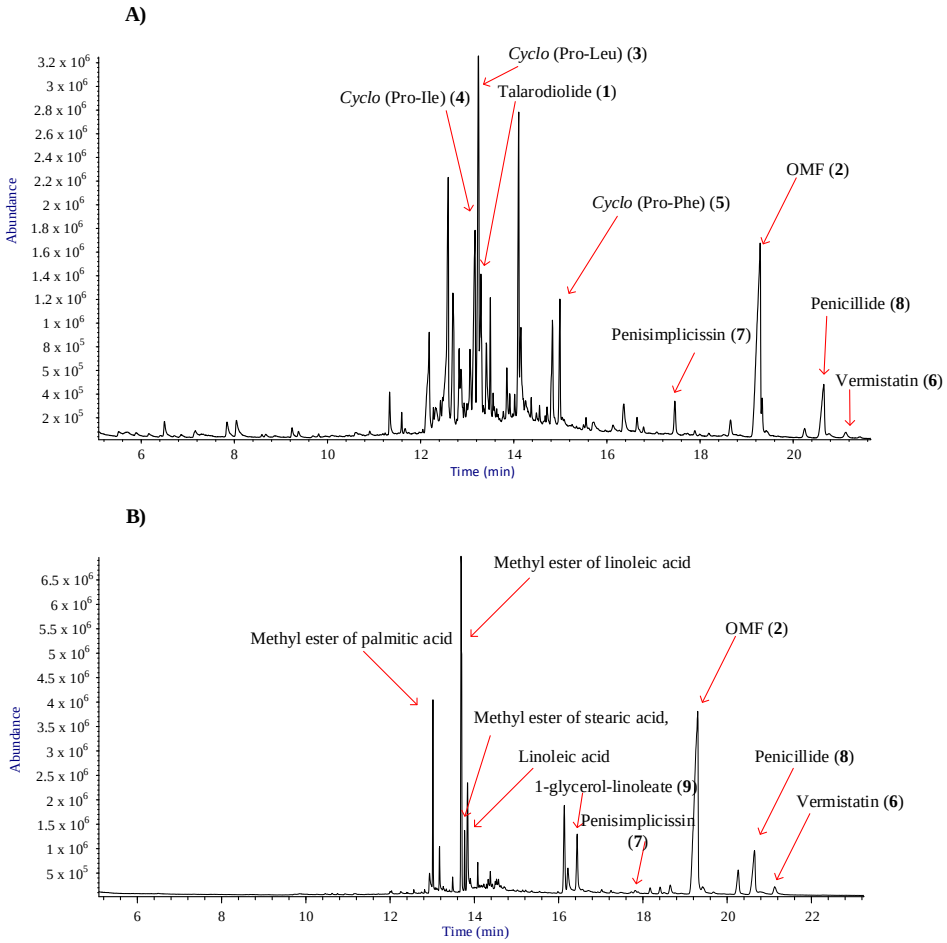

Figure 5.2. Annotated total ion chromatograms (TICs) acquired by culture filtrate extract (A) and mycelial extract (B) of *T. pinophylus*.

Within the frame of the overall strategy, a very important outcome of the procedures arises from the fact that crude extracts were analyzed by GC-MS to check the presence of the isolated metabolites. Notwithstanding some metabolites were not isolated from the culture filtrate, AMDIS attributes peaks in the TIC, as in the case of penicillide, vermistatin and penisimplicissin. Hence, GC-MS analysis is very useful in assessing the possible diversity in the pattern of metabolites extracted from the different sources. With exception of talarodiolide,

1-glycerol-linoleate and the diketopiperazines, all metabolites were detected in both crude extracts, while fatty acids and their esters are present in the mycelial extract only. This is in line with the reported occurrence of the latter compounds in the cell membrane of fungi[27].

5.4. References

1. Benjamin, C.R. (1955). Ascocarps of *Aspergillus* and *Penicillium*. Mycologia, 47, 669-687.
2. Hawksworth, D.L., Crous, P.W., Redhead, S.A., Reynolds, D.R., Samson, R.A., Seifert, K.A., Taylor, J.W., Wingfield, M.J., Abaci, O., Aime, C., et al. (2011). The Amsterdam declaration on fungal nomenclature. IMA Fungus *2*, 105–112.
3. Yilmaz, N., Visagie, C.M., Houbraken, J., Frisvad, J.C., Samson, R.A. (2014). Polyphasic taxonomy of the genus *Talaromyces*. Stud. Mycol. *78*, 175–341.
4. Nicoletti, R., De Stefano, M., De Stefano, S., Trincone, A., Marziano, F. (2004). Antagonism against *Rhizoctonia solani* and fungitoxic metabolite production by some *Penicillium* isolates. Mycopathologia *158*, 465–474.
5. Nicoletti, R., Salvatore, M.M., Andolfi, A. (2018). Secondary matabolites of mangrove-associated strains of *Talaromyces*. Mar. Drugs *16*, 12.
6. Nicoletti, R., Trincone, A. (2016). Bioactive compounds produced by strains of *Penicillium* and *Talaromyces* of marine origin. Mar. Drugs *14*, 37.
7. Pandey, A., Das, N., Kumar, B., Rinu, K., Trivedi, P. (2008). Phosphate solubilization by *Penicillium* spp. isolated from soil samples of Indian Himalayan region. World J. Microbiol. Biotechnol. *24*, 97–102.
8. Wani, Z.A., Mirza, D.N., Arora, P., Riyaz-Ul-Hassan, S. (2016). Molecular phylogeny, diversity, community structure, and plant growth promoting properties of fungal endophytes associated with the corms of saffron plant: An insight into the microbiome of *Crocus sativus* Linn. Fungal Biol. *120*, 1509–1524.
9. Hansen, G.H., Lübeck, M., Frisvad, J.C., Lübeck, P.S., Andersen, B. (2015). Production of cellulolytic enzymes from ascomycetes: Comparison of solid state and submerged fermentation. Process Biochem. *50*, 1327–1341.

10. Li, C.X., Zhao, S., Zhang, T., Xian, L., Liao, L.S., Liu, J.L., Feng, J.X. (2017). Genome sequencing and analysis of *Talaromyces pinophilus* provide insights into biotechnological applications. Sci. Rep. *7*, 490.
11. Ohte, S., Matsuda, D., Uchida, R., Nonaka, K., Masuma, R., Omura, S., Tomoda, H. (2011). Dinapinones, novel inhibitors of triacylglycerol synthesis in mammalian cells, produced by *Penicillium pinophilum* FKI-3864. J. Antibiot. *64*, 489–494.
12. Nicoletti, R., Scognamiglio, M., Fiorentino, A. (2014). Structural and bioactive properties of 3-O-methylfunicone. Mini Rev. Med. Chem. *14*, 1043–1047.
13. De Stefano, S., Nicoletti, R., Milone, A., Zambardino, S. (1999). 3-*O*-Methylfunicone, a fungitoxic metabolite produced by the fungus *Penicillium pinophilum*. Phytochemistry, 52, 1399–1401.
14. Adamczeski, M., Reed, A.R., Crews, P. (1995). New and known diketopiperazines from the Caribbean sponge, *Calyx* cf. *podatypa*. J. Nat. Prod. *58*, 201–208.
15. Wang, G., Dai, S., Chen, M., Wu, H., Xie, L., Luo, X., Li, X. (2010). Two diketopiperazine cyclo-(Pro-Phe) isomers from marine bacteria *Bacillus subtilis* sp. 13–2. Chem. Nat. Compd. *46*, 583–585.
16. Fuska, J., Uhrin, D., Proksa, B., Votický, Z., Ruppeldt, J. (1986). The structure of vermistatin, a new metabolite from *Penicillium vermiculatum*. J. Antibiot. *39*, 1605–1608.
17. Komai, S.I., Hosoe, T., Itabashi, T., Nozawa, K., Yaguchi, T., Fukushima, K., Kawai, K. (2005). New vermistatin derivatives isolated from *Penicillium simplicissimum*. Heterocycles *11*, 2771–2776.
18. Komai, S.I., Hosoe, T., Itabashi, T., Nozawa, K., Yaguchi, T., Fukushima, K., Kawai, K.I. (2006). New penicillide derivatives isolated from *Penicillium simplicissimum*. J. Nat. Med. *60*, 185–190.

19. Nicoletti, R., Manzo, E., Ciavatta, L. (2009). Occurence and bioactivities of funicone-related compounds. Int. J. Mol. Sci. *10*, 1430–1444.
20. Buommino, E., Paoletti, I., De Filippis, A., Nicoletti, R., Ciavatta, M.L., Menegozzo, S., Menegozzo, M., Tufano, M.A. (2010). 3-*O*-Methylfunicone, a metabolite produced by *Penicillium pinophilum*, modulates ERK1/2 activity, affecting cell motility of human mesothelioma cells. Cell Prolif. *43*, 114–123.
21. Buommino, E., Tirino, V., De Filippis, A., Silvestri, F., Nicoletti, R., Ciavatta, M.L., Pirozzi, G., Tufano, M.A. (2011). 3-*O*-Methylfunicone, from *Penicillium pinophilum*, is a selective inhibitor of breast cancer stem cells. Cell Prolif. *44*, 401–409.
22. Buommino, E., De Filippis, A., Nicoletti, R., Menegozzo, M., Menegozzo, S., Ciavatta, M.L., Rizzo, A., Brancato, V., Tufano, M.A., Donnarumma, G. (2012). Cell-growth and migration inhibition of human mesothelioma cells induced by 3-*O*-methylfunicone from *Penicillium pinophilum* and cisplatin. Investig. New Drugs *30*, 1343–1351.
23. Nicoletti, R., Buommino, E., De Filippis, A., Lopez-Gresa, M.P., Manzo, E., Carella, A., Petrazzuolo, M., Tufano, M.A. (2008). ioprospecting for antagonistic Penicillium strains as a resource of new antitumor compounds. World J. Microbiol. Biotechnol. *24*, 189–195.
24. Baroni, A., De Luca, A., De Filippis, A., Petrazzuolo, M., Manente, L., Nicoletti, R., Tufano, M.A., Buommino, E. (2009). 3-*O*-methylfunicone, a metabolite of *Penicillium pinophilum*, inhibits proliferation of human melanoma cells by causing G2 + M arrest and inducing apoptosis. Cell Prolif. *42*, 541–553.
25. Nieva-Echevarría, B., Goicoechea, E., Manzanos, M.J., Guillén, M.D. (2014). A method based on 1H-NMR spectral data useful to evaluate the hydrolysis level in complex lipid mixtures. Food Res. Int. *66*, 379–387.

26. NIST Standard Reference Data. Available online: http://www.nist.gov/srd/nist1a.cfm (accessed on 14 12 2019).
27. Vinale, F., Nicoletti, R., Lacatena, F., Marra, R., Sacco, A., Lombardi, N., d'Errico, G., Digilio, M.C., Lorito, M., Woo, S.L. (2017). Secondary metabolites from the endophytic fungus *Talaromyces pinophilus*. Nat. Prod. Res. *31*, 1778–1785.

.

CHAPTER 6

Experimental Section

6.1. General Experimental Procedures

6.1.1. Fungi

Fungi studied in this work were isolated by diverse researchers which take part to this project. Strains of *Lasiodiplodia theobromae* and *Macrophomina phaseolina* have been provided by Prof. Artur Alves, Department of Biology – University of Aveiro (PT). The isolate of *Neofusicoccum vitifusiforme* was provided by Prof Santelle Burruano, Department of Agricultural, Food and Forest Sciences (SAAF) – University of Palermo (IT). Marine-derived fungi and *Talaromyces pinophilus* have been provided by Dr. Rosario Nicoletti, Council for Agricultural Research and Economics, Research Centre for Olive, Citrus and Tree Fruit, Caserta (IT).

6.1.2. Conventional Chromatographic Techniques

Thin-layer chromatography (TLC) was performed on silica gel plates (Kieselgel 60, F_{254}; 0.25; Merck, Darmstadt, Germany). The spots were visualized by exposure to ultraviolet (UV) radiation (253 nm) or by spraying first with 10% sulfuric acid (H_2SO_4) in methanol followed by heating at 110°C for 10 min. Chromatography was performed on silica gel column (Kieselgel 60, 0.063–0.200 mm; Merck).

6.1.3. Optical Rotation and NMR Analysis

Optical rotations of pure metabolites were measured in chloroform ($CHCl_3$) or in methanol (CH_3OH) on a Jasco polarimeter (Tokyo, Japan). ^{1}H and ^{13}C nuclear magnetic resonance (NMR) spectra were recorded at 400 and 100 MHz, respectively, in deuterated chloroform ($CDCl_3$) or in deuterated methanol (CD_3OD), on Bruker (Karlsruhe, Germany) spectrometers, and the same solvents were used as internal standards. Carbon multiplicities were determined by COSY (Correlation Spectroscopy)-45, HSQC (Heteronuclear Single Quantum Coherence), HMBC (Heteronuclear Multiple Bond Correlation) and NOESY

(Nuclear Overhauser Enhancement Spectroscopy) experiments were performed using standard Bruker microprograms.

6.1.4. GC-MS Analysis

Gas chromatography–mass spectrometry (GC-MS) measurements were performed using an Agilent 6850 GC instrument equipped with an HP-5ms capillary column (5% phenyl methyl polysiloxane stationary phase) and the Agilent 5973 Inert MS detector (used in the scan mode). Helium was employed as the carrier gas, at a flow rate of 1 mL min^{-1}. Unless otherwise stated, the injector temperature was 250 °C and during the run a temperature ramp raised the column temperature from 70 °C to 280 °C: 70 °C for 1 min; 10 °C min^{-1} until reaching 170 °C and 30 °C min^{-1} until reaching 280 °C; 280 °C for 20 min. The electron impact (EI) ion source was operated at 70 eV and at 200 °C. The quadrupole mass filter was kept at 250 °C and was programmed to scan the range 45-550 m/z at a frequency of 3.9 Hz.

GC-MS data were acquired on samples (i.e. crude extracts, chromatographic fractions and purified metabolites) directly, after methylation with diazomethane or trimethylsililation with *N,O*-bis(trimethylsilyl)trifluoroacetamide (BSTFA).

For GC-MS sample processing after trimethylsilylation, 1 g L^{-1} solutions were prepared by dissolving a small amount (typically a few mg) of each sample in a small volume of a volatile solvent (typically methanol or chloroform). For derivatization, 200 μL of the solution were transferred to a 2 mL vial and the solvent evaporated under vacuum in order to completely remove water which destroys BSTFA. Next, 100 μL of acetonitrile (or other aprotic solvent) and 100 μL of BSTFA were added to the residue in the vial which, then, was hermetically closed with a screw cap fitted with a double-faced PTFE/Silicone liner and sonicated for 1 min. The vial was finally submitted to a thermal treatment to speed up trimethylsilylation reactions which tend to be slow at room temperature and,

after cooling, 1 µL of the derivatized mixture was injected in the GC. The heat treatment of the derivatization mixture was performed either in the conventional way by mounting the tightly sealed 2 ml vials in a heated aluminum block with holes for vials (typically 30 min at 100 °C) or by heating in a microwave oven (typically 2 min at a microwave power output of 800 W)[1].

For GC-MS sample processing after methylation, an ethereal solution of CH_2N_2 was slowly added to 2 mg of sample (i.e. crude extract or chromatographic fraction) dissolved in MeOH (1.5 mL) until a yellow colour was persistent. The reaction mixture was stirred at room temperature for 4 h. The solvent was evaporated under a N_2 stream andthe residue used for GC-MS analysis.

Compounds were identified by retention index (RI) and its mass spectrum compared with those present in databases by employing the National Institute of Standards and Technology (NIST) Mass Spectral Search Program v2.0g which explore, among others, NIST 14 Mass Spectral library[2], the Golm Metabolome Database and target custom mass spectra library. High-quality mass spectra were obtained employing the NIST deconvolution software Automatic Mass spectral Deconvolution & Identification System (AMDIS)[3].

6.1.5. LC-MS Analysis

LC-MS analyses were conducted on an Agilent HP 1260 Infinity Series liquid chromatography equipped with a DAD system coupled to a Q-TOF mass spectrometer. An Ascentis® Express C18 column (3.0 x 50 mm, 2.7 µm, Supelco, Bellefonte, PA, USA) was used for chromatographic separation. The UV spectra were collected by DAD every 0.4 s from 190 to 750 nm with a resolution of 2 nm. The MS system was equipped with a Dual Electrospray Ionization (ESI) source and operated with Agilent MassHunter Data Acquisition Software, rev. B.05.01 in the positive mode. Mass spectra were recorded within *m/z* range 50-1700 as centroid spectra, with 3 scans per second. The mass spectrometer was calibrated

using the ESI-L Low Concentration Tuning Mix (Agilent Technologies). Additionally, real-time lock mass correction was performed using purine ($C_5H_4N_4$ at *m/z* 121.050873, 10 µmol L^{-1}) and hexakis ($^1H,^1H$, 3H-tetrafluoropentoxy)-phosphazene ($C_{18}H_{18}O_6N_3P_3F_{24}$ at *m/z* 922.009798, 2 µmol L^{-1}), according to manufacturer's instructions (Agilent Technologies). Solvents were LC–MS grade, and all other chemicals were analytical grade purchased from Sigma-Aldrich, (Saint Louis, MO, USA), unless otherwise stated.

Data were evaluated using MassHunter Qualitative Analysis Software B.06.00 and comparisons were made to known compounds in an in-house database combined with data from the literature. Positive identifications of fungal metabolites were considered for analysis if the compound was detected with a mass error below 10 ppm and with a sufficient score.

6.2. Experimental Procedures for Chemical and Biological Analysis of Secondary Metabolites by *Lasiodiplodia theobromae* Strains

6.2.1. Production, Extraction of Secondary Metabolites by L. theobromae *Strains*

Strain CAA019 was originally isolated from a coconut tree in Brazil, strain CBS339.90 (obtained from the Westerdijk Fungal Biodiversity Institute) was isolated from a human patient from Jamaica and LA-SV1 and LA-SOL3 were isolated from grapevines in Peru[4]. Cultures were maintained at room temperature on potato dextrose agar (PDA) (Merck). Before inoculation, each strain was cultured on PDA at 25 °C for 4 d. Mycelium was scraped from PDA plates and suspended in 5 mL of sterilized ultrapure water. This mycelial suspension was added to 1 L Erlenmeyer flasks containing 250 mL of liquid medium. All the strains under examination were grown in Czapek medium amended with 2% cornmeal (pH 5.7) and incubated for 21d in the dark at 25 or 37 °C, without

agitation. Grapevine strains (i.e. LA-SV1 and LA-SOL3) were also grown in Potato Dextrose Broth (pH 5.6) with 0 mM and 10 mM of GABA and incubated for 4 days in the dark at 25 °C. For convenience, the preparation of samples is represented in a schematic form in Figure 6.1.

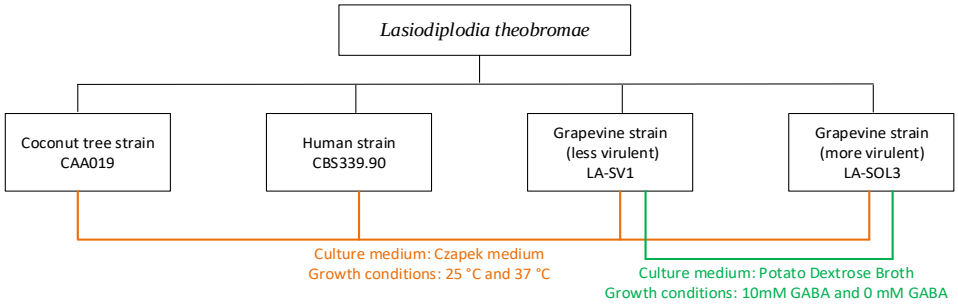

Figure 6.1. Schematic representation of *Lasiodiplodia theobromae* strains under examination and growth conditions.

Culture filtrates were obtained by filtering culture through sterile 0.45 µm cellulose membranes in a vacuum system. The culture filtrates were extracted three times with same volume of ethyl acetate. The crude extracts were dried with sodium sulfate anhydrous (Na_2SO_4) and evaporated under reduced pressure, yielding a brown oil residues (Table 6.1).

Table 6.1. Summary of cultural conditions and crude extracts weights.

Strain	Culture medium	Growth temperature	GABA concentration	Volume culture filtrate (L)	Crude extract weight (mg)
CAA019	Czapek	25 °C	/	1.60	128.4
	Czapek	37 °C	/	0.40	160.6
CBS339.90	Czapek	25 °C	/	3.00	147.8
	Czapek	37 °C	/	1.60	252.2
LA-SOL3	Czapek	25 °C	/	0.65	120.3
	Czapek	37 °C	/	1.60	432.7
	PDB	25 °C	10 mM	0.95	84.7

	PDB	25 °C	0 mM	0.91	113.7
LA-SV1	Czapek	25 °C	/	2.50	413.9
	Czapek	37 °C	/	1.00	524.4
	PDB	25 °C	10 mM	0.90	76.1
	PDB	25 °C	0 mM	0.95	114.6

These extracts were purified by silica gel chromatography (column chromatography (CC) and/or thin layer chromatography (TLC)) giving the metabolites reported in Figure 3.3.

6.2.2. Phytotoxicity Assays

Phytotoxicity was assessed on tomato cuttings and on tomato leaves. Phytotoxicity of culture filtrates diluted in distilled sterile water, were tested on tomato cuttings. Tomato stems of rootless plants (2 weeks old) were dipped in a vial with 2 mL of culture filtrate. After 24 h incubation at room temperature, the solution was replaced by 2 mL of sterile distilled water for additional 48 h. Sterile distilled water, PDB medium and 10 mM solution of GABA were used as controls. Using a 0-4 scale (0: no symptoms; 1: slight withering; 2: intermediate withering; 3: severe withering; 4: full withering), symptoms were recorded and converted to a percentage to evaluate the phytotoxic activity (Figure 6.2). All assays were conducted in triplicate.

Figure 6.2. Typical outcome of phytotoxic assays on tomato cuttings.

For the leaf puncture assay, young tomato plant leaves punctured with a sterile needle were used. Crude extracts/pure compounds were dissolved in methanol and then a stock solution (4 % methanol) was made with distilled water. A droplet of sample solution was applied on the adaxial surface of leaves. As control, a droplet of 4 % methanol was used. The leaves were kept in a moist chamber to prevent the droplets from drying and were observed daily. The visual symptoms were recorded after 10 days of incubation. The lesion diameter was expressed in cm. All assays were carried out in triplicate.

6.2.3. Cytotoxicity Assays on Mammalian Cell Lines

In vitro cytotoxicity was performed as previously reported with slight modifications[5,6]. Two cell lines were grown and maintained according to Ammerman et al. (2009)[7]: a Vero cell line (ECACC 88020401, African Green Monkey Kidney cells, GMK clone) and a 3T3 cell line (ECACC 86110401, mouse embryonic fibroblasts, A31 clone A31). The microtiter plates were incubated at 37 °C in 5 % CO_2 for 24 h. Vero and 3T3 cells were treated, for 20 h, with culture filtrates or pure metabolites (1:1 in DMEM - Dulbecco's Modified Eagle

Medium). Two different concentrations of each sample were analyzed [crude extracts: 1 mg mL^{-1} and 0.5 mg mL^{-1}; pure compounds: 1 and 0.5 mg mL^{-1}] in Phosphate Buffered Saline (PBS)]. After the incubation period, the medium was removed by aspiration and 50 µL of DMEM with 10 % resazurin (0.1 mg mL^{-1} in PBS) was added to each well to assess cell viability. The microtiter plates were incubated at 37 °C in 5 % CO_2 during 3 h. The absorbance was read at 570 and 600 nm wavelengths in a microtiter plate spectrophotometer (Biotek Synergy, Winooski, VT, USA). PBS and Czapek medium were used as controls.

6.2.4. Statistical Analysis

Two-way analysis of variance (ANOVA), followed by a Bonferroni multiple comparison test, was used to determine the statistical significance of cytotoxicity of each strain within the same temperature against the control or between pure metabolites and control ($P < 0.05$, $P < 0.01$, $P < 0.001$, $P < 0.0001$). All the analyses were performed with GraphPad Prism 6 (GraphPad Software, La Jolla, California, USA). Data are shown as the average of three independent replicates of each condition.

6.2.5. Metabolite Purification of CAA019 Crude Extract Obtained at 25 °C in Czapek Medium

The culture filtrate was obtained as described above, acidified to pH 2 with 1 M of formic acid and extracted exhaustively with ethyl acetate. After solvent evaporation, 128.4 mg of crude extract, which had the appearance of brown oil was obtained. The crude extract was submitted to fractionation by column chromatography eluted with $CHCl_3$/*i*-PrOH (95:5, *v/v*), originating ten homogeneous fractions of which the last fraction was eluted with methanol (fractions A 4.8 mg, B 4.3 mg, C 5.3 mg, D 4.9 mg, E 24.2 70 mg, F 14.5 mg, G 10.5 mg, H 3.3 mg, I 0.9 mg, L 51.8 mg). TLC spots were visualized by exposure to UV radiation (253 nm), or by spraying first with 10% of sulfuric acid in

methanol followed by heating at 110 °C for 10 min. The residue from fraction B, obtained as yellow oil, was identified as lasiodiplodin (**3**). An additional small amount of lasiodiplodin was obtained after purification of residue from fraction C by TLC on silica gel eluted with $CHCl_3$/*i*-PrOH (95:5, *v/v*) and 6:4 *n*-hexane/Me_2CO mixtures [*Rf* = 0.50 (TLC on silica gel: $CHCl_3$/*i*-PrOH (95:5, *v/v*) eluent); *Rf* = 0.78 (TLC on silica gel: *n*-hexane/Me_2CO (6:4, *v/v*) eluent)]. From this same TLC run a further metabolite, identified as (-)- jasmonic acid (**2**), was obtained as yellow oil [0.7 mg, *Rf* = 0.48 (TLC on silica gel: $CHCl_3$/*i*-PrOH (95:5, *v/v*) eluent) and *Rf* = 0.58 (TLC on silica gel: *n*-hexane/Me_2CO (6:4, v/v) eluent)]. Residue from fraction E was purified by preparative TLC on silica gel eluted with $CHCl_3$/*i*-PrOH (9:1, *v/v*) mixture and on reversed phase eluted with EtOH/H_2O (6:4, *v/v*) mixture. A white solid, which could be identified as 3-indolecarboxylic acid (**1**) was recovered [15.3 mg, *Rf* = 0.60 (TLC on silica gel: $CHCl_3$/*i*-PrOH (9:1, *v/v*) eluent) and *Rf* = 0.60 (TLC on reversed phase: 6:4, EtOH/H_2O eluent)] (Scheme 6.1).

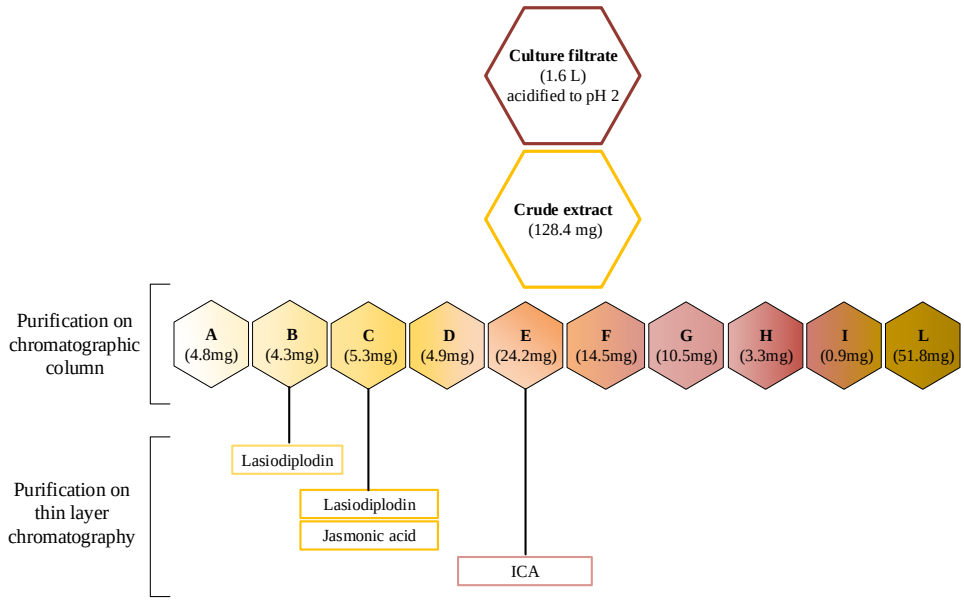

Scheme 6.1. Schematic representation of purification process of CAA019 crude extract obtained at 25 °C in Czapek medium.

6.2.6. Metabolite Purification of CAA019 Crude Extract Obtained at 37 °C in Czapek Medium

The crude extract (160.6 mg) was dissolved in ethyl acetate and extracted with a saturated solution of sodium bicarbonate (pH 8.5). For convenience, we will refer to this ethyl acetate phase from extraction with sodium bicarbonate as *primary organic phase*. The aqueous phase and the ethyl acetate organic phase were further processed. The aqueous phase was acidified with concentrated hydrochloric acid and re-extracted with ethyl acetate giving a brownish solid residue (69.5mg) (*secondary organic phase*) composed essentially of acid compounds. This latter was purified by TLC on silica gel eluted with CH_2Cl_2/MeOH/HCOOH (9:1:1, *v/v/v*) mixture. 21.3 mg of 3-indolecarboxylic acid and 6.4 mg of yellow oil were recovered. This yellow oil [*Rf* = 0.85 (TLC on silica gel: CHCl3/*i*-PrOH (95:5, *v/v*) eluent)] could be identified as a mixture of

(3*S*,4*S*)-4-acetyl-3-methyl-2-dihydrofuranone (**6**) and (3*R*,4*S*)-4-acetyl-3-methyl-2-dihydrofuranone (**7**).

Primary organic phase was dried, filtered and evaporated under vacuum yielding a brownish oily residue (55.2 mg). This residue was purified by preparative TLC on silica gel eluted with $CHCl_3$/*i*-PrOH (93:7, *v/v*) mixture, yielding 7.4 mg of a yellow oil identified as lasiodiplodin and a second main fraction from which a 13.7 mg residue was recovered. The main fraction was further purified by another TLC step under the same chromatographic conditions yielding 1.5 mg of a colourless oil identified as botryosphaerilactone A (**4**) [*Rf* = 0.50 (TLC on silica gel: $CHCl_3$/*i*-PrOH (93:7, *v/v*) eluent); *Rf* = 0.64 (TLC on reversed phase: EtOH/H_2O (6:4, *v/v*) eluent)] and 2.4 mg of an amorphous solid identified as (3*S*,4*R*,5*R*)-4-hydroxymethyl-3,5-dimethyldihydro-2-furanone (**5**). Finally, the residue of the most polar fraction, obtained as a white solid [6.1 mg, Rf = 0.15, TLC on silica gel eluent $CHCl_3$/*i*-PrOH (93:7, *v/v*)] was identified as *cyclo*-(Trp-Ala) (**11**) (Scheme 6.2).

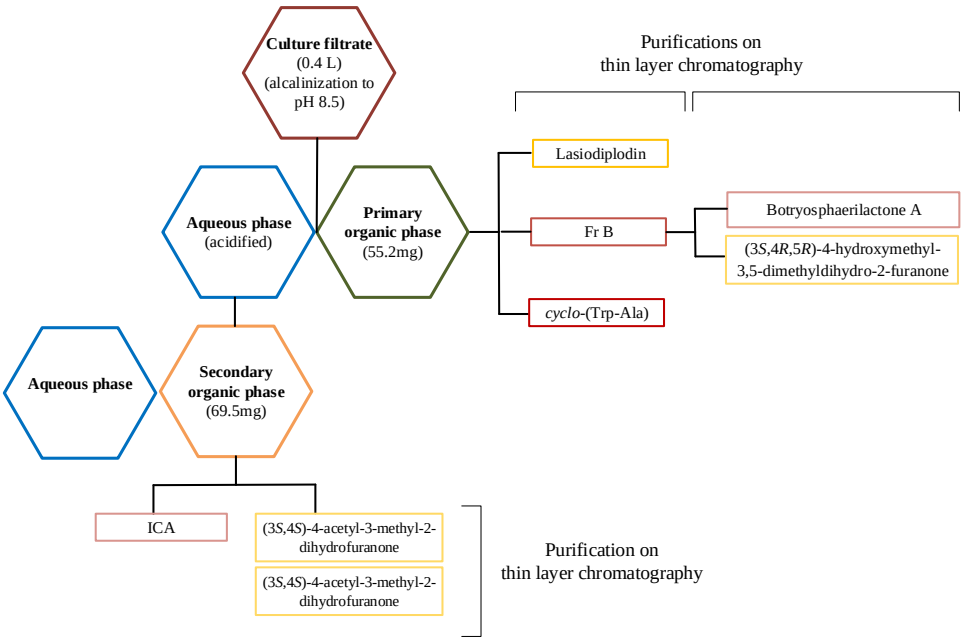

Scheme 6.2. Schematic representation of purification process of CAA019 crude extract obtained at 37 °C in Czapek medium.

6.2.7. Metabolite Purification of CBS339.90 Crude Extract Obtained at 25°C in Czapek Medium

The crude extract (147.8 mg, brown oil) was submitted to a fractionation through CC on silica gel, eluted with $CHCl_3$/*i*-PrOH (95:5, *v/v*), yielding six homogeneous fractions (fractions A 7.6 mg, B 4.8 mg, C 13.0mg, D 51.2 mg, E 19 mg, F 10.3 mg), of which the last was eluted with methanol. The residue from fraction C was purified by TLC on silica gel eluted with $CHCl_3$/*i*-PrOH (97:3, *v/v*) mixture. 1.8 mg of (-)-jasmonic acid (**2**) could be recovered along with an additional white solid residue. This last residue was further purified by TLC on reversed phase eluted with 1:1 ethanol/water mixture. Two metabolites identified as (-)-(3*R*,4*R*)-(*cis*)-hydroxymellein (**8**) and (-)-(3*R*,4*S*)-(*trans*)-hydroxymellein (**9**) were recovered as white solids [1.5 mg, *Rf* = 0.48 and 1.0 mg, *Rf* = 0.52 (TLC on reversed phase: ethanol/H_2O (1:1, *v/v*) eluent), respectively]. Residue of

fraction D, that showed the presence of main metabolite, was purified by preparative TLC on silica gel eluted with $CHCl_3$/*i*-PrOH (9:1, *v/v*) mixture. 18.2 mg of a white solid, identified as 3-indolecarboxylic acid (**1**), were recovered. Residue of fraction F was purified by TLC on silica gel eluted with $CHCl_3$/*i*-PrOH (93:3, *v/v*) mixture, yielding 1.1 mg of a white solid, which was identified as scytalone (**10**) [(*Rf* = 0.51 (TLC on silica gel: $CHCl_3$/*i*-PrOH (93:3, *v/v*) eluent)] (Scheme 6.3).

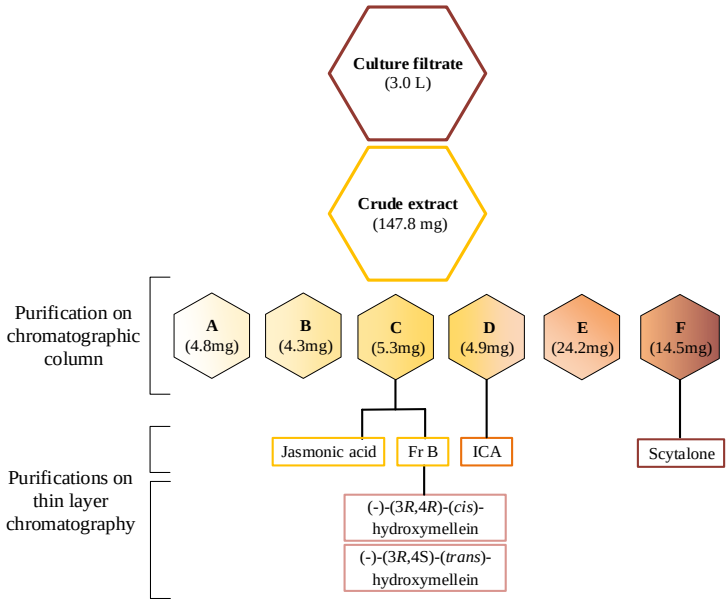

Scheme 6.3. Schematic representation of purification process of CBS339.90 crude extract obtained at 25 °C in Czapek medium.

6.2.8. Metabolite Purification of CBS339.90 Crude Extract Obtained at 37°C in Czapek Medium

The crude extract (252.2 mg) was dissolved in ethyl acetate and extracted with a saturated solution of sodium bicarbonate (pH 8.5). The aqueous phase and the ethyl acetate organic phase (*primary organic phase*) were further processed. The aqueous phase was acidified with concentrated HCl and re-extracted with

ethyl acetate. The organic phase from this liquid-liquid extraction (*secondary organic phase*) was recovered, dried with Na_2SO_4 anhydrous, and filtered.

From secondary organic phase, a solid residue (90.3 mg) containing acid compounds was obtained after evaporation of EtOAc under reduced pressure.

This residue was purified by column chromatography on silica gel eluted with CH_2Cl_2/*i*-PrOH (9:1, *v/v*), being the last fraction eluted with MeOH. It was possible to obtain 6 homogeneous fractions (A = 5.3 mg, B = 15.1 mg, C = 10.2 mg, D = 7.3 mg, E = 22.3 mg, F = 18.5 mg)

The residue from fraction C was identified as an equimolecular mixture of (3*S*,4*S*)- and (3*R*,4*S*)-4-acetyl-3-methyl-2-dihydrofuranons (**6**-**7**). The residue from fraction D was identified as 3-indolecarboxylic acid (**1**).

The primary organic phase (containing essentially neutral or phenolic compounds) was dried, filtered and evaporated under vacuum yielding 72.0 mg of a brownish oily residue. This residue was purified by two successive TLC steps on silica gel eluted with $CHCl_3$/*i*-PrOH (93:7, *v/v*) and *n*-hexane/EtOAc (8:2, *v/v*) mixtures and fractions (A 3.5 mg, B 15.6 mg, C 2.4 mg, D 2.3 mg) were finally recovered. Residue from fraction A was identified as botryosphaerilactone A (**4**), residue from fraction B was identified as (3*S*,4*R*,5*R*)-4-Hydroxymethyl-3,5-dimethyldihydro-2-furanone (**5**) and residue from fraction C contained a mixture of *cis*-(3*R*,4*R*)-4-hydroxymellein and *trans*-(3*R*,4*S*)-4-hydroxymellein (**8**-**9**) the residue from fraction D was identified as *cyclo*-(Trp-Ala) (**11**) (Scheme 6.4).

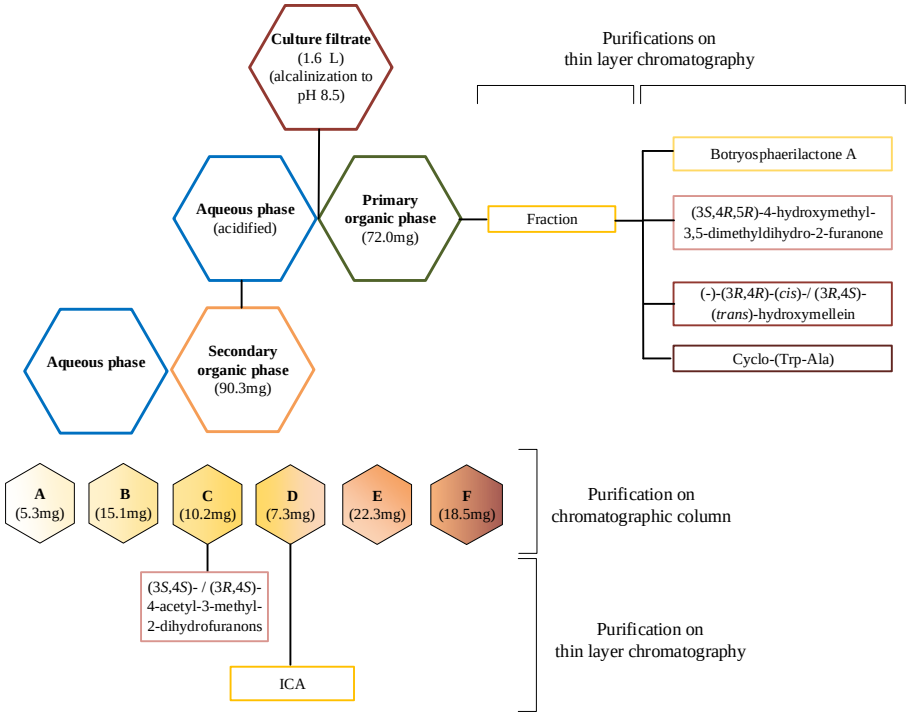

Scheme 6.4. Schematic representation of purification process of CBS339.90 crude extract obtained at 37 °C in Czapek medium.

6.2.9. Metabolite Purification of LA-SOL3 Crude Extract Obtained at 25°C in Czapek Medium

The crude extract (120.3 mg) was fractionated by CC on silica gel (30 x 1.5 cm) eluted with $CHCl_3$/*i*-PrOH (9:1, *v/v*) to yield 7 fractions (A 4.6 mg, B 2.4 mg, C 6.7 mg, D 14.5 mg, E 5.9 mg, F 23.4 mg, G 12.8 mg). The residue of fraction D was dissolved in EtOAc and then washed with a saturated solution of $NaHCO_3$ to remove jasmonic acid [**2**, 5.3 mg; *Rf* 0.44 on TLC on silica gel eluted with $CHCl_3$/*i*-PrOH (92:8, *v/v*)]. The organic phase was dried with Na_2SO_4 and evaporated under reduced pressure originating the amorphous solid (3*S*,4*R*,5*R*)-4-hydroxymethyl-3,5-dimethyldihydro-2-furanone [**5**, 6.7 mg, *Rf* 0.60 on TLC on silica gel eluted with $CHCl_3$/*i*-PrOH (92:8, *v/v*)]. Fraction F was purified by

preparative TLC on silica gel eluted with $CHCl_3$/*i*-PrOH (9:1, *v/v*). Two more metabolites were obtained as amorphous solid and yellow oil, respectively, and identified as 3-indolecarboxylic acid [**1**, 3.5 mg; *Rf* 0.38 on TLC on silica gel eluted with $CHCl_3$/*i*-PrOH (9:1, *v/v*)] and lasiolactols A and B [**12-13**, 12.4 mg; *Rf* 0.33 on TLC on silica gel eluted with $CHCl_3$/*i*-PrOH (9:1, *v/v*)] (Scheme 6.5).

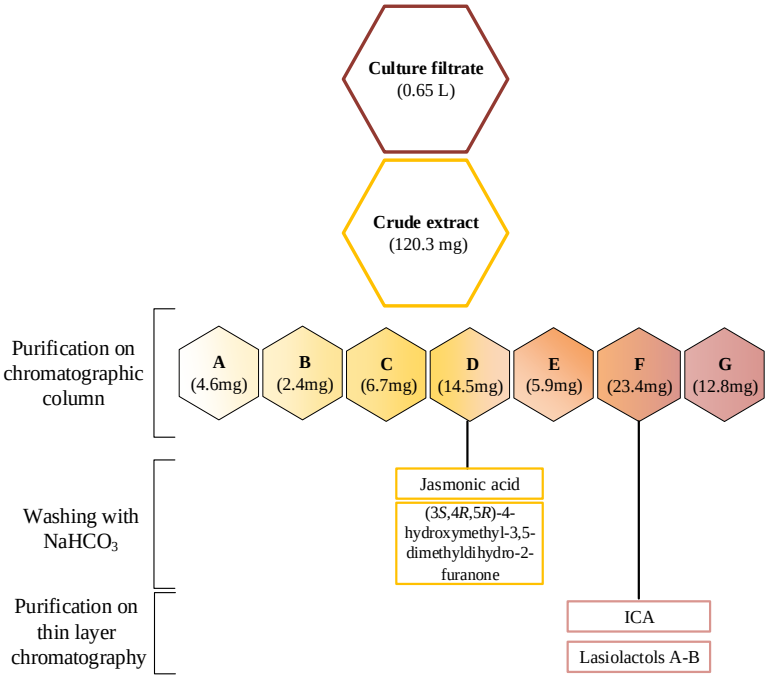

Scheme 6.5. Schematic representation of purification process of LA-SOL3 crude extract obtained at 25 °C in Czapek medium.

6.2.10. Metabolite Purification of LA-SOL3 Crude Extract Obtained at 37°C in Czapek Medium

The crude extract (432.7 mg), obtained as a brown oil, was fractionated by CC on silica gel (45 x 1.5 cm) eluted with $CHCl_3$/*i*-PrOH (9:1, *v/v*) originating 9 homogeneous fractions (A 3.3 mg, B 4.3 mg, C 6.3 mg, D 5.6 mg, E 64.0 mg, F 18.3 mg, G 16.4 mg, H 102.3 mg, I 12.3 mg). The residue of fraction B, an amorphous solid, was identified as (*R*)-mellein (**14**, *Rf* 0.69 on TLC on silica gel

eluted with $CHCl_3$). The residue of fraction C, a yellow oil, was identified as (3*S*,4*S*)-4-acetyl-3-methyl-2-dihydrofuranone [**6**, *Rf* 0.85 on TLC on silica gel eluted with $CHCl_3$/*i*-PrOH (95:5, *v/v*)], and the residue of fraction D, a yellow oil, was identified as (3*R*,4*S*)-4-acetyl-3-methyl-2-dihydrofuranone [**7**, *Rf* 0.84 on TLC on silica eluted with $CHCl_3$/*i*-PrOH (95:5, *v/v*)]. Fraction E, after purification by preparative TLC on silica gel eluted with *n*-hexane/ethyl acetate (1:1, *v/v*), produced yellow oils identified as botryodiplodin (**15**, 22.3 mg *Rf* 0.24) and 3-*epi*-botryodiplodin [**16**, 16.8 mg *Rf* 0.26 on TLC on silica gel eluted with *n*-hexane/ethyl acetate (1:1, *v/v*)]. The residue from fraction F was further purified by preparative TLC on silica gel eluted with $CHCl_3$/*i*-PrOH (92:8, *v/v*), originating (3*S*,4*R*,5*R*)-4-hydroxymethyl-3,5- dimethyldihydro-2-furanone (**5**, 13.4 mg) and an amorphous solid identified as tyrosol [**17**, 3.2 mg, *Rf* 0,52 on TLC on silica gel eluted with $CHCl_3$-*i*-PrOH (92:8, *v/v*)]. The residue from fraction G, an amorphous solid, was identified as 3-indolecarboxylic acid. Finally, the fraction H, obtained as yellow oil, was identified as a mixture of lasiolactols A and B (**12-13**) (Scheme 6.6).

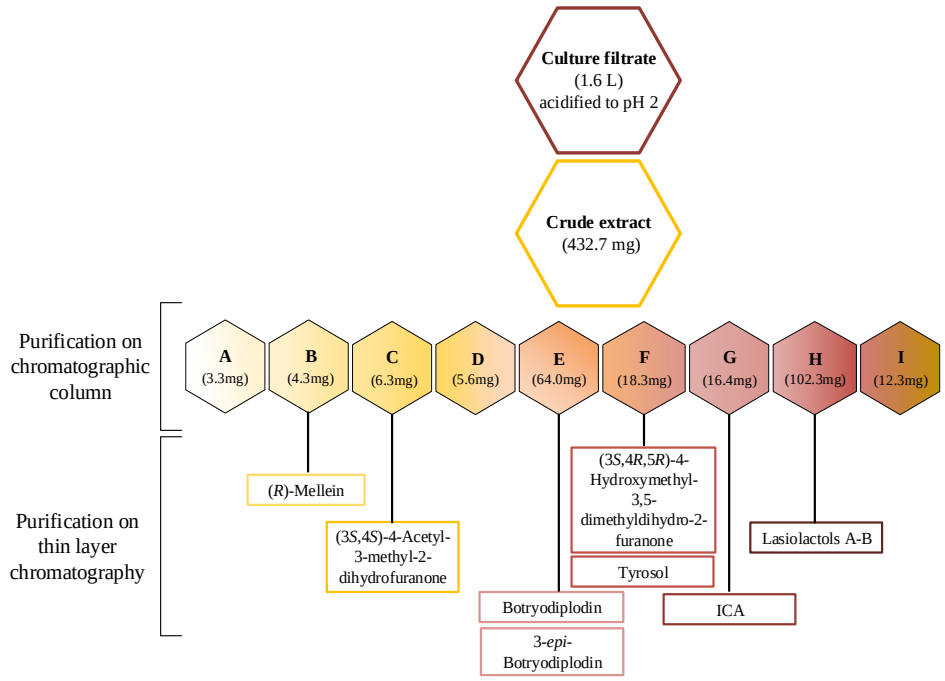

Scheme 6.6. Schematic representation of purification process of LA-SOL3 crude extract obtained at 37 °C in Czapek medium.

6.2.11. Metabolite Purification of LA-SOL3 Crude Extract Obtained at 25°C in PDB

The crude extract (113.7 mg) was fractionated by CC on silica gel (40 cm x 1.5 cm) eluted with $CHCl_3$/*i*-PrOH (9:1, *v/v*) originating 10 homogeneous fractions and last fraction was eluted with methanol (A 3.7 mg, B 2.2 mg, C 10.3 mg, D 10.4 mg, E 10.2 mg, F 9.1 mg, G 9.9 mg, H 10.6 mg, I 8.2 mg, L 26.6 mg). Fraction B was identified as (*R*)-mellein and fraction D was identified as botryodiplodin. Fraction G was identified as indole-3-carboxylic acid.

6.2.12. Metabolite Purification of LA-SOL3 Crude Extract Obtained at 25°C in PDB in Presence of 10 mM of GABA

The crude extract (84.7 mg) was fractionated by CC on silica gel (40 cm x 1.5 cm) eluted with $CHCl_3$/*i*-PrOH (9:1, *v/v*) originating 11 homogeneous

fractions and last fraction was eluted with methanol (A 1.5 mg, B 1.1 mg, C 2.2 mg, D 1.4 mg, E 4.9 mg, F 4.1 mg, G 4.0 mg, H 6.2 mg, I 23.2 mg, L 6.4, M 21.0 mg). Fraction A was identified as (*R*)-mellein, fraction D was identified as 4-hydroxymellein and fraction F was identified as botryodiplodin.

6.2.13. Metabolite Purification of LA-SV1 Crude Extract Obtained at 25°C in Czapek Medium

The crude extract (413.9 mg), obtained as brown oil residue, was submitted to fractionation by CC (45 x 1.5 cm) on silica gel eluted with $CHCl_3$/*i*-PrOH (9:1, *v/v*) originating 8 fractions (A 10.3 mg, B 5.5 mg, C 15.2 mg, D 6.1 mg, E 135.1 mg, F 36.5 mg, G 185.5 mg, and H 9.1 mg). The residue from fraction A was further purified by preparative TLC on silica gel eluted with $CHCl_3$ and identified as (*R*)-mellein (**14**, 2.0 mg). The residue of fraction B was identified as (3*S*,4*S*)-4-acetyl-3-methyl- 2-dihydrofuranone. The residue of fraction C was purified by preparative TLC on silica gel eluted with a mixture of *n*-hexane/EtOAc (1:1, *v/v*), originating an amorphous solid identified as *cis*-(3*R*,4*R*)-4-hydroxymellein [**8**, 3.2 mg *Rf* 0.45 on TLC on silica gel eluted with *n*-hexane/ethyl acetate (1:1, *v/v*)]. The residue of fraction E (30.5 mg) was dissolved in ethyl acetate and then washed with a saturated solution of $NaHCO_3$ to remove jasmonic acid (**2**, 7.5 mg). The organic phase was dried with Na2SO4 and evaporated under reduced pressure giving (3*S*,4*R*,5*R*)-4-hydroxymethyl-3,5-dimethyldihydro-2-furanone (**5**, 12.4 mg). The residue of fraction F was identified as jasmonic acid (**2**). Finally, the residue of fraction G (yellow oil) was obtained and identified as a mixture of lasiolactols A and B (**12**-**13**) (Scheme 6.7).

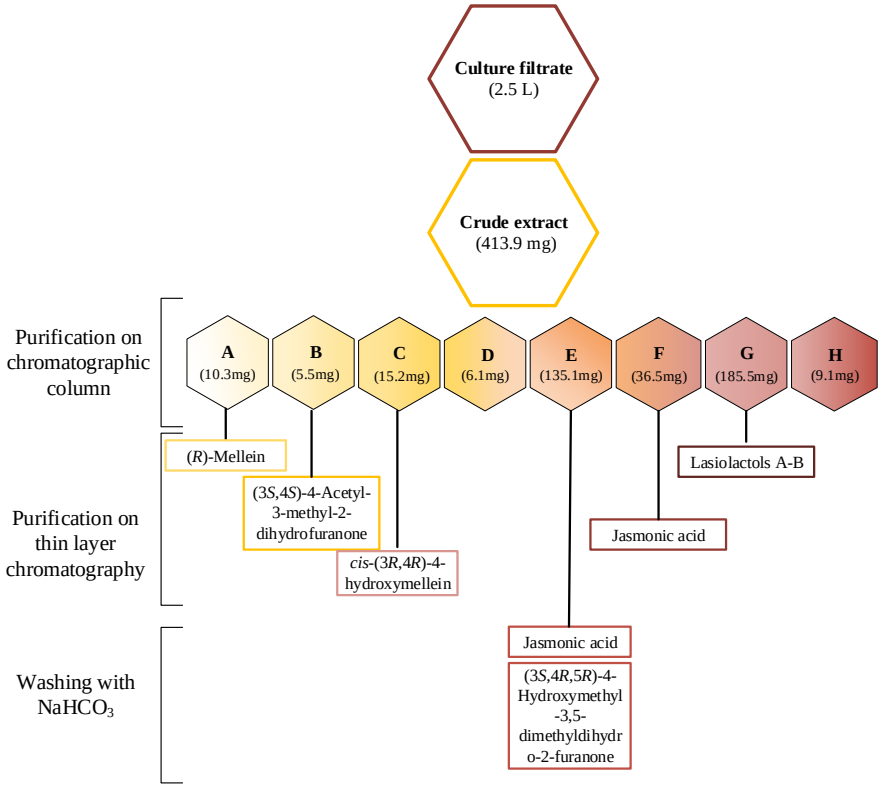

Scheme 6.7. Schematic representation of purification process of LA-SV1 crude extract obtained at 25 °C in Czapek medium.

6.2.14. Metabolite Purification of LA-SV1 Crude Extract Obtained at 37°C in Czapek Medium

The crude extract (524.4 mg), obtained as brown oil, was fractionated by CC (45 x 1.5 cm) on silica gel, eluted with $CHCl_3$/*i*-PrOH (9:1, *v/v*), originating 11 fractions (A 2.8 mg, B 11.6 mg, C 13.6 mg, D 22.5 mg, E 116.0 mg, F 35.4 mg, G 47.1 mg, H 7.4 mg, I 33.5 mg, L 113.8 mg, and M 9.6 mg). The residue of fraction B was identified as (*R*)-mellein (**14**). The residue of fraction C was identified as (3*S*,4*S*)-4- acetyl-3-methyl-2-dihydrofuranone (**6**). Part of the residue of fraction E (37.4 mg) was further purified by preparative TLC on silica gel eluted with *n*-hexane/EtOAc (1:1, *v/v*) (three times) originating (-)-botryodiplodin

and 3-*epi*-botryodiplodin (**15-16**, 7.4 and 8.3 mg, respectively). The residue of fraction F was identified as 3-indolecarboxylic acid. Finally, the residue of fraction L, yellow oil, was identified as a mixture of lasiolactols A and B (**12-13**) (Scheme 6.8).

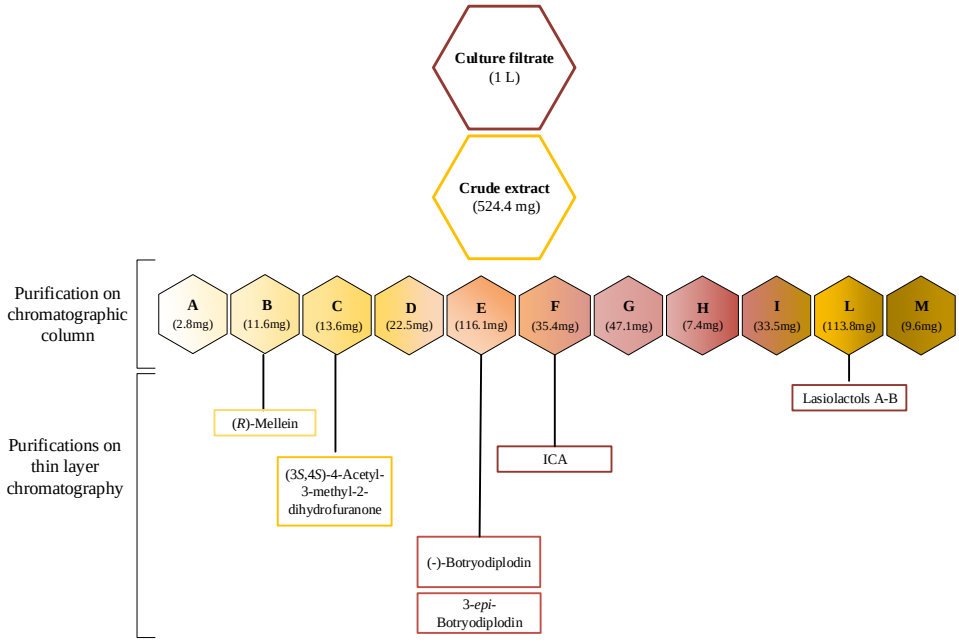

Scheme 6.8. Schematic representation of purification process of LA-SV1 crude extract obtained at 37 °C in Czapek medium.

6.2.15. Metabolite Purification of LA-SV1 Crude Extract Obtained at 37°C in PDB

The crude extract (114.6 mg) was fractionated by CC on silica gel (40 cm x 1.5 cm) eluted with $CHCl_3$/*i*-PrOH (9:1, *v/v*) originating 10 homogeneous fractions and last fraction was eluted with methanol (A 1.7 mg, B 1.8 mg, C 4.1 mg, D 4.4 mg, E 1.8 mg, F 7.9 mg, G 0.8 mg, H 2.3 mg, I 14.0 mg, L 19.5 mg). Fraction B was identified as (*R*)-mellein, and I was identified as indole-3-carboxylic acid

6.2.16. Metabolite Purification of LA-SV1 Crude Extract Obtained at 25°C in PDB in Presence of 10 mM of GABA

The crude extract (76.1 mg) was fractionated by CC on silica gel (40 cm x 1.5 cm) eluted with $CHCl_3$/*i*-PrOH (9:1, *v/v*) originating 11 homogeneous fractions and last fraction was eluted with methanol (A 1.3 mg, B 2.0 mg, C 4.4 mg, D 3.8 mg, E 2.1 mg, F 6.3 mg, G 3.6 mg, H 1.7 mg, I 6.2 mg, L 5.2 mg, M 10.3 mg). Fraction E was identified as botryodiplodin.

6.2.17. Quantification of indole-3-carboxylic acid (ICA)

Certified standard of indole-3-carboxylic acid (Sigma-Aldrich, Saint Louis, MO, USA) and weighted amounts of crude extracts were treated with diazomethane in ether in order to obtain methyl derivative of indole-3-carboxylic acid (ICA-ME).

Quantification of ICA-ME was obtained by linear regression of the chromatographic peak areas and known concentrations of certified standards (ranging from 50 to 200 mg L^{-1}). The response of target compounds was normalized to the response of an internal standard (anthracene), which was added to the sample prior to the analysis at the constant concentration of 100 mg L^{-1}

6.2.18. Acetylation of 4-hydroxymethyl-3,5-dimethylhydro-2-furanone

4-Hydroxymethyl-3,5-dimethyldihydro-2-furanone (4.9 mg), dissolved in pyridine (30 μL), Ac2O was added to solution. The reaction was stopped by addition of CH_3OH, and the azeotrope formed by addition of benzene was evaporated in a N_2 stream. The oily residue (6.2 mg) was purified by TLC on silica gel, eluent toluene-EtOAc (1:1, *v/v*), yielding derivative **22** (5.1 mg, Rf 0.23) as an oil.

6.2.19. Acetylation of botryodiplodin.

(3*R*,4*S*)-Botryodiplodin (5.3 mg) was acetylated with pyridine (30 μL) and Ac_2O (30 μL) in the same conditions above reported to convert (3*S*,4*R*,5*R*)-4-hydroxymethyl-3,5-dimethyldihydro-2-furanone in the corresponding 2-*O*-acetyl derivative. Also, the reaction work-up is the same and the residue was purified by TLC on silica gel, eluent *n*-hexane-ethyl acetate (1:1, *v/v*), originating (2*R*,3*R*,4*S*)-botryodiplodin acetate (**23**, 4.3 mg, R*f* 0.56), whose physic and spectroscopic data were comparable to those previously reported[8].

6.2.20. Acetylation of epi-botryodiplodin

epi-Botryodiplodin (6.4 mg), dissolved in pyridine (30 μL), was converted into the corresponding 2-*O*-acetyl derivatives by acetylation with Ac_2O (30 μl) at room temperature for 12 h. The reaction (room temperature for 12 h), was stopped with CH_3OH and work up as above reported. The oily residue (7.3 mg) was purified by TLC on silica gel, eluent toluene-EtOAc (1:1, *v/v*), yielding derivatives **24A** (2.3 mg, *Rf* 0.52) and **24B** (3.2 mg, *Rf* 0.49) as oils.

(-)-Jasmonic acid (**2**). $[\alpha]_D^{25}$ -68 (*c* = 0.3, CH_3OH) [optical rotation was very similar to that reported[9]]. ^1H NMR ($CDCl_3$): 5.49-5.44 (m, H-10), 5.28-5.24 (m, H-9), 2.78 (d, *J* = 8.9, H-4), 2.41-2.25 (m, H-4, H-5, H-6 and H2-8,), 2.14 (dd, *J* = 8.0 and 19.9, H-1), 2.06 (dd, *J* = 7.4 and 7.4, H_2-11), 1.92 (m, H-2), 1.53 (m, H-5), 0.96 (t, *J* = 7.3, H_3-12). ^1H NMR spectrum was similar to data previously reported[10]. ESIMS (+) *m/z*: 233 $[M + Na]^+$.

*(3S,4*R,*5*R*)-4-Hydroxymethyl-3,5-dimethyldihydro-2-furanone* (**5**). $[\alpha]_D^{25}$ -21 (*c* = 0.5) [Optical rotation was very similar to that previously reported[11]]; ^1H NMR (400 MHz, in $CDCl_3$): δ 4.39 (dq *J* = 6.2, 9.4, H-5), 3.83 (dd, *J* = 4.0, 10.8, H-8), 3.75 (dd, *J* = 5.4, 10.8, H-8) 2.60 (dq, *J* = 7.1, 11.5, H-3), 1.87 (m, H-4),

1.46 (3H, d, *J* = 6.2, H_3-6), 1.28 (d, *J* = 7.1, H_3-7). ^{1}H NMR spectrum was similar to data previously reported[12]; ESIMS (+) *m/z*: 167 $[M+Na]^+$.

(*3*S,*4*S*)-4-Acetyl-3-methyl-2(3H)-dihydrofuranone* (**6**). $[\alpha]_D^{25}$ -68 (c 0.4, CH3OH); ^{1}H NMR ($CDCl_3$) 4.50 (t, *J* = 8.8, H-5), 4.22 (t, *J* = 9.3, H-5), 3.27 (q, *J* = 9.4, H-4), 2.87 (dq, *J* = 7.0, 10.2, H-3), 2.28 (s, H_3-8), 1.38 (d, *J* = 7.0, H3-6). Optical rotation and ^{1}H NMR spectrum were similar to data previously reported[13]. ESI MS (+) *m/z*: 165 $[M+Na]^+$.

*(3*R,*4*S*)-4-Acetyl-3-methyl-2-dihydrofuranone* (**7**). $[\alpha]_D^{25}$ -11.2 (c 0.3, CH3OH), ^{1}H NMR (400 MHz, $CDCl_3$) 4.55 (dd, *J* = 6.2, 9.6, H-5), 4.31 (dd, *J* = 6.9, 9.6, H-5), 3.63 (*ddd*, *J* = 6.2, 6.9, 8.8, H-4), 2.98 (dq, *J* = 7.5, 8.8, H-3), 2.26 (s, H_3-8), 1.24 (*d*, *J* = 7.5, H_3-6). Optical rotation and ^{1}H NMR spectrum were similar to data previously reported[13]. ESI MS (+) *m/z*: 165 $[M+Na]^+$.

*(3*R,*4*R*)-4-hydroxymellein* (**8**)**.** $[\alpha]_D^{25}$ -42 (c 0.4, CH_3OH) [Optical rotation was very similar to that previously reported[14]]; ^{1}H NMR (CD3OD) δ: 11.06 (*s*, OH-8), 7.56 (dd, *J* = 1.1, 7.3, H-6), 7.08 (dd, *J* = 1.1, 7.3, H-5), 7.00 (br*d*, *J* = 7.3, H-7), 4.73 (*dq*, *J* = 6.6, 1.8, H-3), 4.61 (brd, *J* = 1.8), 1.62 (*d*, *J* = 6.6, 3-CH3). ^{1}H NMR spectrum was similar to data previously reported[9]. ESIMS (+) *m/z*: 217 $[M + Na]^+$, 195 $[M + H]^+$.

Lasiolactol A (**12**). ^{1}H NMR (400 MHz, in $CDCl_3$,): δ 5.08 (s, H-2), 4.22 (quint *J* = 6.3, H-5), 3.85-3.66 (m, H2-8), 2.11 (ddq, *J* = 6.0, 7.2, 8.5 , H-3), 1.63 (brs, OH), 1.61-1.56 (m, H-4), 1.35 (d, *J* = 6.3 Hz, H3-6), 1.15 (3H, d, *J* = 7.2, H3-7).

Lasiolactol B (**13**). ^{1}H NMR (400 MHz, in $CDCl_3$): δ 5.26 (d, 4.0, H-2), 4.02 (dq *J* = 6.3, 8.2, H-5), 3.85-3.66 (m, H2-8), 2.05 (ddq, *J* = 6.0, 7.2, 8.5 H-3), 1.86-1.79 (m, H-4), 1.63 (brs, OH), 1.41 (d, *J* = 6.3, H3-6), 1.08 (3H, d, *J* = 7.2, H3-

7). ^{1}H NMR spectrum was similar to data previously reported[15]. ESI MS(+) *m/z*: 313 $[M+K]^+$, 297 $[M+Na]^+$.

*(*R*)-Mellein* (**14**). $[\alpha]_D^{25}$ -95 (c 0.5, CH_3OH) [Optical rotation was very similar to that previously reported[14]]; ^{1}H NMR ($CDCl_3$) δ: 11.03 (s, OH-8), 7.41 (t, *J* = 8.0, H-6), 6.89 (d, *J* = 8.0, H-5), 6.69 (d, *J* = 8.0, H-7), 4.78-4.69 (m, H-3), 2.93 (d, *J* = 7.2, H2-4), 1.53 (d, *J* = 6.2, 3-CH_3). ^{1}H NMR spectrum was similar to data previously reported[16]. ESIMS (+) *m/z*: 217 $[M + Na]^+$, 195 $[M + H]^+$.

(-)-Botryodiplodin (**15**). $[\alpha]_D^{25}$ -62 (c 0.3, $CHCl_3$); ^{1}H NMR ($CDCl_3$, 400 MHz) δ 5.22-5.18 (m, H-2 and H-2'), 4.86 (d, *J* = 12.0, OH′), 4.31 (t, *J* = 8.8, H5), 4.12-4.02 (m, H5 and H5′), 3.69 (q, *J* = 7.1, H4′), 3.44 (dt, *J* = 2.7, 7.7, H4), 2.63 (quint, *J* = 7.1, H3), 2.51-2.46 (m, H3′), 2.32 (s, H_3-8), 2.23 (s, H_3-8'), 1.09 (d, *J* = 7.2, H_3-6), 0.89 (d, *J* = 7.2, H3-6). Optical rotation and ^{1}H NMR spectrum were similar to data previously reported[17]. ESI MS(+) *m/z*: 167 $[M+Na]^+$.

*(2*R*/2*S*,3*S*,4*S*)-3-epi-Botryodiplodin* (**16**). $[\alpha]_D^{25}$ +75 ($CHCl_3$, *c* 0.7) [Optical rotation was very similar to that previously reported[18]]; ^{1}H and ^{13}C NMR ($CDCl_3$); HR-ESI-MS (+) spectrum *m/z*: 167.0660 [$C_7H_{12}NaO_3$, calcd. 167.0684, $M+Na]^+$.

Tyrosol (**17**). ^{1}H NMR (CD_3OD) δ: 7.03 (*d, J* = 8.2 Hz, H-3 e H-5), 6.70 (*d, J* = 8.2 Hz H-2 and H-6), 3.67 (*t, J* = 7.2 Hz, H-8), 2,70 (*t, J* = 7.2 Hz, H-7). ^{1}H NMR spectrum was similar to data previously reported[19]. ESIMS (+) *m/z*: 295 $[2M + Na]^+$, 159 $[M + Na]^+$.

(3S,4R,5R)-4-Hydroxymethyl-3,5-dimethyldihydro-2-furanone acetate (**22**): ^{1}H NMR (400 MHz, in $CDCl_3$,): δ 4.28 (1H, m, H-5), 4.26 (1H, dd, *J* = 4.4, 11.5 Hz, H-8a), 4.18 (1H, dd, *J* = 5.9, 11.5 Hz, H-8b), 2.52 (1H, m, H-3), 2.11 (3H, s, COCH3), 2.03 (1H, m, H-4), 1.48 (3H, d, *J* = 6.1, Hz, H3-6), 1.32 (3H, d, *J* = 7.6 Hz, H3-7). ESI MS(+) m/z: 209 $[M+Na]^+$, 187 $[M+H]^+$, 127 $[M+CH3COO]^+$.

Botryodiplodin acetate (**23**): ^{1}H NMR ($CDCl_3$, 400 MHz) δ 6.00 (brs, H-2), 4.38 (t, *J* = 9.0 Hz, H5), 4.12 (t, *J* = 9.0 Hz, H5), 3.63-3.57 (m, *J* = 7.1 Hz, H4), 2.71 (quint, *J* = 7.0 Hz, H3), 2.25 (s, $COCH_3$), 2.08 (s, H_3-8); 0.96 (d, *J* = 7.3 Hz, H_3-6); ESIMS (+) *m/z*: 209 $[M+Na]^+$.b

(2S)-epi-Botryodiplodin acetylate (**24A**): ^{1}H NMR (400 MHz, in $CDCl_3$,): δ 1.25 (3H, d, *J* = 7.2 Hz, CH_3C(3)), 2.05 (3H, s, $\underline{C}H_3COO$), 2.25 (3H, s, $\underline{C}H_3CO$), 2.70 (1H, m, H-3), 2.84 (1H, m, H-4), 4.29 (1H, t, *J* = 8.1 Hz, H-5), 4.23 (1H, t, *J* = 8.1 Hz, H-5), 5.91 (1H, brs, H-2); ^{13}C NMR (100 MHz, in $CDCl_3$,): δ 17.8 ($\underline{C}H_3$C-3), 22.5 ($\underline{C}H_3COO$), 30.2 ($\underline{C}H_3CO$), 42.8 (C-3), 58.4 (C-4), 68.9 (C-5), 104.0 (C-2), 166.1 ($\underline{C}OO$), 206.5 (CO); ESIMS (+), *m/z* 209 $[M+Na]^+$.

(2R)-epi-Botryodiplodin acetylate (**24B**)*:* ^{1}H NMR (400 MHz, in $CDCl_3$): δ 1.11 (3H, d, *J* = 6.8 Hz, C$\underline{H}_3$C-3), 2.10 (3H, s, CH_3COO), 2.25 (3H, s, $\underline{CH}_3CO$), 2.61 (1H, m, H-3), 3.13 (1H, dt, *J* = 9.0, 10.0 Hz, H-4), 3.98 (1H, t, *J* = 9.0 Hz, H-5), 4.31 (1H, t, *J* = 9.0 Hz, H-5), 6.27 (1H, d, *J* = 4.5 Hz, H-2); ^{13}C NMR (100 MHz, in $CDCl_3$,): δ 12.1 ($\underline{C}H_3$C-3), 21.2 ($\underline{C}H_3COO$), 30.3 ($\underline{C}H_3CO$), 41.5 (C-3), 56.0 (C-4), 70.0 (C-5), 99.8 (C-2), 170.2 (COO), 207.0 (CO); ESIMS (+) *m/z* 225 $[M+K]^+$, 209 $[M+Na]^+$.

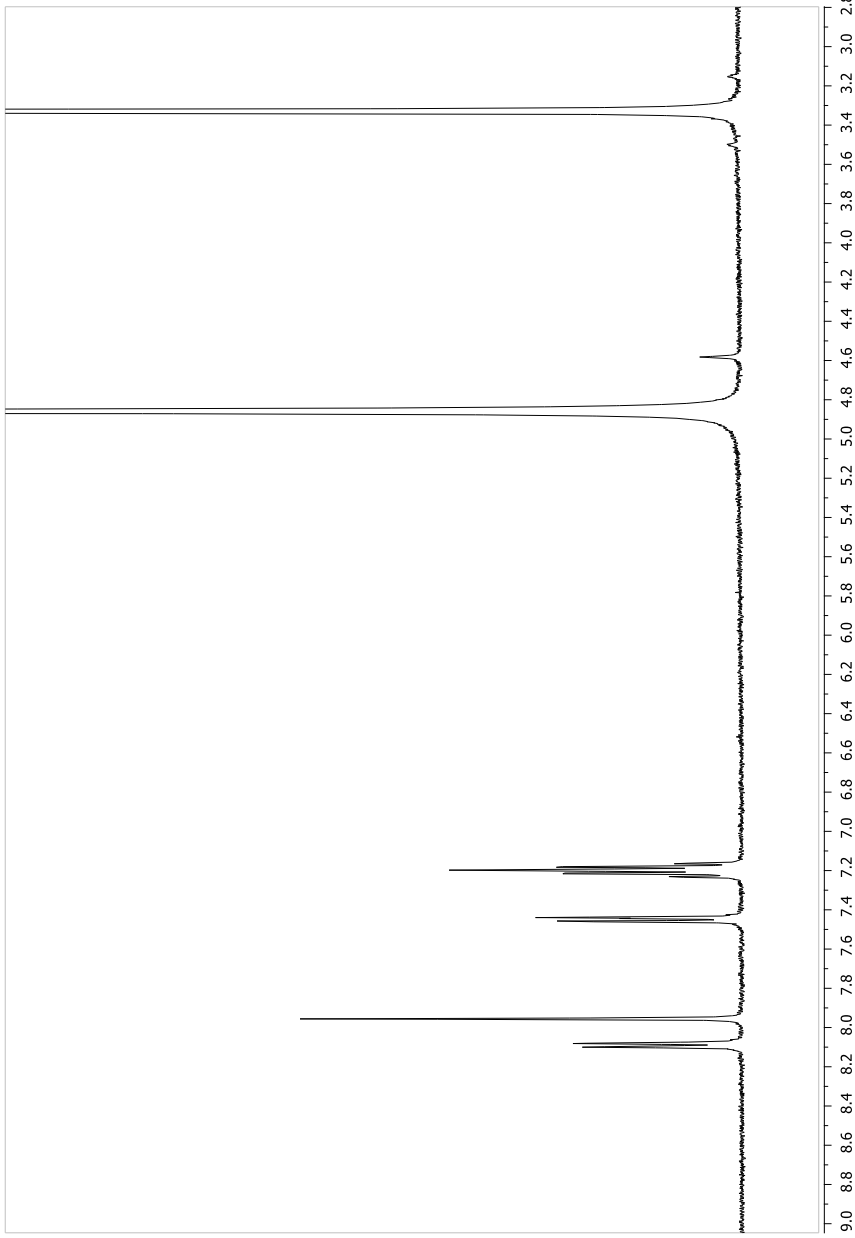

Figure 6.3. ^{1}H NMR spectrum of 3-indolecarboxylic acid (**1**) recorded at 400 MHz in $CDCl_3$

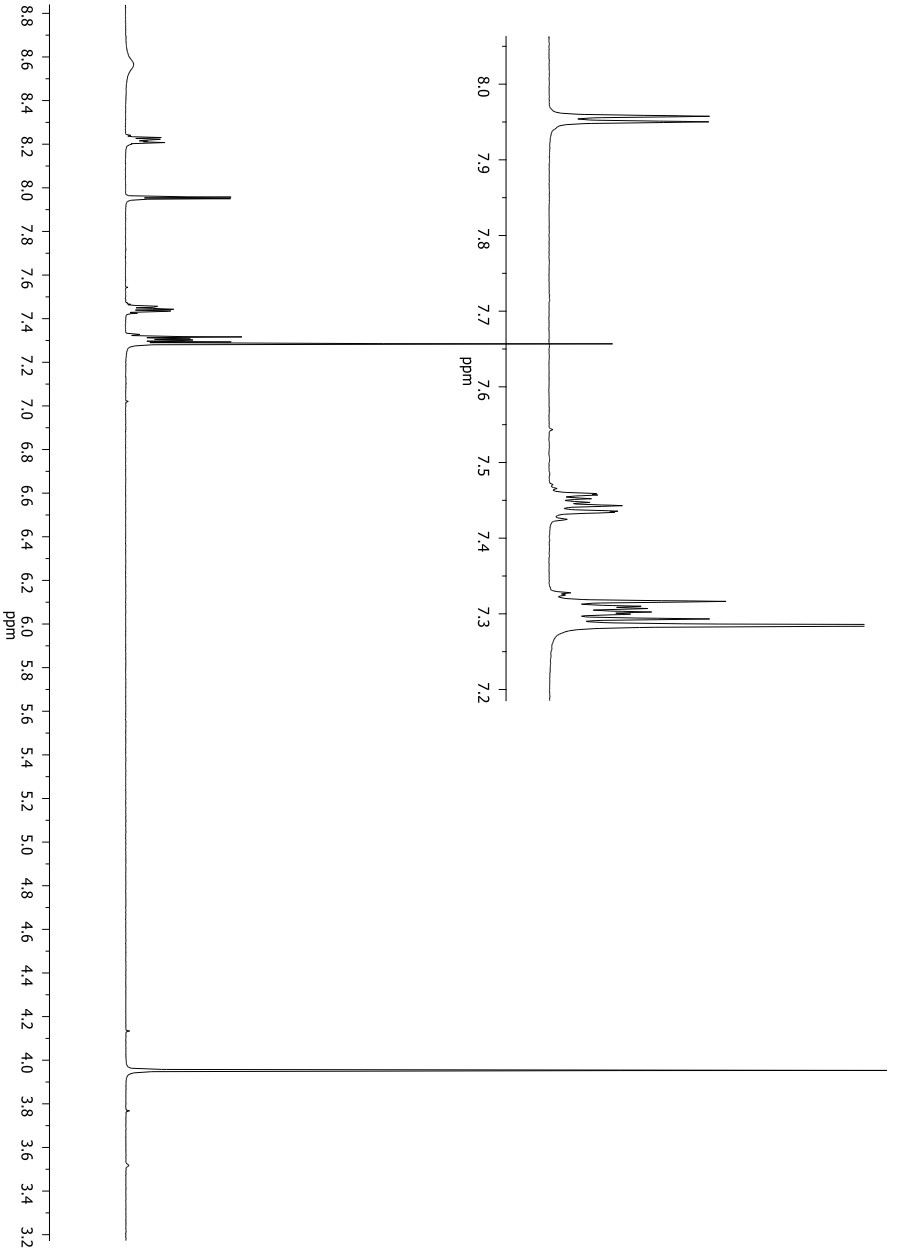

Figure 6.4. ^{1}H NMR spectrum of methyl-3-indolecarboxylate recorded at 400 MHz in $CDCl_3$

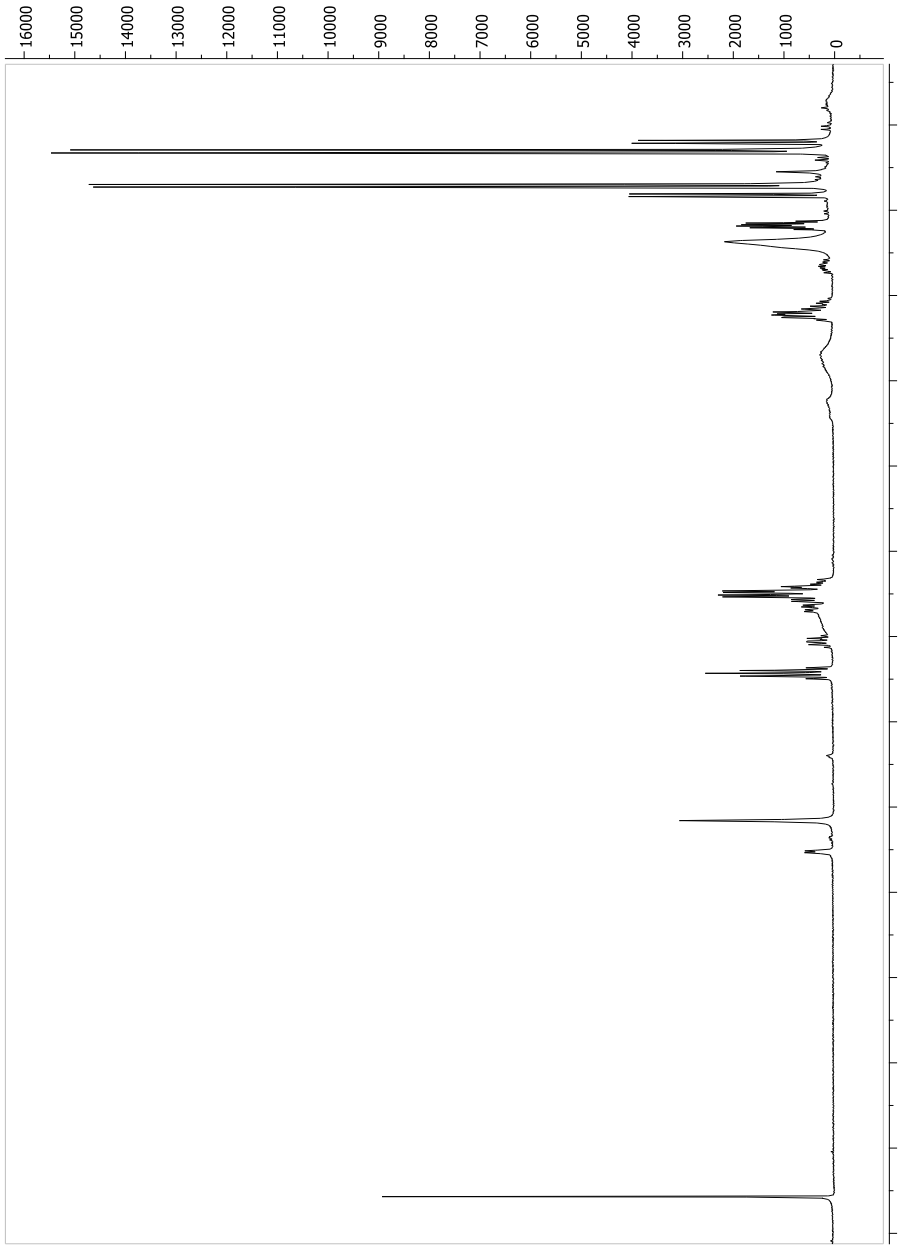

Figure 6.5. ^{1}H NMR spectrum of lasiolactols (**12-13**) recorded at 400 MHz in $CDCl_3$

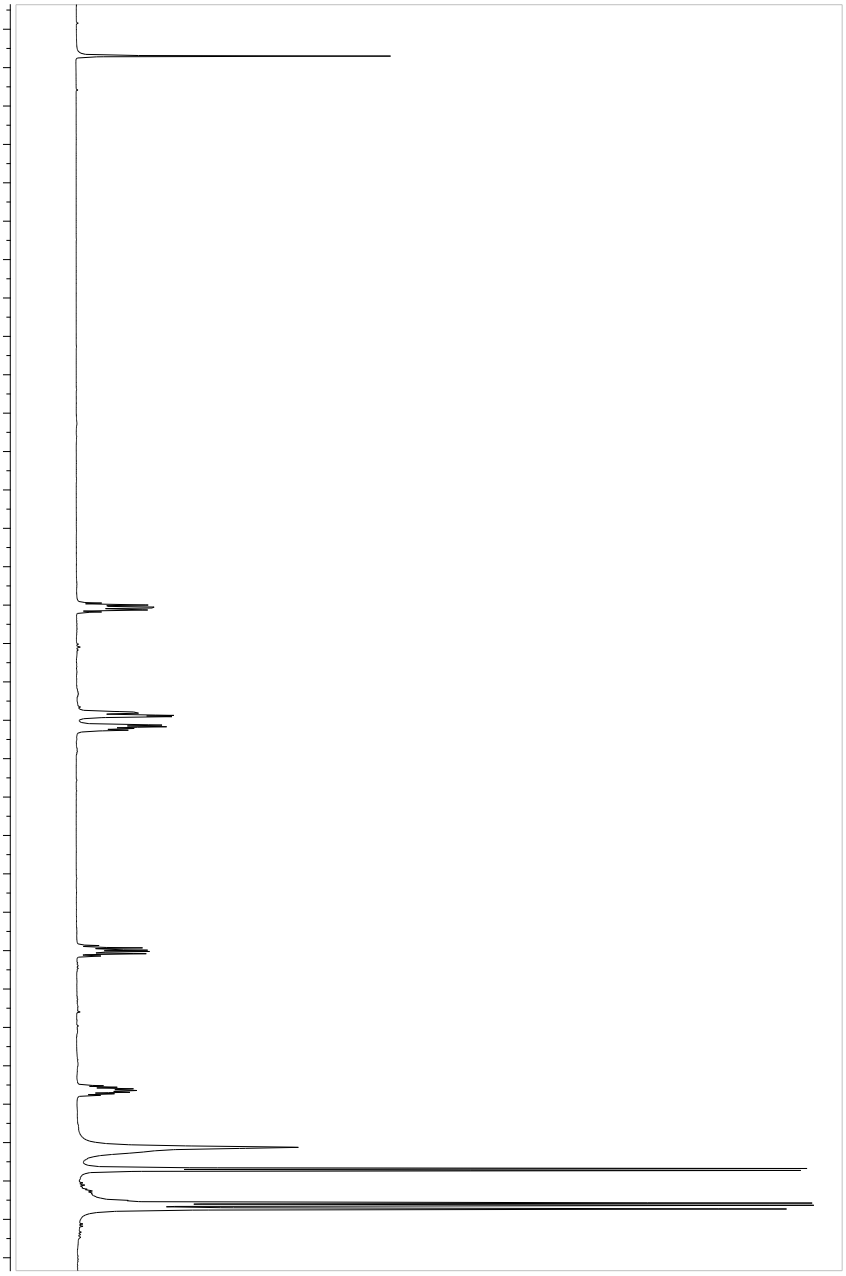

Figure 6.6. ^{1}H NMR spectrum of (3*S*,4*R*,5*R*)-4-hydroxymethyl-3,5-dimethyldihydro-2-furanone (**5**) recorded at 400 MHz in $CDCl_3$

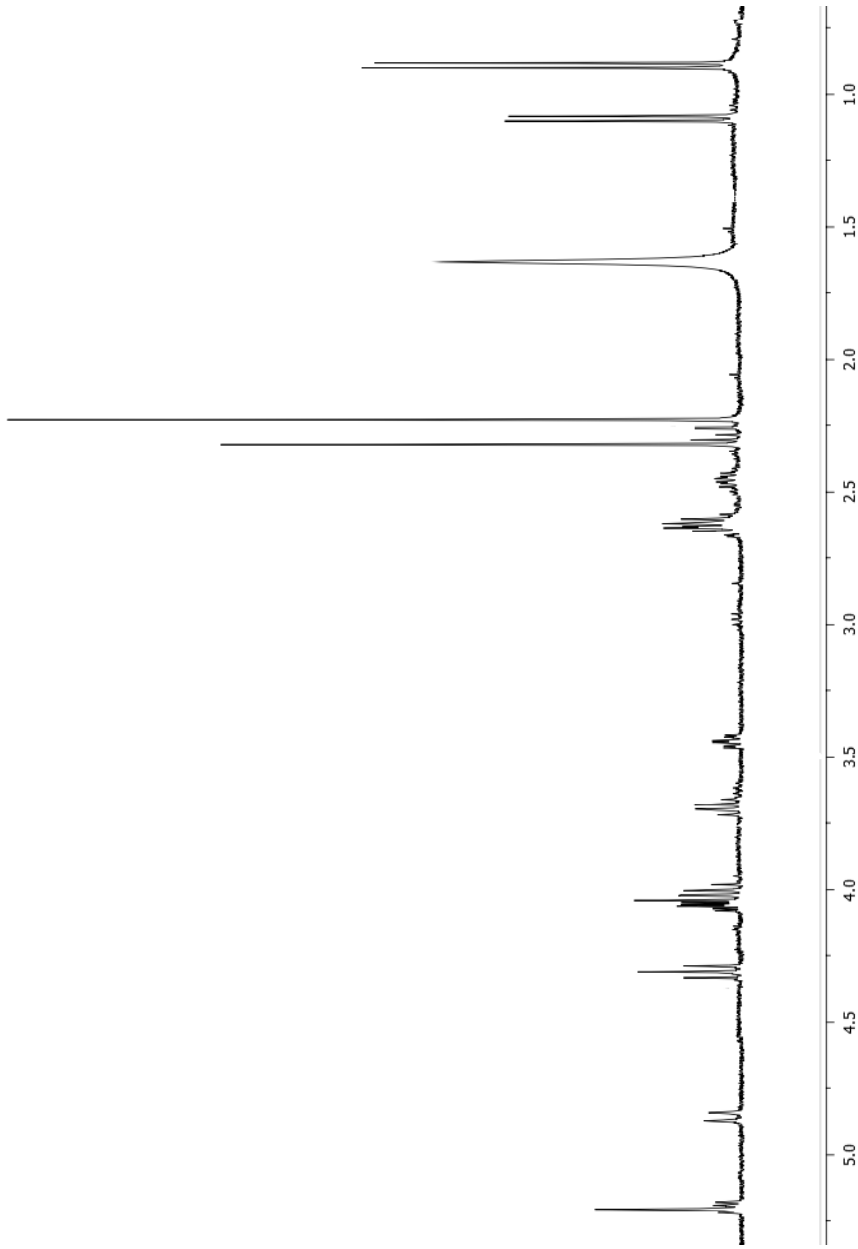

Figure 6.7. ^{1}H NMR spectrum of (-)-botryodiplodin (**15**) recorded at 400 MHz in $CDCl_3$

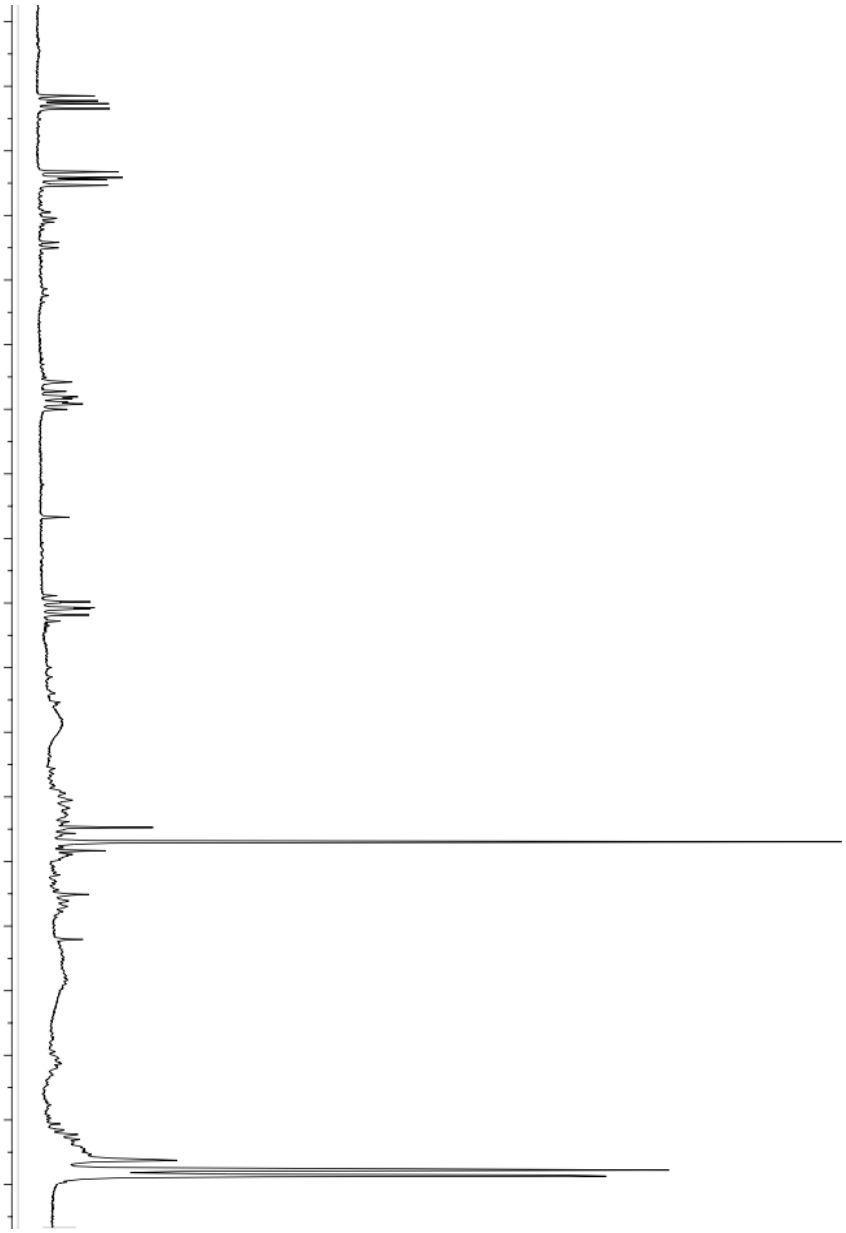

Figure 6.8. ^{1}H NMR spectrum of (3*R*,4*S*)-4-acetyl-3-methyl-2-dihydrofuranone (**7**) recorded at 400 MHz in $CDCl_3$

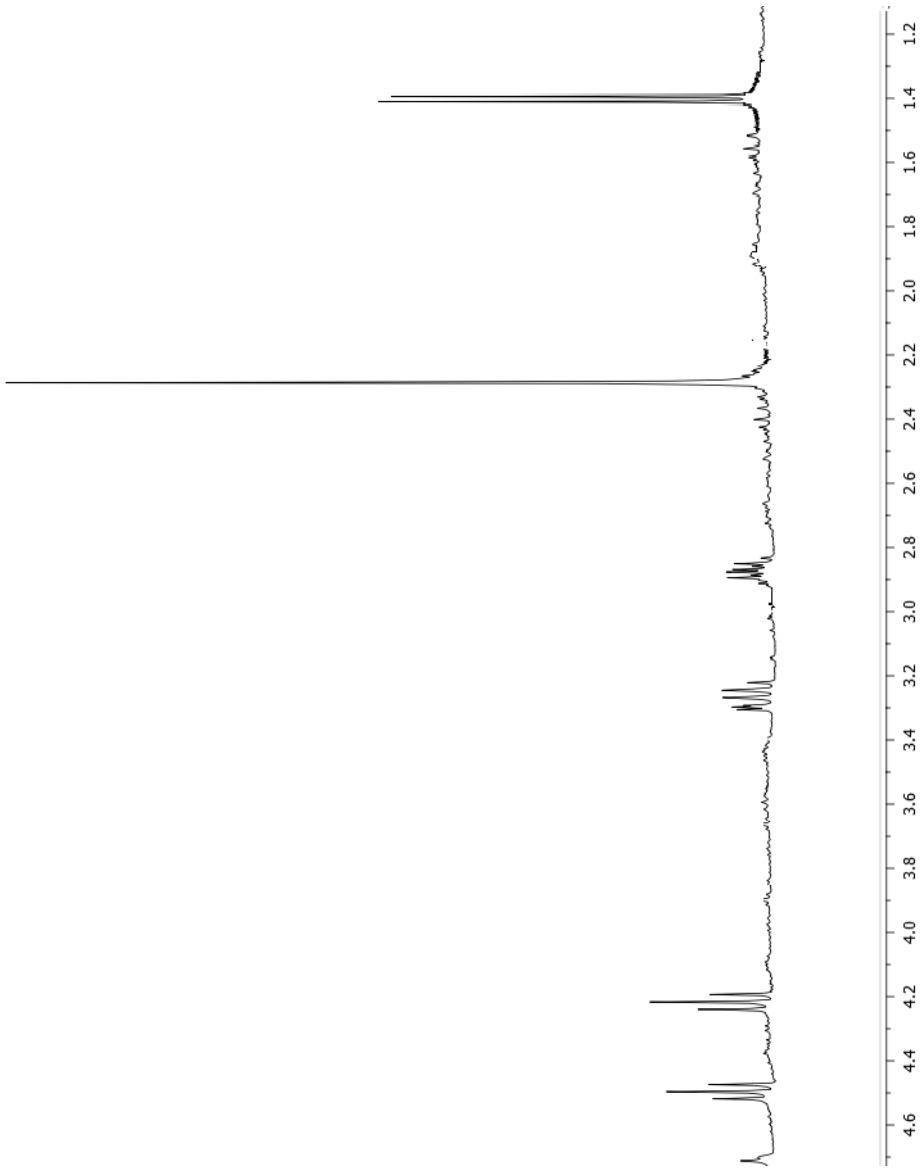

Figure 6.9. ^{1}H NMR spectrum of (3*S*,4*S*)-4-acetyl-3-methyl-2-dihydrofuranone (**6**) recorded at 400 MHz in $CDCl_3$

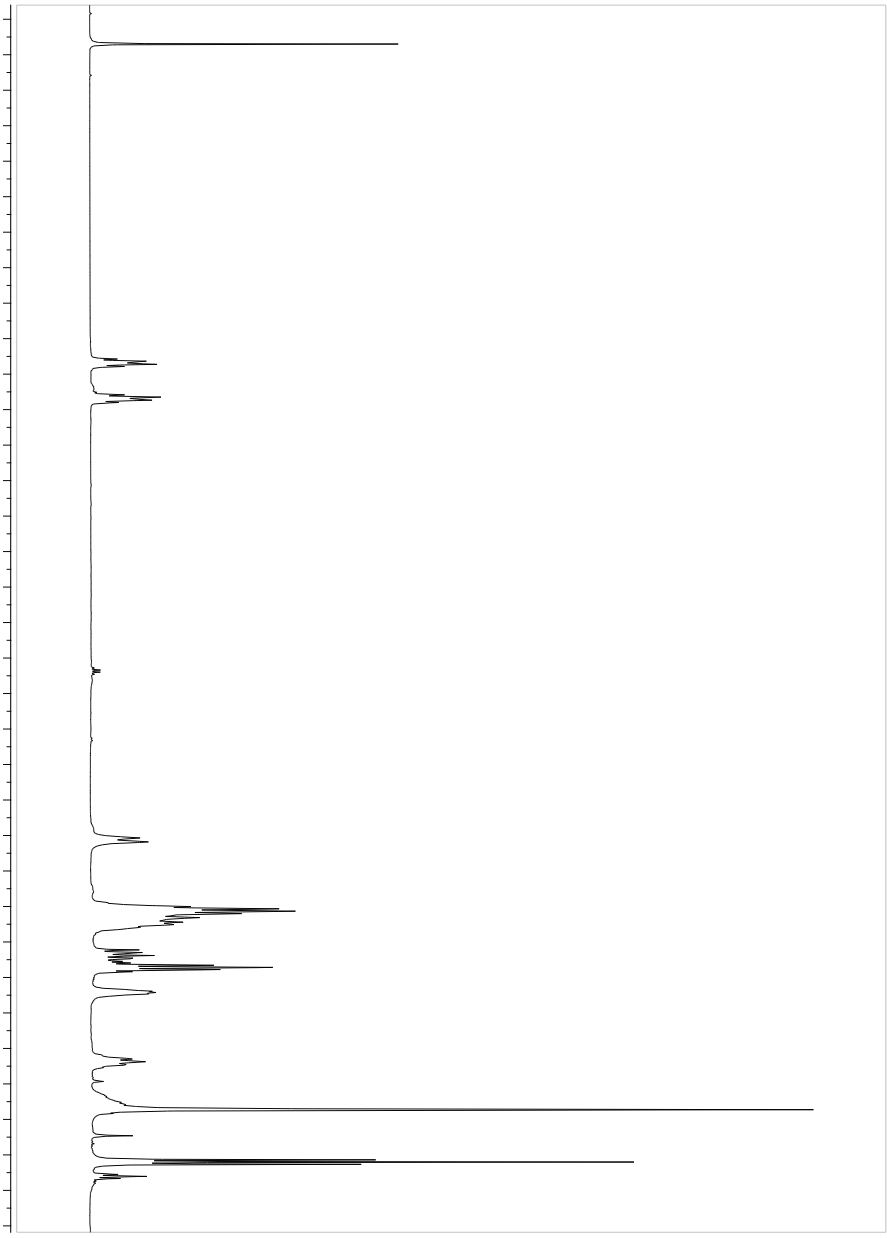

Figure 6.10. ^{1}H NMR spectrum of (-)-jasmonic acid **(2)** recorded at 400 MHz in $CDCl_3$

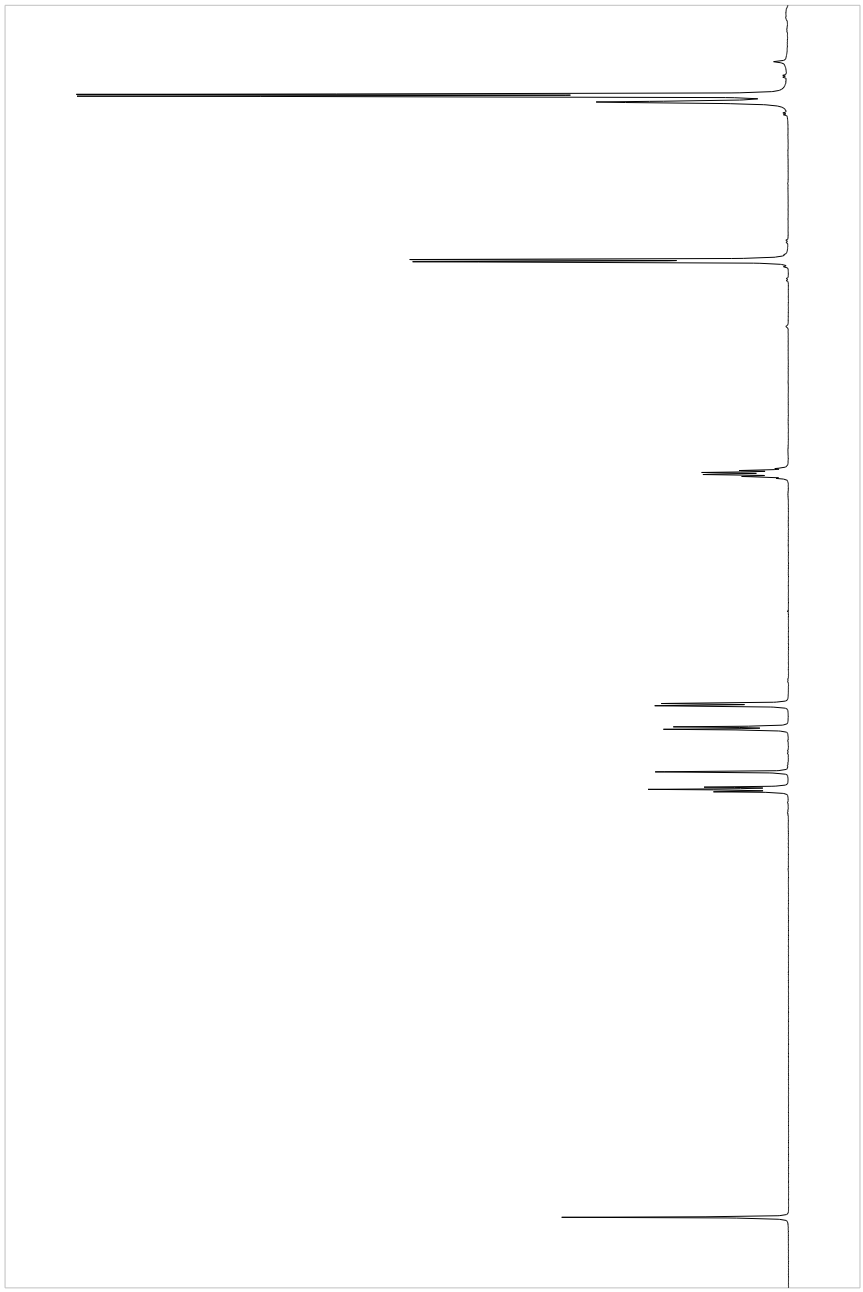

Figure 6.11. ^{1}H NMR spectrum of (*R*)-mellein (**14**) recorded at 400 MHz in $CDCl_3$

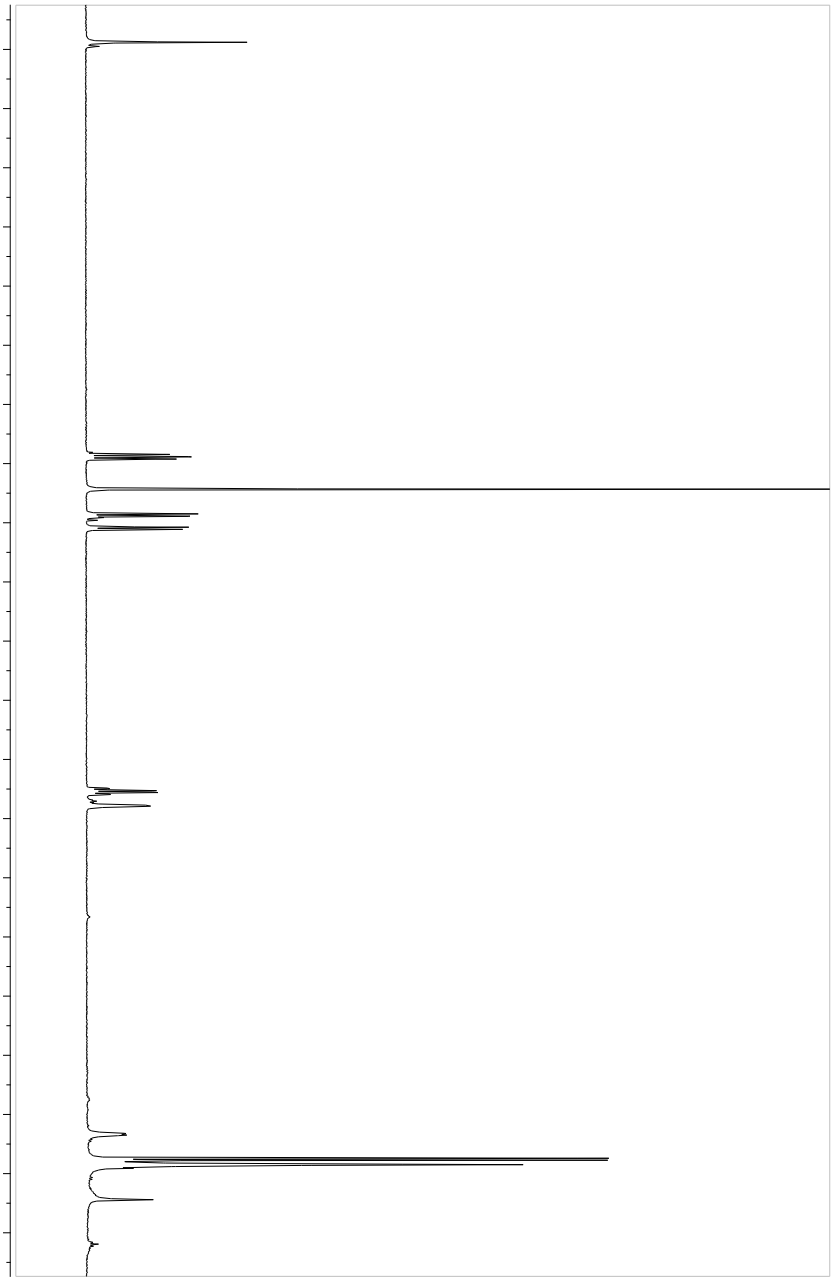

Figure 6.12. ^{1}H NMR spectrum of (3*R*, 4*R*)-4-hydoxymellein (**8**) recorded at 400 MHz in $CDCl_3$

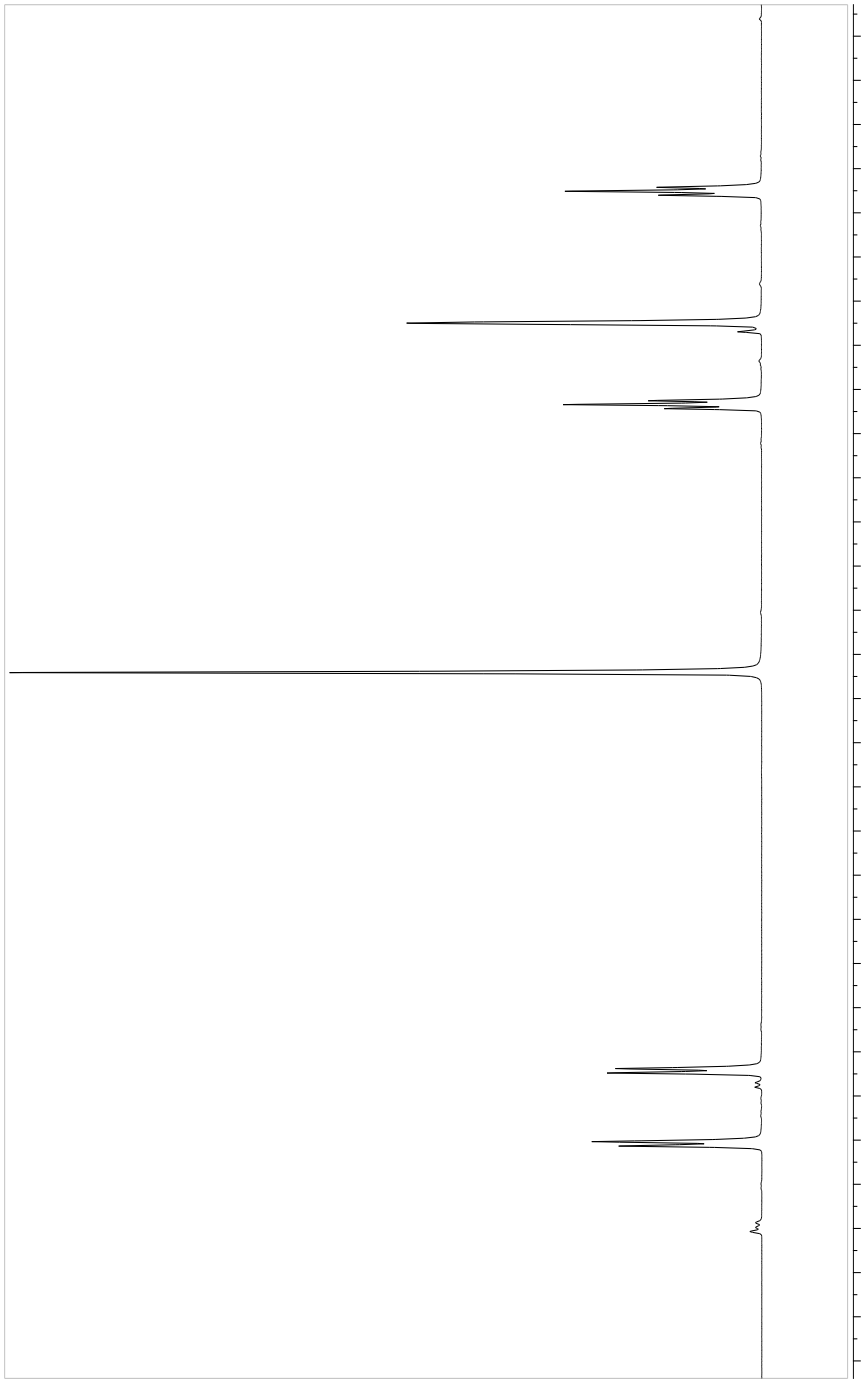

Figure 6.13. ^{1}H NMR spectrum of tyrosol (**17**) recorded at 400 MHz in $CDCl_3$

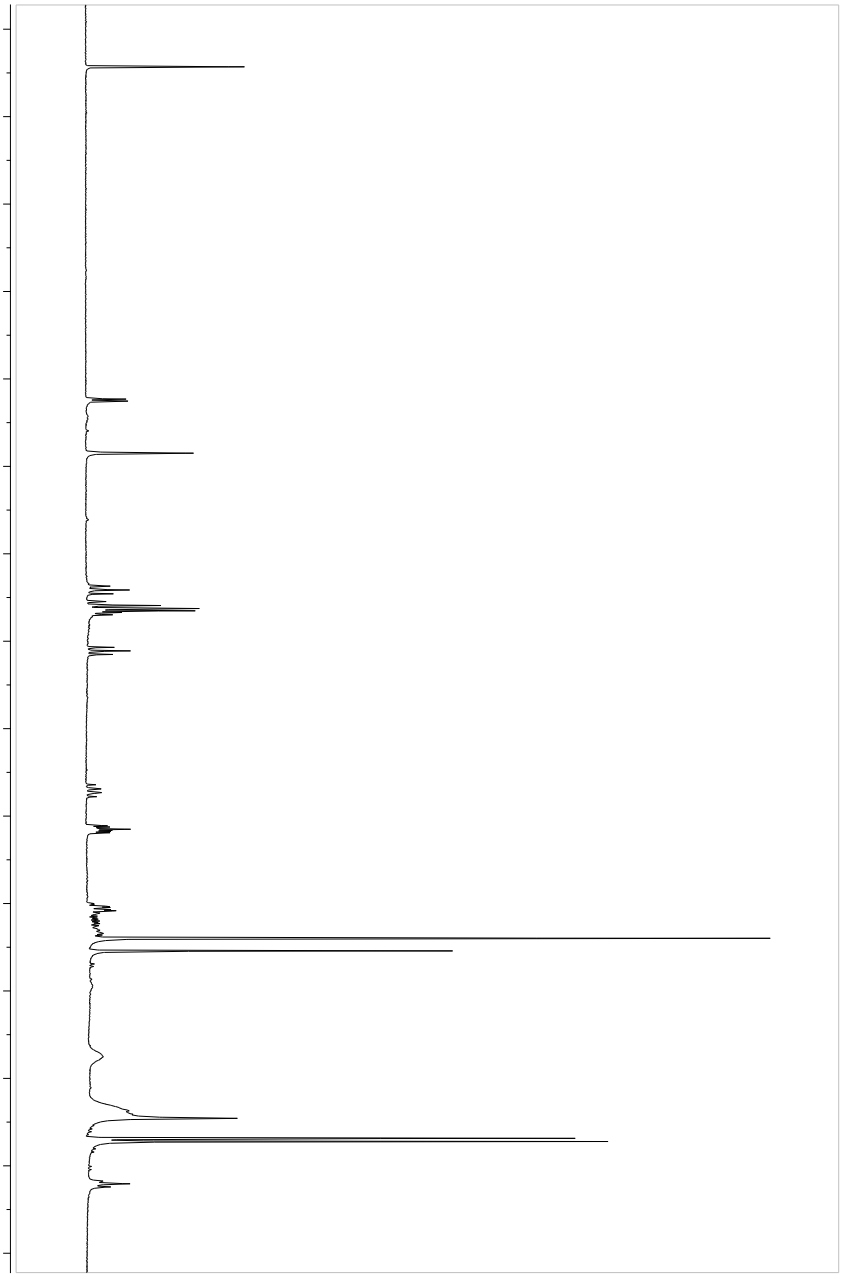

Figure 6.14. ^{1}H NMR spectrum of (2*R*/2*S*-3*S*,4*S*)-3-*epi*-botryodiplodin (**16**) recorded in $CDCl_3$ at 400 MHz

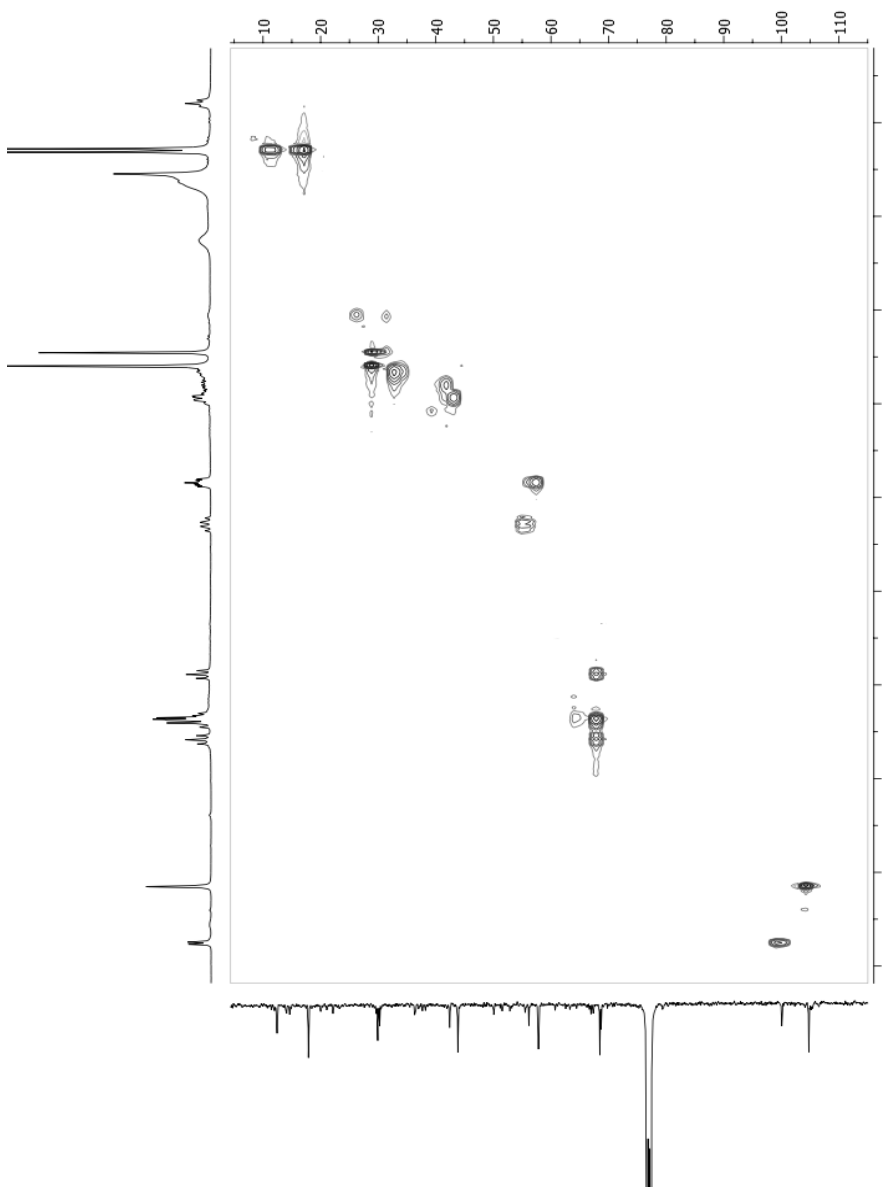

Figure 6.15. HSQC spectrum of (2*R*/2*S*-3*S*,4*S*)-3-*epi*-botryodiplodin (**16**) recorded at 400 MHz in $CDCl_3$

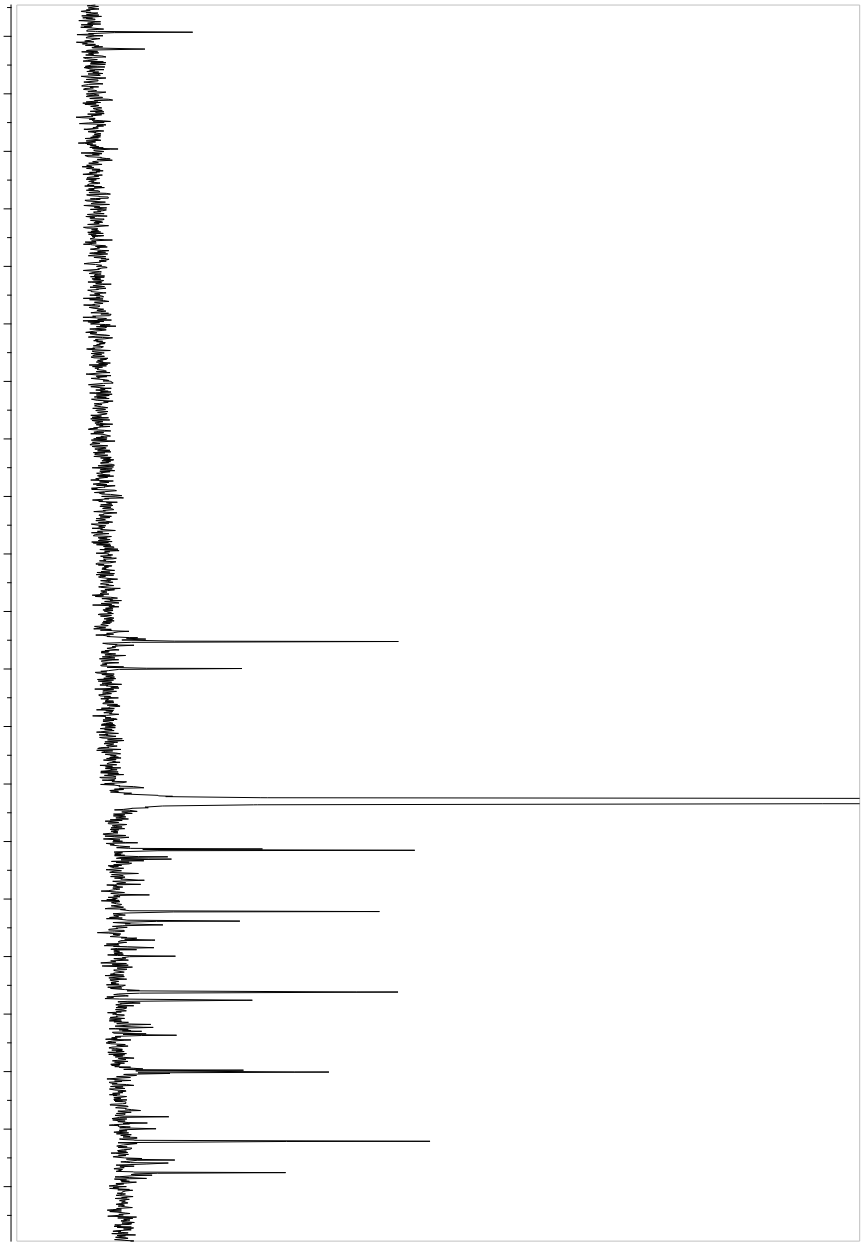

Figure 6.16. ^{13}C NMR spectrum of (2*R*/2*S*-3*S*,4*S*)-3-*epi*-botryodiplodin (**16**) recorded at 100 MHz in $CDCl_3$

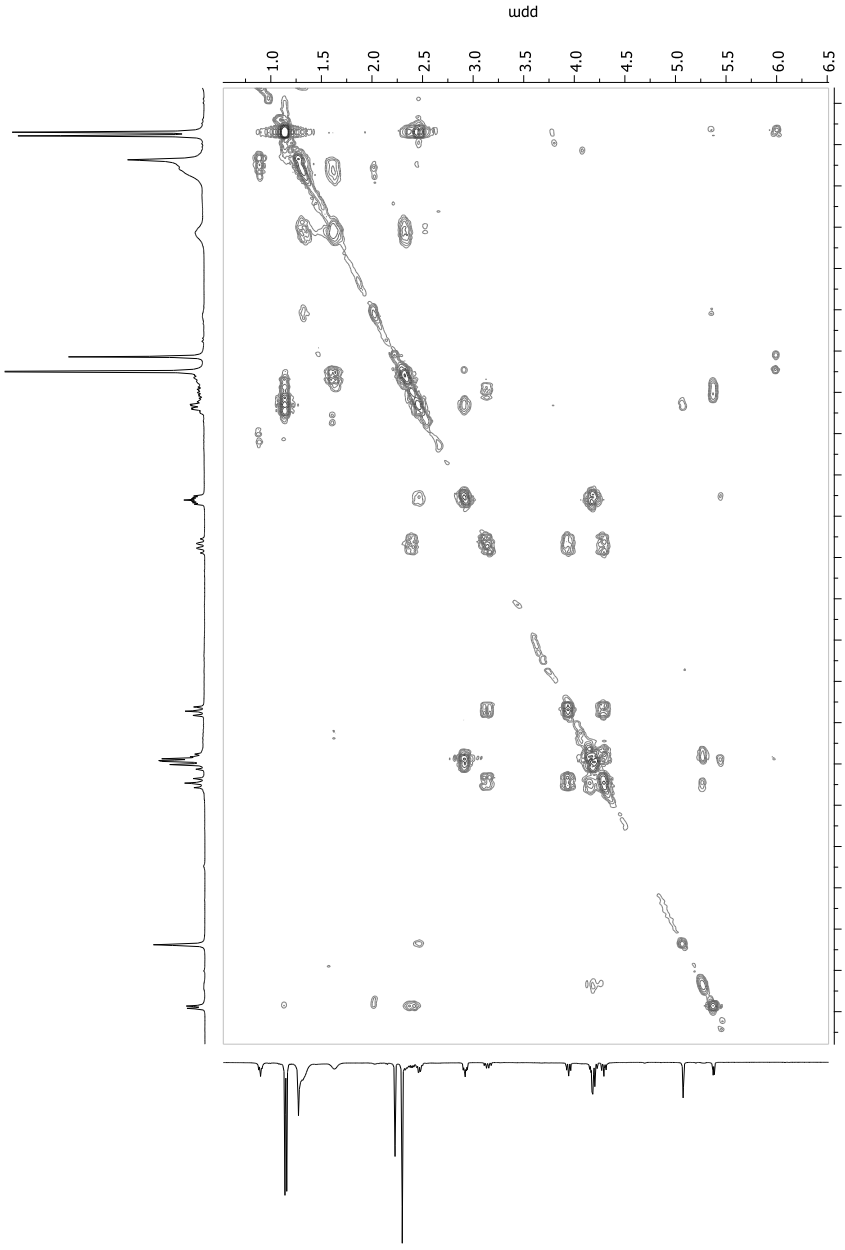

Figure 6.17. ^{1}H, ^{1}H COSY spectrum of (2*R*/2*S*-3*S*,4*S*)-3-*epi*-botryodiplodin (**16**) recorded at 400 MHz in $CDCl_3$

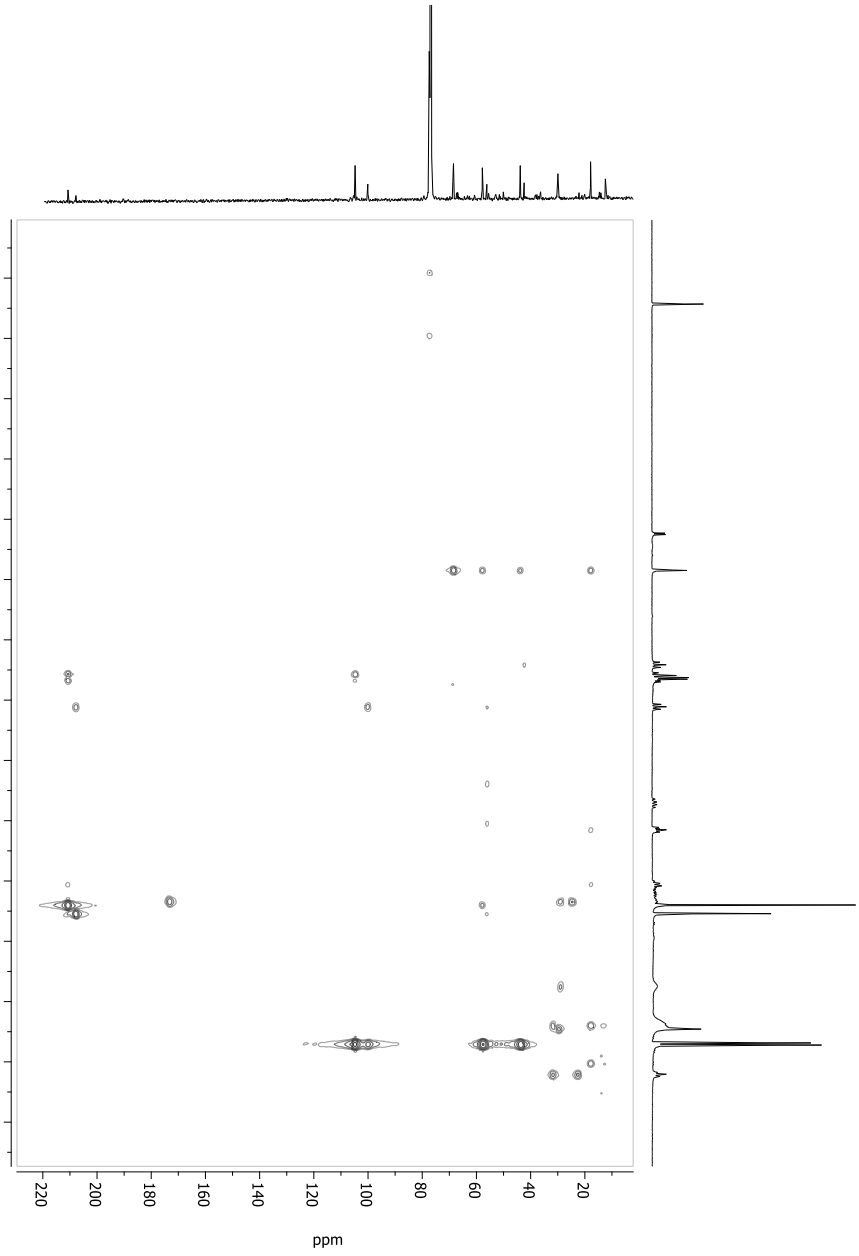

Figure 6.18. HMBC spectrum of (2*R*/2S-3S,4S)-3-*epi*-botryodiplodin (**16**) recorded at 400 MHz in $CDCl_3$

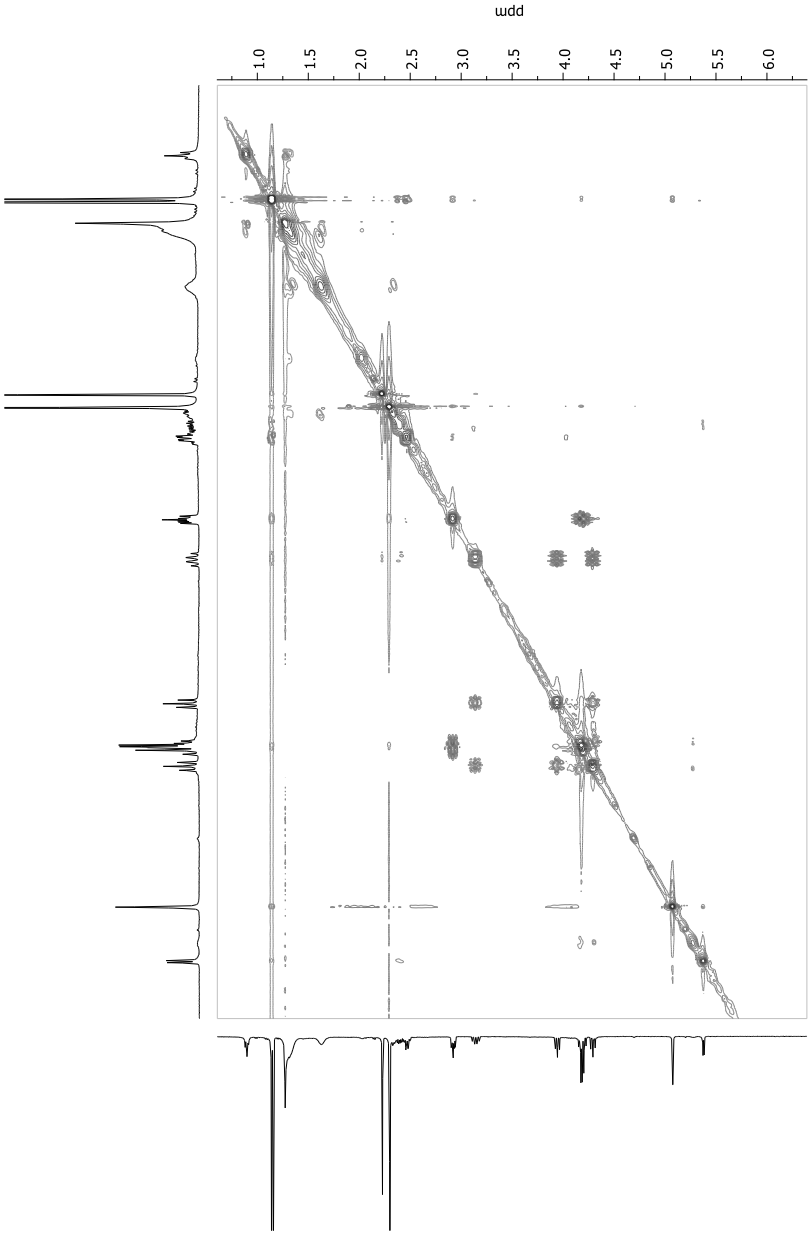

Figure 6.19. NOESY spectrum of (2*R*/2*S*-3*S*,4*S*)-3-*epi*-botryodiplodin (**16**) recorded at 400 MHz in $CDCl_3$

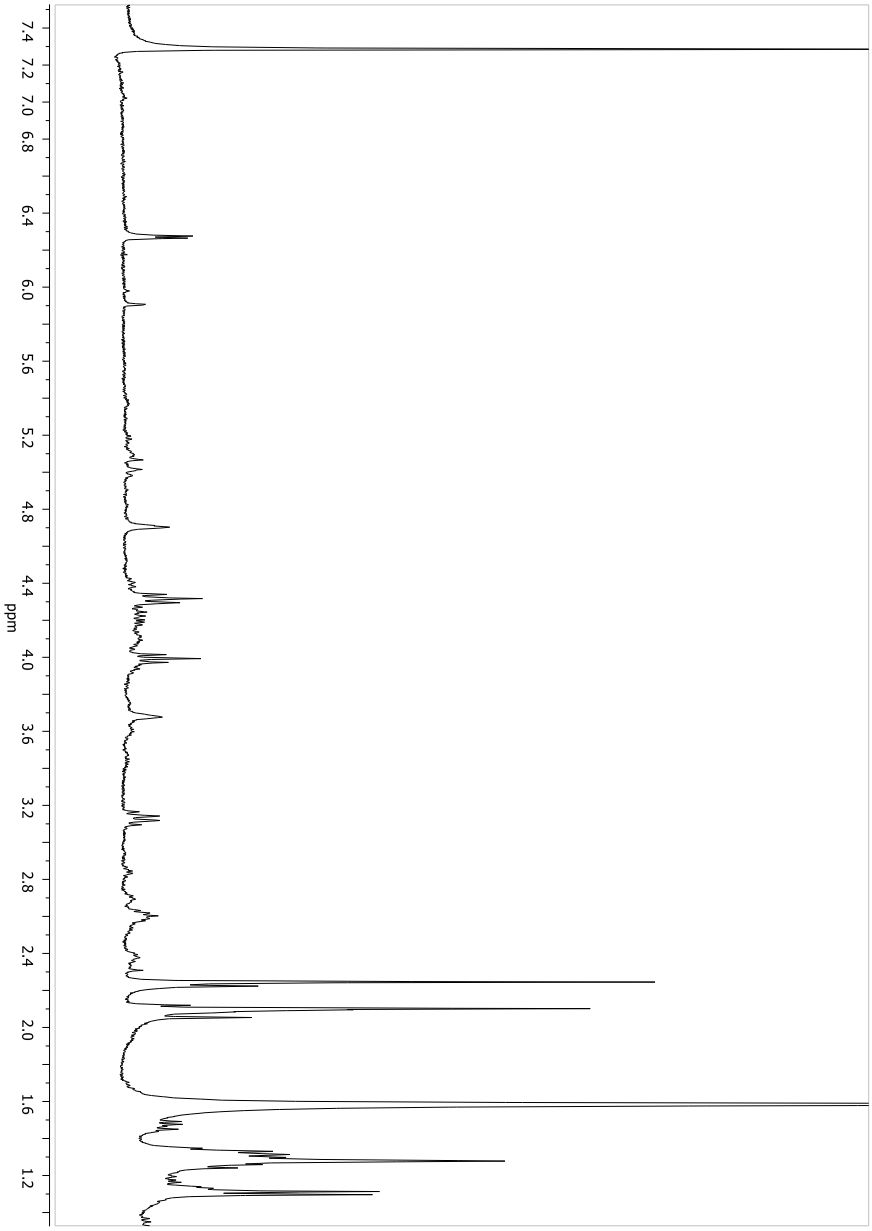

Figure 6.20. ^{1}H NMR spectrum of (2*R*,3*S*,4*S*)-3-*epi*-botryodiplodin acetate (**24B**) recorded in $CDCl_3$ at 400 MHz

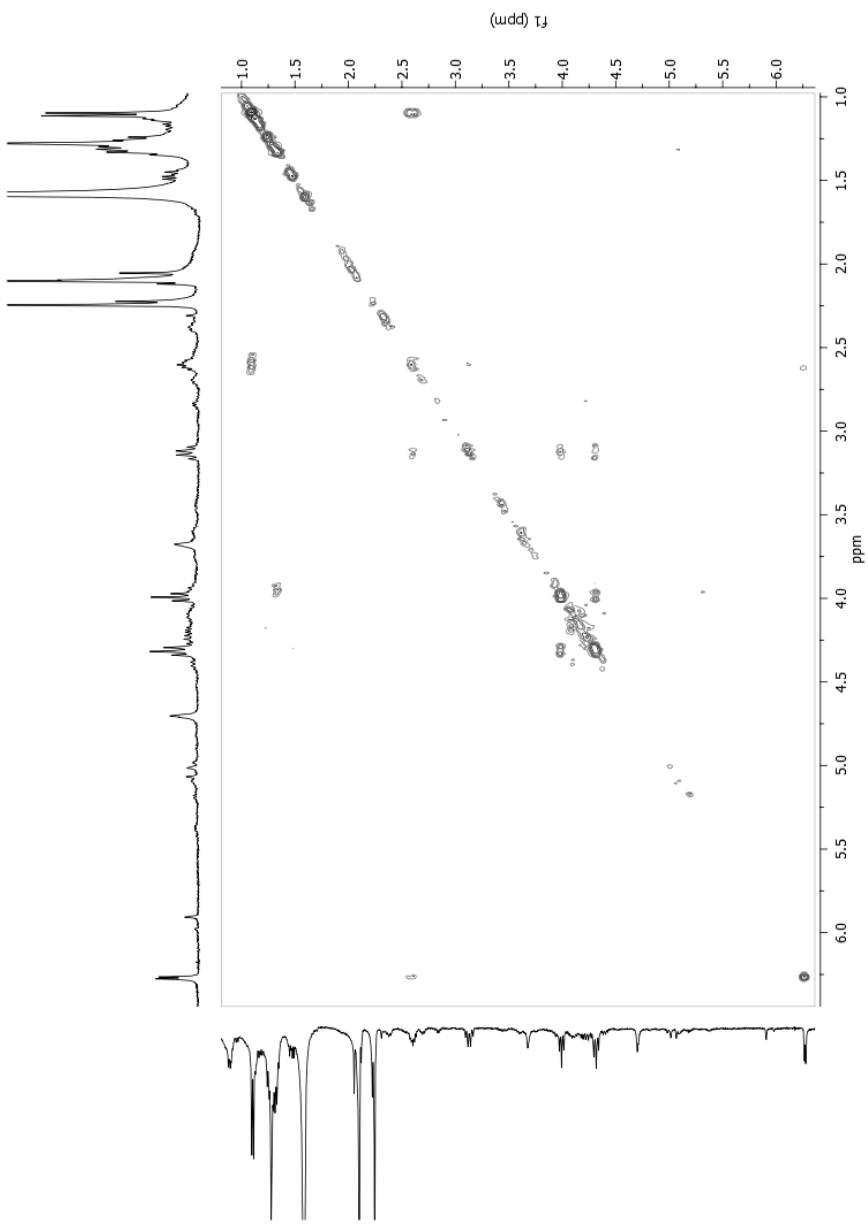

Figure 6.21. ^{1}H, ^{1}H COSY spectrum of (2*R*,3*S*,4*S*)-3-*epi*-botryodiplodin acetate (**24B**) recorded at 400 MHz in $CDCl_3$

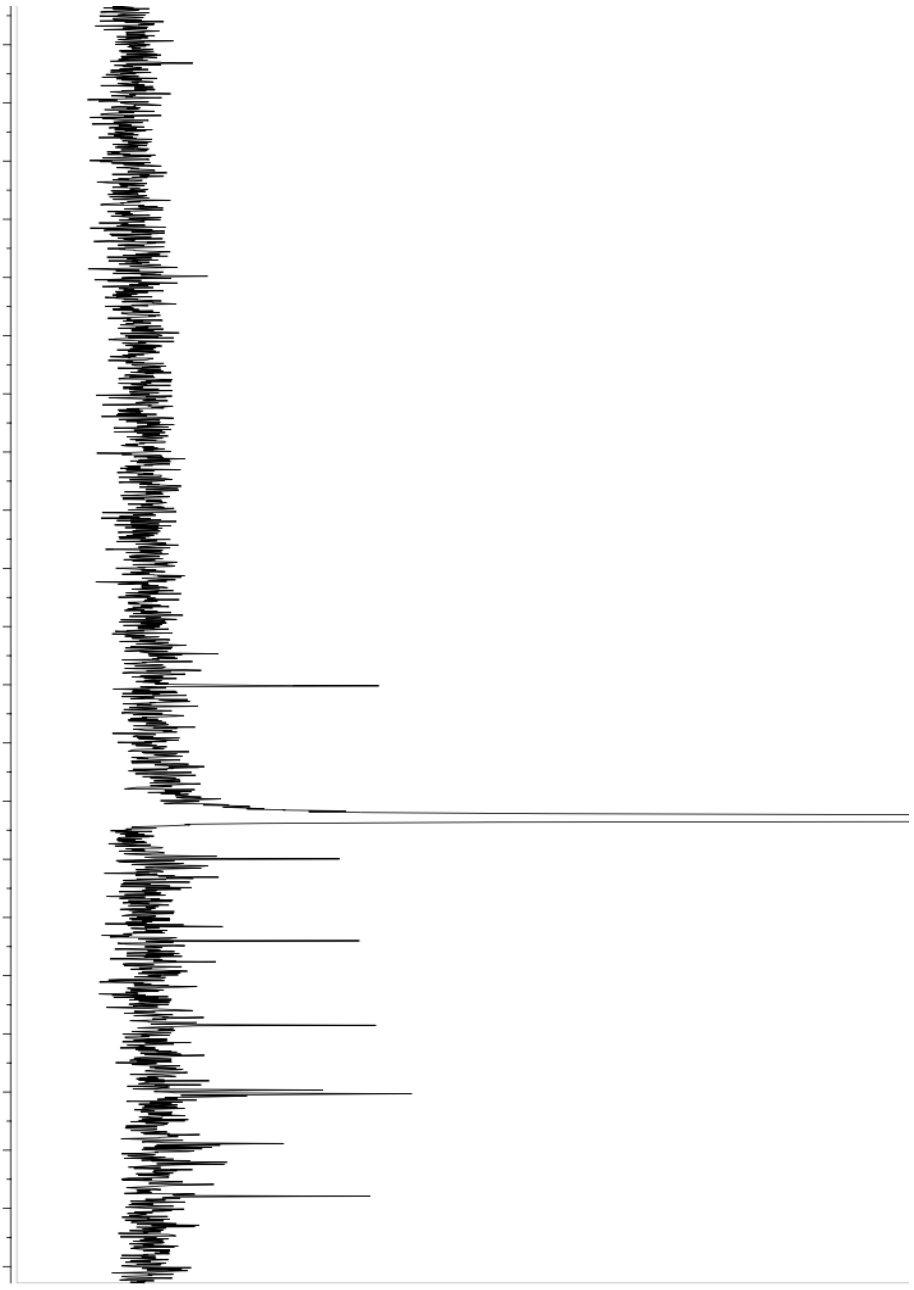

Figure 6.22. ^{13}C NMR spectrum of (2*R*,3S,4S)-3-*epi*-botryodiplodin acetate (**24** B) recorded at 100 MHz in $CDCl_3$

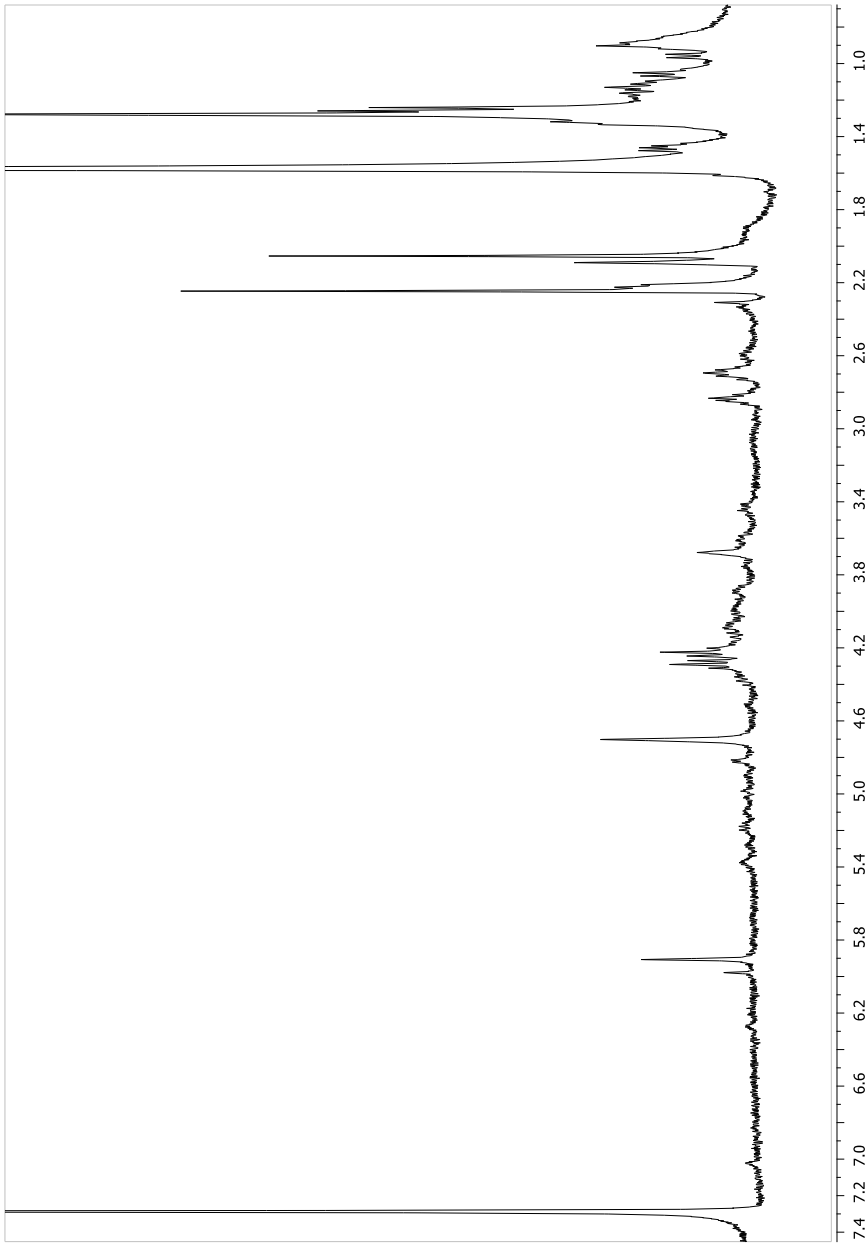

Figure 6.23. ^{1}H NMR spectrum of (2*S*,3*S*,4*S*)-*epi*-botryodiplodin acetate (**24A**) recorded in $CDCl_3$ at 400 MHz

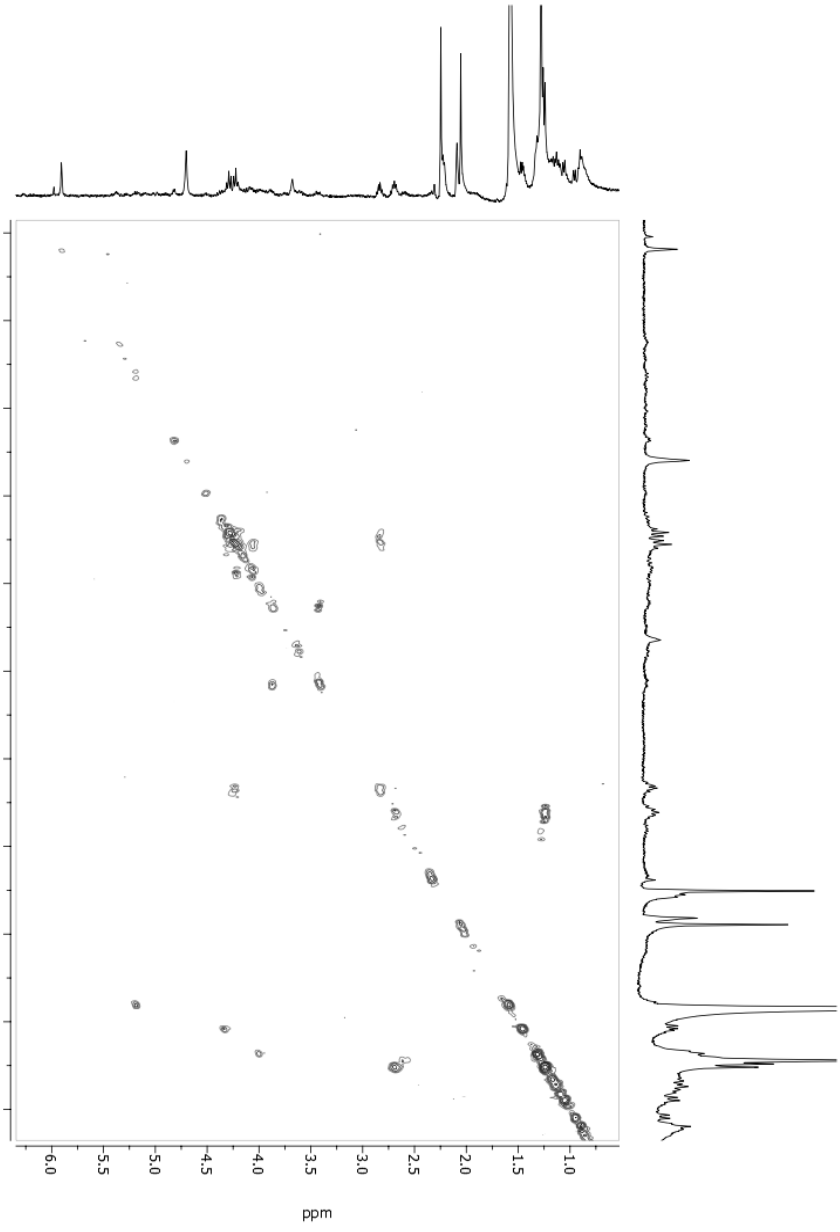

Figure 6.24. ^{1}H, ^{1}H COSY spectrum of (2*S*,3*S*,4*S*)-*epi*-botryodiplodin acetate (**24A**) recorded at 400 MHz in $CDCl_3$

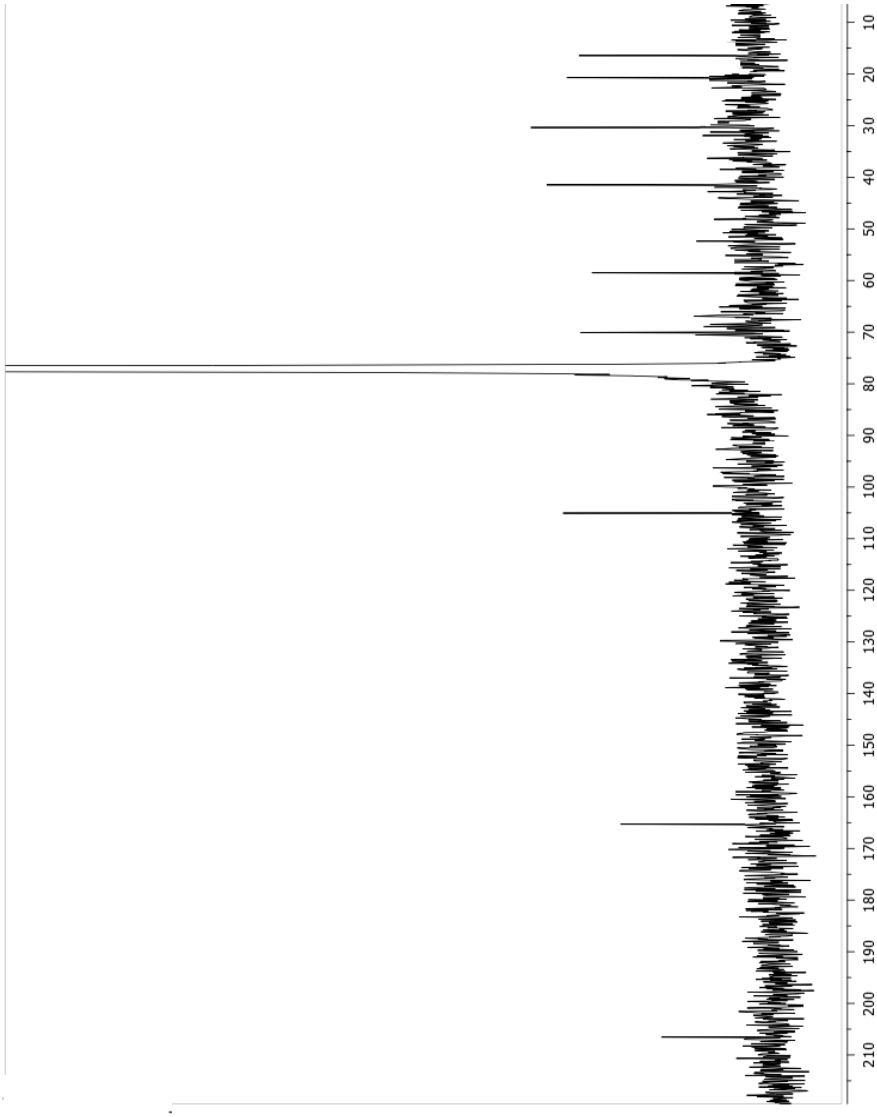

Figure 6.25. ^{13}C NMR spectrum of (2*S*,3*S*,4*S*)-3-*epi*-botryodiplodin acetate (**24** A) recorded at 100 MHz in $CDCl_3$

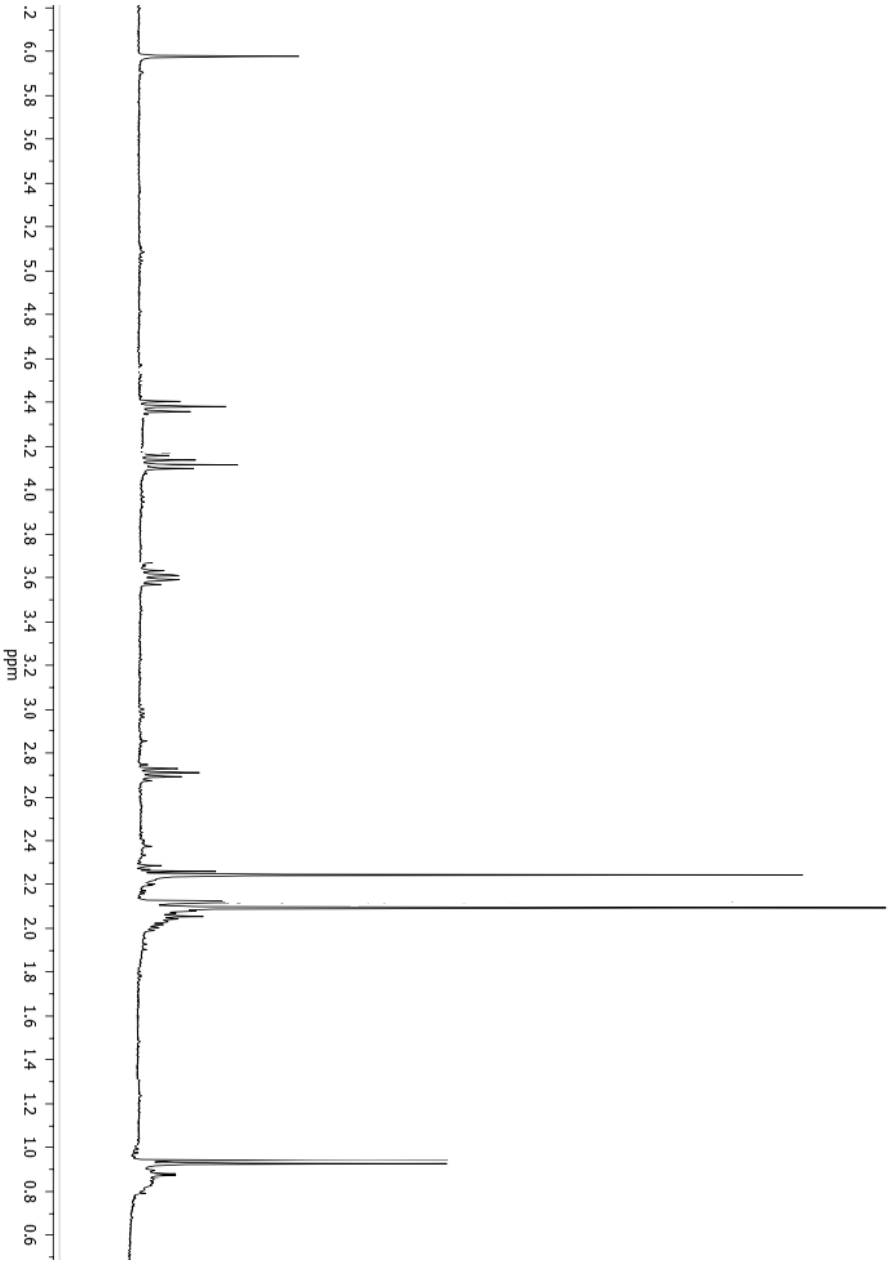

Figure 6.26. ^{1}H NMR spectrum of (2*S*,3*R*,4*S*)-botryodiplodin acetate **(23)** recorded at 400 MHz in $CDCl_3$

Table 6.2. Mass spectra of metabolites reported in Figure 3.3. RI represents the kovats non isothermal retention index; panel "MS peaks annotations" reports mass, formula (in square brackets) and normalized abundance (in round brackets) of identified fragments in mass spectra whenever available, the molecular ion is alwais represented by M, Me indicates methyl (-CH_3); TMS represents -Si(CH_3)$_3$. Abundance is normalized taking abundance of base peak equal 100.

1· (TMS)	RI: 1608	MS peaks annotations: 233 $[M]^+$ (39), 218 $[M\text{-}Me]^+$ (47), 174 $[M\text{-}Me\text{-}CO_2]^+$ (100), 144 $[M\text{-}3Me\text{-}CO_2]^+$ (57), 116 $[M\text{-}TMS\text{-}CO_2]^+$ (19), 73 $[TMS]^+$ (1)

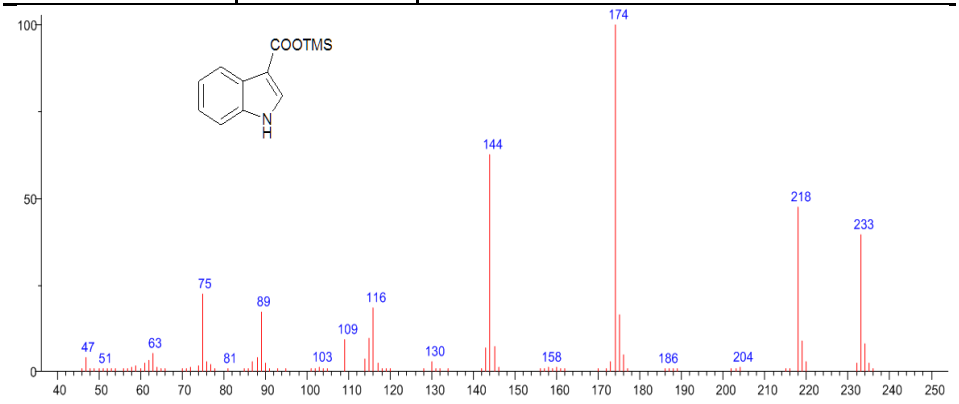

1·(2TMS)	RI: 1618	MS peaks annotations: 305 $[M]^+$ (57), 290 $[M\text{-}Me]^+$ (47), 246 $[M\text{-}Me\text{-}CO_2]^+$ (100), 216 $[M\text{-}3Me\text{-}CO_2]^+$ (57), 73 $[TMS]^+$ (71)

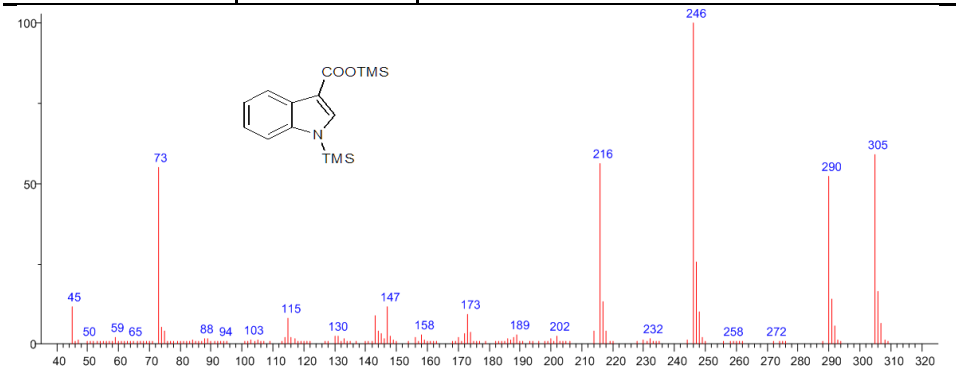

1 ·(ME)	RI: 1535	MS peaks annotations: 175 $[M]^+$ (50)

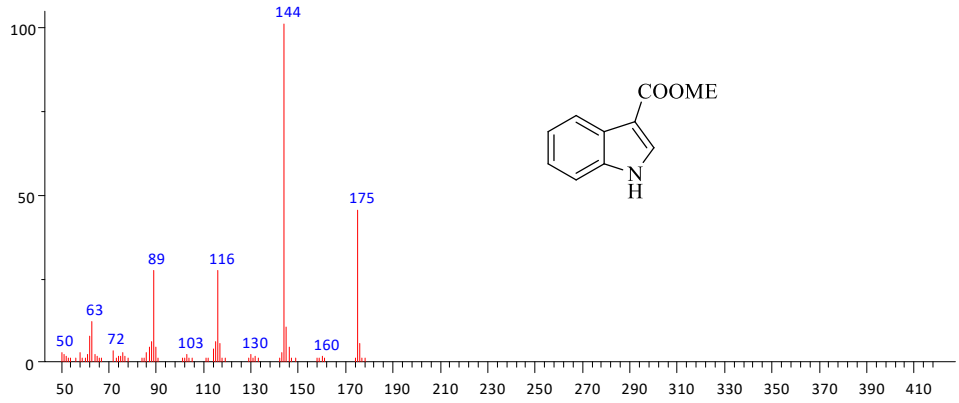

2 (TMS)	RI: 1521	MS peaks annotations: 282 $[M]^+$ (31), 267 $[M\text{-}Me]^+$ (2), 151 $[M\text{-}TMS\text{-}CO_2\text{-}CH_2]^+$ (53), 133 $[M\text{-}TMS\text{-}CO_2\text{-}CH_2\text{-}H_2O]^+$ (39), 109 $[M\text{-}TMS\text{-}CO_2\text{-}CH_2\text{-}C_3H_6]^+$ (20), 96 $[M\text{-}TMS\text{-}CO_2\text{-}CH_2\text{-}C_4H_7]^+$ (24), 73 $[TMS]^+$ (100)

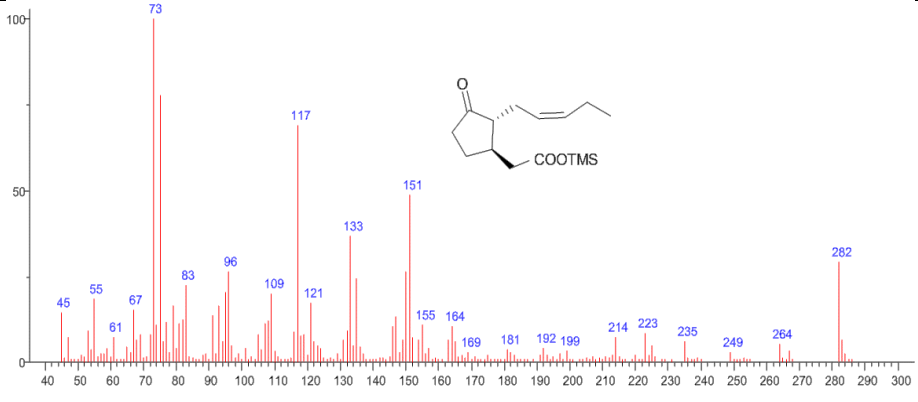

2 (2TMS)	RI: 1542	MS peaks annotations: 354 $[M]^+$ (20), 339 $[M\text{-}Me]^+$ (47), 237 $[M\text{-}TMS\text{-}CO_2]^+$ (10), 223 $[M\text{-}TMS\text{-}CO_2\text{-}CH_2]^+$ (100), 154 $[M\text{-}TMS\text{-}CO_2\text{-}CH_2\text{-}C_5H_9]^+$ (28), 73 $[TMS]^+$ (96)

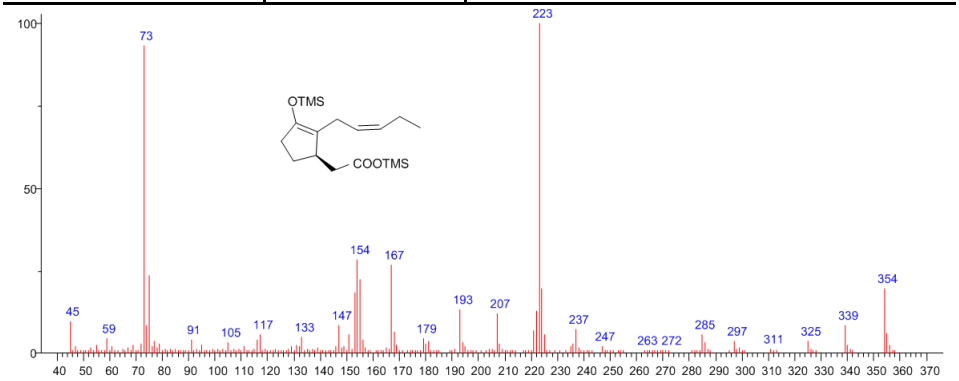

3 (TMS)	RI: 1753	MS peaks annotations: 364 $[M]^+$ (51), 349 $[M\text{-}Me]^+$ (17), 291 $[M\text{-}TMS]^+$ (5), 277 $[M\text{-}TMS\text{-}CH_2]^+$ (10), 254 (72), 210 (100), 73 $[TMS]^+$ (61)

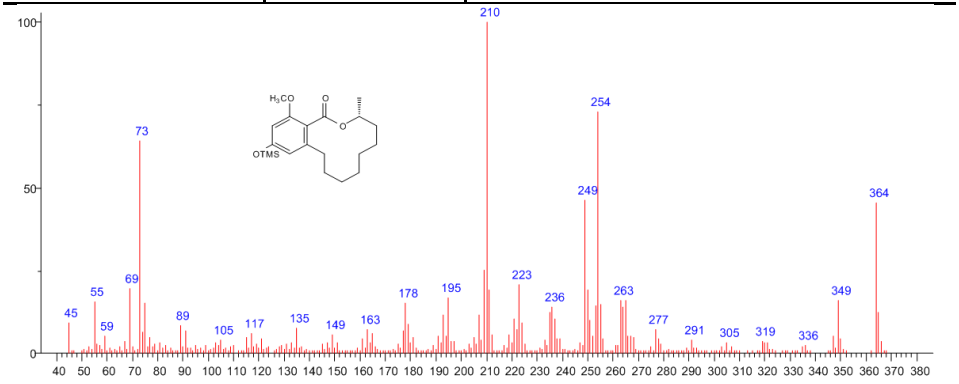

4 (TMS)	RI: 1602	MS peaks annotations: 344 $[M]^+$ (1), 329 $[M\text{-}Me]^+$ (6), 271 $[M\text{-}TMS]^+$ (2), 245 (30), 145 $[C_7H_{13}O_3]^+$ (25), 111 $[C_7H_{11}O]^+$ (100), 73 $[TMS]^+$ (65)

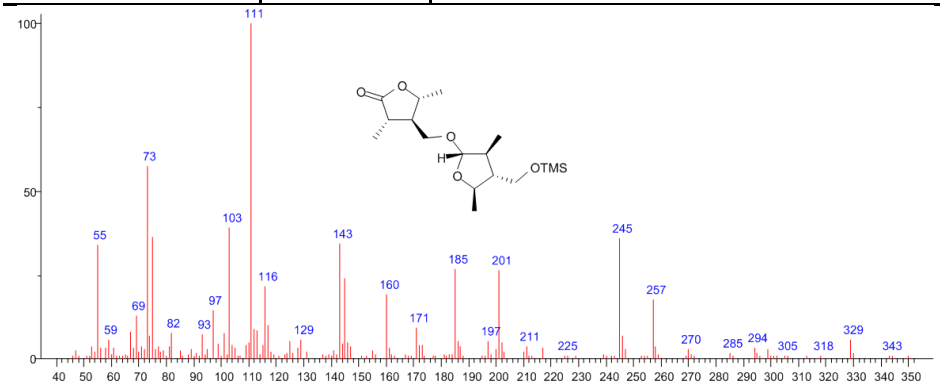

5 (TMS)	RI: 1255	MS peaks annotations: 201 $[M\text{-}Me]^+$ (17), 183 $[M\text{-}Me\text{-}H_2O]^+$ (3), 171 $[M\text{-}2Me]^+$ (100), 157 $[M\text{-}2Me\text{-}CH_2]^+$ (10), 143 $[M\text{-}TMS]^+$ (5), 129 $[M\text{-}TMS\text{-}CH_2]^+$ (14), 73 $[TMS]^+$ (56)

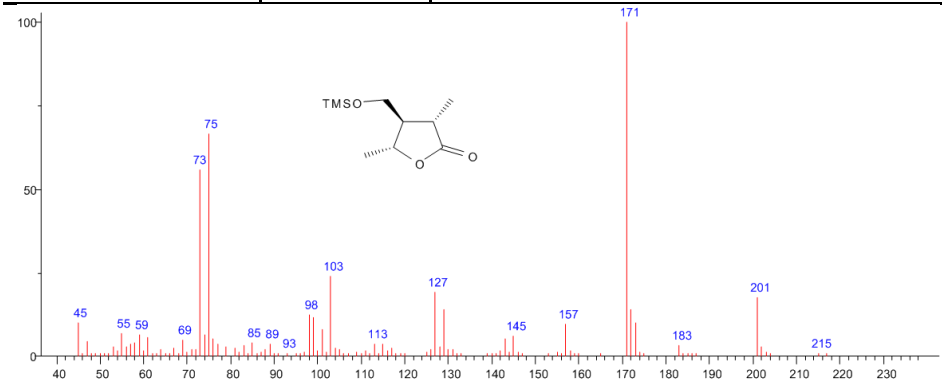

6-7 (TMS)	RI: 1115	MS peaks annotations: 199 $[M\text{-}Me]^+$ (31), 155 $[M\text{-}Me\text{-}CO_2]^+$ (72), 73 $[TMS]^+$ (100)

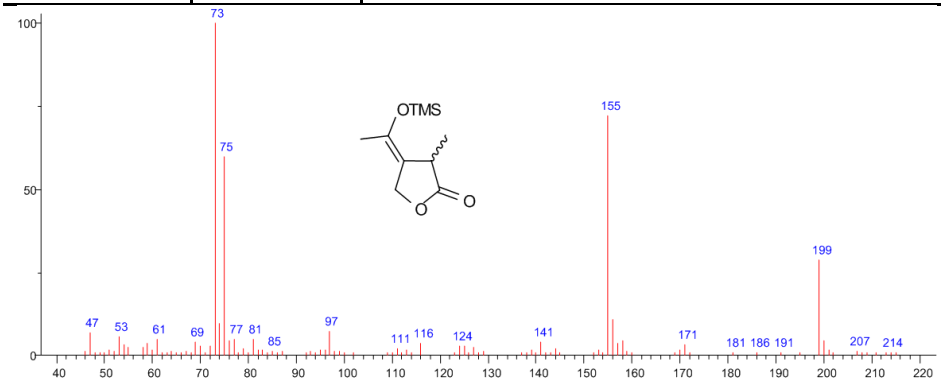

8-9 (2TMS)	RI: 1605	MS peaks annotations: 323 $[M\text{-}Me]^+$ (100), 265 $[M\text{-}TMS]^+$ (14), 249 $[M\text{-}OTMS]^+$ (2), 233 $[M\text{-}OTMS\text{-}Me]^+$ (48), 205 $[M\text{-}OTMS\text{-}Me\text{-}CO]^+$ (17), 73 $[TMS]^+$ (50)

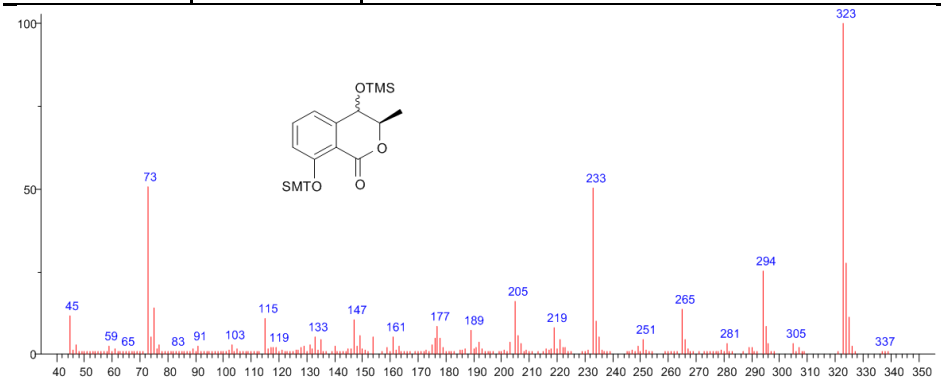

10 (2TMS)	RI: 1635	MS peaks annotations: 338 $[M]^+$ (36), 323 $[M\text{-}CH_3]^+$ (48), 249 $[M\text{-}OTMS]^+$ (14), 221 $[M\text{-}OTMS\text{-}CO]^+$ (4), 73 [TMS] (58)

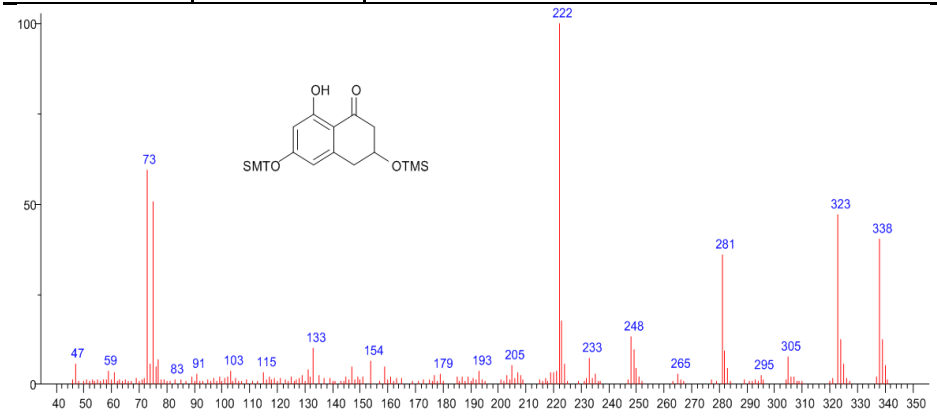

11 (TMS)	RI: 1617	MS peaks annotations: 329 $[M]^+$ (2), 328 $[M\text{-}H]^+$ (5), 313 $[M\text{-}H\text{-}Me]^+$ (91), 129 $[M\text{-}C_5H_7N_2O_2\text{-}TMS]^+$ (52), 73 [TMS] (93)

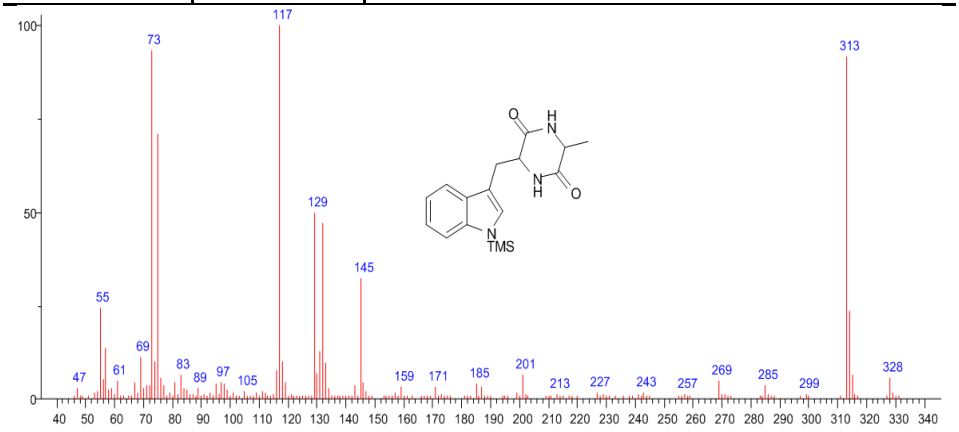

12-13 (2TMS)	RI: 1325	MS peaks annotations: 289 $[M]^+$(1), 275$[M-Me]^+$(1), 259$[M-2Me]^+$(1), 217 $[M-TMS]^+$(2), 200 $[M-OTMS]^+$(6), 143 $[M-2TMS]^+$(91)

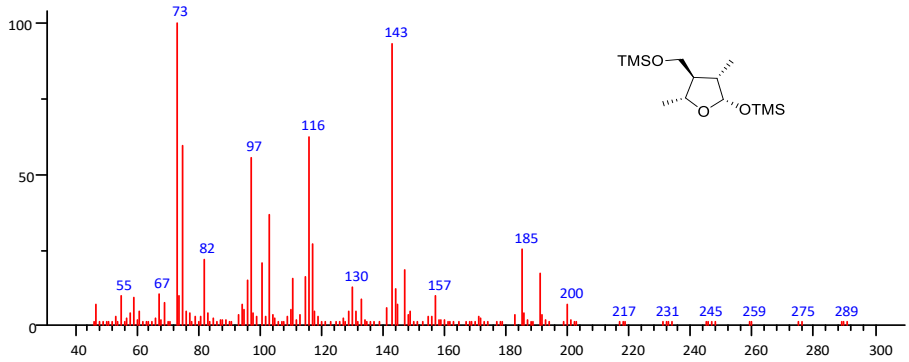

14 (TMS)	RI: 1877	MS peaks annotations: 235$[M-Me]^+$ (100)

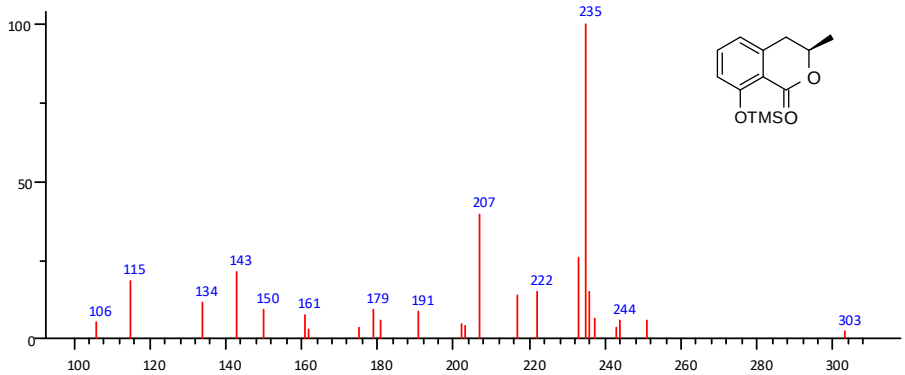

14	RI: 1656	MS peaks annotations: 178[M]$^+$(85),134 [M-C_2H_4O]$^+$(100)

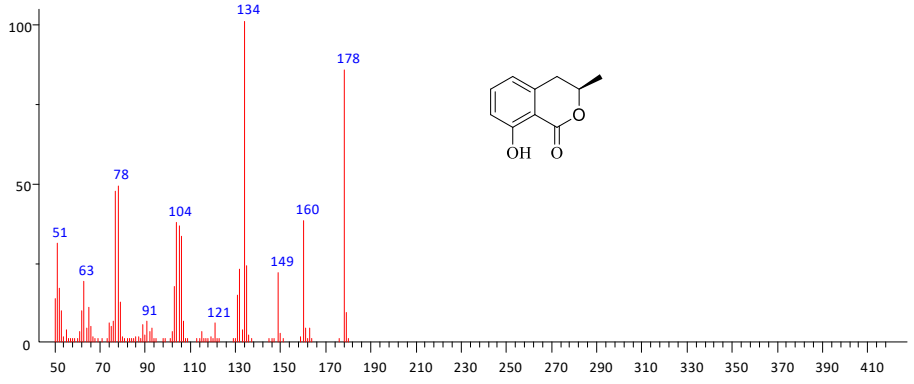

15-16 (TMS)	RI: 1282	MS peaks annotations: 216[M]$^+$(5), 201[M-Me]$^+$(20), 143[M-TMS]$^+$(25), 171[M-C_3H_9]$^+$(70) , 127[M-OTMS]$^+$(4), 100[M-TMS-CH_3CO]$^+$(3)

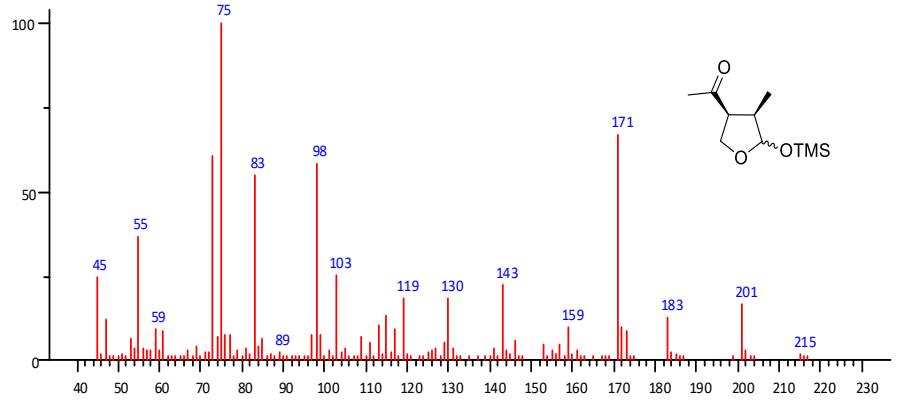

15-16 (2TMS)	RI: 1403	MS peaks annotations: 287[M-H]$^+$(15), 273[M-Me]$^+$(13), 199[M-OTMS]$^+$ (15), 157[M-OTMS-C_3H_6]$^+$(45), 142[M-2TMS]$^+$(65)

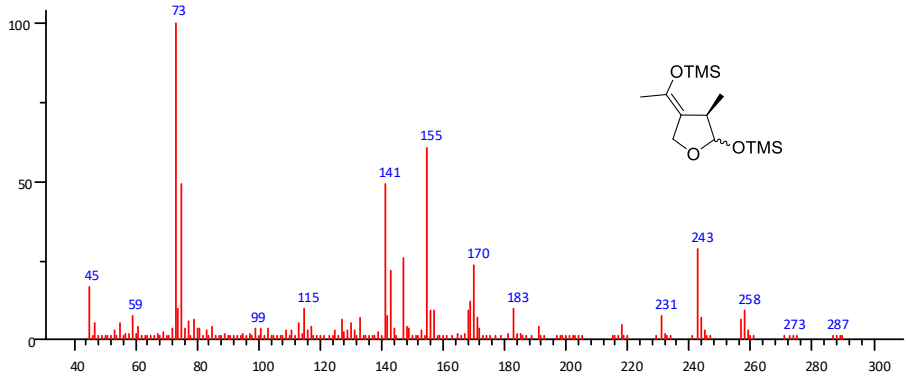

17 (2TMS)	1575	MS peaks annotations: 282 [M]$^+$(19), 267 [M-Me]$^+$(13), 193 [M-OTMS]$^+$(13), 179 [M-OTMS-CH_2]$^+$(100), 103 [M-2OTMS]$^+$(10)

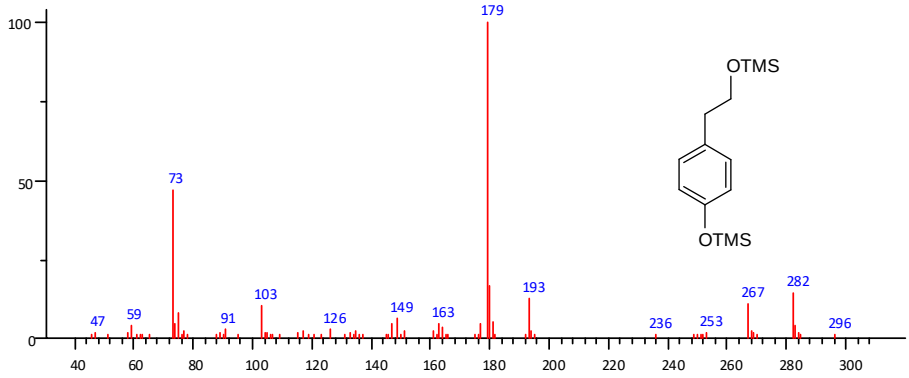

18	RI: 1452	MS peaks annotations: 144 $[M]^+$(100)

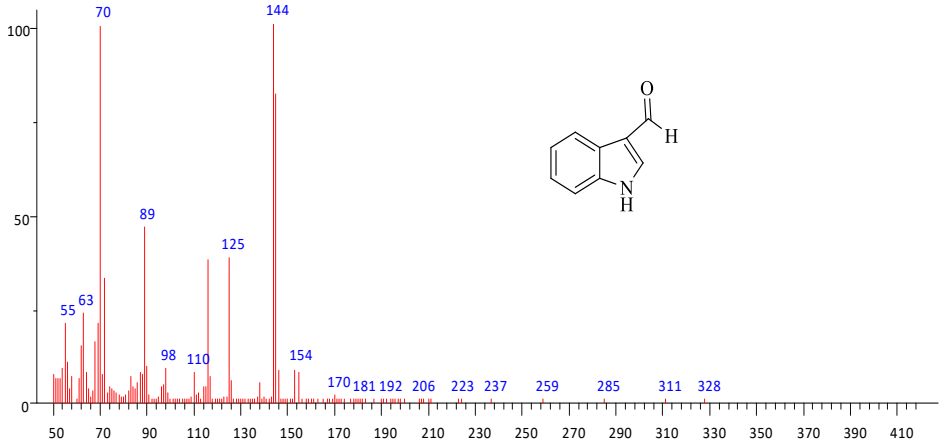

19	RI: 1172	MS peaks annotations: 117 $[M]^+$(100), 90 $[M-C_2H_2]^+$(50)

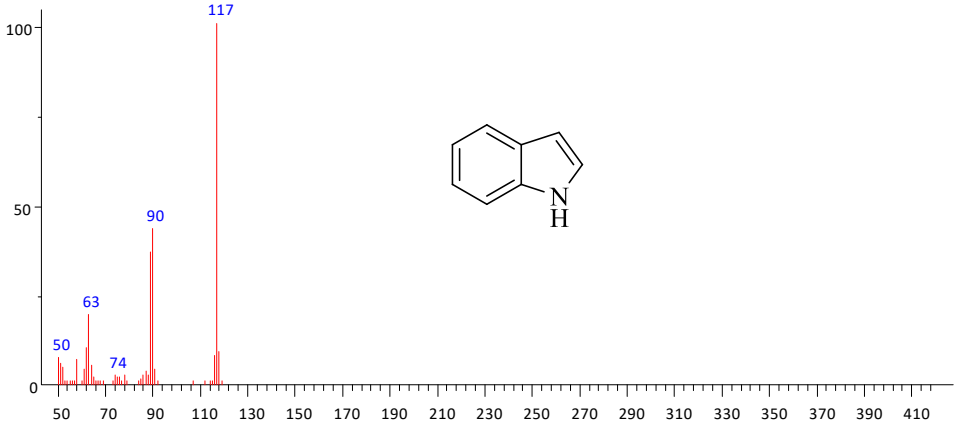

20	RI: 2068	MS peaks annotations: 195 $[M\text{-}Me]^+$ (5), 154 $[M\text{-}C_4H_9]^+$ (100), 125 $[M\text{-}C_6H_{13}]^+$ (15), 111 $[M\text{-}C_7H_{15}]^+$ (3), 70 $[M\text{-}C_7NO_2H_{11}]^+$ (75)

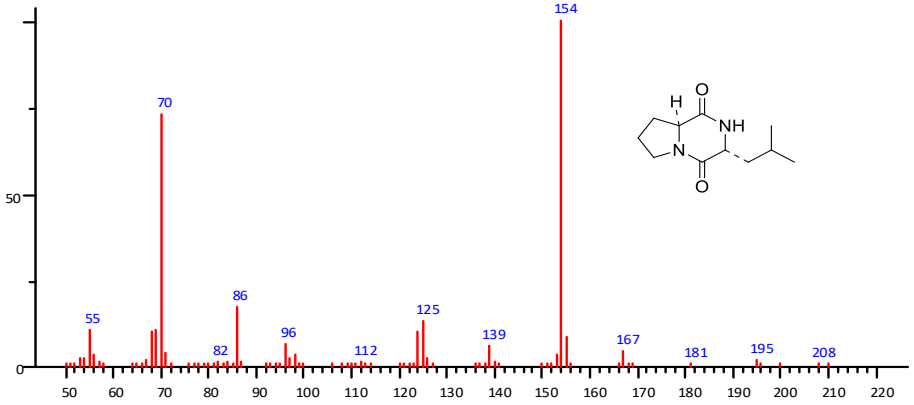

21	RI: 2443	MS peaks annotations: 244 $[M]^+$ (32), 215 $[M\text{-}C_2H_4]^+$ (3), 153 $[M\text{-}C_7H_7]$ (28), 125 $[M\text{-}C_3H_6\text{-}C_6H_5]$ (100)

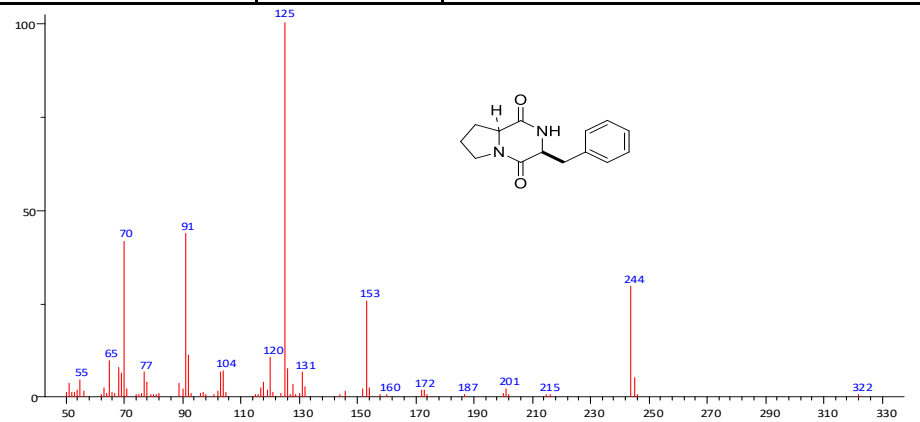

6.3. Experimental Procedures for Chemical and Biological Analysis of Secondary Metabolites by *Macrophomina phaseolina* PE35

6.3.1. Production, Extraction and Purification of Secondary Metabolites

Macrophomina phaseolina PE35 used in this study were originally isolated from *Eucalyptus globulus* in Portugal. The culture was maintained at room temperature on Potato Dextrose Agar (PDA) medium (Merck, Germany). Before inoculations the strain was cultured on PDA at 25 °C for 7 days. Mycelium was scraped from PDA plates and suspended in 5 mL of sterilized ultra-pure water. This mycelial suspension was added to 1 L Erlenmeyers, containing 250 mL of Potato Dextrose Broth (pH 5.6) and incubated for 7 days at 25°C.

Culture filtrate (1 L) was extracted 3 times with EtOAc. The crude extract was dried with Na_2SO_4, and evaporated under reduced pressure originating a brown oil residue (90.2 mg). The crude was fractionated by CC on silica gel (40 cm x 1.5 cm) eluted with $CHCl_3$/*i*-PrOH (9:1, *v/v*) originating 10 homogeneous fractions and the last fraction was eluted with methanol (A 0.7 mg, B 1.3 mg, C 11.0 mg, D 7.1 mg, E 1.1 mg, F 9.3 mg, G 1.9 mg, H 6.7 mg, I 6.8, L 15.0 mg). The residue from fraction B, an amorphous solid, was identified as (*R*)-mellein (Rf 0.67 on TLC on silica gel eluted with $CHCl_3$). The residue of fraction C was purified by preparative TLC on silica gel eluted with a mixture of *n*-hexane/EtOAc (1:1, *v/v*), originating an amorphous solid identified as *cis*-(3*R*,4*R*)-4-hydroxymellein [4.5 mg Rf 0.46 on TLC on silica gel eluted with *n*-hexane/EtOAc (1:1, *v/v*)]. Fraction F, after purification by CC on silica gel (25 cm x 1.0 cm) eluted with *n*-hexane/EtOAc (1:1, *v/v*), produced yellow oil identified as (3*R*,4*S*)-botryodiplodin [7.2 mg Rf 0.24 on TLC on silica gel eluted with n-hexane/EtOAc (1:1, *v/v*)].

6.3.2. Phytotoxicity and Cytotoxicity Assays

Phytotoxicity and cytotoxicity tests were assessed on culture filtrates and crude extracts of *M. phaseolina* PE35 as reported in Section 6.2.2 and 6.2.3.

6.3.3. Statistical Analysis

Two-way analysis of variance (ANOVA), followed by a Tukey multiple comparison test, was used to determine the statistical significance of cytotoxicity between each dilution/concentration and control of crude extract or culture filtrate ($p < 0.05$, $p < 0.01$, $p < 0.001$, $p < 0.0001$). All the analyses were performed with GraphPad Prism 6. Data are shown as the average of three independent replicates of each condition.

6.4. Experimental Procedures for Chemical and Biological Analysis of Secondary Metabolites by *Neofusicoccum vitifusiforme* B8

6.4.1. Pathogenicity Test

Strain B8 of *N. vitifusiforme* was isolated from stem cankers of symptomatic grapevines showing subcortical discolourations and xylematic sectorial necrosis, but without foliar symptoms, in a vineyard in western Sicily and identified in a previous study[20]. The pathogenicity re-isolation test of strain B8 were performed on 2-year-old grapevine plants of cv. Inzolia in this study according to Burruano et al. (2016)[21] .

6.4.2. Production, Extraction and Quantification of Fatty Acids

The fungus grown in stationary conditions in 2 L Erlenmeyer flasks containing 400 mL of Czapek medium amended with corn meal (pH 5.7). For seeding liquid cultures, 5 mL of mycelial suspension by a 1-week-old colony were inoculated in each flask and incubated at 25 °C for 4 weeks in darkness[21]. The culture filtrates were obtained by sterile filtering the culture in a vacuum on a 500

mL Stericup (0.45 lmHV Durapore membrane; Millipore Corp., Billerica, MA, USA) and stored at -20 ◦C.

The freeze-dried culture filtrate (10 L) was dissolved in ultrapure water (1 L) and extracted at native pH (i.e., pH ≈ 6.0) three times with ethyl acetate (1 L for each). The organic phases were combined, dried with Na_2SO_4, and evaporated under reduced pressure to give the crude extract as brown-red oil (550.2 mg).

6.4.3. Preparation of Samples for Quantification via GC-MS

Fatty acids were methylated as reported above. Quantification of individual methylated (ME) fatty acids was obtained by linear regression of the chromatographic peak areas and known concentrations of certified standards (ranging from 50 to 200 mg L^{-1})[22]. The response of target compounds was normalized to the response of an internal standard (nonanoic acid ME), which was added to the sample prior to the analysis at the constant concentration of 100 mg L^{-1}.

6.5. Experimental Procedures for Chemical and Biological Analysis of Secondary Metabolites by *Trichoderma citrinoviride* A12

6.5.1. Isolation, Cultivation and Identification of Fungal Strain

The green alga *Cladophora* sp. was collected from a rock on the shoreline in Miliscola, near Naples, Italy (40.788046 N, 14.068539 E). The alga was morphologically identified by Prof. Antonino Pollio, Department of Biology University of Naples Federico II, Naples, Italy. Two-cm cuttings from this specimen were aseptically excised and plated on potato dextrose agar (PDA) amended with 1% lactic acid. Plates were incubated in the dark at 25°C and after 48 h, a plug of the mycelium emerging from the cuttings was sub-cultured on fresh plates. Strain A12 was provisionally identified as *Trichoderma* sp. according to its morphological characters, i.e. the production of sparsely branched

conidiophores bearing the typically flask-shaped phialides. Molecular analyses of rDNA-ITS sequence were carried out for a more conclusive taxonomic identification. To this purpose, fungal mycelium grown for 7 days on PDA plates was collected and genomic DNA was extracted using NucleoSpin® Soil kit, following manufacturer's instructions. DNA quantification was performed using dsDNA BR assay on a Qubit 2.0 fluorometer (Life Technologies, Carlsbad, CA, USA). The internal transcribed spacer region (ITS) of rDNA was amplified using the primer pair ITS1 (5′-TCC GTA GGT GAA CCT GCG G-3′) and ITS4 (5′-TCC TCC GCT TAT TGA TAT GC-3′), according to White et al. (1990). PCR amplifications was carried out in a total reaction volume of 50 µl, with 0.5 µM each primer, 0.2 mM dNTP Mix, 1 × DreamTaq Green Buffer (Thermo Fisher Scientific, Waltham, MA, USA), and 1.25 U of DreamTaq DNA Polymerase (Thermo Fisher Scientific). PCR was conducted as follows: initial denaturation (3 min at 95 °C), 35 cycles of primer denaturation (30 s at 95 °C), annealing (30 s at 52 °C), and elongation (45 s at 72 °C), followed by a final elongation step (10 min at 72 °C). PCR products were sequenced by Eurofins Genomics using the ITS1 primer. Sequences alignments were carried out through Clustal Omega multiple sequence alignment program tool of the EMBL-EBI web site[23]. ITS sequence has been deposited in GenBank under the reference number MG878433.

6.5.2. Isolation and Identification of Metabolites

Mycelial plugs from actively growing cultures of strain A12 were inoculated in 2 L Erlenmayer flasks each containing 1 L of potato dextrose broth (PDB). The stationary cultures (3 L) were incubated in the dark at 25 ± 2 °C for 21 days. The fungal cultures were vacuum filtered through filter paper (Whatman No. 4) to remove the biomass, and the culture filtrate was collected and extracted exhaustively with ethyl acetate. The organic extracts were combined, dried with Na_2SO_4, and evaporated under reduced pressure at 37°C to give a brown-red oil residue (338.4 mg). The crude organic extract was submitted to fractionation on

silica gel column (1.5 x 40 cm), eluted with $CHCl_3$/*i*-PrOH (9:1, *v/v*). The last fraction was eluted with MeOH. Fraction D (30.0 mg) was further purified by silica-gel preparative TLC eluted with $CHCl_3$/*i*-PrOH (95:5, *v/v*), yielding six homogeneous sub-fractions. The residue of first sub-fraction obtained as yellow oil, was identified as sorbicillin [**4**, 1.0 mg, *Rf* 0.75], while the residue of the second subfraction, obtained as colourless oil, was identified as 2-phenylethanol [**5**, 9.7 mg, *Rf* 0.55]. The residue of the sixth sub-fraction was further purified by TLC on silica gel eluted with $CHCl_3$/*i*-PrOH (9:1, *v/v*) giving, as yellow amorphous solid, spirosorbicillinol A [**2**, 0.8 mg, *Rf* 0.59]. Fraction 5 was purified in two steps by TLC on silica gel eluted with $CHCl_3$/*i*-PrOH (95:5, *v/v*), then with *n*-hexane/Me_2CO (6:4, *v/v*), yielding two metabolites: a yellow solid, identified as (*R*)-vertinolide [**3**, 1.8 mg, *Rf* 0.15, eluent *n*-hexane/Me_2CO (6:4, *v/v*), and *Rf* 0.37, eluent $CHCl_3$/*i*-PrOH (95:5, *v/v*)], and a white solid, identified as tyrosol [**6**, 1.2 mg, *Rf* 0.34, eluent *n*-hexane/Me_2CO (6:4, *v/v*)]. Finally, the residue of Fraction 7 was further purified by TLC on silica gel with $CHCl_3$/*i*-PrOH (9:1, *v/v*) to give a yellow oil, found to be trichodermanone C [**1**, 4.8 mg, *Rf* 0.27, eluent $CHCl_3$/*i*-PrOH (9:1, *v/v*), and *Rf* 0.25, eluent *n*-hexane/Me_2CO (6:4, *v/v*)].

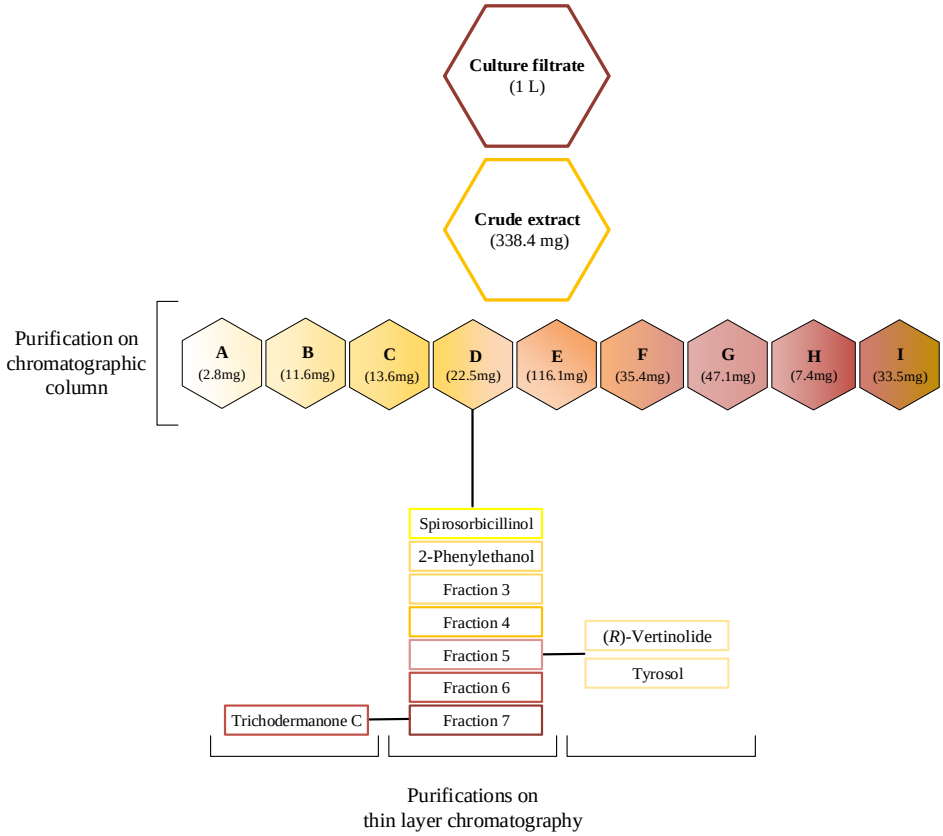

Scheme 6.9. Schematic representation of purification process of *M. phaseolina* PE35 crude extract.

Trichodermanone C ***(1)***. $[\alpha]_D^{25}$ +257 (MeOH, *c* 0.6); ^{1}H NMR (400 MHz, $CDCl_3$, *J* in Hz): δ 13.90 (s, OH), 7.36 (dd, 14.9, 10.5, H-14), 6.28-6.21 (m, H-13,14 and 15), 4.26 (d, 12.2, H-11), 3.86 (d, 12.2, H-11), 3.41 (s, H-6), 3.43 (d, 11.0, H-20), 3.36 (d, 11.0, H-20), 2.63 (dd, 9.7, 7.6, H-8), 2.21 (dd, 14.1,9.9, H-9), 1.92 (d, 6.3, H3-17), 1.62 (dd, 14.1, 7.4, H-9), 1.23 (s, H3-19), 1.22 (s, H_3-18); ^{13}C NMR (100 MHz, $CDCl_3$) δ 211.5 (C-4), 198.1 (C-2), 168.7 (C-12), 143.1 (C-14), 140.4 (16), 130.8 (C-15), 117.6 (C-13), 109.4 (C-1), 106.8 (C-10), 88.9 (C-7), 74.5 (C-5), 68.3 (C-11), 63.1 (C-3), 50.2 (C-8), 47.0 (C-6), 38.4 (C-9), 27.0

(C-19), 18.9 (C-17), 10.7 (C-18); HR ESI MS (+) spectrum *m/z*: 811.3141 [$C_{40}H_{52}O_{16}Na$, calcd. 811.3148, 2M+Na]$^+$, 417.1520 [$C_{20}H_{26}O_8Na$, calcd. 417.1525, M+Na]$^+$, 377.1598 [$C_{20}H_{25}O_7$, calcd. 377.1600, M-OH]$^+$, 359 [M-OH-H_2O]$^+$.

*Spirosorbicillinol A (**2**)*. $[\alpha]_D^{25}$ +158 (MeOH, *c* 0.2); NMR (400 MHz, $CDCl_3$, *J* in Hz) δ: 13.81 (s, OH), 7.38 (dd, 14.9, 10.1, H-3'), 6.76 (brs, H-13), 6.29 (m, H-4' and H-5'), 6.18 (d, *J* = 14.9 Hz, H-2'), 4.70 (s, OH), 4.55 (m, H-12), 4.36 (dd, 9.5, 0.7, H-11), 3.88 (dt, 9.5, 6.2, H-10), 3.79 (s, $COOCH_3$), 3.67 (brs, OH), 3.27 (t, 2.9, H-1), 3.08 (dd, 13.7, 2.9, H-7), 2.93 (dd, 17.8, 6.2, H-15), 2.37 (m, H-15), 2.10 (dd, 13.7, 2.9, H-7), 1.93 (d, 6.0, H_3-6'), 1.34 (s, CH_3-4), 1.28 (s, CH_3-6); HR ESI MS (+) spectrum *m/z*: 999.3245 [$C_{50}H_{56}O_{20}Na$, calcd.999.3257, 2M+Na]$^+$, 511.1568 [$C_{25}H_{28}O_{10}Na$, calcd. 511.1575, M+Na]$^+$, 489.1753 [$C_{25}H_{29}O_{10}$, calcd. 489.1761, M+H]$^+$, 471.1651 [$C_{25}H_{27}O_9$, calcd. 471.1656, M-OH]$^+$.

*Vertinolide (**3**)*. HR ESI MS (+) spectrum *m/z*: 523.2293 [$C_{28}H_{36}O_8Na$, calcd. 523.2302, 2M+Na]$^+$, 273.1089 [$C_{14}H_{18}O_4Na$, calcd. 273.1097, M+Na]$^+$, 251.1271 [$C_{14}H_{19}O_4$, calcd. 251.1278, M+H]$^+$, 233.1139 [$C_{14}H_{17}O_3$, calcd. 233.1178, M-H_2O]$^+$.

*Sorbicillin (**4**)*. HR ESI MS (+) spectrum *m/z*: 233.1172 [$C_{14}H_{17}O_3$, calcd. 233.1172, M+H]$^+$.

Trichodimerol (**7**). HR ESI MS (+) spectrum *m/z*: 535.1713 [$C_{28}H_{32}O_8$, calcd. 535.1734, M+K]$^+$, 519.1981 [$C_{28}H_{32}O_8Na$, calcd. 511.1995, M+Na]$^+$, 497.2166 [$C_{28}H_{33}O_8$, calcd. 497.2175, M+H]$^+$, 479.2056 [$C_{28}H_{31}O_7$, calcd. 479.2070, M-OH]$^+$.

*Rezishanone A (**8**)*. HR ESI MS (+) spectrum *m/z*: 363.1436 [$C_{19}H_{23}O_7$, calcd. 363.1438, M+H]$^+$, 345.1327 [$C_{19}H_{21}O_6$, calcd. 345.1338, M-OH]$^+$.

*2',3'-Sorbicillin (**9**)*. HR ESI MS (+) spectrum *m/z*: 235.1339 [$C_{14}H_{19}O_3$, calcd. 235.1329, M+H]$^+$, 217.1223 [$C_{14}H_{17}O_2$, calcd. 217.1229, M-OH]$^+$.

*Bisvertinol (**10**)*. HR ESI MS (+) spectrum *m/z*: 499.2332 [$C_{28}H_{35}O_8$, calcd. 499.2332, M+H]$^+$.

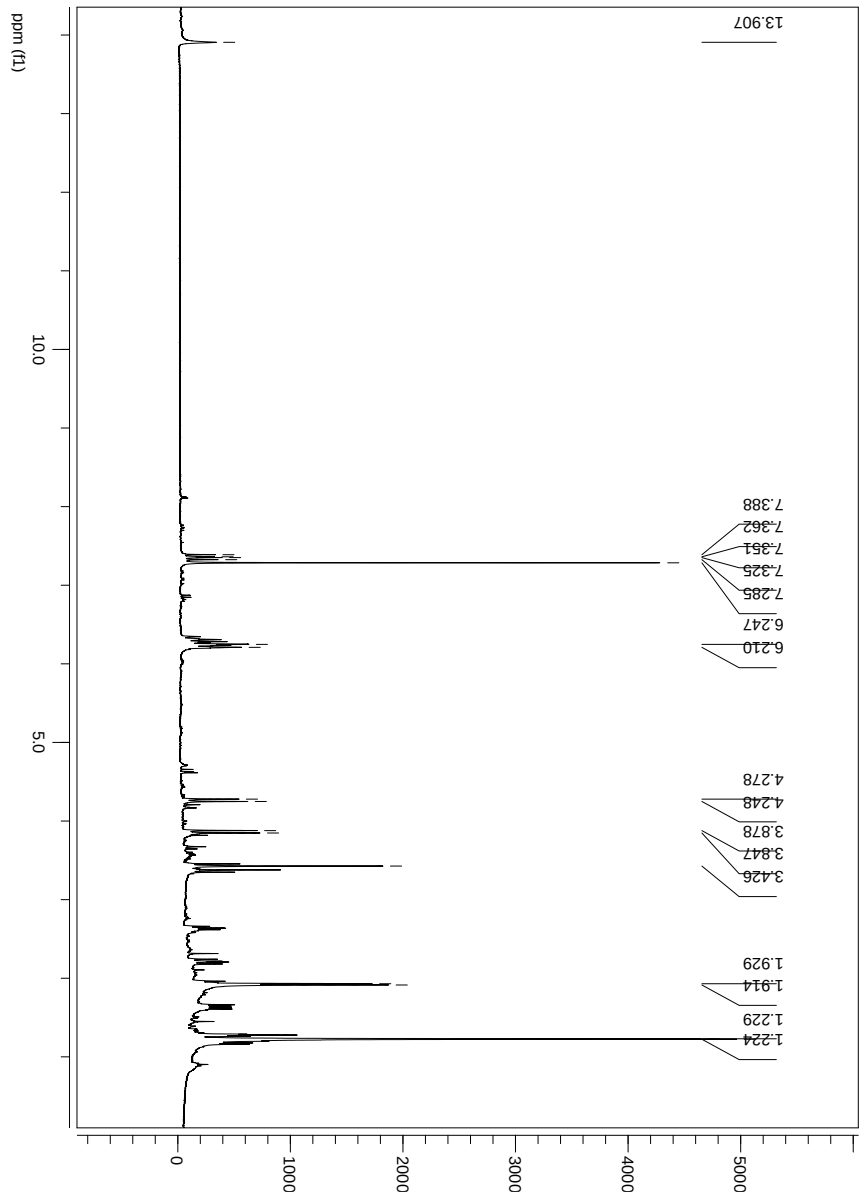

Figure 6.27. ^{1}H NMR spectrum of trichodermanone C (**1**) recorded in $CDCl_3$ at 400 MHz

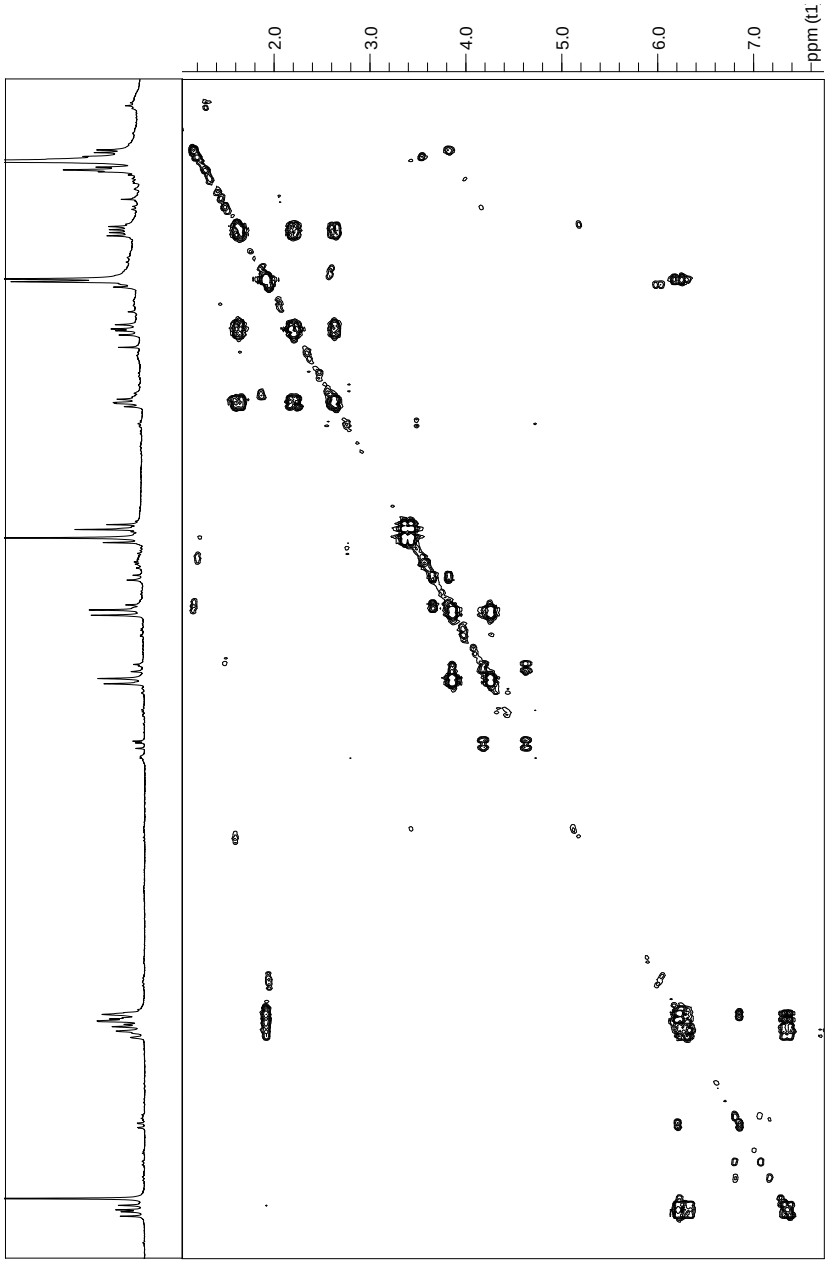

Figure 6.28. COSY spectrum of trichodermanone C(**1**) recorded in $CDCl_3$ at 400 MHz

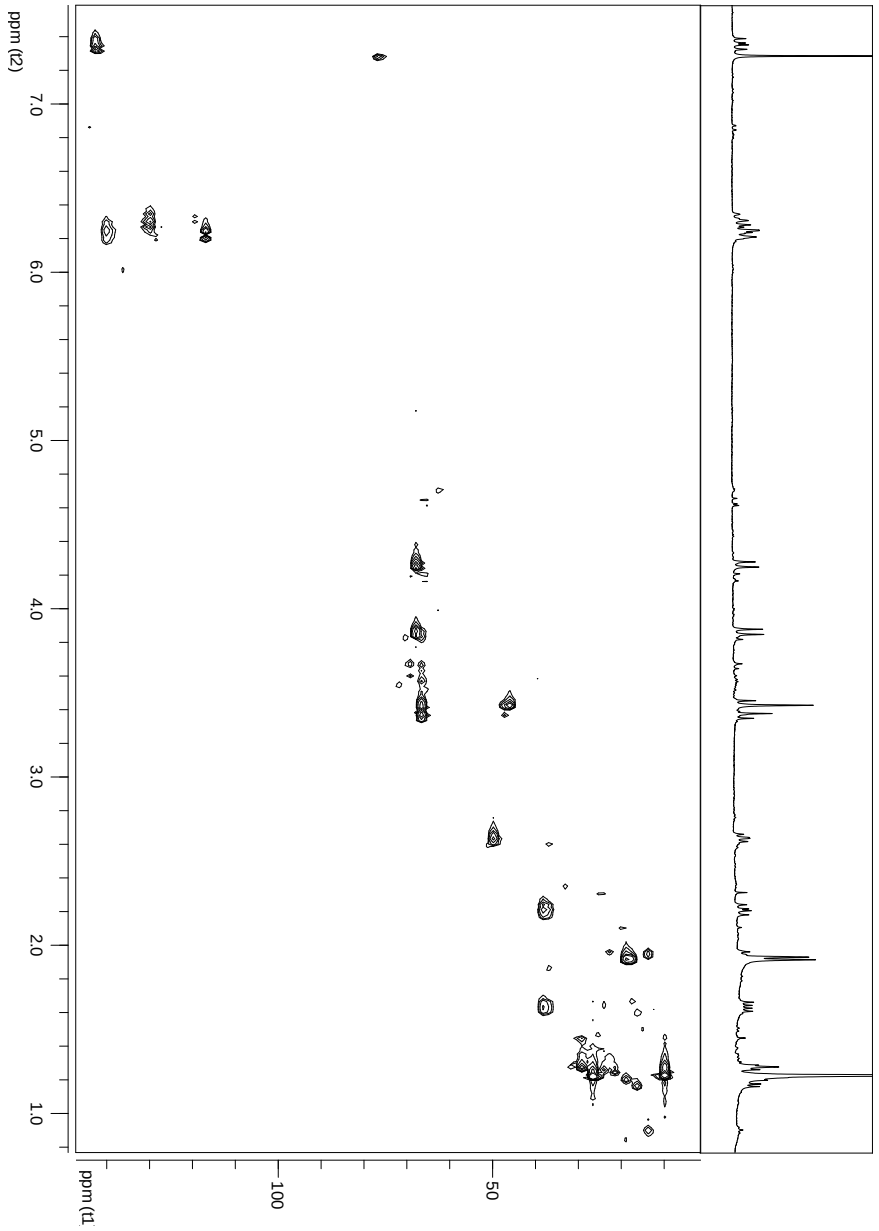

Figure 6.29. HSQC spectrum of trichodermanone C (**1**) recorded in $CDCl_3$ at 400 MHz

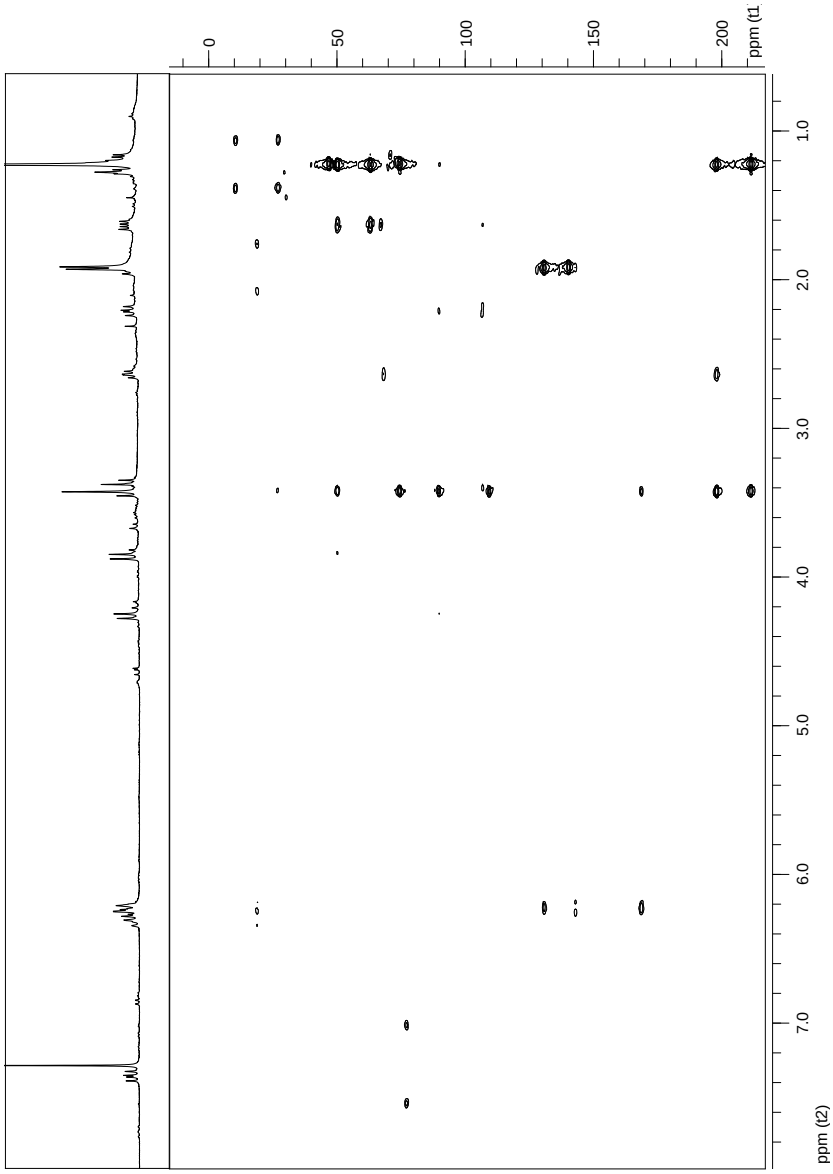

Figure 6.30. HMBC spectrum of trichodermanone C (**1**) recorded in $CDCl_3$ at 400 MHz

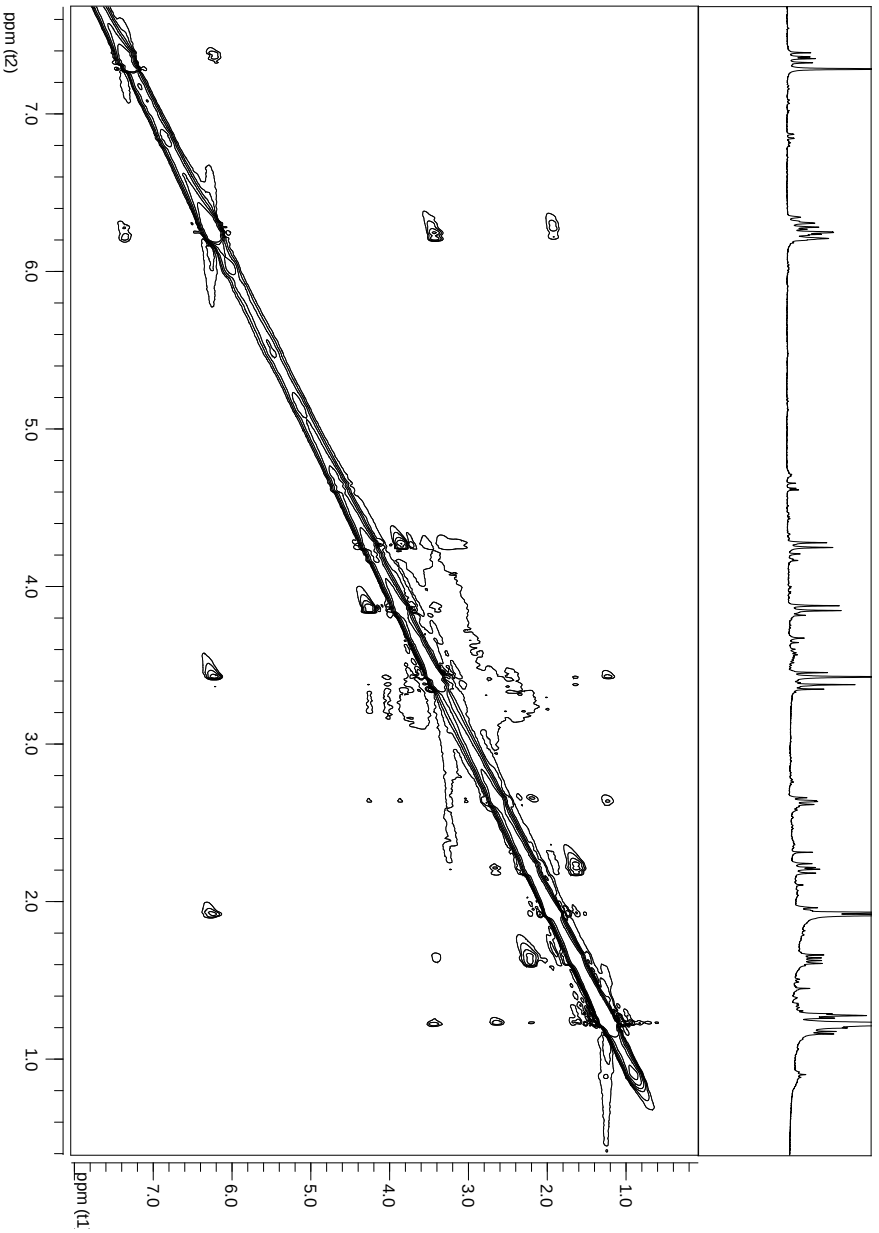

Figure 6.31. NOESY spectrum of trichodermanone C (**1**) recorded in $CDCl_3$ at 400 MHz

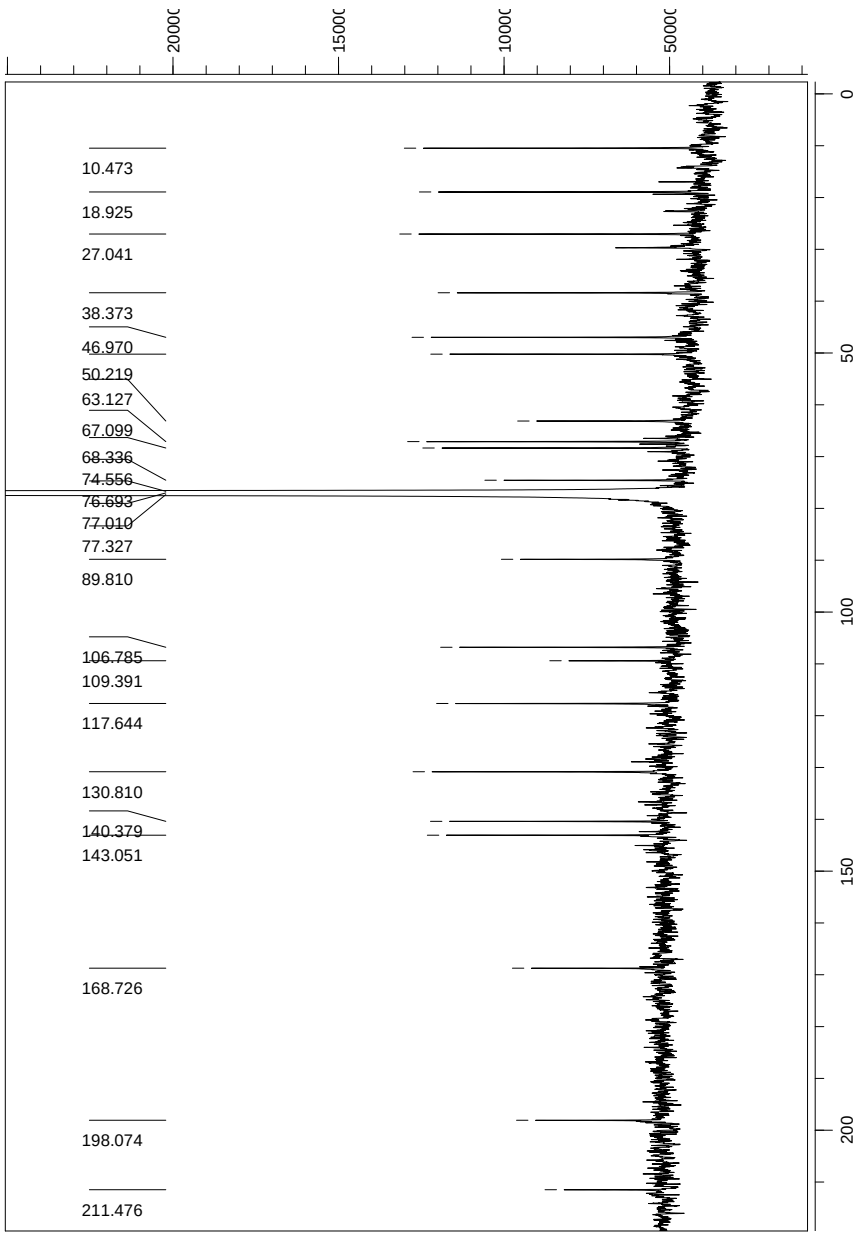

Figure 6.32. ^{13}C NMR spectrum of trichodermanone C (**1**) recorded in $CDCl_3$ at 100 MHz.

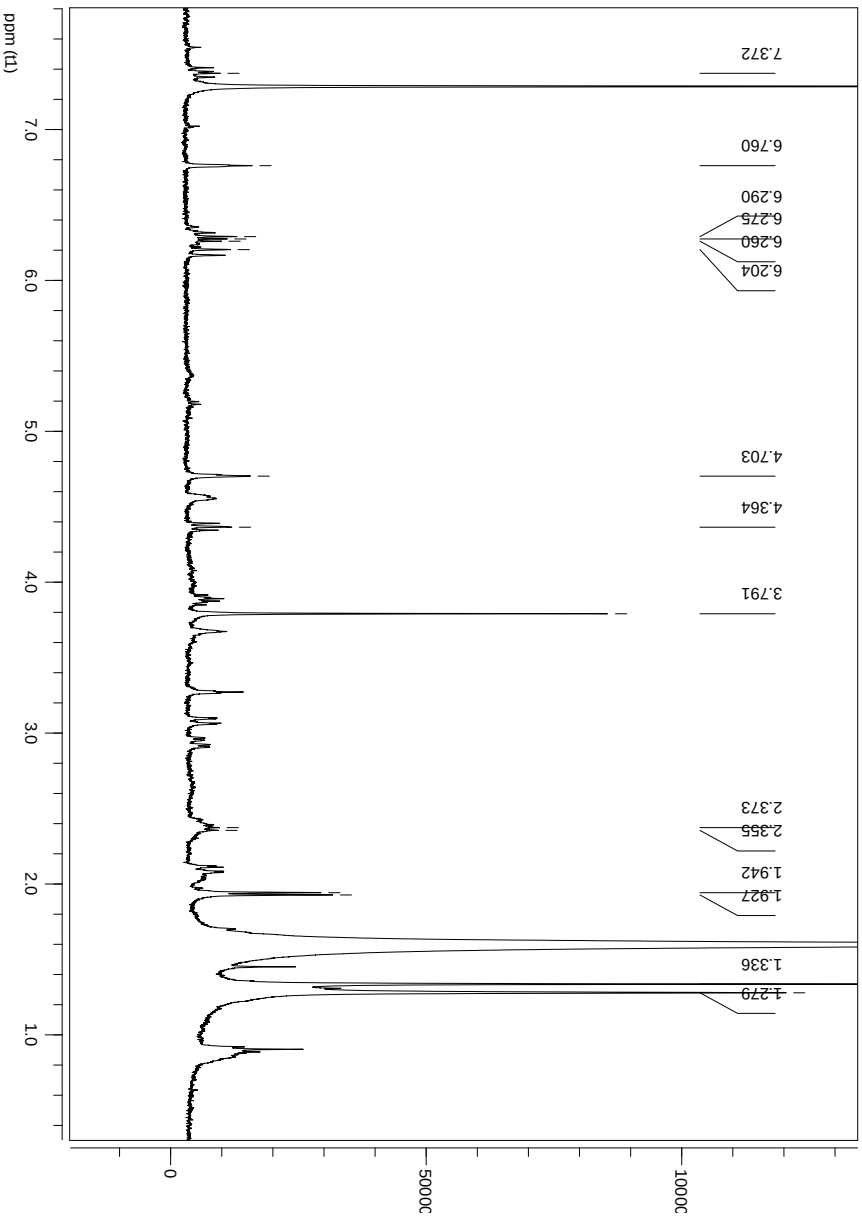

Figure 6.33. ^{1}H NMR spectrum of spirosorbicillinol A (**2**) recorded in $CDCl_3$ at 400 MHz.

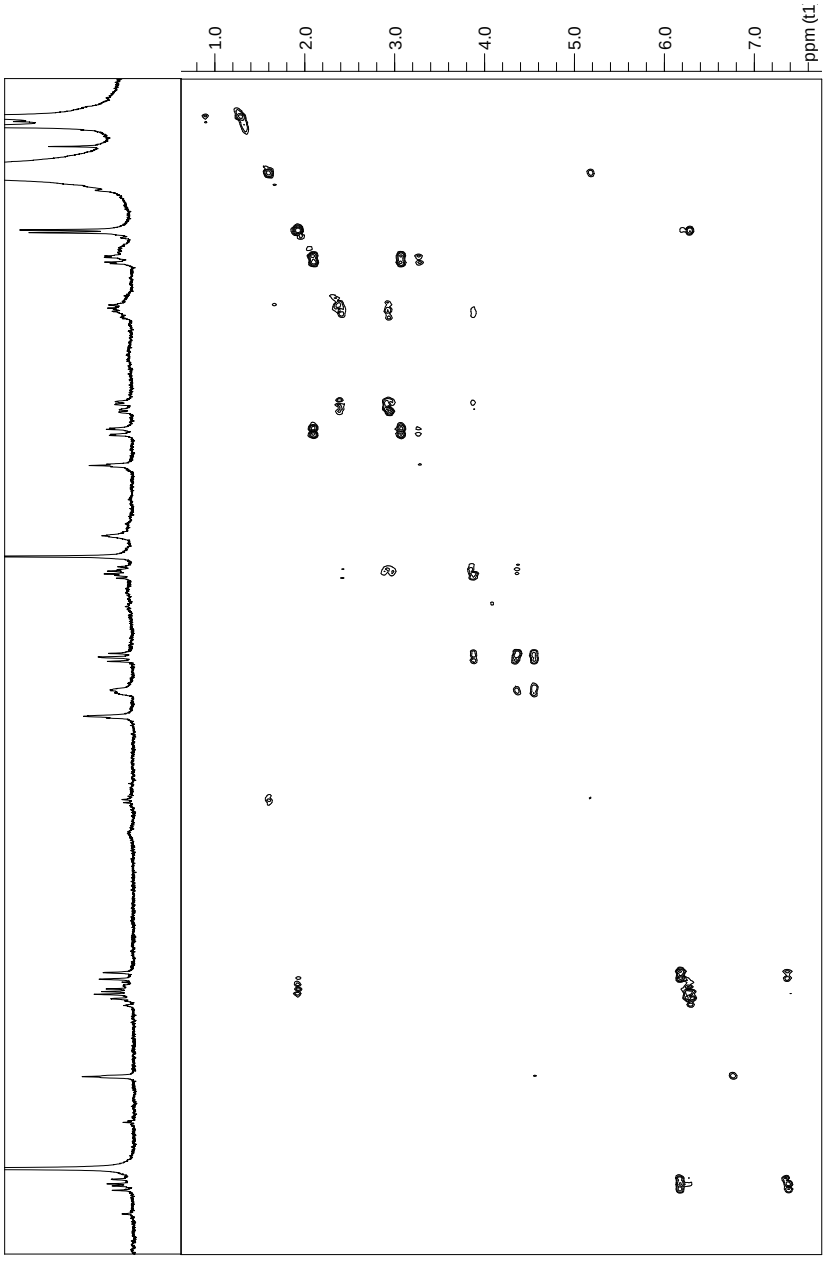

Figure 6.34. COSY spectrum of spirosorbicillinol A (**2**) recorded in $CDCl_3$ at 400 MHz.

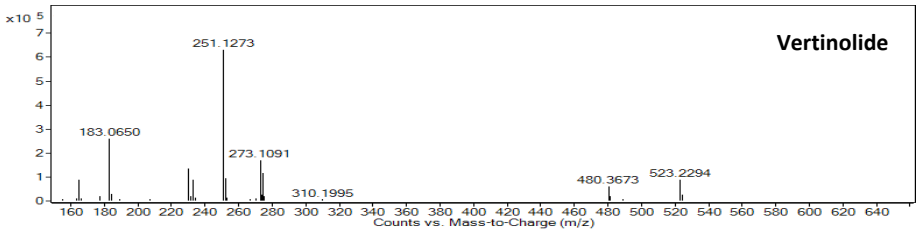
Vertinolide
x10 5
251.1273
183.0650
273.1091
310.1995
480.3673
523.2294
Counts vs. Mass-to-Charge (m/z)

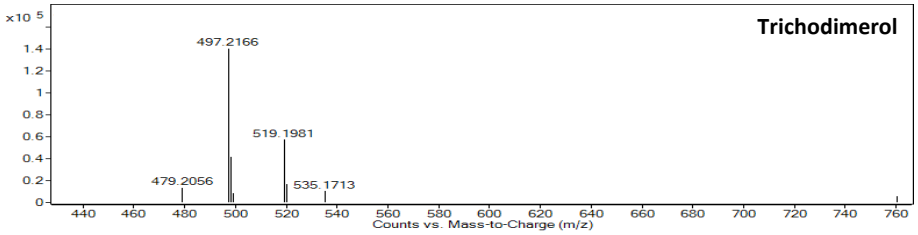
Trichodimerol
x10 5
497.2166
519.1981
479.2056
535.1713
Counts vs. Mass-to-Charge (m/z)

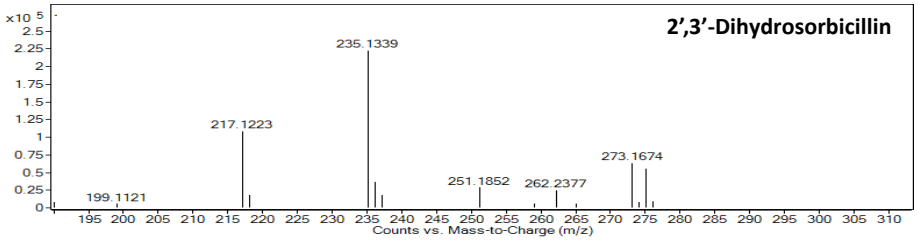
2',3'-Dihydrosorbicillin
x10 5
235.1339
217.1223
273.1674
251.1852
262.2377
199.1121
Counts vs. Mass-to-Charge (m/z)

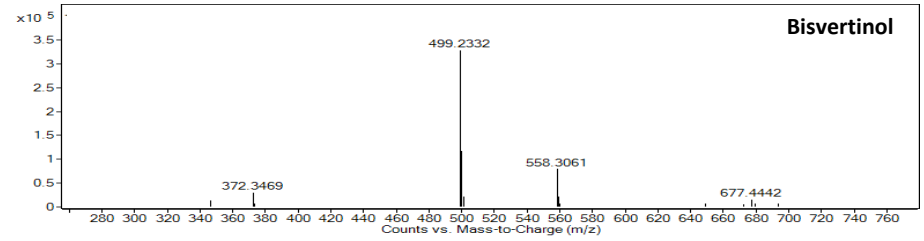
Bisvertinol
x10 5
499.2332
558.3061
372.3469
677.4442
Counts vs. Mass-to-Charge (m/z)

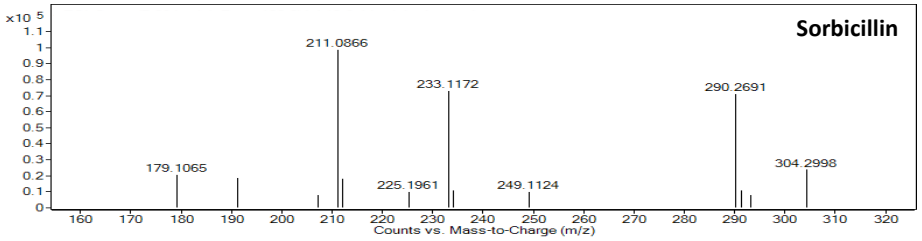
Sorbicillin
x10 5
211.0866
233.1172
290.2691
304.2998
179.1065
225.1961
249.1124
Counts vs. Mass-to-Charge (m/z)

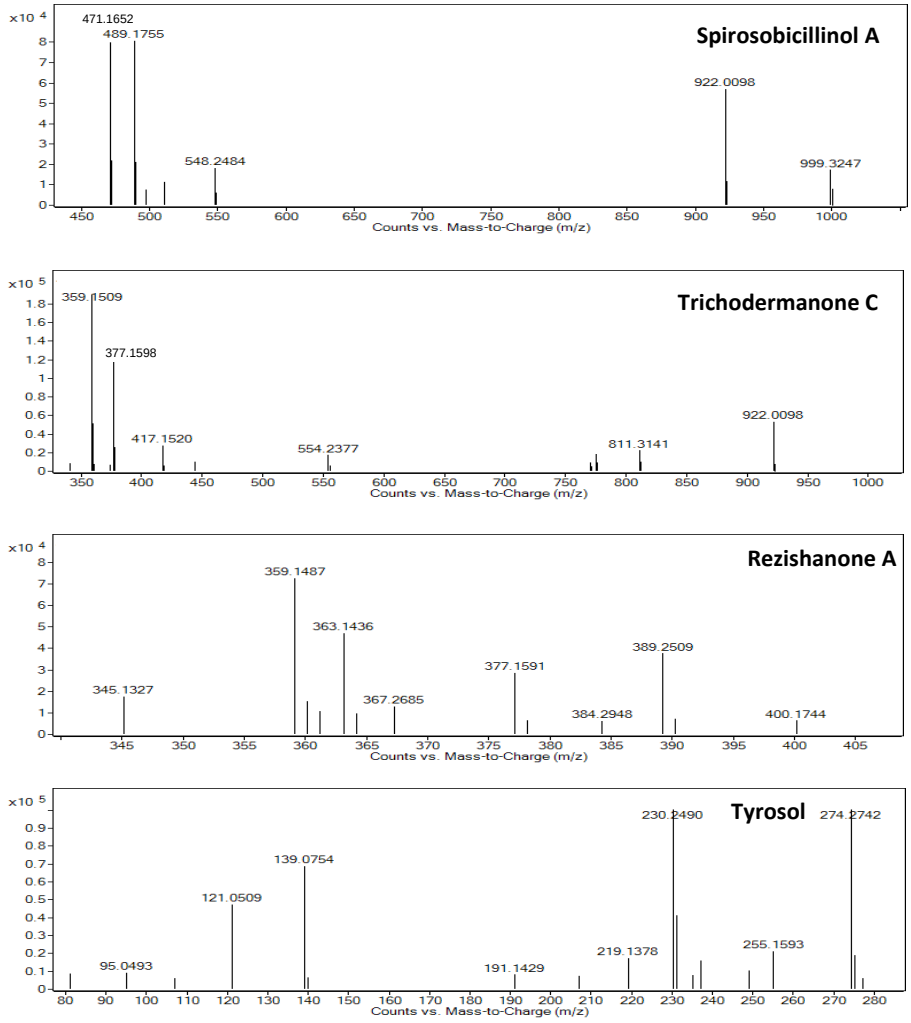

Figure 6.35. ESI MS (+) spectra of compounds produced by strain A12 of T. citrinoviride in liquid culture.

6.5.3. Biological Activity

J774A.1 murine macrophages (ATCC, from LGC Standards, Milan, Italy) were maintained at 37°C in a humidified atmosphere of 5% CO_2. The cells were cultured in Dulbecco's Modified Eagle's medium (DMEM, Lonza Group) supplemented with 10% fetal bovine serum (FBS), 100 U/mL penicillin and 100

μg/L streptomycin, 2 mM L-glutamine, 20 mM Hepes [4-(2-hydroxyethyl)-1-piperazineethanesulphonic acid] and 1 mM Na pyruvate. The medium was changed every 48h in conformity with the manufacturer's protocols. Cell viability was evaluated by measuring the mitochondrial reductase activity (MTT assay). Briefly, J774A.1 macrophages were seeded in 96-well plates at a density of 3 x 104 cells per well and allowed to adhere for 24h. Then, the cells were treated with trichodermanone C (1-60 μM) for 24h. Subsequently, the cells were incubated with 3-(4,5-dimethylthiazolyl-2)-2,5-diphenyltetrazolium bromide (MTT, 250 μg/mL, for 1h at 37°C) and, after the solubilization in DMSO, the mitochondrial reduction of MTT to formazan was quantitated at 490nm. All results were expressed as percentage of cell viability.

The effect of **1** on the nitric oxide (NO) production was assessed by measuring nitrites via colorimetric Griess assay, as previously. Briefly, J774A.1 macrophages (1,5 × 105 cells per well seeded in a 24-well plates) were treated with **1** (3-60 μM) for 30 min and subsequently with LPS (1 μg/mL) for 24 h. The cell supernatant was incubated with 100 μL of Griess reagent at room temperature for 10 minutes, then a highly coloured azo dye was formed and determined at 550 nm. Serial-diluted sodium nitrite (Sigma-Aldrich) was used to generate a standard curve. The data were expressed as nM of nitrite. Each sample was determined in triplicate.

6.5.4. Statistical Analysis

Results are expressed as the mean ± standard error of the mean (S.E.M.) of 3 independent experiments. The data were analysed using one-way ANOVA followed by Tukey post hoc test. A value of $P < 0.05$ was considered significant.

6.6. Experimental Procedures for Chemical Analysis of Secondary Metabolites by *Aspergillus niger* A7

6.6.1. Isolation, Cultivation and Extraction of Fungal Strain

Aspergillus niger A7 was isolated together with the *Trichoderma citrinoviride* A12 from the green alga *Cladophora* sp. from a rock on the shoreline in Miliscola (Naples, Italy) as reported in the previous pragraph. Strain A7 was identified as *Aspergillus niger* according to its morphological characters. Mycelial plugs from actively growing cultures of strain A12 were inoculated in 250 ml Erlenmayer flasks each containing 100 ml of Czapek dextrose broth. The culture filtrate (100ml) was extracted with same volume of EtOAc at native pH (2.5) for three times. The organic extracts were combined, dried with Na_2SO_4, and evaporated under reduced pressure to give a brown oil residue (28 mg).

6.7. Experimental Procedures for Chemical and Biological Analysis of Secondary Metabolites by *Penicillium brevicompactum* AN-4

6.7.1. Isolation and Identification of Fungal Strain

Strain AN4 was recovered from a Mediterranean snakelocks sea anemone (A. sulcata) collected in intertidal zone along the coastline of the isle of Procida (Naples Bay, Italy) by plating a tissue fragment excised from the pedal disc on potato dextrose agar (PDA) amended with streptomycin sulphate (200 mg L^{-1}). The fungal isolate was transferred in pure culture, and stored at 4 °C. Subcultures were prepared on Czapek-Dox agar (CDA) and malt extract agar (MEA) for morphological observations. The strain formed slow growing velutinous colonies, which turned dull green as sporulation progressed. Finely roughened ellipsoidal conidia were produced on short terverticillate conidiophores, with all elements adpressed, which were clearly indicative of its belonging in the section Brevicompacta of the genus *Penicillium*[25,26]. For a more circumstantial species

ascription, the translation elongation factor 1-alpha (TEF) gene sequence was extracted according to a previously published procedure[27], which showed a 100% homology with TEF sequences of a few strains of *P. brevicompactum* available in GenBank, including the type strain NRRL2011. Our sequence has in turn been deposited in GenBank under the code MN548283.

6.7.2. Production, Extraction and Fractionation of Culture Filtrate

Mycelial plugs from actively growing cultures of strain AN4 were inoculated in 1 L Erlenmayer flasks containing 500 mL of Czapek-Dox broth (Oxoid, Hampshire, UK). The liquid cultures (3 L) were incubated in the dark at 25 ± 2 °C on stationary phase. After 14 days the fungal biomass was removed through filtration (Whatman No. 4 filter paper), and the culture filtrate was extracted at native pH (4.2) with ethyl acetate. The organic extracts were combined, dried with Na_2SO_4, and evaporated under reduced pressure at 37 °C to give a yellow oily residue (29.4 mg). The crude organic extract was submitted to fractionation on silica gel column (1.0 x 40 cm i. d.), eluted with $CHCl_3$/*i*-PrOH (95:5, *v/v*). The last fraction was eluted with MeOH. Six homogeneous fractions were collected and pooled on the basis of similar TLC profiles (A 1.6 mg, B 5.2 mg, C 1.5, D 1.6 mg, E 7.2 mg, F 11.9 mg). The residue of fraction B after purification by TLC on silica gel eluted with n-hexane/ethyl acetate (6:4, *v/v*), produced yellow solid identified as **1** (Figure 3.9, 3.5 mg, Rf 0.85). The residue from fraction E was further purified by preparative TLC on silica gel eluted with $CHCl_3$/*i*-PrOH (92:8, *v/v*), originating solid mycophenolic acid (**8**, Figure 3.9, 5.8 mg, Rf 0.48) (Scheme 6.10).

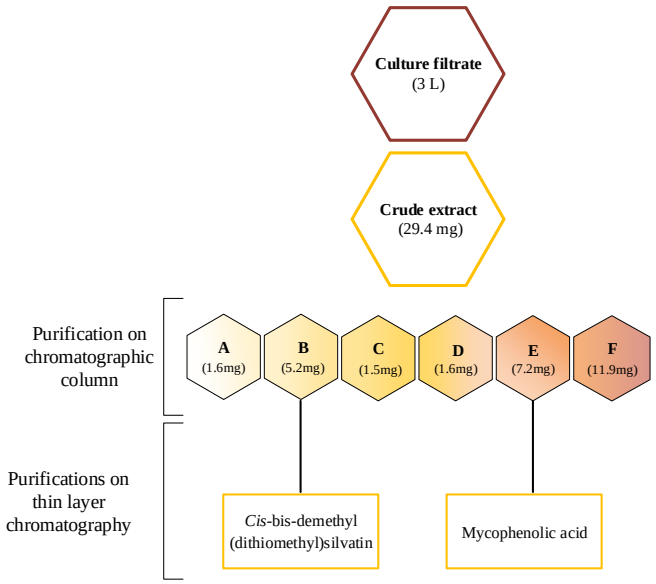

Scheme 6.10. Schematic representation of purification process of *P. brevicompactum* crude extract.

Cis-bis-demethyl(dithiomethyl)silvatin (**1**). $[\alpha]_D^{25}$ -47.5 ($CHCl_3$, *c* 0.2); HR ESI MS (+) spectrum *m/z*: 839.2969 [$C_{40}H_{56}N_4O_6S_4Na$, calcd. 839.2980, 2M+Na]$^+$, 431.1433 [$C_{20}H_{28}N_2O_3S_2Na$, calcd. 431.1439, M+Na]$^+$, 361.1579 [$C_{19}H_{25}N_2O_3S$, calcd. 361.1586, M-CH_3]$^+$.

Saroclazine A/B (**2**).HR ESI MS (+) spectrum *m/z*: 395.1623 [$C_{19}H_{27}N_2O_3S_2$, calcd. 251.1278, M+H]$^+$.

Fusaperazine E/F (**3**). HR ESI MS (+) spectrum *m/z*: 383.1822 [$C_{19}H_{24}O_3N_2SNa$, calcd. 383.1405, M+Na]$^+$, 361.1574 [$C_{19}H_{25}O_3N_2SNa$, calcd. 361.1586, M+H]$^+$.

6-Oxo-methylthiosilvatin (**4**). HR ESI MS (+) spectrum *m/z*: 775.2817 [$C_{38}H_{48}N_4O_8S_2Na$, calcd. 775.2811, 2M+Na]$^+$, 399.1354 [$C_{19}H_{24}N_2O_4SNa$, calcd.

399.1345, M+Na]$^+$, 377.1528 [$C_{19}H_{25}N_2O_4S$, calcd. 377.1535, M+H]$^+$, 361.1575 [M-CH_3calcd. 361.1222]$^+$.

Bilain B (**5**). HR ESI MS (+) spectrum *m/z*: 443.3332 [$C_{20}H_{31}N_2O_5S_2$, calcd. 443.1674, M+H]$^+$.

Deprenyl-bis(methylthio)silvatin (**6**). HR ESI MS (+) spectrum*m/z*: 363.3094 [$C_{15}H_{20}O_3N_2O_3S_2Na$, calcd. 363.0815, M+Na]$^+$, 341.2656 [$C_{15}H_{21}O_3N_2O_3S_2$, 341.4688, M+H]$^+$.

Fusaperazine A (**7**). HR ESI MS (+) spectrum *m/z*: 335.2791 [$C_{13}H_{16}N_2O_3S_2Na$, calcd. 335.2804, M+Na]$^+$, 313.2351 [$C_{13}H_{17}N_2O_3S_2$, calcd. 313.2278, M+H]$^+$.

Mycophenolic acid (**8**). HR ESI MS (+) spectrum *m/z*: 663.24092 [C34H40O12Na, calcd. 663.2417, 2M+Na]$^+$, 343.1153 [$C_{17}H_{20}O_6Na$, calcd. 343.1158, M+Na]$^+$, 321.1331 [$C_{17}H_{21}O_6$, calcd. 321.1338, M+H]$^+$, 303.1228 [$C_{17}H_{19}O_5$, calcd. 303.1232, M-OH]$^+$.

Brevianamide A/B (**9**). HR ESI MS (+) spectrum *m/z*: 753.3359 [$C_{42}H_{46}O_6N_6Na$, calcd. 753.3356, 2M+Na]$^+$, 731.3549 [$C_{42}H_{47}O_6N_6$, calcd. 753.3557, 2M+H]$^+$, 388.1620 [$C_{21}H_{23}O_3N_3Na$, calcd. 388.1637, M+Na]$^+$, 366.1810 [$C_{21}H_{24}O_3N_3$, calcd. 366.1818, M+H]$^+$.

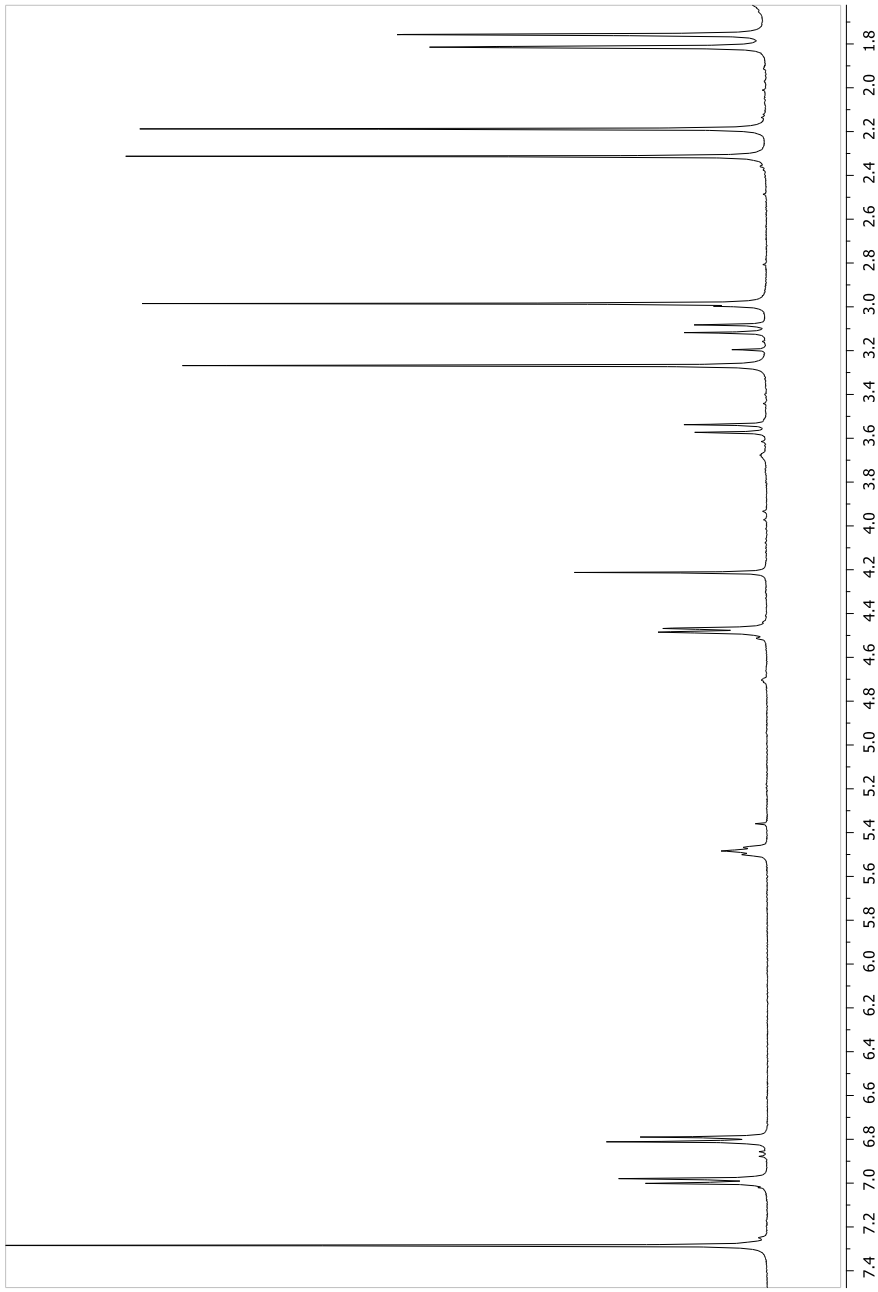

Figure 6.36. ^{1}H NMR spectrum of *cis*-bis(methylthio)silvatin (**1**) recorded in $CDCl_3$ at 400 MHz.

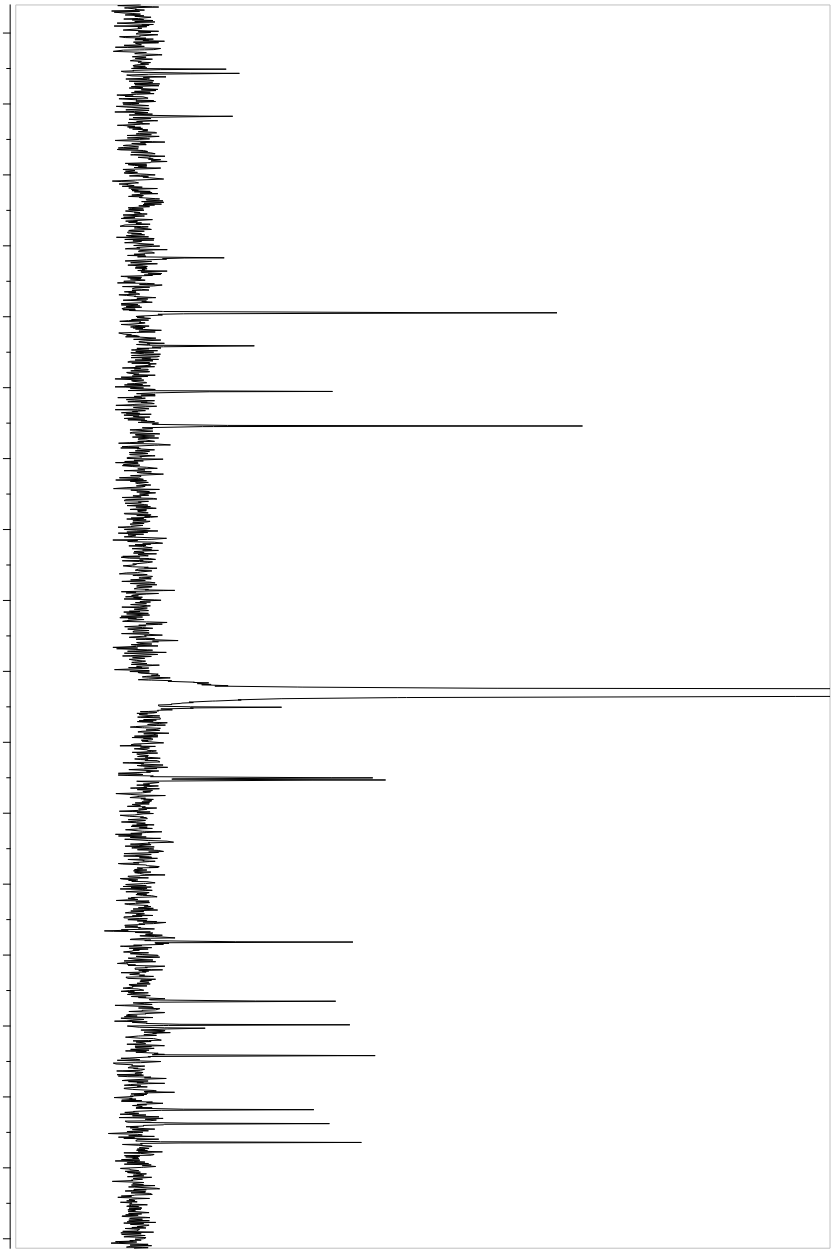

Figure 6.37. ^{13}C NMR spectrum of *cis*-bis(methylthio)silvatin (**1**) recorded in $CDCl_3$ at 100 MHz.

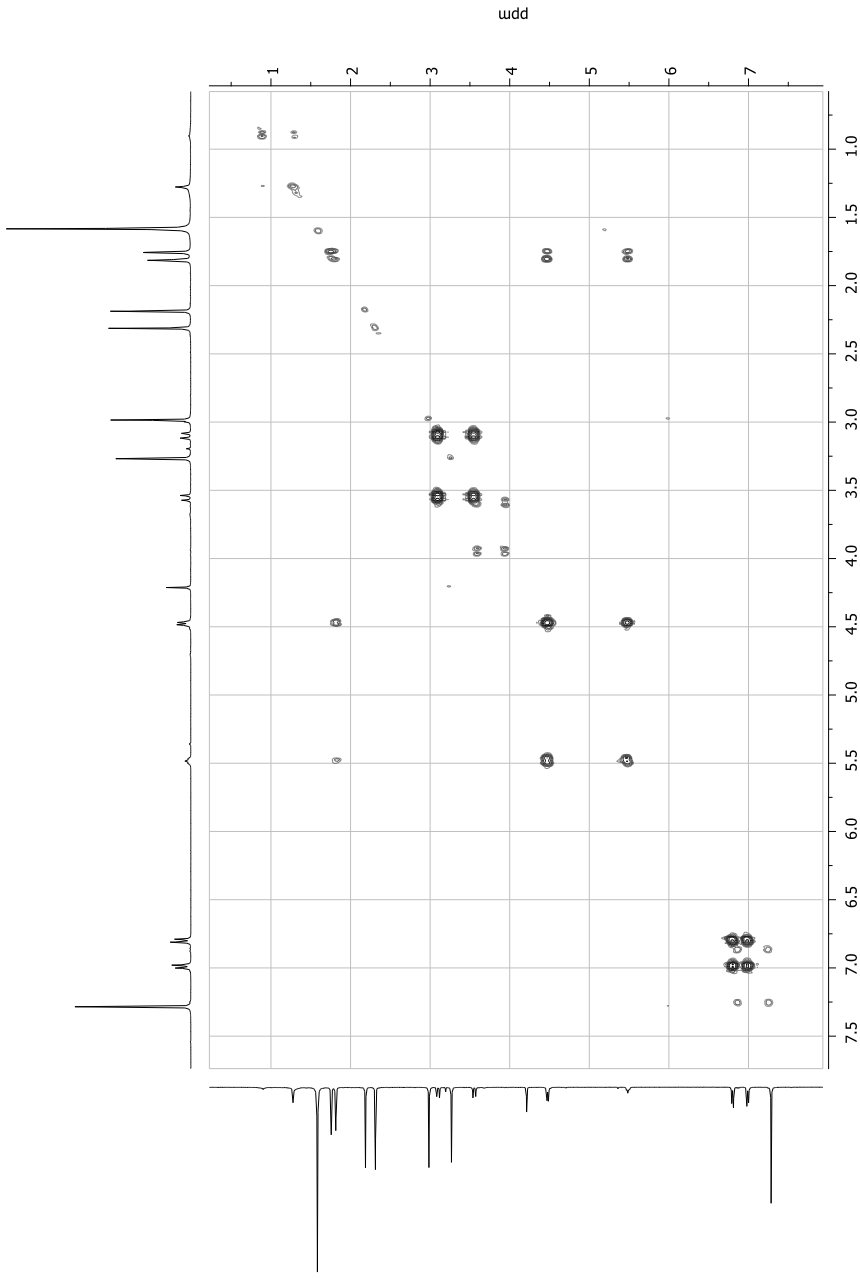

Figure 6.38. COSY spectrum of *cis*-bis(methylthio)silvatin (**1**) recorded in $CDCl_3$ at 400 MHz.

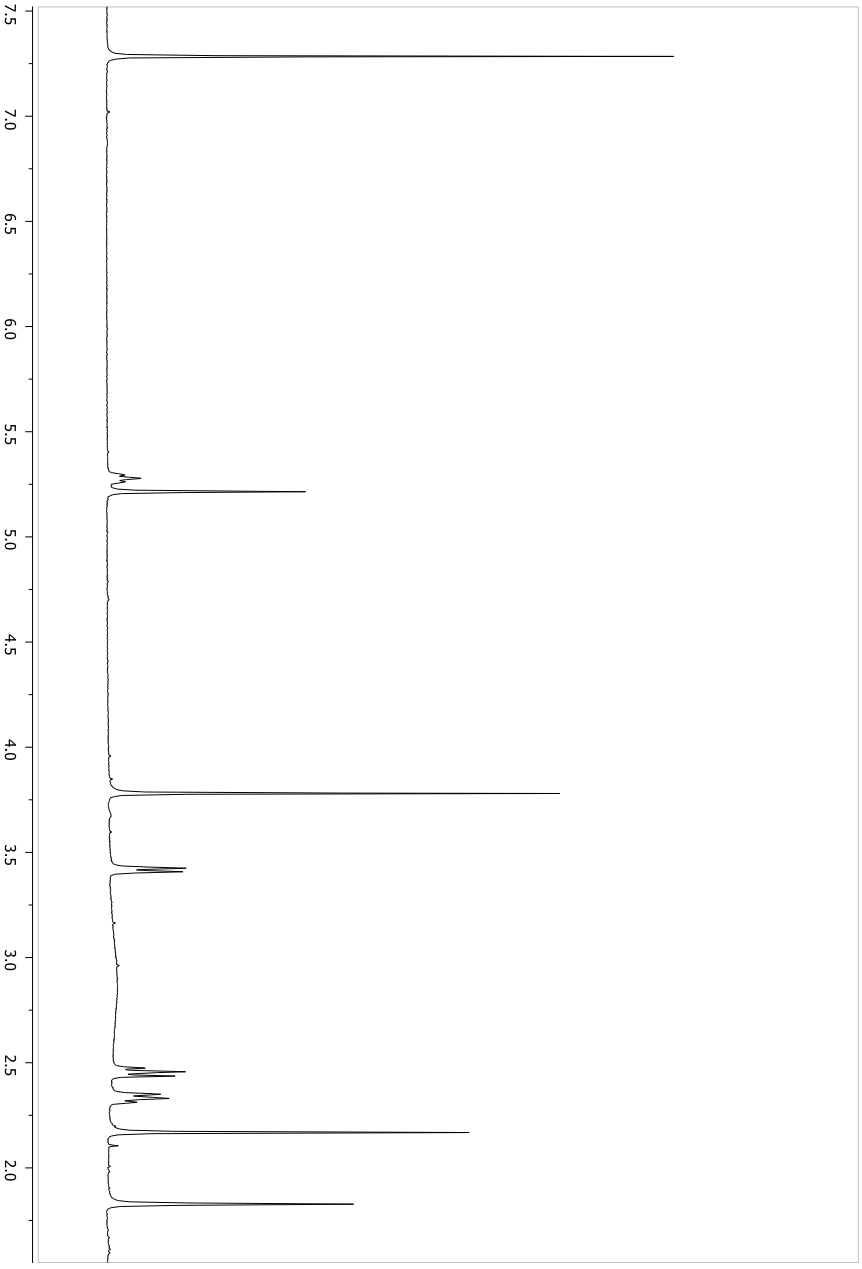

Figure 6.39. ^{1}H NMR spectrum of mycophenolic acid (**2**) recorded in $CDCl_3$ at 400 MHz.

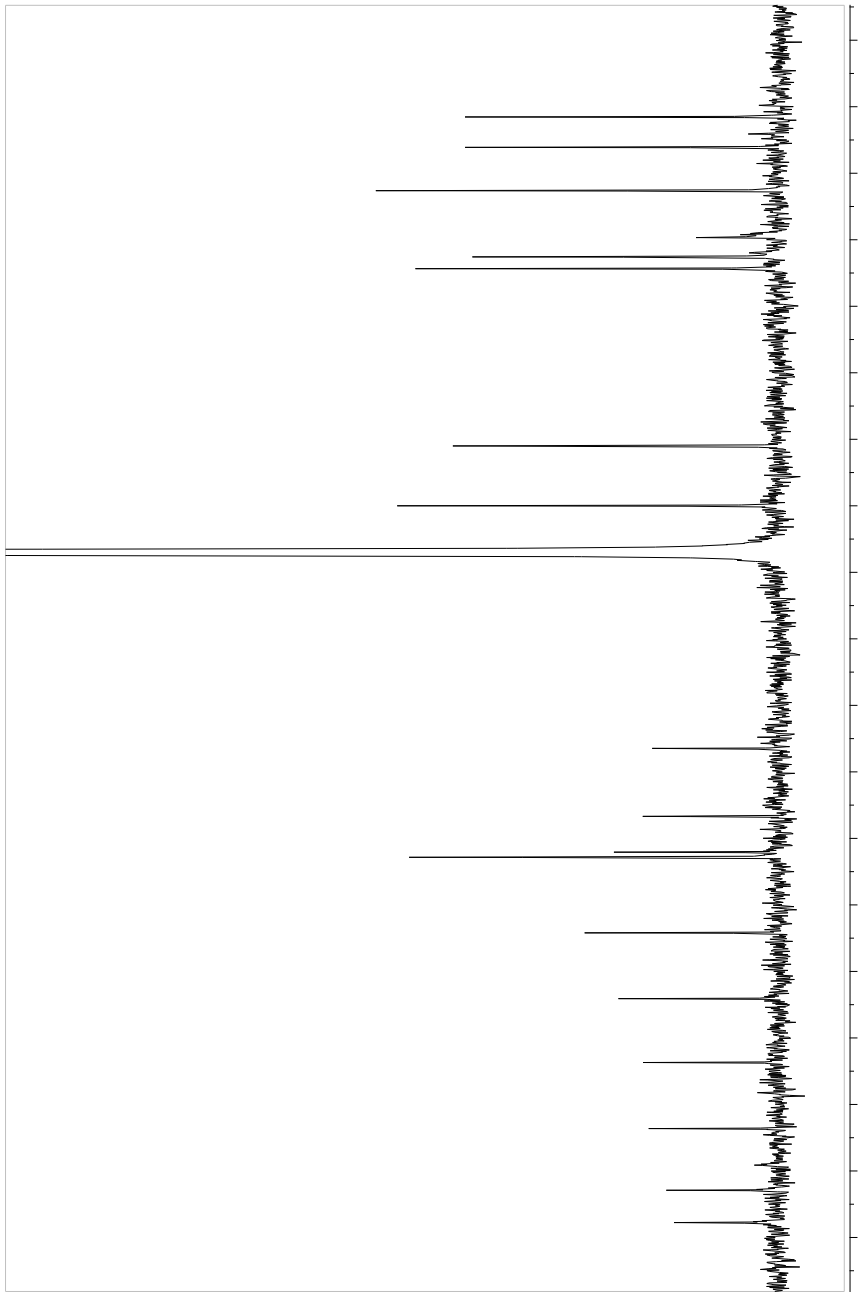

Figure 6.40. ^{13}C NMR spectrum of mycophenolic acid (**2**) recorded in $CDCl_3$ at 100 MHz

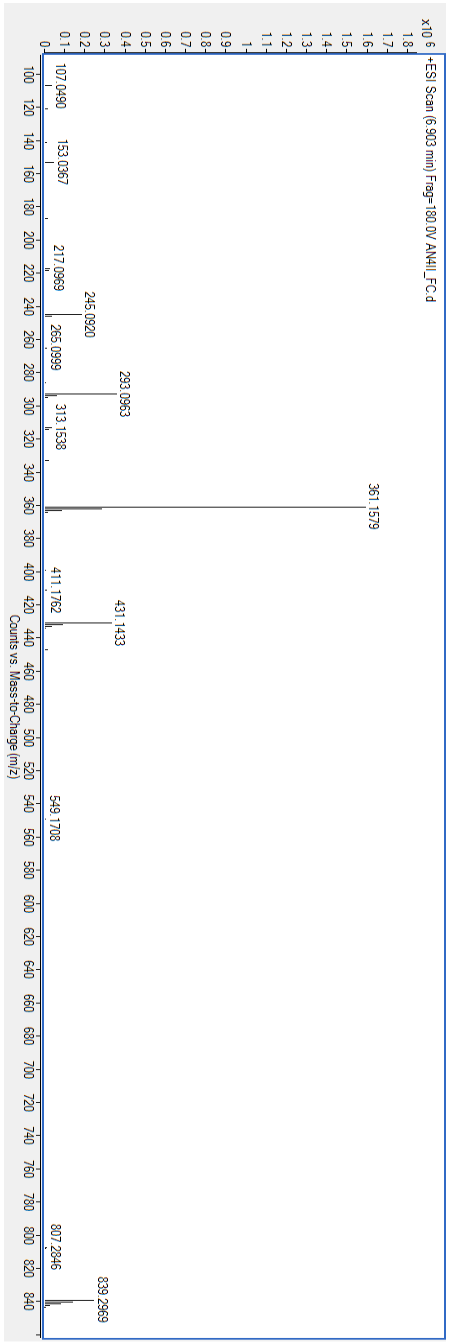

Figure 6.41. *Cis*-bis(methylthio)silvatin mass spectrum recorded in positive mode.

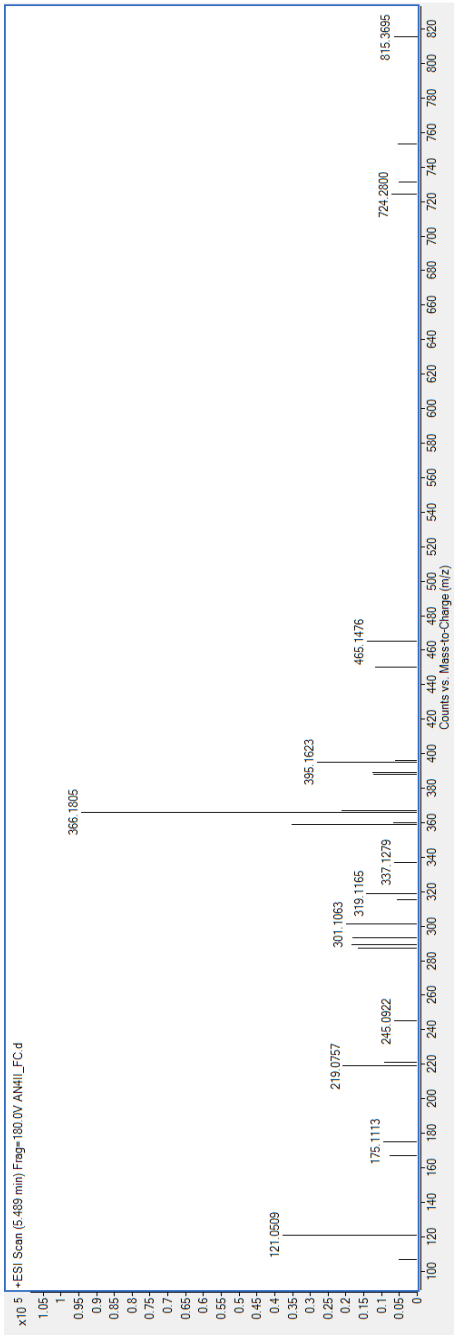

Figure 6.42. Saroclazine A/B mass spectrum recorded in positive mode.

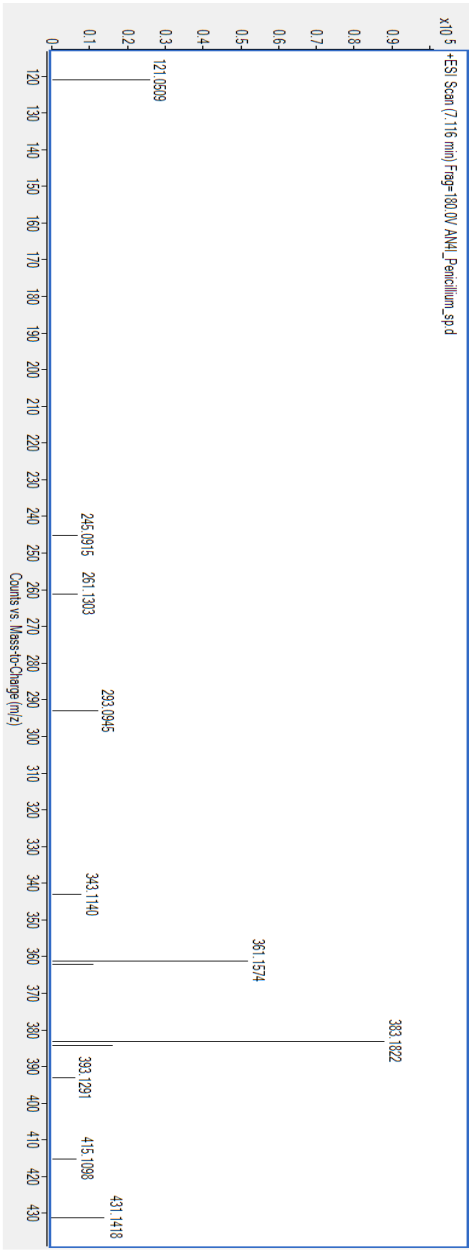

Figure 6.43. Fusaperazine E/F mass spectrum recorded in positive mode.

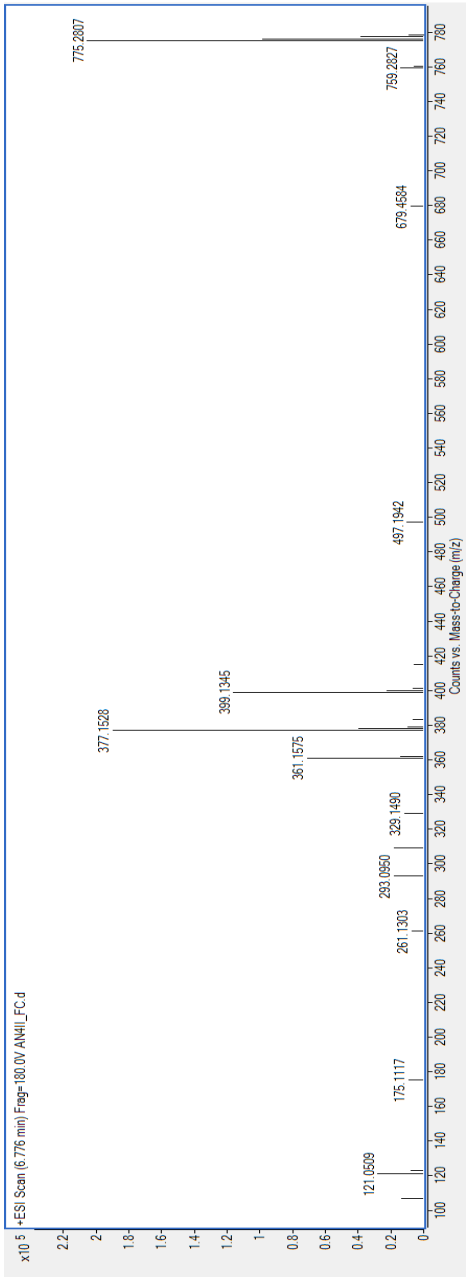

Figure 6.44. 6-Oxo-methylthiosilvatin mass spectrum recorded in positive mode.

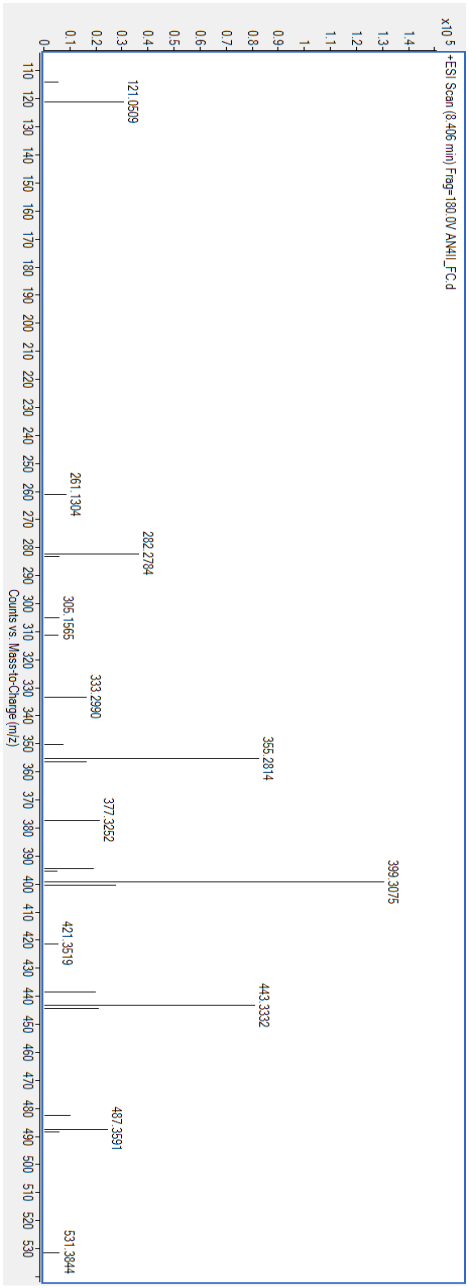

Figure 6.45. Bilain B mass spectrum recorded in positive mode.

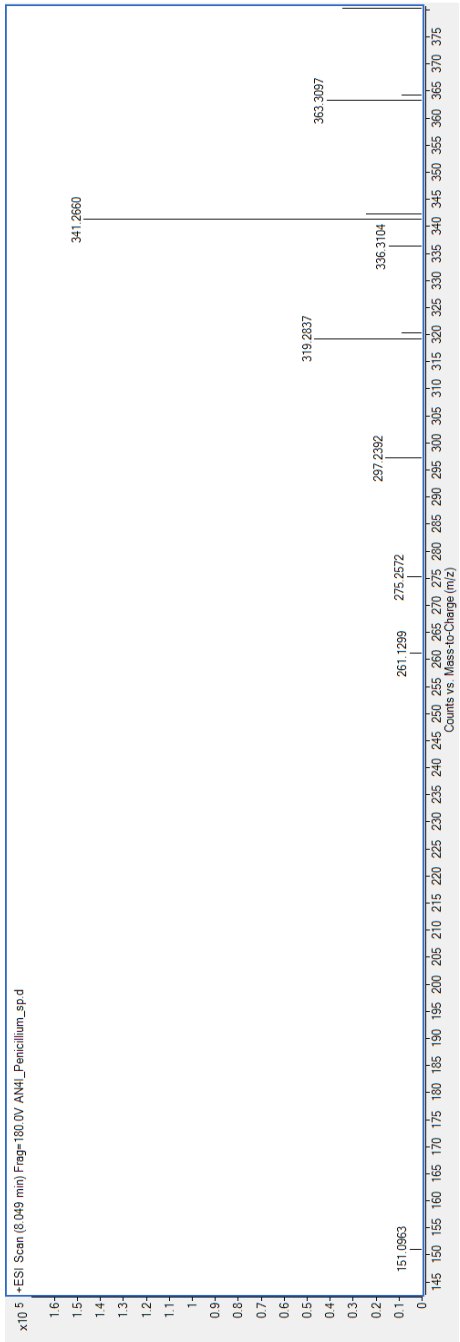

Figure 6.46. Deprenyl-bis(methylthio)silvatin mass spectra recorded in positive mode.

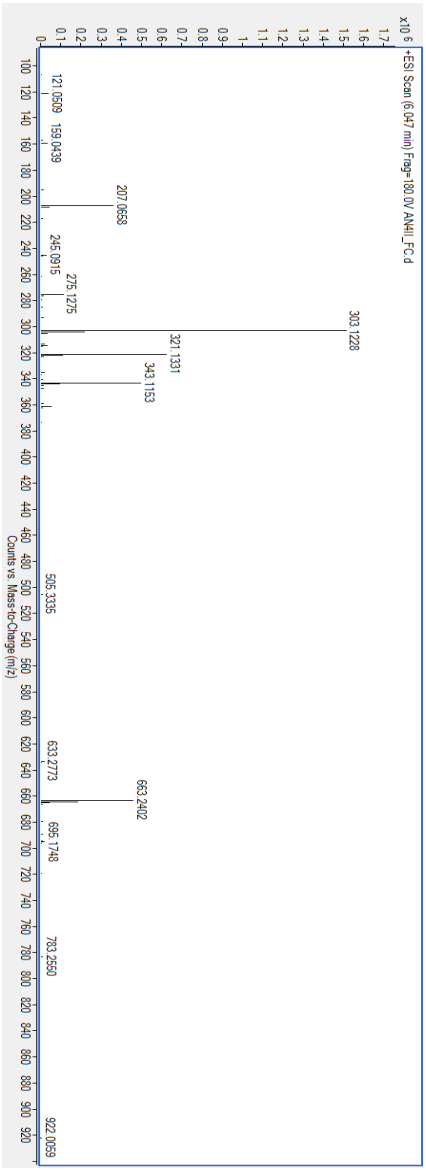

Figure 6.47. Mycophenolic acid mass spectrum recorded in positive mode.

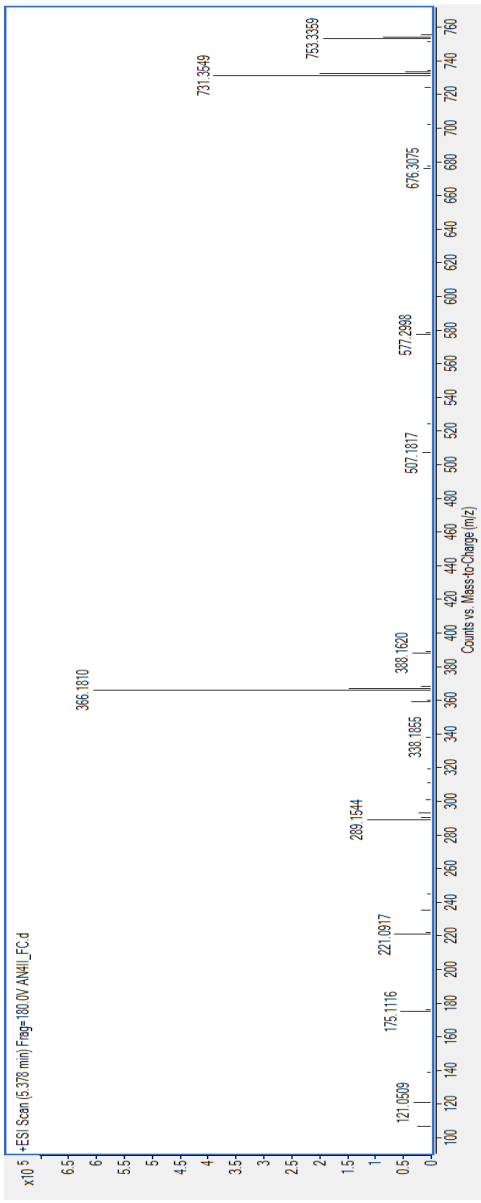

Figure 6.48. Brevianamide A/B mass spectrum recorded in positive mode

Table 6.3. Mass spectra of i metabolites reported in Figure 4.5. RI represents the kovats non isothermal retention index; panel "MS peaks annotations" reports mass, formula and normalized abundance of identified fragments in mass spectra whenever available, the molecular ion is alwais represented by M, Me indicates methyl (-CH_3); TMS represents -$Si(CH_3)_3$. Abundance is normalized taking abundance of base peak equal 100.

1	RI: 3229	Mass peak annotations: 361 [M-CH_3S]$^+$ (26), 293 [M-$C_6H_{11}S$]$^+$ (23), 245 [M-$C_5H_8NO_2S$-H_2O]$^+$ (46), 233 [M-$C_{12}H_{16}O$]$^+$ (60), 217 [M-$C_{13}H_{21}O$]$^+$ (21), 186 [M-$C_{13}H_{19}OS$]$^+$ (40), 107 [M-$C_{13}H_{21}N_2O_2S_2$]$^+$ (100)
2	RI: 2892	Mass peak annotations: 340 [M-C_4H_7]$^+$(3), 293 [M-$C_6H_{14}O$]$^+$(76), 245 [M-$C_4H_8N_2OS$-H_2O]$^+$(28), 235 [M-$C_{11}H_{14}N_2O$]$^+$(35), 218 [M-$C_{11}H_{14}O$-CH_3]$^+$(33), 187 [M-$C_{12}H_{20}N_2O_2S_2$]+ (100)

3	RI: 2083	Mass peak annotations: 361 $[M]^+$(100), 312 $[M\text{-}CH_4S]^+$(47), 234 $[M\text{-}C_7H_{13}NO]^+$(52), 187 $[M\text{-}C_8H_{16}NOS]^+$(76)

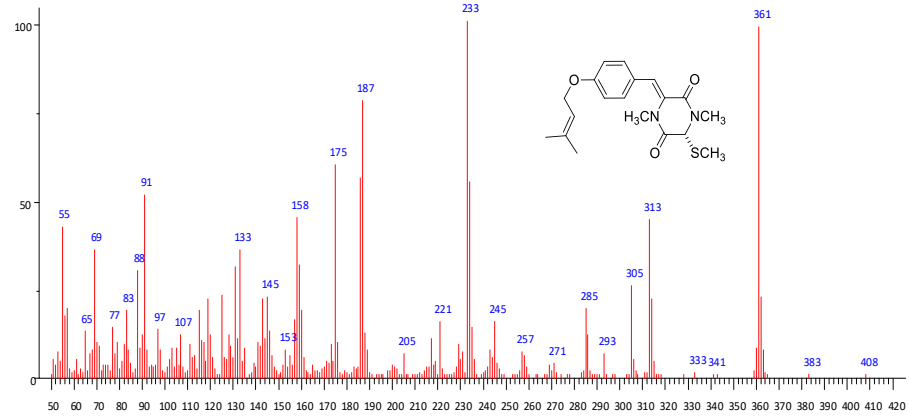

4	RI: 3203	Mass peak annotations: 360 $[M\text{-}CH4]^+$ (14), 292 [M-C5H8O]+ (33), 245 [M-C4H4NO3-H2O]+ (100), 217 [M-C5H5NO3S]+ (64), 146 [M-C8H12N2O3S-CH3]+ (46)

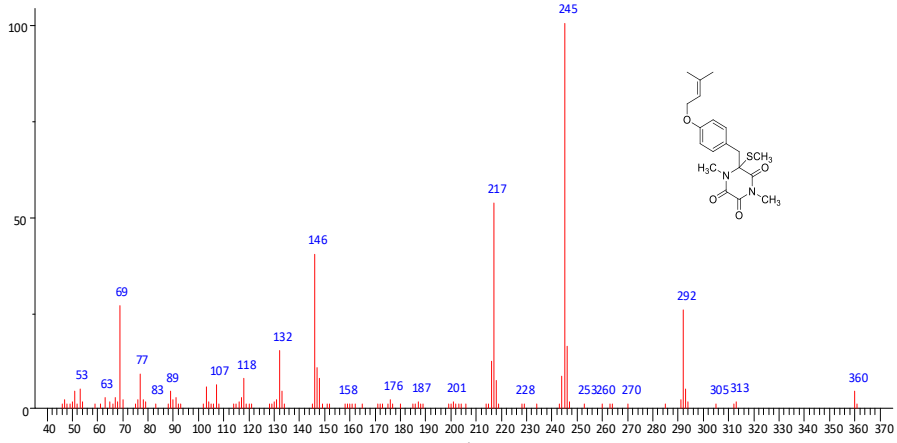

5 (2TMS)	RI 3047	Mass peak annotations: 280 $[M\text{-}C_{13}H_{31}SSi_2]^+$(50), 218 $[M\text{-}C_{15}H_{18}N_2O_2S_2\text{-}H_2O]^+$(25)

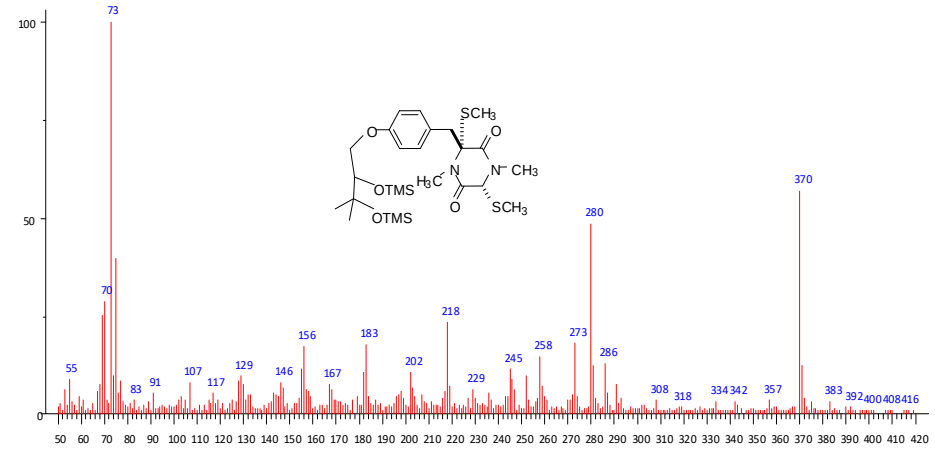

6 (TMS)	RI: 2014	Mass peak annotations: 412 $[M]^+$(25), 369 $[M\text{-}C_2H_4O]^+$(25), 321 $[M\text{-}C_3H_{10}S\text{-}H_2O]^+$(47), 294 $[M\text{-}C_4H_9NOS]^+$ (12)

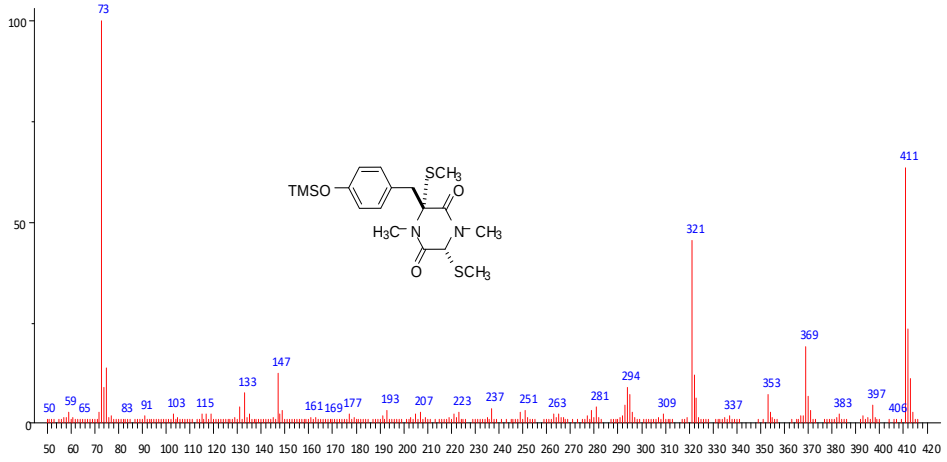

7 (TMS)	RI: 1876	Mass peak annotations: 384 $[M]^+$(5), 369 $[M\text{-}CH_3]^+$(100), 353 $[M\text{-}2(CH_3)]^+$(5), 295 $[M\text{-}C_3H_8Si\text{-}H_2O]^+$ (12), 237 $[M\text{-}C_4H_7NO_2S\text{-}CH_3]^+$(10).

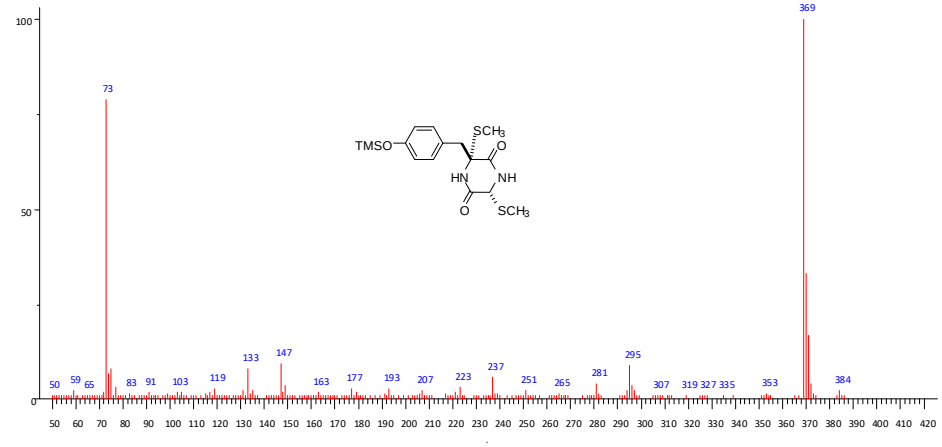

8	RI: 2871	Mass peak annotations: 320 $[M]^+$ (19), 302 $[M\text{-}H_2O]^+$ (15), 247 $[M\text{-}C_3H_6O_2]^+$ (57), 207 $[M\text{-}C_6H_{10}O_2]^+$

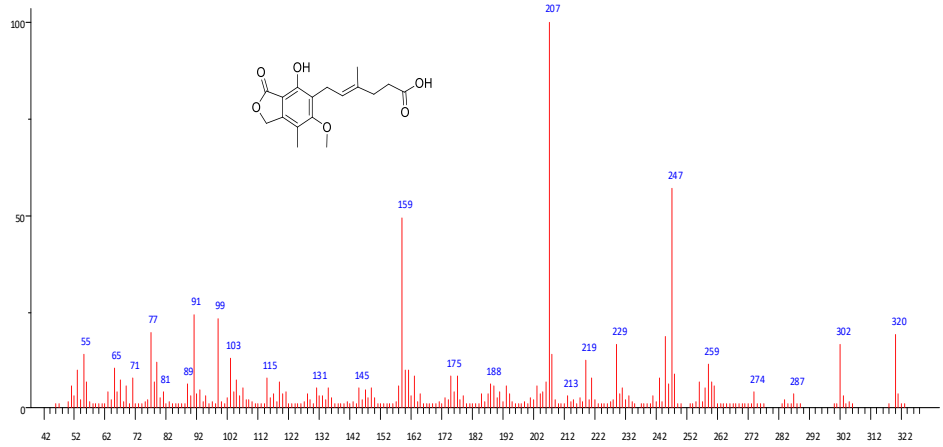

9 (TMS)	RI: 3227	Mass peak annotations: 361 $[M\text{-}C_6H_5]^+$(45), 245 $[M\text{-}C_9H_{10}N_2O_2\text{-}CH_3\text{-}CH_3]^+$(48), 233 $[M\text{-}C_{11}H_{15}NOS]^+$ (73), 217 $[M\text{-}C_{12}H_{17}N_2O_2]^+$(18), 186 $[M\text{-}C_{12}H_{20}N_2O_2Si]^+$(50)

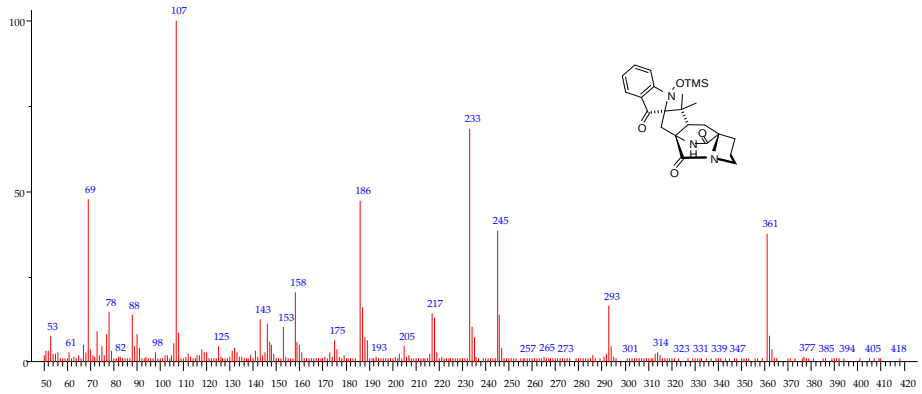

6.7.3. Cytotoxicity Assays

For *in vitro* experiments, two human colon adenocarcinoma cell lines (i.e. Caco-2 and HCT116, ATCC from LGC Standards, Milan, Italy) and a healthy colonic epithelial cell (HCEC, a kind gift of Fondazione Callerio Onlus, Trieste, Italy) have been used. Caco-2 and HCT116 were cultured in Dulbecco's modified Eagle's medium (DMEM) containing 10% fetal bovine serum (FBS), 100 U mL^{-1} penicillin and 100 μg mL^{-1} streptomycin, 1% non-essential amino acids, 2 mM L-glutamine and 1 M HEPES, in conformity with the manufacturer's protocols. The immortalized HCEC, derived from human colon biopsies and used as a comparison with tumor cells, were cultured in DMEM supplemented with 10% FBS, 100 U mL^{-1} penicillin, 100 μg mL^{-1} streptomycin, 200 mM L-glutamine, 100 mM Na-pyruvate and 1 M HEPES.

Cell viability was evaluated by measuring the mitochondrial reductase activity (MTT assay). Cells were seeded in presence of 10% FBS in 96-well plates at a density of 10^4 cells per well and allowed to adhere for 24 h. After this period,

cells were incubated with medium containing 10% FBS in presence or absence of increasing concentrations of *cis*-bis(methylthio)silvatin (0.3÷100 μM, previously dissolved in DMSO 0.1%) or DMSO 20% used as positive control, for 24 h. Subsequently, the treatment medium was replaced with fresh medium containing MTT (250 μg mL^{-1}, for 1h at 37 °C). After solubilization in DMSO, the mitochondrial reduction of MTT to formazan was quantitated at 490 nm (iMarkTM microplate reader, Bio-Rad). All results are expressed as percentage of cell viability.

6.7.4. Statistical Analysis

Data are expressed as the mean ± SEM of 3 experiments. Statistical analysis was performed with the software GraphPad Prism 6 using one-way ANOVA followed by a Tukey multiple comparisons test (for analysis of multiple treatment means). EC50 values were calculated by non-linear regression analysis using the equation for a sigmoid concentration–response curve (GraphPad Prism 6). P-value < 0.05 was considered to be significant.

6.8. Experimental Procedures for Chemical Analysis of Secondary Metabolites by *Talaromyces pinophilus* LT6

6.8.1. Production, Extraction and Fractionation of Culture Filtrate

Liquid cultures were prepared by inoculating mycelial plugs from actively growing cultures of strain LT6 in 1 L Erlenmayer flasks containing 500 mL potato-dextrose broth (PDB, Himedia), (which were kept in darkness on stationary phase at 25°C. After 21 days cultures were filtered at 0.45 μm, and the culture filtrates were concentrated in a lyophilizer until reduction to 1/10 of the starting volume. The mycelial cake floating on the broth was collected separately and stored at -20°C.

The freeze-dried culture filtrates (6 L) were dissolved in 600 mL of pure water and extracted with same volume of $CHCl_3$ (pH 4) for three times. The organic extracts were combined, dried on Na_2SO_4, and evaporated under reduced pressure to give a yellowish oil residue (75.3 mg).

The residue was submitted to fractionation on silica gel column (1.5 x 30 cm i. d.), eluted with $CHCl_3$/*i*-PrOH (98:2, *v/v*). Seven homogeneous fraction groups were collected (A 0.7 mg, B 2.7 mg, C 9.5 mg, D 0.8 mg, E 3.4 mg, F 9.3 mg, G 8.2 mg).The residue of fraction C was purified by TLC on silica gel eluted with *n*-hexane/Me_2CO (6:4, *v/v*) yielding an amorphous solid, talarodiolide [(**1**, 1.5 mg, R_f 0.41 on TLC on silica gel eluent *n*-hexane/Me_2CO (6:4, *v/v*)], and a cristalline solid, 3-*O*-methylfunicone (OMF) [(**2**, 3.5 mg, R_f 0.47 on TLC on silica gel eluent *n*-hexane/Me_2CO (6:4, *v/v*)].The residue of the fraction F was further purified by TLC on silica gel eluted with $CHCl_3$/*i*-PrOH (95:5, *v/v*) giving as amorphous solids: *cyclo*-(*S*-Pro-*R*-Leu) [(**3**, 1.0 mg, R_f 0.49 on TLC on silica gel eluent $CHCl_3$/*i*-PrOH (95:5, *v/v*)], *cyclo*-(*S*-Pro-*S*-Ile) [(**4**, 2.3 mg, R_f 0.35 on TLC on silica gel eluent $CHCl_3$/*i*-PrOH (95:5, *v/v*)], and *cyclo*-(*S*-Pro-*S*-Phe) [(**5**, 1.5 mg, R_f 0.32 on TLC on silica gel eluent $CHCl_3$/*i*-PrOH (95:5, *v/v*)] (Scheme 6.11).

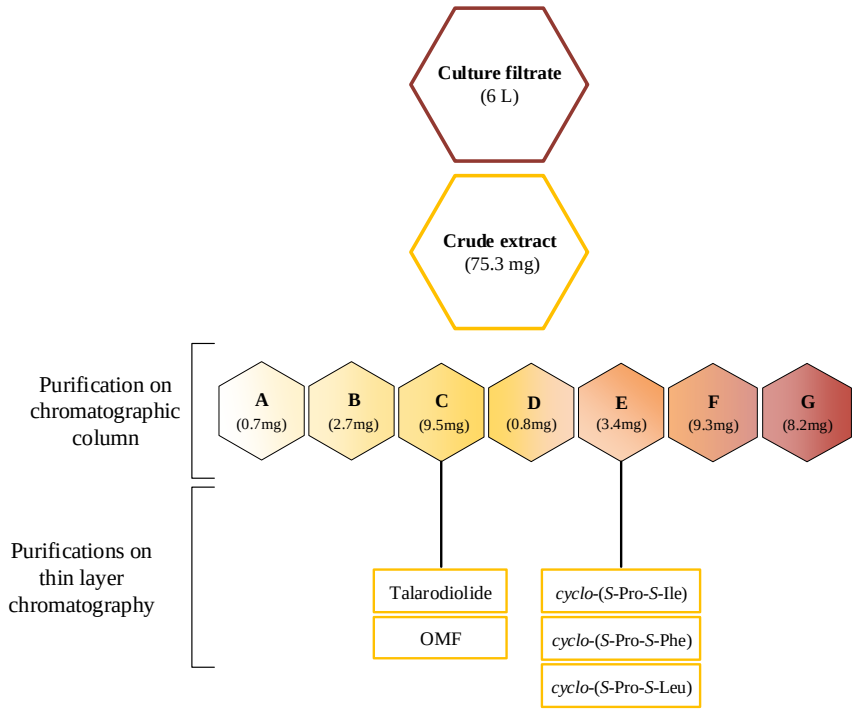

Scheme 6.11. Schematic representation of purification process of crude extract of culture filtrate of *T. pinophilus*.

6.8.2. Extraction and Isolation of Metabolites from Mycelium

Fresh mycelium was homogenized in a mixer with 440 mL of MeOH-H_2O (NaCl 1%) mixture (55:45, *v/v*). The suspension was stirred in the dark at room temperature for 4h. After this period, the suspension was centrifuged (40 min at 7000 rpm, 10°C) and separated from the supernatant. The residue was overnight extracted with 250 mL of the mixture reported above. The suspension was centrifuged, and both supernatants were combined for the subsequent extraction with $CHCl_3$. The organic extracts were combined, dried on anhydrous Na_2SO_4, and evaporated under reduced pressure yielding crude extract as a red oil (230.2 mg). The extract was fractionated by CC on silica gel (1.5 x 40 cm i. d.), eluting with $CHCl_3$/*i*-PrOH (97:3, *v/v*). The last fraction was eluted with MeOH. Seven

homogeneous fraction groups were collected (A 16.0 mg, B 16.4 mg, C 12.2 mg, D 14.2 mg, E 9.8 mg, F 29.1 mg, G 66.2 mg). The residue of fraction B was identified as OMF (**2**). Fraction C was purified by TLC on silica gel eluted with *n*-hexane/Me_2CO (6:4, *v/v*) to afford a further amount of OMF (5.6 mg), a crystalline compound identified as vermistatin [(**6**, 1.5 mg, R_f 0.37 on TLC on silica gel eluent *n*-hexane/Me_2CO (6:4, *v/v*)], and an amorphous solid identified as penisimplicissin [(**7**, 0.5, mg, R_f 0.29 on TLC on silica gel eluting with *n*-hexane/ Me_2CO (6:4, *v/v*)]. Fraction D was purified using the same condition described for C giving penicillide [(**8**, 6.9, mg, R_f 0.29 on TLC on silica gel eluent *n*-hexane/Me_2CO (6:4, *v/v*)] as amorphous solid. Finally, the residue of fraction F was further purified on TLC on silica gel eluting with $CHCl_3$/*i*-PrOH (9:1, *v/v*) giving 1-glycerol-linoleate [(**9**, 1.5 mg, R_f 0.40 on TLC on silica gel eluent $CHCl_3$/*i*-PrOH (9:1, *v/v*)] as soft solid (Scheme 6.12).

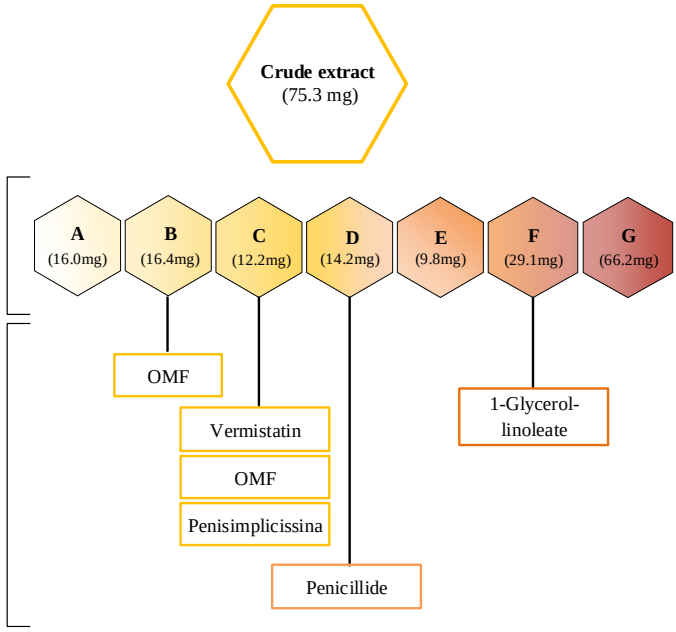

Scheme 6.12. Schematic representation of purification process of crude extract of mycelium of *T. pinophilus*.

*Talarodiolide (**1**)*: amorphous solid; UV (CH_3CN) λ_{max} (log ε) 260 (3.15); HRESIMS (+): 471.1990 ([calcd. 471.1995 for $C_{24}H_{32}O_8Na$ 2M+Na]$^+$), 449.2182 ([calcd. 449.2175 for $C_{24}H_{33}O_8$ 2M+H]$^+$), 247.0950 ([calcd. 247.0941 for $C_{12}H_{16}O_4Na$ M+Na]$^+$), 225.1118 ([calcd. 225.1127 for $C_{12}H_{17}O_4$ M+H]$^+$); ^{1}H-NMR ($CDCl_3$, 400 MHz) and ^{13}C-NMR ($CDCl_3$, 100 MHz) data: see Table 5.1.

*Cyclo-(S-Pro-R-Leu) (**3**)*: amorphous solid, HR ESI MS (+): 443.2636 ([calcd. 443.2629 for $C_{22}H_{36}N_4O_4Na$ 2M+Na]$^+$), 233.1269 ([calcd. 233.1260 for $C_{11}H_{18}N_2O_2Na$ M+Na]$^+$), 211.1448 ([calcd. 211.1441 for $C_{11}H_{19}N_2O_2$ M+H]$^+$); NMR data are in agreement with those previously reported[28].

Cyclo-(S-Pro-S-Ile) *(**4**)*: amorphous solid, HR ESI MS (+): 233.1272 ([calcd. 233.1260 for $C_{11}H_{18}N_2O_2Na$ M+Na]$^+$), 211.1451 ([calcd. 211.1441 for $C_{11}H_{19}N_2O_2$ M+H]$^+$); NMR data are in agreement with those previously reported[28].

*Cyclo-(S-Pro-S-Phe) (**5**)*: amorphous solid, HR ESI MS (+): 267.1115 ([calcd. 267.1109 for $C_{14}H_{16}N_2O_2Na$ M+Na]$^+$), 245.1296 ([calcd. 245.1290 for $C_{14}H_{17}N_2O_2$ M+H]$^+$); NMR data are in agreement with those previously reported[29].

*Vermistatin (**6**)*: crystalline compound HR ESI MS (+): 351.0841 ([calcd. 351.0845 for $C_{18}H_{16}O_6Na$ M+Na]$^+$), 329.1025 ([calcd. 329.1029 for $C_{18}H_{17}O_6$ M+H]$^+$). NMR data are in agreement with those previously reported[30].

*Penisimplicissin (**7**)*: amorphous solid HR ESI MS (+): 627.1475 ([calcd. 627.1473 for $C_{32}H_{28}O_{12}Na$ 2M+Na]$^+$), 325.0686 ([calcd. 325.0683 for $C_{16}H_{14}O_6Na$ M+Na]$^+$), 303.0869 ([calcd. 303.0863 for $C_{16}H_{15}O_6$ M+H]$^+$); NMR data are in agreement with those previously reported [Komai et al 2005].

*Penicillide (**8**)*: amorphous solid HR ESI MS (+): 409.2565 ([calcd. 409.1627 for $C_{22}H_{26}O_6Na$ M+Na]$^+$), 371.1493 ([calcd. 371.1489 for $C_{21}H_{23}O_6$ M-CH_3]$^+$), 359 [M+H-CO]$^+$. NMR data are in agreement with those previously reported[31].

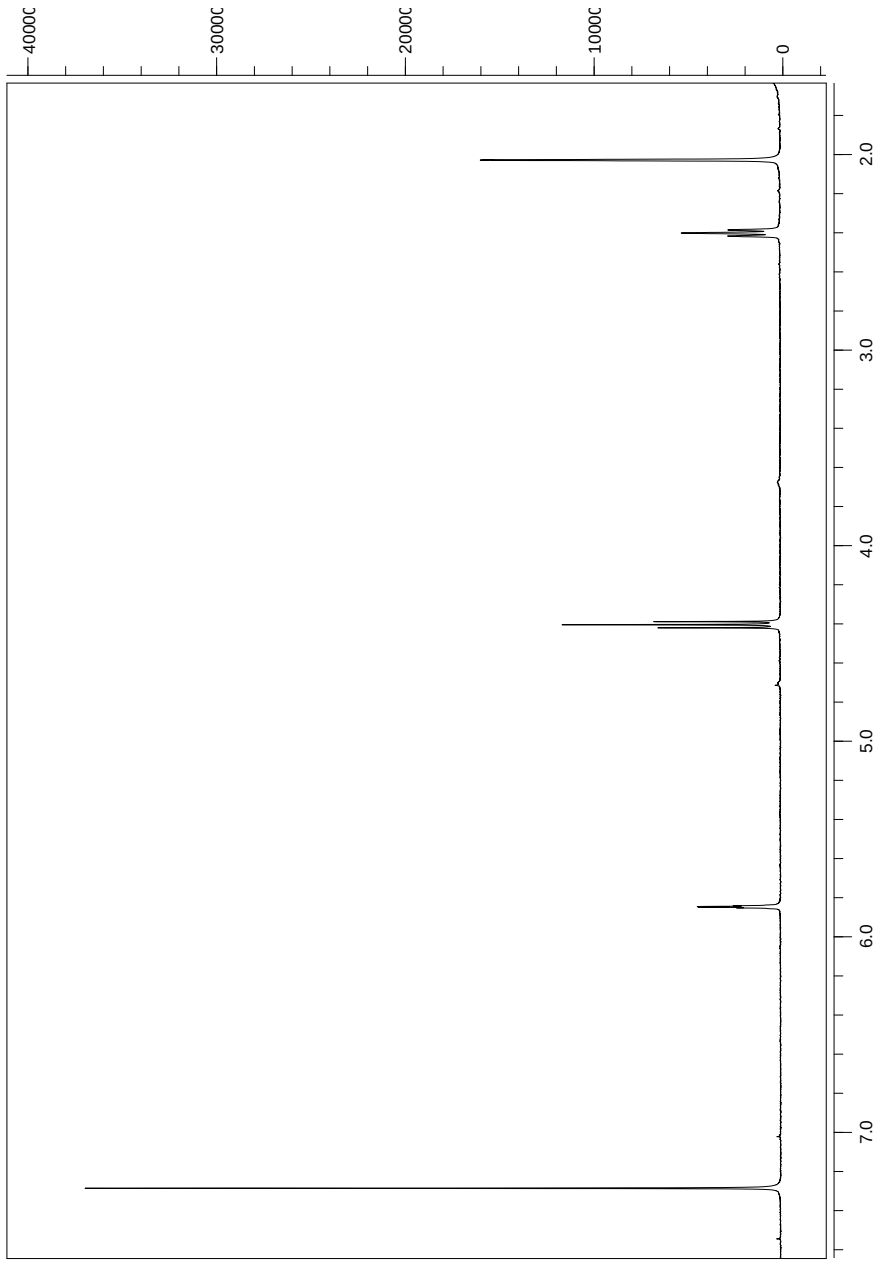

Figure 6.49. ^{1}H NMR spectrum of talarodiolide (**1**) recorded in $CDCl_3$ at 400 MHz.

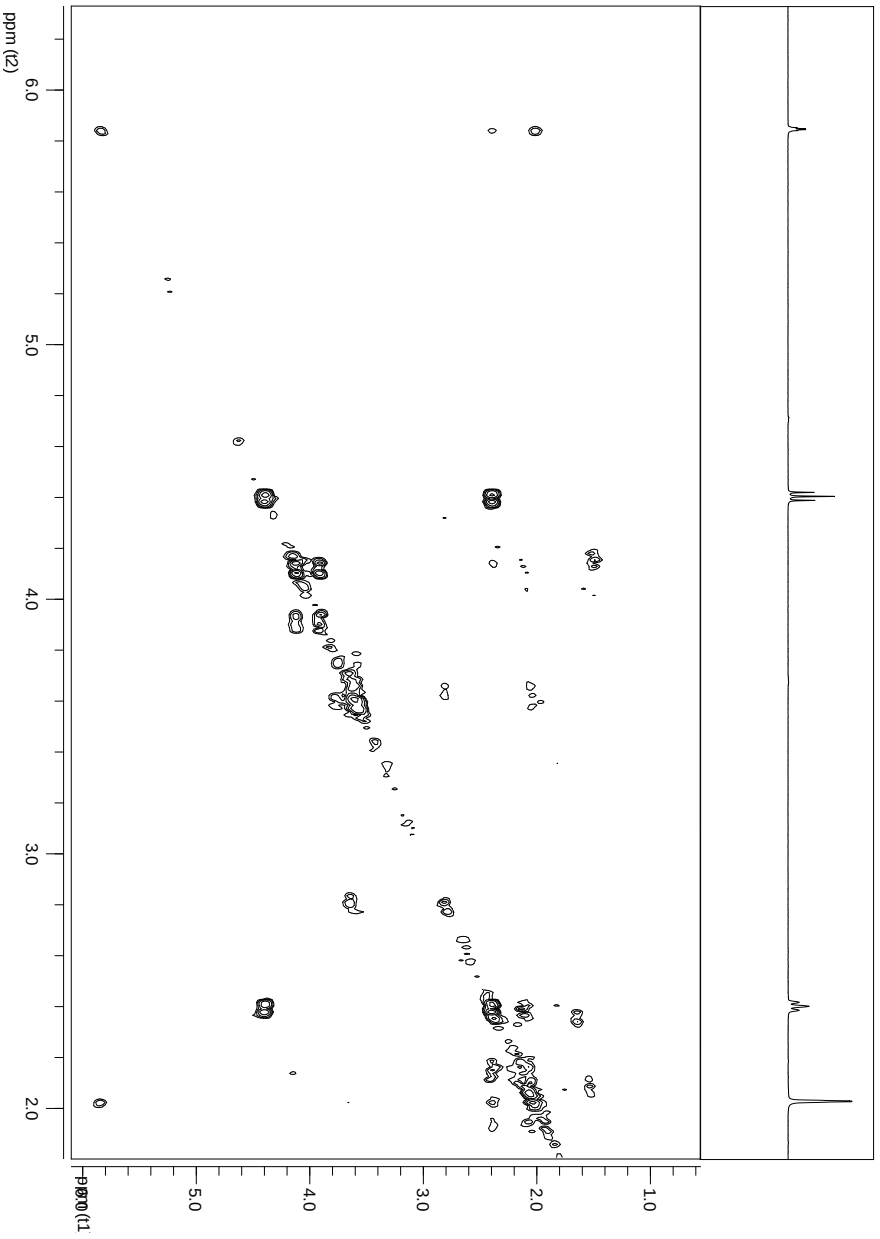

Figure 6.50. COSY spectrum of talarodiolide (**1**) recorded in $CDCl_3$ at 400 MHz.

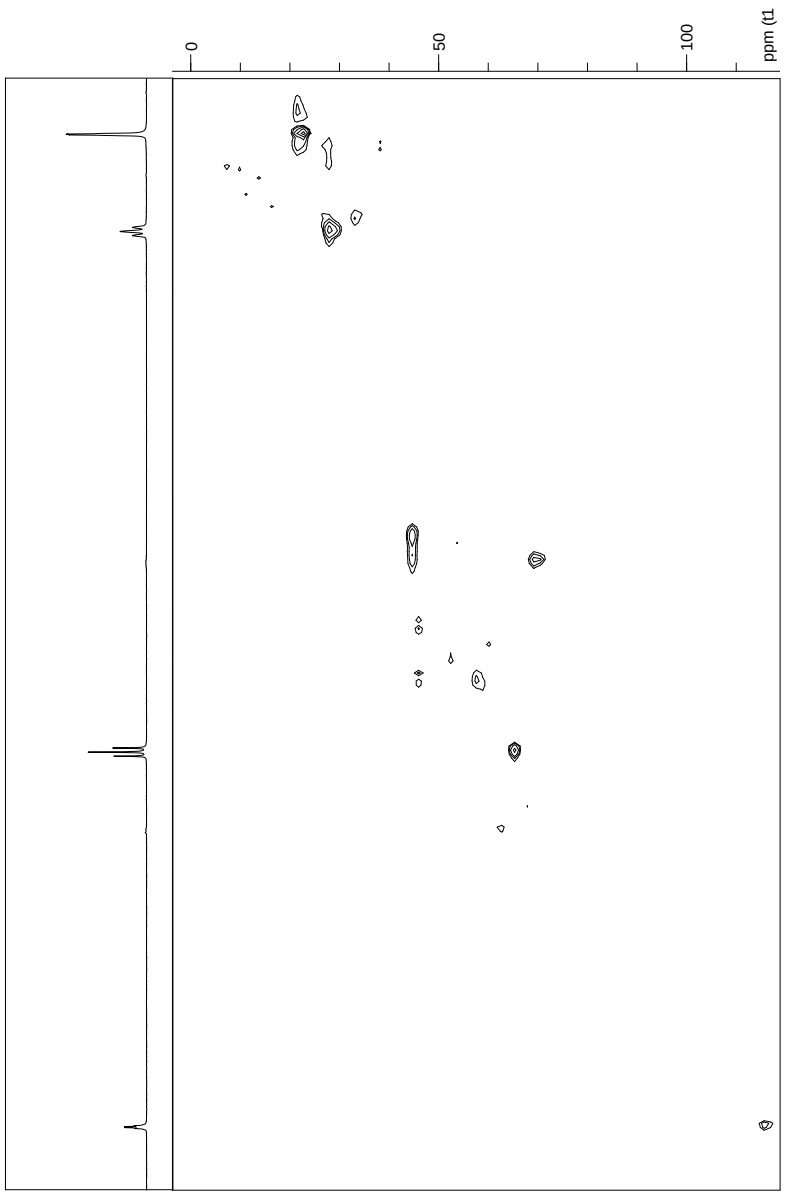

Figure 6.51. HSQC spectrum of talarodiolide (**1**) recorded in $CDCl_3$ at 400 MHz.

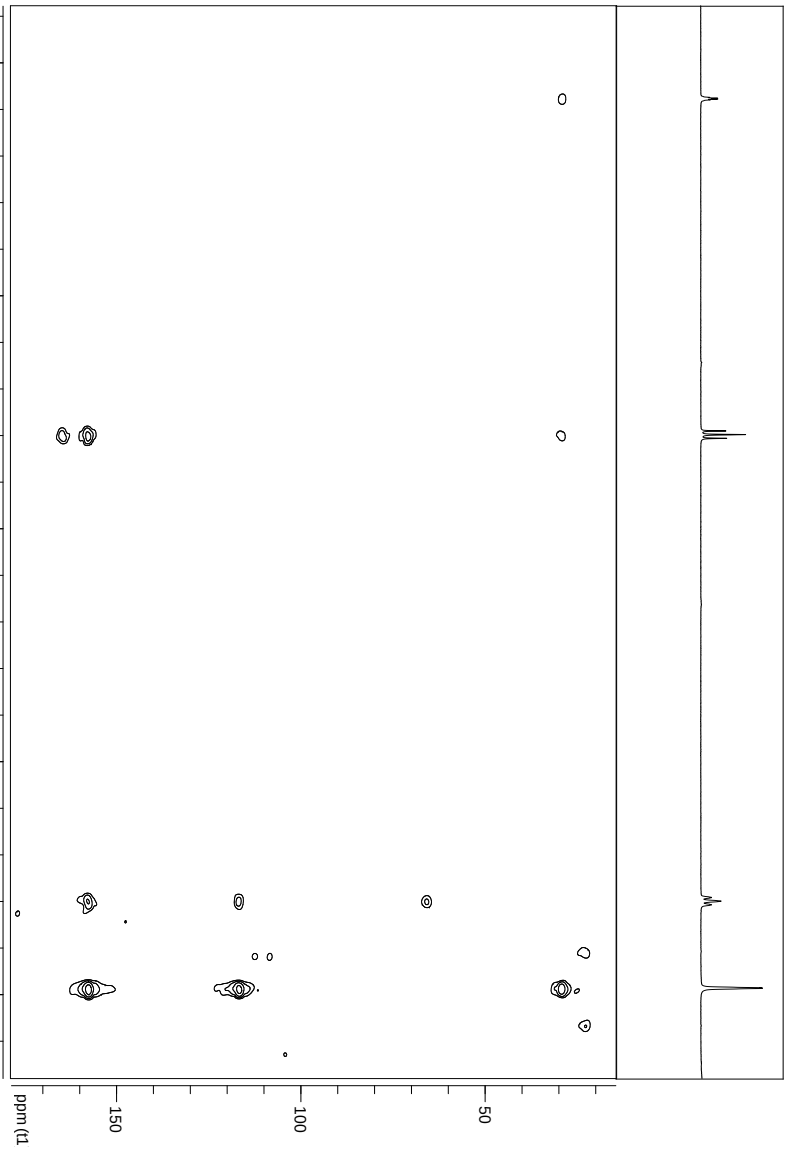

Figure 6.52. HMBC spectrum of talarodiolide (**1**) recorded in $CDCl_3$ at 400 MHz.

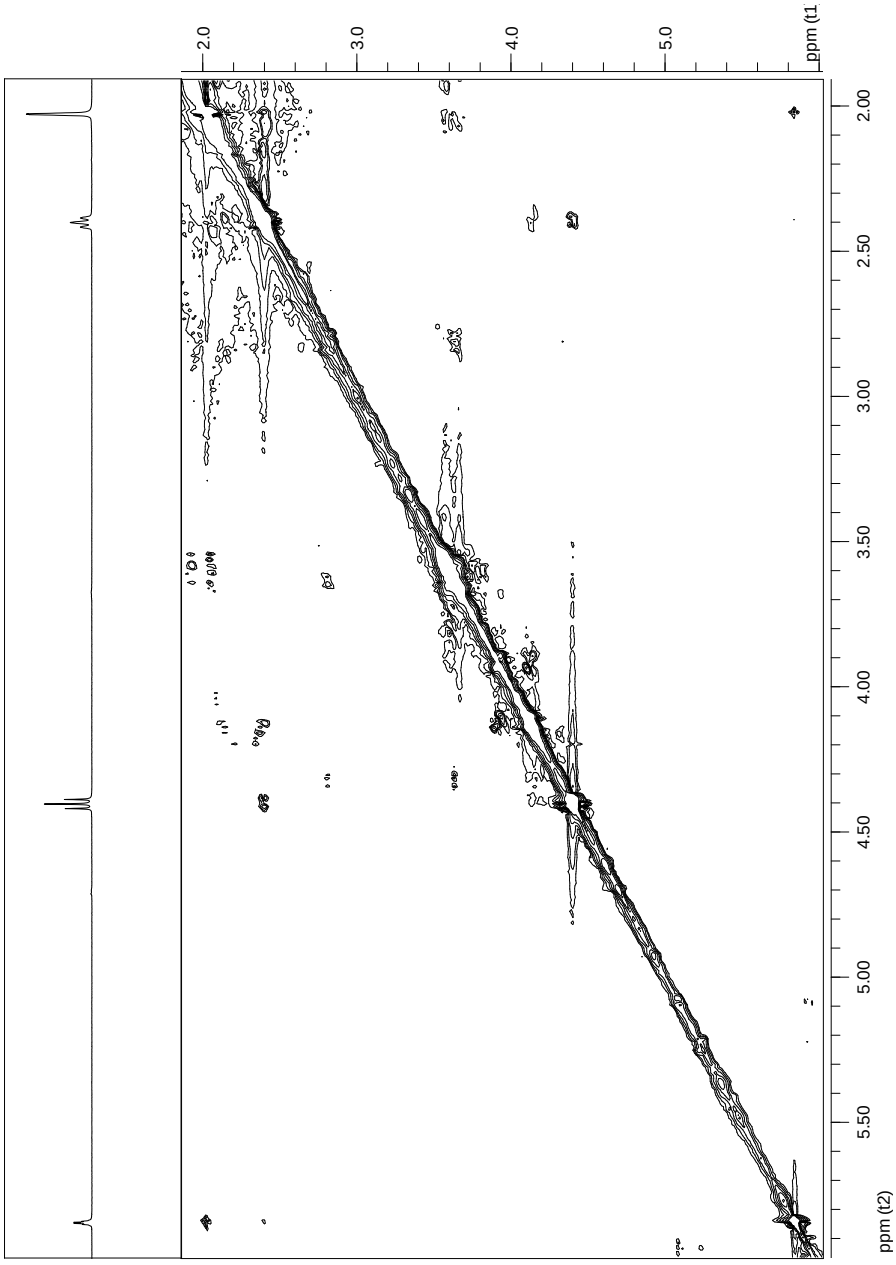

Figure 6.53. NOESY spectrum of talarodiolide (**1**) recorded in $CDCl_3$ at 400 MHz.

Table 6.4. Mass spectra of metabolites reported in Figure 5.1. RI represents the Kovats non isothermal retention index. Panel "MS peaks annotations" reports mass, formula (in square brackets) and normalized abundance (in round brackets) of identified fragments in mass spectra; the molecular ion is always represented by M; Me indicates methyl (-CH_3). Abundance is normalized taking abundance of base peak equal 100.

1	RI: 2064	MS peaks annotations: 224 [M] (5), 209 $[M\text{-}Me]^+$ (4), 194 $[M\text{-}2Me]^+$ (35), 149 $[M\text{-}2Me\text{-}CO_2\text{-}O]^+$ (60), 70 $[M\text{-}C_8H_9O_3]^+$ (100)

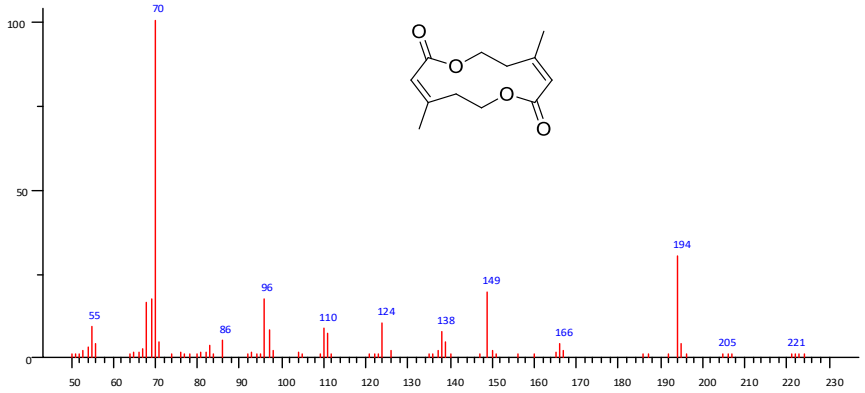

2	RI: 3006	MS peaks annotations: 388 $[M]^+$ (40), 373 $[M\text{-}Me]^+$ (15), 357 $[M\text{-}2Me]^+$, 223 $[M\text{-}C_9O_3H_9]^+$ (65), 192 $[M\text{-}2Me\text{-}C_9O_3H_9]^+$ (100)

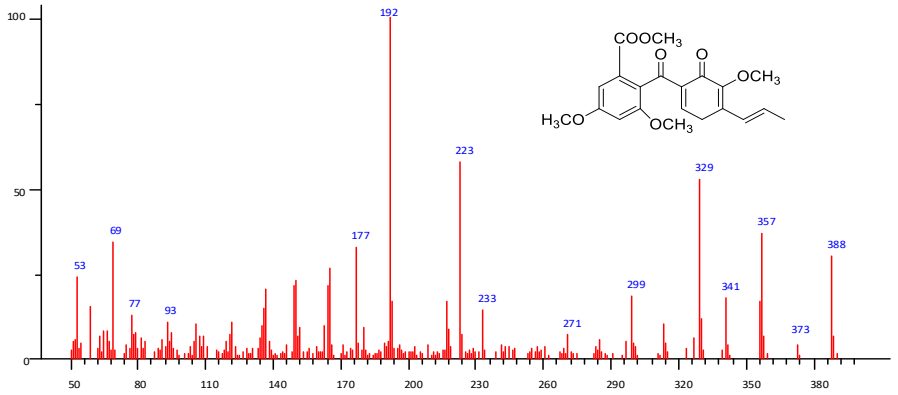

3	RI: 2068	MS peaks annotations: 195 $[M\text{-}Me]^+$ (5), 154 $[M\text{-}C_4H_9]^+$ (100), 125 $[M\text{-}C_6H_{13}]^+$ (15), 111 $[M\text{-}C_7H_{15}]^+$ (3), 70 $[M\text{-}C_7NO_2H_{11}]^+$ (75)

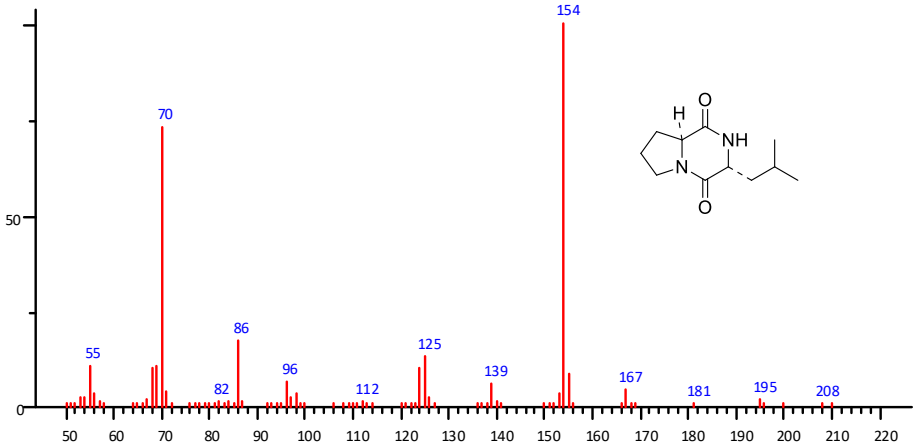

4	RI: 2039	MS peaks annotations: 154 $[M\text{-}C_4H_9]^+$ (100), 125 $[M\text{-}C_6H_{13}]^+$ (120), 111 $[M\text{-}C_7H_{15}]^+$ (5), 70 $[M\text{-}C_7NO_2H_{11}]^+$ (65)

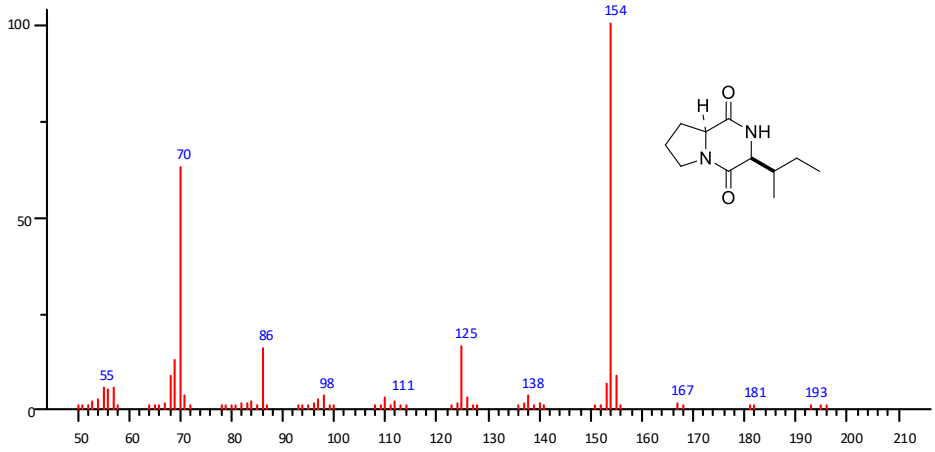

5	RI: 2443	MS peaks annotations: 244 $[M]^+$ (32), 215 $[M\text{-}C_2H_4]^+$ (3), 153 $[M\text{-}C_7H_7]$ (28), 125 $[M\text{-}C_3H_6\text{-}C_6H_5]$ (100)

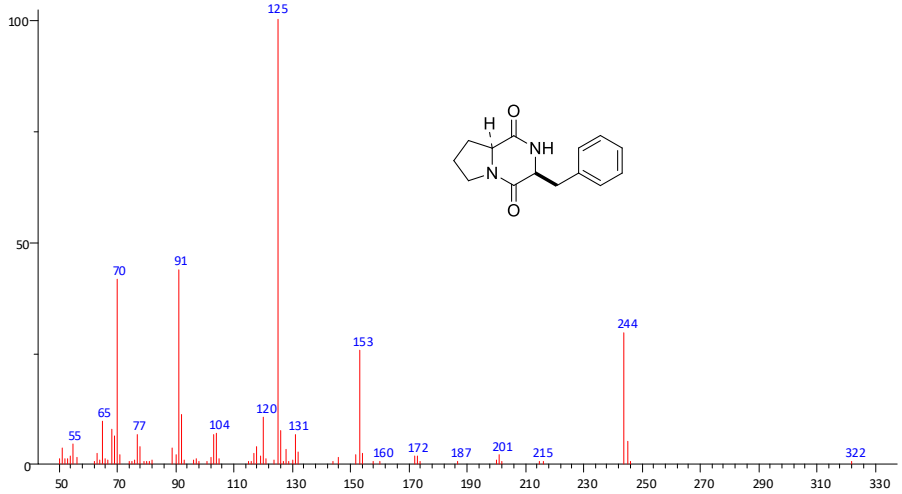

6	RI: 3105	MS peaks annotations: 328 $[M]^+$ (100), 313 $[M\text{-}Me]^+$ (10), 285 $[M\text{-}Me\text{-}C_2H_4]^+$ (48), 165 $[M\text{-}C_2H_4\text{-}C_8O_2H_8]^+$ (43)

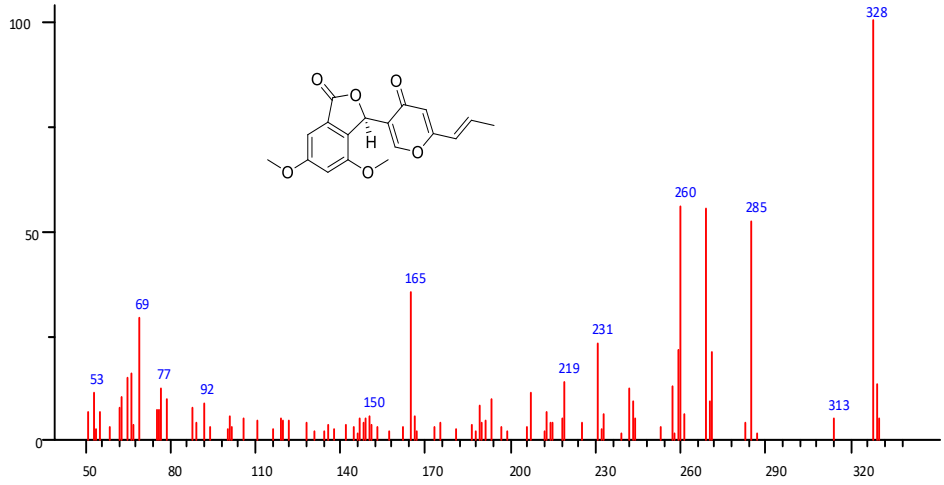

7	RI: 2835	MS peaks annotations: 302 $[M]^+$ (100), 287 $[M\text{-}Me]^+$, 273 $[M\text{-}2Me]^+$ (17), 175 $[M\text{-}Me\text{-}C_6H_7O_2]$ (14), 165 $[M\text{-}C_8O_2H_8]^+$ (47)

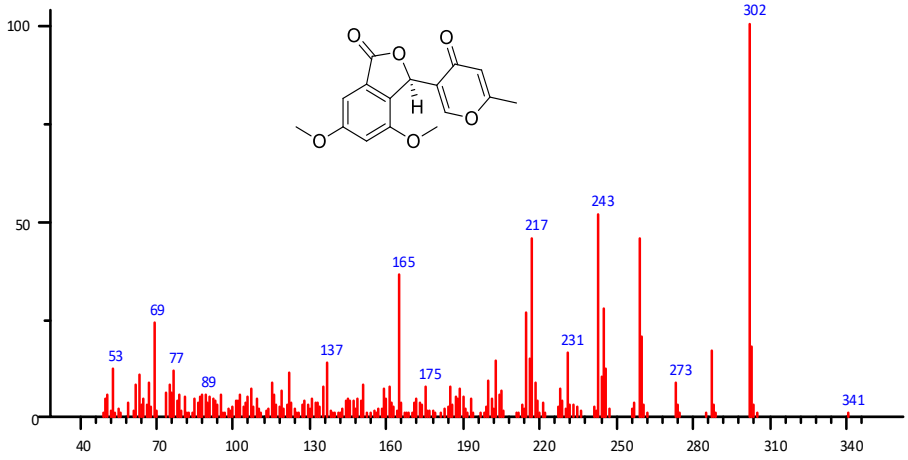

8	RI: 3103	MS peaks annotations: 372 $[M\text{-}Me]^+$ (16), 269 $[M\text{-}2Me\text{-}C_5OH_{10}]$ (100), 253 $[M\text{-}Me\text{-}OCH_3\text{-}C_5OH_{10}]$ (20)

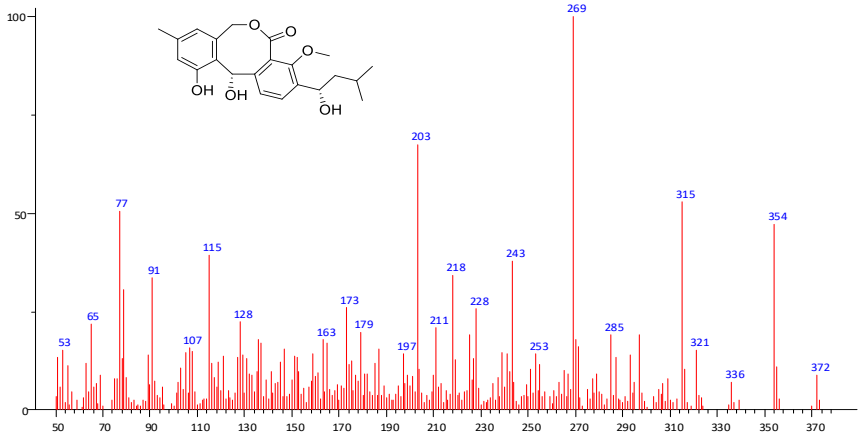

9	RI: 2076	MS peaks annotations: 354 $[M]^+$ (4), 336 $[M\text{-}OH]^+$, 262 $[M\text{-}C_3O_3H_7]^+$ (63), 234 $[M\text{-}C_4O_4H_7]^+$ (12)

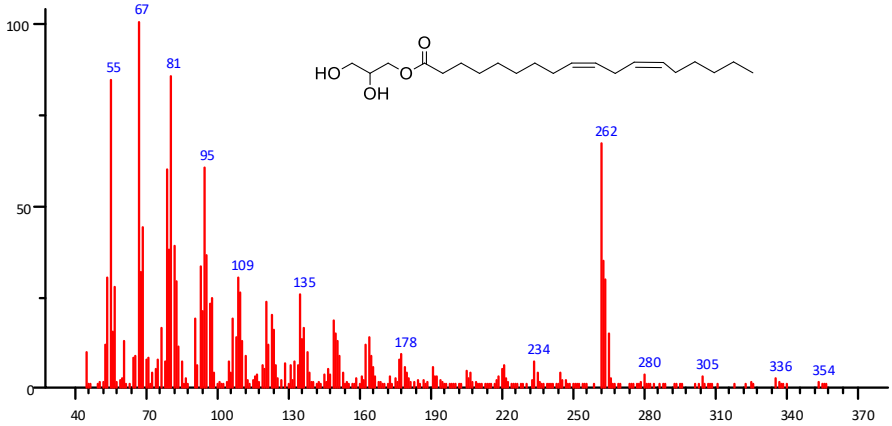

References

1. Guida, M., Salvatore, M.M., Salvatore, F. (2015). A Strategy for GC/MS quantification of polar compounds via their silylated surrogates: silylation and quantification of biological amino acids. J. Anal. Bioanal. Tech. *6*, 263–279.
2. NIST Standard Reference Data. Available online: http://www.nist.gov/srd/nist1a.cfm (accessed on 14 12 19)
3. AMDIS NET. AMDIS. Available from: http://www.amdis.net/ (accessed on 14 12 2019).
4. Rodríguez-Gálvez, E., Maldonado, E., Alves, A. (2015). Identification and pathogenicity of *Lasiodiplodia theobromae* causing dieback of table grapes in Peru. Eur. J. Plant Pathol. *141*, 477–489.
5. Félix, C., Duarte, A.S., Vitorino, R., Guerreiro, A.C., Domingues, P., Correia, A.C., Alves, A., Esteves, A.C. (2016). Temperature modulates the secretome of the phytopathogenic fungus *Lasiodiplodia theobromae*. Front. Plant Sci. *7*, 1096.
6. Duarte, A.S., Cavaleiro, E., Pereira, C., Merino, S., Esteves, A.C., Duarte, E.P., Tomás, J.M., Correia, A.C. (2015). *Aeromonas piscicola* AH-3 expresses an extracellular collagenase with cytotoxic properties. Lett. Appl. Microbiol. *60*, 288–297.
7. Ammerman, N.C., Beier-Sexton, M., Azad, A.F. (2008). Growth and maintenance of vero cell lines. Curr. Protoc. Microbiol. *S1*, A.4E.1–A.4E.7.
8. Moreau, S., Lablache-Combier, A., Biguet, J., Foulon, C., Delfosse, M. (1982). Botryodiplodin, a mycotoxin synthesized by a strain of *P. roqueforti*. J. Org. Chem. *47*, 2358–2359.
9. Aldridge, D.C., Galt, S., Giles, D., Turner, W.B. (1971). Metabolites of *Lasiodiplodia theobromae*. J. Chem. Soc. C 1623–1627.
10. Carvajal, M., Espinoza, L., Caggia, S., Cardile, V., Garbarino, J.A., Peña-Cortés, H., Russo, A. (2011). New stereoisomeric derivatives of jasmonic acid

generated by biotransformation with the fungus *Gibberella fujikuroi* affect the viability of human cancer cells. Electron. J. Biotechnol. *14*, 7.

11. Andolfi, A., Maddau, L., Cimmino, A., Linaldeddu, B.T., Basso, S., Deidda, A., Serra, S., Evidente, A. (2014). Lasiojasmonates A–C, three jasmonic acid esters produced by *Lasiodiplodia* sp., a grapevine pathogen. Phytochemistry *103*, 145–153.
12. Ravi, B.N., Armstrong, R.W., Faulkner, D.J. (1979). Some aromatic compounds from the marine sponge *Plakortis halichondrioides*. J. Org. Chem. *44*, 3109–3113.
13. Forzato, C., Furlan, G., Nitti, P., Pitacco, G., Marchesan, D., Coriani, S., Valentin, E. (2005). A combined experimental and computational strategy in the assignment of absolute configurations of 4-methyl-5-oxo-tetrahydrofuran-3-carboxylic acids and their esters. Tetrahedron: Asymmetry *16*, 3011–3023.
14. Cabras, A., Mannoni, M.A., Serra, S., Andolfi, A., Fiore, M., Evidente, A. (2006). Occurrence, isolation and biological activity of phytotoxic metabolites produced in vitro by *Sphaeropsis sapinea*, pathogenic fungus of *Pinus radiata*. Eur. J. Plant Pathol. *115*, 187–193.
15. Andolfi, A., Basso, S., Giambra, S., Conigliano, G., Lo Piccolo, S., Alves, A., Burruano, S. (2016). Lasiolactols A and B produced by the grapevine fungal pathogen *Lasiodiplodia mediterranea*. Chem. Biodivers. *13*, 395–402.
16. Dimitriadis, C., Gill, M., Harte, M.F. (1997). The first stereospecific approach to both enantiomers of mellein. Tetrahedron: Asymmetry *8*,2153–2158.
17. Ramezani, M., Shier, W.T., Abbas, H.K., Tonos. J.L., Baird. R.E., Sciumbato, G.L. (2007). Soybean charcoal rot disease fungus *Macrophomina phaseolina* in Mississippi produces the phytotoxin (−)-botryodiplodin but no detectable phaseolinone. J. Nat. Prod. *70*, 128–129.

18. Rehnberg N, Magnusson G. (1990). Total synthesis of (−)- and (+)-botryodiplodin and (+)- and (−)-epibotryodiplodin. Acta Chem. Scand. *44*, 377–383.
19. Capasso, R., Cristinzio, G., Evidente, A., Scognamiglio, F. (1992). Isolation, spectroscopy and selective phytotoxic effects of polyphenols from vegetable waste waters. Phytochemistry *31*, 4125–4128.
20. Mondello, V., Lo Piccolo, S., Conigliaro, G., Alfonzo, A., Torta, L., Burruano, S. (2013). First report of *Neofusiccoccum vitifusiforme* and presence of other Botryosphaeriaceae species associated with Botryosphaeria dieback of,grapevine in Sicily (Italy). Phytopathol. Mediterr. *52*, 388–396.
21. Burruano, S., Giambra, S., Mondello, V., DellaGreca, M., Basso, S., Tuzi, A., Andolfi, A. (2016). Naphthalenone polyketides produced by *Neofusicoccum parvum*, a fungus associated with grapevine Botryosphaeria dieback. Phytopathol. Mediterr. *55*, 197–206.
22. Sparkman, O.D., Penton, Z., Kitson, F.G. (2011). Gas chromatography and mass spectrometry: a practical guide, 2nd ed. Academic Press, Oxford, UK ISBN: 978-0-12-373628-4.
23. EMBL-EBI website. Available online: https://www.ebi.ac.uk/Tools/msa/clustalo (accessed on 14 12 2019).
24. Alupei, M.C., Licarete, E., Patras, L., Banciu, M. (2015). Liposomal simvastatin inhibits tumor growth via targeting tumor-associated macrophages-mediated oxidative stress. Cancer Lett. *356*, 946–952.
25. Frisvad, J.C., Houbraken, J., Popma, S., Samson, R.A. (2013). Two new *Penicillium* species *Penicillium buchwaldii* and *Penicillium spathulatum*, producing the anticancer compound asperphenamate. FEMS Microbiol. Lett. 339, 77–92.

26. Frisvad, J.C., Samson, R.A. (2004) Polyphasic taxonomy of *Penicillium* subgenus *Penicillium.* A guide to identification of food and air-borne terverticillate Penicillia and their mycotoxins. Stud. Mycol. *49*, 1–174
27. Manganiello, G., Marra, R., Staropoli, A., Lombardi, N., Vinale, F., Nicoletti, R. (2019). The shifting mycotoxin profiles of endophytic *Fusarium* strains: A case study. Agriculture *9*, 143.
28. Adamczeski, M.; Reed, A.R.; Crews, P. (1995). New and known diketopiperazines from the Caribbean sponge, *Calyx* cf. *podatypa*. J. Nat. Prod. *58*, 201–208.
29. Wang, G., Dai, S., Chen, M., Wu, H., Xie, L., Luo, X., Li, X. (2010). Two diketopiperazine *cyclo*-(Pro-Phe) isomers from marine bacteria *Bacillus subtilis* sp. 13–2. Chem. Nat. Compd. *46*, 583–585.
30. Fuska, J., Uhrin, D., Proksa, B., Votický, Z., Ruppeldt, J. (1986). The structure of vermistatin, a new metabolite from *Penicillium vermiculatum*. J. Antibiot. *39*, 1605–1608.
31. Komai, S.I., Hosoe, T., Itabashi, T., Nozawa, K., Yaguchi, T., Fukushima, K., Kawai, K. (2005). New vermistatin derivatives isolated from *Penicillium simplicissimum*. Heterocycles *11*, 2771–2776.

CHAPTER 7

Final Remarks

Fungi are organisms of great importance and have proven to be a rich source of useful compounds with a wide variety of biological activities. Research is needed to understand their remarkable metabolic features, considering the broad spectrum of fungal biodiversity.

In this thesis, an attempt has been made to present some of more widely used analytical methods in the detection and isolation of bioactive natural products, according to the words of Gilbert K. Chesterton's *Father Brown*, "No machine can lie, nor can it tell the truth".

The data presented in this thesis show a vast range of compounds produced by fungi from different environmental contexts. The secondary metabolites production with enormous structural diversity might be linked to the fungal capacity to occupy areas with a wide variety of environmental conditions with possible implications in the fungal interactions with other organisms. There is a general lack of information regarding the effect of environmental conditions on secondary metabolites produced by fungi. This critical issue has been adressed for strains of *Lasiodiplodia theobromae*, as phytopathogenic fungus with particular relevance in the agrarian field. Data about the effect of growth conditions on virulence and metabolite profile of *L. theobromae* strains have been collected.

In this work was also studied the metabolome of other phytopathogenic fungal species (i.e. *Macrophomina phaseolina* and *Neofusicoccum vitifusiforme*) involved in plant diseases, in order to increase the knowledge on potential correlations between secondary metabolites and plant disease.

Fungi represent an abundant and dependable source of bioactive and chemically original compounds with potential exploitation in a wide variety of economically important applications. In this respect, the parallel application of several instrumental techniques was used for the detection of valuable compounds produced by terrestrial (e.g. *Talaromyces pinophilus*) and marine-derived fungi

(e.g. *Trichoderma citrinoviride*, *Aspergillus niger* and *Penicillium brevicompactum*).

Obviosly, despite the contribution of the present work, the reported data are just a piece of the puzzle.